PALACKÝ UNIVERSITY OLOMOUC

Faculty of Science

Department of Biophysics

in cooperation with

UNIVERSITY OF OSTRAVA

Faculty of Science

Department of Physics

Spectral characteristics of photosynthetic pigments and their relation to structure-functional aspects of pigment-protein complexes *in vivo* and *in vitro*

Doctoral Thesis

Author: Mgr. Václav Karlický

Study program: P1703/ Physics

Program field: Biophysics

Supervisor: Doc. RNDr. Vladimír Špunda, CSc.

Olomouc 2017

BIBLIOGRAPHICAL IDENTIFICATION

Name of the author: Václav Karlický

Title of the doctoral thesis: Spectral characteristics of photosynthetic pigments and their relation to structure-functional aspects of pigment-protein complexes *in vivo* and *in vitro*

Study program: P1703/ Physics

Degree program field: Biophysics

Year of defense: 2017

Supervisor: Doc. RNDr. Vladimír Špunda, CSc.

Co-supervisor: prof. RNDr. Petr Ilík, Ph.D.

Number of pages: 140 (76 without attachments)

Number of attachments: 4

Annotation: In this thesis, spectral characteristics of Norway spruce photosynthetic apparatus are studied using circular dichroism and low temperature fluorescence spectroscopy and compare to those of model plants Arabidopsis thaliana and spring barley. Main goal of this thesis was to obtain new information about the pigment-protein complexes of spruce, their supramolecular organization and stability in the thylakoid membranes.

Keywords: Norway spruce; Spring barley; *Arabidopsis thaliana*; Fluorescence spectra; Circular dichroism; Photosystem II organization; Thylakoid membrane; Thermal stability

BIBLIOGRAFICKÉ IDENTIFIKAČNÍ ÚDAJE

Jméno autora: Václav Karlický

Název doktorské práce: Spektrální charakteristiky fotosyntetických pigmentů a jejich vztah ke strukturně-funkčním aspektům pigment-proteinových komplexů *in vivo* a *in vitro*

Studijní program: P1703/Fyzika

Studijní obor: Biofyzika

Rok obhajoby: 2017

Školitel: Doc. RNDr. Vladimír Špunda, CSc.

Konzultant: prof. RNDr. Petr Ilík, Ph.D.

Počet stran: 140 (76 bez příloh)

Počet příloh: 4

Anotace: V této práci jsou studovány spektrální charakteristiky fotosyntetického aparátu smrku ztepilého pomocí spektroskopie cirkulárního dichroismu a nízkoteplotní fluorescenční spektroskopie a porovnány vůči vybraným modelovým rostlinám (huseníček rolní, ječmen jarní). Hlavním cílem této práce bylo získat informace o pigment-proteinových komplexech smrku, jejich makro-organizaci a stabilitě v thylakoidní membráně.

Klíčová slova: Smrk ztepilý; Ječmen jarní; Arabidopsis thaliana; Fluorescenční spektra; Cirkulární dichroismus; Organizace fotosystému II; Thylakoidní membrána; Teplotní stabilita

DECLARATION

I hereby declare that the Ph.D thesis is my original work and effort and that it has not been submitted anywhere for any award. I have written this thesis by myself and where other information has been used, they have been acknowledged in the section „References“. All the results were included in this study after the consent of the co-authors.

Signature: ……..

Date and Place: ……..

CONTENT

LIST OF PUBLICATIONS

Published:

1) *Karlický, V., Podolinská, J., Nadkanská, L., Štroch, M., Čajánek, M., Špunda, V. (2010) Pigment composition and functional state of the thylakoid membranes during preparation of samples for pigment-protein complexes separation by nondenaturing gel electrophoresis. Photosynthetica 48: 475-480
2) *Miloslavina, Y., Lambrev, P.H., Jávorfi, T., Várkonyi, Z., Karlický, V., Wall, J.S., Hind, G., Garab, G (2012) Anisotropic circular dichroism signatures of oriented thylakoid membranes and lamellar aggregates of LHCII. Photosynthesis Research 111: 29-39
3) Štroch, M., Materová, Z., Vrábl, D., Karlický, V., Šigut, L., Nezval, J., Špunda, V. (2015) Protective effect of UV-A radiation during acclimation of the photosynthetic apparatus to UV-B treatment. Plant Physiology and Biochemistry 96: 90-96
4) *Karlický, V., Kurasová, I., Ptáčková, B., Večeřová, K., Urban, O., Špunda, V. (2016) Enhanced thermal stability of the thylakoid membranes from spruce. A comparison with selected angiosperms. Photosynthesis Research 130: 357-371

Submitted:

5) *Karlický, V., Strouhal, O., Ilík, P., Štroch, M., Kurasová, I., Garab, G., Šebela, M., Špunda, V. The effect of growth light intensity on pigment-protein composition and efficiency of excitation energy transfer within photosystem II in barley leaves. Photosynthesis Research
6) VI. Materová, Z., Sobotka, R., Zdvihalová, B., Oravec, M., Nezval, J., Karlický, V., Vrábl, D., Štroch, M., Špunda, V. Monochromatic green light induces an aberrant accumulation of geranylgeranyl-chlorophyll in plants. Plant Physiology and Biochemistry

Peer-reviewed conference papers (ISI Web of Science):

7) Karlický, V., Kurasová, I., Špunda, V. (2015) The thermostability of photosystem II photochemistry is related to maintenance of thylakoid membranes organization. Global Change: A Complex Challenge: 142-145
8) Kurasová, I., Svrčinová, K., Karlický, V., Špunda, V. (2015) CN-PAGE as a tool for separating pigment-protein complexes and studying their thermal stability in spruce and barley thylakoid membranes. Global Change: A Complex Challenge: 146-149

Peer-reviewed conference papers:

9) Karlický, V., Nezval, J., Štroch, M., Špunda, V. (2013) Response of epidermal blue-green fluorescence emission from Barley leaves to UV radiation stress. Global Change and Resilience: From Impacts to Responses: Proceedings of the 3rd annual Global Change and Resilience Conference, ISBN 978-80-904351-8-6

*These publications are the basis of the present Ph.D. thesis

ABBREVIATIONS

Car – Carotenoid

CD – Circular dichroism

CN-PAGE – Clear-native polyacrylamide gel electrophoresis

DGDG – Digalactosyldiacylglycerol

Chl – Chlorophyll

F_V/F_M – maximum efficiency of PSII photochemistry

HL – High light

Lhc – Light-harvesting complex

Lhca (LHCI) – Light-harvesting complex of PSI

Lhcb – Light-harvesting complex of PSII

LHCII – Major light-harvesting complex of PSII

Lhcb4 (CP29), Lhcb5 (CP26), Lhcb6 (CP24) – Minor light-harvesting complex of PSII

Lhcsr – stress-related LHC protein

LL – Low light

MGDG – Monogalactosyldiacylglycerol

ML – Moderate light

NPQ – Non-photochemical quenching of chlorophyll *a* fluorescence

PPC – Pigment-protein complex

PSI – Photosystem I

PSII – Photosystem II

ROS – Reactive oxygen species

T_m – Transition temperature

VDE – Violaxanthin de-epoxidase

Ψ – Polymer and salt induced

ABSTRACT

In this thesis, spectral characteristics of Norway spruce photosynthetic apparatus were studied using circular dichroism and low temperature fluorescence spectroscopy and compared to those of model plants *Arabidopsis thaliana* and spring barley. Main goal of this thesis was to obtain new information about the pigment-protein complexes of spruce, their supramolecular organization and stability in the thylakoid membranes. Red shift of 77K chlorophyll *a* fluorescence emission maximum of isolated PSII-LHCII supercomplexes and smaller macrodomain organization of pigment-protein complexes were confirmed in spruce membranes in comparison with *Arabidopsis* and barley, which can be related to recently described, different structure of spruce PSII-LHCII supercomplexes. It was shown that main signatures of low temperature fluorescence emission of isolated PSII-LHCII and also PSI-LHCI supercomplexes remain distinguishable in 77K chlorophyll *a* fluorescence emission spectra of isolated thylakoids and even intact leaves/needles, indicating that they reflect native state of those pigment-protein complexes. Further, thylakoid membranes of spruce revealed enhanced thermal stability PSII photochemistry than *Arabidopsis* and barley cultivated under the same temperatures. We have proved that higher thermal stability of PSII photochemistry of spruce is accompanied by the maintenance of PSII macro-organization and stability of PSII-LHCII supercomplexes at elevated temperatures. Finally, we documented the specific long-term acclimation response to different growth light intensity in spruce photosynthetic apparatus, in comparison with other higher plants such as *Arabidopsis* or barley. Similarly as observed in *Arabidopsis* and barley, young spruce seedlings exhibited ability to adjust light harvesting antennas during acclimation to different light intensity, but the pronounced increase in lutein content in seedlings acclimated to high light is not typical for other higher plants, but rather for algae (e.g. *Chlamydomonas reinhardtii*). This work thus contributes to the knowledge of the specific aspects of the Norway spruce photosynthetic apparatus and its unusual short- and long-term responses to different environmental conditions.

SOUHRN

V této práci byly studovány spektrální charakteristiky fotosyntetického aparátu smrku ztepilého pomocí spektroskopie cirkulárního dichroismu a nízkoteplotní fluorescenční spektroskopie a porovnány vůči vybraným modelovým rostlinám (huseníček rolní, ječmen jarní). Hlavním cílem této práce bylo získat informace o pigment-proteinových komplexech smrku, jejich makro-organizaci a stabilitě v thylakoidní membráně. U superkomplexu PSII-LHCII smrku při 77 K byl potvrzen posun emisního maxima fluorescence chlorofylu *a* k delším vlnovým délkám a menší makro-organizace pigment-proteinových komplexů v thylakoidních membránách ve srovnání s huseníčkem a ječmenem. Toto je pravděpodobně způsobeno díky odlišné struktuře PSII-LHCII superkomplexů smrku, jež byla nedávno popsána. Dále jsme prokázali, že hlavní rysy nízkoteplotní emise fluorescence chlorofylu *a* izolovaných superkomplexů PSII-LHCII, ale i PSI-LHCI zůstávají patrné nejen v nízkoteplotních emisních spektrech fluorescence chlorofylu *a* izolovaných thylakoidních membrán, ale i intaktních listů či jehlic, což ukazuje, že odráží nativní stav těchto pigment-proteinových komplexů. Navíc thylakoidní membrány smrku vykázaly zvýšenou teplotní stabilitu fotochemie PSII ve srovnání s rostlinami huseníčku a ječmene, které byly pěstovány při stejných teplotách. Prokázali jsme, že vyšší teplotní stabilita fotochemie PSII u smrku je doprovázena schopností udržet makro-organizaci PSII a stabilitu superkomplexů PSII-LHCII při zvýšených teplotách. Rovněž jsme prokázali, že fotosyntetický aparát smrku má odlišnou aklimační odezvu na různé intenzity světla než ostatní druhy vyšších rostlin jako huseníček či ječmen. Podobně jak bylo pozorováno u huseníčku a ječmene, semenáčky smrku vykazovaly schopnost přizpůsobit světlosběrné antény během aklimace na různé intenzity světla, nicméně výrazný nárůst obsahu luteinu semenáčků smrku aklimovanch na vysokou intenzitu světla není typické pro vyšší rostliny, ale spíše řasy (např. *Chlamydomonas reinhardtii*). Tato práce přispívá ke znalostem specifických aspekty fotosyntetického aparátu smrku ztepilého a jeho neobvyklé krátkodobé i dlouhodobé odezvy na různé environmentální odezvy.

1 INTRODUCTION

1.1. General introduction

Nowadays, one of the main scientific challenges is solution of problems related to the rapidly increasing energy consumption of humankind. Fossil fuels cannot be maintained in the long term perspective as a prevailing producer of the global energy due to the rapid decrease of its resources and increasing atmospheric carbon dioxide concentration. Therefore, scientific studies on the utilization of renewable resources became important. Amongst various energy resources, solar energy has a special role, because light energy reaching the Earth's surface is many times greater than the needs of world's energy. In the Biosphere, efficient collection, utilization and storage of solar energy through conversion to chemical energy is performed by photosynthetic organisms. Photosynthesis is the biochemical process in plants, algae and certain bacteria that serves as the energy input for the current life of terrestrial and aquatic organisms and it regulates the oxygen concentration and carbon dioxide in the atmosphere. On the basis of this natural process, a substantial contribution to industrial energy production can originate from modified photosynthetic organisms or artificial devices converting solar energy.

Moreover, the plants are exposed to extremely different climatic conditions, such as irradiances or temperatures that undergo considerable changes in very diverse time scales. As sessile organisms plants have to evolve highly sophisticated acclimation responses during evolution to allow survival under these environmental conditions. There is still a lack of information on diversity of photosynthetic apparatus, particularly if the importance of individual regulatory mechanisms that control the resistance of plants to environmental stresses and influence different acclimation strategies among different plant species is taken into account. In this work, we focused on higher plants, which form a large group of plants as regards the plant species, but relatively narrow group from the viewpoint of evolutionary history. Nevertheless, there are still differences in architecture and composition of photosynthetic apparatus components among land plant families and probably also in acclimation responses to environmental stresses.

This thesis is related to specific structural and functional aspects of photosynthetic apparatus of Norway spruce belonging to the *Pinaceae* family of gymnosperms, which were always less studied than angiosperms.

1.1. Thylakoid membrane of the chloroplast

The photosynthetic processes of higher plants and eukaryotic algae occur in an organelle, called the chloroplast. Evolutionary, the chloroplast became a plant cell organelle through an endosymbiotic event, during which a non-photosynthesizing eukaryotic organism engulfed a cyanobacterium. The chloroplasts contain the thylakoid membranes, the multilamellar lipid bilayer membrane assembly located in the aqueous matrix called stroma. Carbon fixation, the 'dark reactions', happen in the stroma, while thylakoid membranes are the site for the 'light reactions' of photosynthesis, and thus have a crucial role in the primary steps of photosynthesis. The thylakoid membranes separate two aqueous phases (the stroma and the lumen) and incorporate almost all components of the photosynthetic electron transfer pathway, including main protein complexes photosystem II (PSII), the cytochrome b_6/f complex, photosystem I (PSI) and the ATP-synthase. Further, between PSII and cytochrome b_6/f and between cytochrome b_6/f and PSI the mobile plastoquinone and small water-soluble protein plastocyanin serve as electron carriers. These components, their role in the photosynthetic electron transport or in the energy conversion are presented in Figure 1.

The matrix of thylakoid membranes is composed of specific lipid classes (monogalactosyl-diacylglycerol - MGDG, digalactosyl-diacylglycerol - DGDG, sulfoquinosyl-diacylglycerol - SQDQ and phosphatidyl-glycerol - PG) forming the bulk lipid phase, interface with protein complexes and filling their cavities (Garab et al. 2016). Although for each of the thylakoid lipids a specific role in the assembly and functioning of both photosystems in thylakoid membrane has been identified (Pali et al. 2003), MGDG, the most abundant thylakoid lipid, constituting about half of total thylakoid lipids in most higher plants, has a specially complex role. Although, MGDG belongs to the class of non-bilayer (or non-lamella-forming) lipids, which do not self-assemble into bilayers in aqueous media (Williams 1998), it has been shown that the non-bilayer lipid MGDG can be forced into a bilayer structure upon its association with the most abundant membrane protein, the light-harvesting complex of PSII (LHCII) (Simidjiev et al. 1998; Simidjiev et al. 2000). Role of MGDG in the operation of the xanthophyll cycle has been well established showing that the functioning of violaxanthin de-epoxidase (VDE) requires the presence of MGDG for its activity (Yamamoto and Higashi 1978) and the presence of non-bilayer lipid phases (Latowski et al. 2004). MGDG form a lipid shield around LHCII and free xanthophylls and thus avoid the formation of aggregates of

hydrophobic xanthophyll cycle pigments in an aqueous medium so that they become accessible to the VDE.

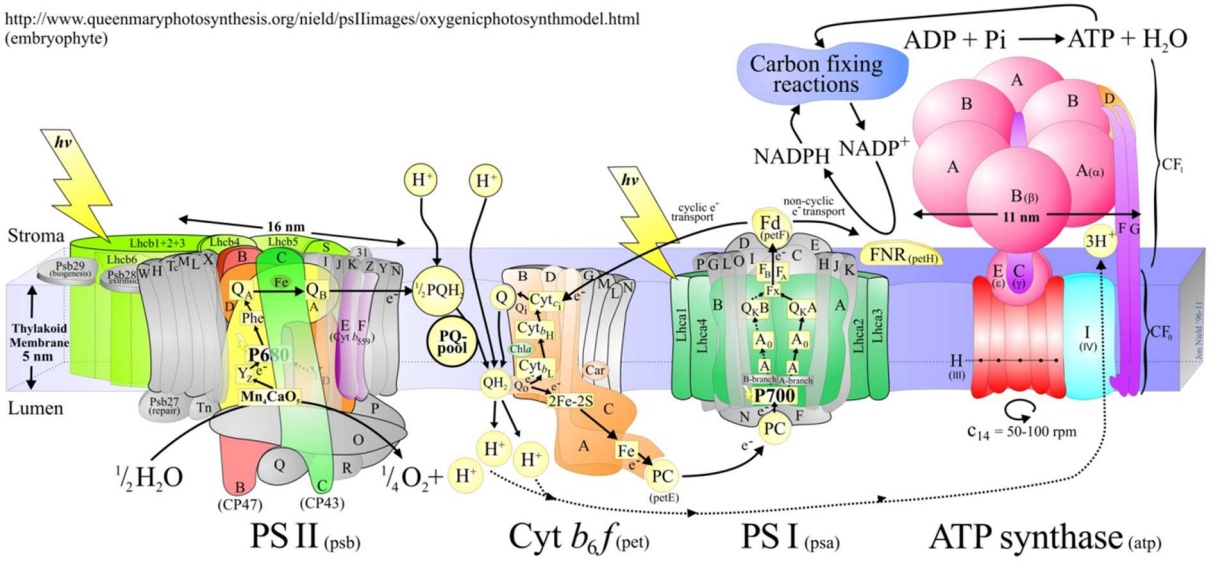

Fig. 1: *Schematic models for the major protein complexes involved in photosynthesis (adopted from (Nield 2011)). In higher plants (eukaryotes), photosynthetic and carbon fixation reactions are housed in the chloroplasts. The so-called light reactions of photosynthesis take place in the thylakoid membranes of chloroplasts and are driven by light captured in the light-harvesting complexes bound to PSI and PSII (LHCI (Lhca), LHCII (Lhcb), respectively). Linear electron transport involves electrons (e^-) being derived from the splitting of water, by PSII, and sequentially passed along the photosynthetic electron transport chain by plastoquinone (PQ), cytochrome b_6f ($Cytb_6f$), plastocyanin (PC), Photosystem I (PSI) and PSI-bound ferredoxin (Fd), before being used for NADPH production in ferredoxin–$NADP^+$ oxido-reductase (not shown) in the stromal matrix (stroma). From this splitting of water (water oxidation), and from the Q-cycle operating around $Cytb_6f$, protons (H^+) accumulate in the thylakoid's lumenal space (lumen), thereby generating a gradient which provides proton motive force for ATP production via chloroplastic ATP synthase (CF_oF_1 ATP synthase). Under conditions causing the phenomenon of cyclic electron transport that operates around PSI, only PSI is active, the energy of the absorbed light is used for increasing the proton gradient, and thus for ATP production. The products of the light reactions, ATP and NADPH, are consumed during carbon dioxide (CO_2) fixation, where a separate enzyme, RuBisCO, is responsible for incorporating CO_2 into Ribulose bisphosphate (RuBP), ultimately forming sugar phosphates*

On the other hand, DGDG plays an important role in the stability and activity of PSII and PSI and also in the stabilization of LHCII trimers (Kalisch et al. 2016). Therefore, changes in the MGDG/DGDG ratio affect the membrane organization and the protein folding and insertion, which exert an impact on the photosynthetic performance. Variations in the MGDG/DGDG ratios influence also the structural flexibility of the thylakoid membranes, as demonstrated by the significant alterations in the organization of the thylakoid membranes and their thermal stability (Krumova et al. 2010).

1.2.1. The structure of thylakoid membrane

Differentiation of the thylakoid membrane into stacked and unstacked regions (forming grana and stromal lamellae, respectively) is known for decades from transmission electron microscopy studies (Fig. 2A). In recent years, structural complexity of thylakoids become clear using more advanced microscopic methods. The grana exist as cylindrical stacks of flattened membrane discs closely appressed at their stromal faces and interconnected by the fret-like stromal lamellae (Austin and Staehelin 2011). The stromal lamellae thus provide contact multiple grana layers in the same stack. In addition to the stromal lamellae non-appressed membranes form two other regions, the non-appressed grana end membranes at the top and bottom of each stack and the junctional slits which connect the grana and stromal lamellae (Ruban and Johnson 2015).

In plants, the distribution of the different protein complexes is not homogenous (Fig. 2B). PSII is mainly found in the granum while PSI and the ATP synthase only in the stroma thylakoids and the end membranes of grana, grana margins. The cytochrome b_6/f complex and the trimeric major LHCII, which serves both PSI and PSII, are found in both, grana and stroma thylakoids (Dekker and Boekema 2005). This lateral segregation of the protein complexes allows the formation of the different structure of the stroma and granum thylakoids. The trimeric LHCII actively participate in the close packing of granum thylakoids (Garab and Mustardy 1999).

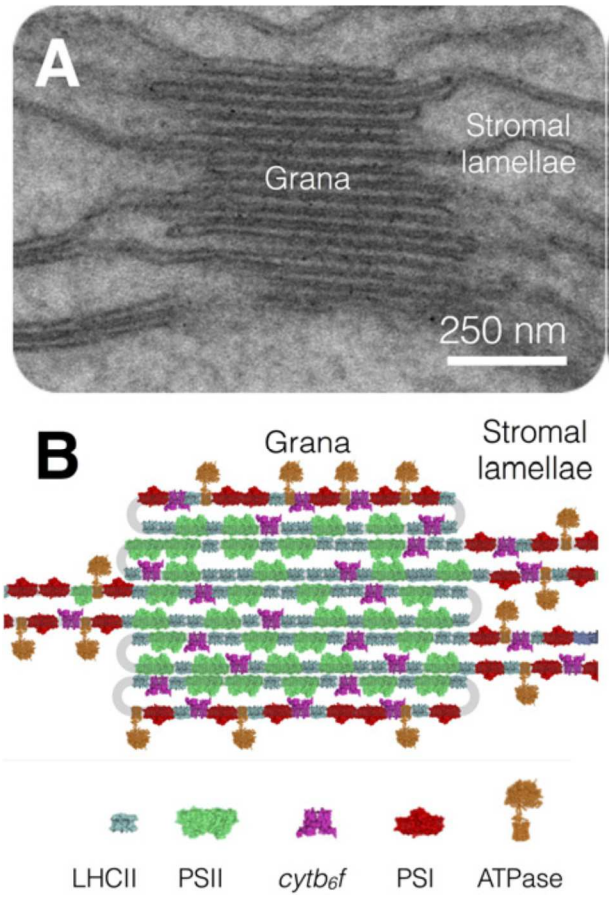

Fig. 2: *Lateral heterogeneity in thylakoid membrane organization (adopted from (Johnson 2016)). (A) Electron micrograph of the thylakoid membrane showing stacked grana and unstacked stromal lamellae regions. (B) Model showing the distribution of the major complexes of photosynthetic electron and proton transfer between the stacked grana and unstacked stromal lamellae regions.*

The biological advantage of the structural and functional segregation of the two different thylakoid membranes, a unique feature for higher plants and green algae (Olive and Vallon 1991), is a widely investigated topic in photosynthesis. In the case of cyanobacterium, thylakoid membranes lacking lateral segregation of the protein complexes do not form grana structures. The evolutionary advantage of thylakoid membrane stacking is considered to be a higher efficiency of electron transport by preventing the fast energy trap PSI from outflowing excitation energy from the slower trap PSII, a phenomenon known as spillover (Johnson 2016). Another possible advantage of membrane stacking in thylakoids may be the segregation of the linear and cyclic electron transfer pathways, which might otherwise compete to reduce plastoquinone (Johnson 2016). Moreover, this lateral heterogeneity enables the flexibility in dynamic redistribution of the protein components,

such that the plant can perform vital self-protective and repair processes that enable rapid responses to its environment (Ruban and Johnson 2015).

1.1. Photosynthetic light-harvesting

Photosynthesis begins with the absorption of light by pigment molecules located in the thylakoid membrane. In plants and green algae most of the light is absorbed by the photosynthetic pigments chlorophyll (Chl) *a* and *b* owning remarkable physicochemical properties allowing efficient light harvesting and ultrafast excitation energy transfer among antenna Chls. Thus energy from sunlight is captured by pigment-protein complexes (PPCs) that subsequently deliver it to reaction centres during 10–100 ps with the highest known quantum and thermodynamic efficiencies (Scholes et al. 2011). In other words, light harvesting count on the process of electronic energy transfer moving electronic excitation energy stored for a very short time (nanoseconds) by the excited states of molecules within highly organized networks of light absorbing chromophores to a target chromophore or trap (Olaya-Castro and Scholes 2011). Timescale of this process limits the size of the chromophore arrays connected to the reactive centre on so-called exciton diffusion length, i.e. how far excitation energy can migrate. The excitation energy flow to the reaction centres thus can be regulated by very fine structural changes in antennas. On this basis, photoprotective mechanisms switch from an arrangement of chromophores that optimizes trapping via energy transfer through the antenna to arrangement that works inefficiently due to excitation traps quenching the excited-states of Chls.

1.1.1. Photosynthetic pigments

The first step of the photosynthetic processes is the absorption of a photon by a photosynthetic pigment. As a result of evolution nature has selected a relatively small group of pigments to serve in the photosynthetic antenna complexes: Chls, carotenoids (Cars) and phycobilins. From them only Chl in plants and algae and bacteriochlorophyll in photosynthetic bacteria serve in photochemically active reaction centre. The antenna pigments are more versatile. The photosynthetic antenna pigments of plants include Chl *a* and *b* and several types of Cars including oxygenated Cars, called xanthophylls.

The majority of photosynthesizing organisms contain Chl *a,* which plays a central role in the photochemical energy conversion. Chl *a* is a magnesium containing chlorin ring, to

which a phytol chain is esterified at pyrrole ring IV (Fig. 3). Chl *b* is the main accessory Chl in higher plants and green algae. Chl *b* differs only in one functional group from Chl *a* (Fig. 3), which confers a slightly lower lipophylic character and shifts of the major absorption bands in the red and blue towards the green.

Higher plant antenna xanthophylls, lutein, neoxanthin, violaxanthin and zeaxanthin are the most common xanthophylls on our planet (Fig. 3). Xanthophylls absorb light in spectral region in which the sun irradiates maximally and transfer excitation energy to Chls. Xanthophylls also contribute to regulation of energy flow within the photosynthetic apparatus and to protection of photosynthetic apparatus against photoinduced damage caused by excess light absorption.

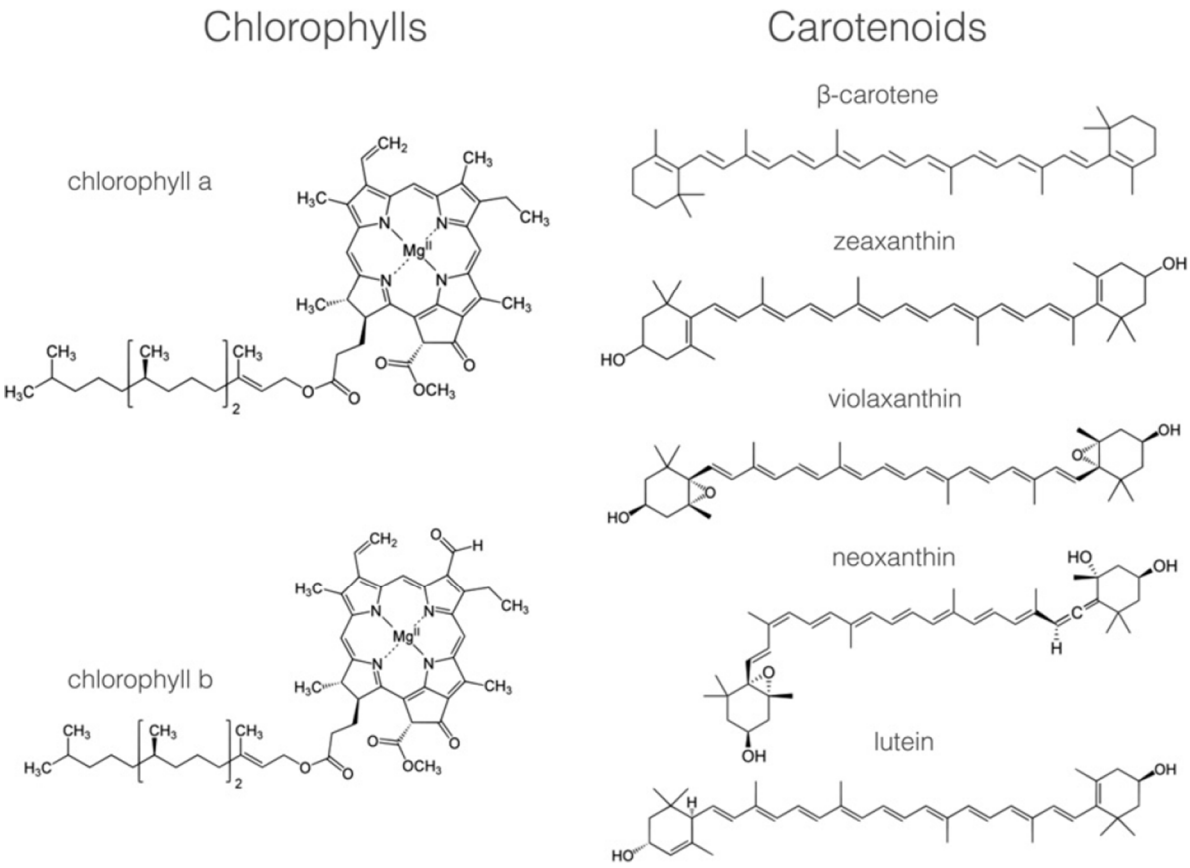

Fig. 3: *Major photosynthetic pigments in plants (adopted from (Johnson 2016)). The chemical structures of the chlorophyll and carotenoid pigments present in the thylakoid membrane. Note the presence of conjugated systems of carbon–carbon double bonds that is responsible for light absorption in the specific spectral regions.*

1.1.2. The structure of the individual light-harvesting complexes

Most of photosynthetic organisms possess an antenna system that increases optical cross-section of the photosystems. During the evolution of photosynthesis in eukaryotes, the membrane-associated phycobilisomes of the cyanobacteria have been substituted by membrane-integral pigment binding complexes, Light-harvesting complexes (Lhc) (Ballottari et al. 2012). All Lhc proteins are encoded by nuclear genes, are homologous to each other and share a similar structure. Although all Lhc antennas have three helix membrane-spanning regions and coordinate Chl *a*, Chl *b* and Car molecules, each Lhc has a specific pigment content which confers them distinct spectroscopic properties (Caffarri et al. 2014). Accordingly to the nomenclature for core subunits, PPCs of PSII and PSI are named Lhcb and Lhca, respectively.

The antenna complexes of PSII from higher plants are composed of 6 different Lhcb proteins Lhcb1-6. Subunits Lhcb1, Lhcb2 and Lhcb3 form heterotrimer of the major antenna complex of PSII, LHCII. Subunits Lhcb4, Lhcb5 and Lhcb6 occur only as monomers and are also commonly named as CP29, CP26 and CP24, respectively (based on the apparent molecular weight on a SDS-PAGE obtained at the time of the first characterization). The structure of a monomeric subunit of trimeric LHCII (Liu et al. 2004) is shown in Fig 4. Each monomer coordinates 8 Chls *a*, 4 Chls *b* and four xanthophylls (one N, two L and one V). The two L are located at sites L1 and L2 in the center of the molecule while N and V are located at the periphery in sites N1 and V1, respectively (Croce et al. 1999; Caffarri et al. 2001; Ruban and Horton 1999). The average distance between the Chls is around 10 A°, which leads to excitonic interactions between the pigments, resulting in fast energy transfer within the complex.

Crystal structure of CP29 at 2.8 Å resolution indicates that this complex binds 3 Cars and 13 Chls with Chls *a*/*b* ratio about 1.9 (Pan et al. 2011). CP29 differs from LHCII subunits in absence of a peripheral V1 site and also in the position of some Chls binding sites. The structure of CP26 is not available, nevertheless, biochemical data and sequence homology suggest that this complex has a similar amount of Chls (13-14 Chls) as CP29 and a Chls *a*/*b* ratio approximately 2 (Dall'Osto et al. 2005). CP24 differs from all the other PSII monomeric antennas. Evolution of this subunit is considered as a more recent, because it is found only in the land plant lineage while CP26, CP29 and LHCII are present in green algae as well (Koziol

et al. 2007). Moreover, it has unusual pigment binding properties due to the lowest Chl *a*/*b* ratio approximately 1, binding only 10-11 Chls and 2 Cars in site L1 and L2 (Passarini et al. 2009).

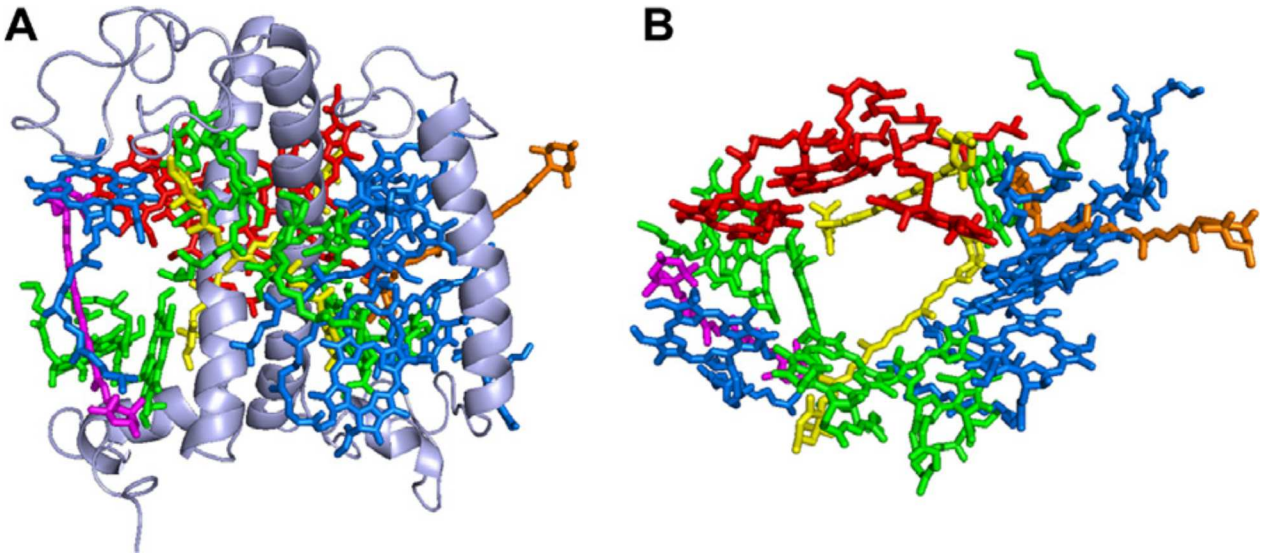

Fig. 4: *Model of the structure of LHCII (adopted from (Liu et al. 2004))(A) membrane view of the pigment-protein complex. (B) top view only showing the pigment organization. The protein is in light blue, Chls a in green, Chls b in blue, Chls 610-611-612 in red. Luteins, yellow; neoxanthin, orange; violaxanthin, magenta.*

The structural and pigment-binding characteristics of the individual Lhca complexes were always less elucidated than for the Lhcb complexes, mainly due the difficulties of purifying intact monomeric complexes. In plants, the absorption cross section of the PSI core is increased by four LHCI subunits Lhca1-4, which form a belt on one side of the PSI core (Ben-Shem et al. 2003) and bind 57 Chls and 13 Cars as revealed 2.8 Å resolution of Lhca from pea (Qin et al. 2015). These high-resolution structures are necessary to understand the molecular basis of light harvesting in Lhca, especially due to the fact that the Lhca contain several Chls with redshifted spectra (called red forms) which extend the light-harvesting capacity of PSI to the far-red region (van Amerongen and Croce 2013).

1.3.3. The structure and function of the photosystem II

The basic role of the PSII is to oxidize water molecules on the lumenal side and to reduce quinones at the stromal side of the thylakoid membrane using the energy of absorbed photons. During the last two decades electron and X-ray crystallography studies have provided more and more detailed information about this multisubunit protein complex

achieving already a resolution of 1.9 Å (Guskov et al. 2009; Loll et al. 2005; Umena et al. 2011). The structure of the PSII core from higher plants is not available at present but it is supposed to be very similar to that of cyanobacteria. The PSII core is composed of four large integral membrane proteins (the products of genes PsbA–PsbD) containing 22 membrane-spanning helices and 14 additional transmembrane helices are formed by a number of small subunits. The products of genes PsbA and PsbD (D1 and D2 proteins, respectively) form a heterodimer which coordinates 6 Chls, 2 pheophytins and 2 plastoquinones (Q_A and Q_B) that participate in the electron transport chain. These complexes together with the two $cytb_{559}$ proteins form complex of reaction center (RC) (Fig. 5). PsbB and PsbC encode for the two inner antenna complexes (core antenna proteins CP47 and CP43) located on the side of D2 and D1, respectively (Fig. 5). Core antenna proteins coordinate 29 Chl *a* (CP47: 16; CP43: 13) and 11-12 β-carotene molecules (Umena et al. 2011).

During the last decade, development of single particle cryo-electron microscopy and cryo-electron tomography enabled improvement of knowledge on the structure of external antenna system of PSII and the architecture of thylakoid membranes (Croce and van Amerongen 2011; Kouřil et al. 2012; Mustardy et al. 2008; van Amerongen and Croce 2013). A variable number of LHCII proteins can be bound to dimeric PSII core PPCs forming different PSII–LHCII supercomplexes (Dekker and Boekema 2005). The largest supercomplex purified so far named C2S2M2 (Caffarri et al. 2009) consist of dimeric core (C2) associated with 2 copies of each of the monomeric complexes CP29 (lhcb4), CP26 (lhcb5) and CP24 (lhcb6) and 4 LHCII trimers (lhcb1-3) (Boekema et al. 1999) (Fig. 5). Two LHCII trimers firmly bound on the CP26 sides (S-trimers) are composed of the products of the Lhcb1 and Lhcb2 genes (Hankamer et al. 2001), while the next two ones, moderately bound on the side of CP29 and CP24 (M-trimers), contain also the product of the Lhcb3 gene (Boekema et al. 1999). Except LHCII trimers contained in the PSII-LHCII supercomplexes there are also extra LHCII trimers that are either functionally connected to PSII (van Amerongen and Croce 2013) or located in the LHCII-only domains (Boekema et al. 2000).

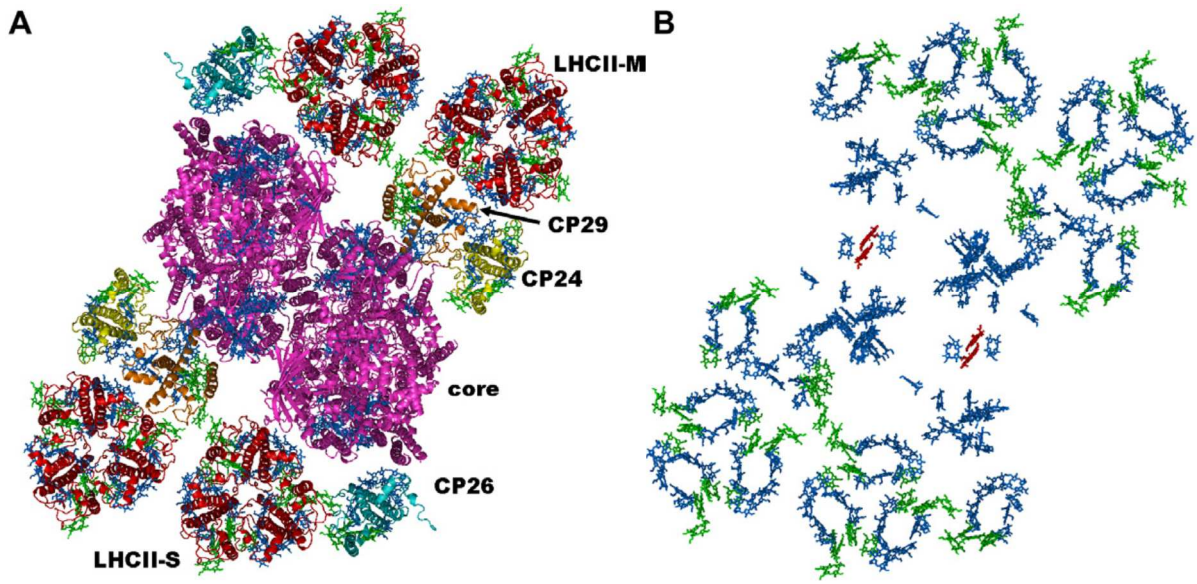

Fig. 5: *Model of the PSII supercomplex C2S2M2 from higher plants (adopted from (Croce and van Amerongen 2011)). The model has been assembled based on (Caffarri et al. 2009) using the crystal structures of the cyanobacterial PSII core (Guskov et al. 2009) and LHCII trimer (Liu et al. 2004). (A) Model showing the protein organization. For the monomeric antennas, the structure of a monomeric LHCII has been used. Proteins of the core, magenta; LHCII, red; CP24, yellow; CP29, orange; CP26, cyan. (B) model shoring only the Chls organization. Chls a, green; Chls b, blue. The "P680" Chls are in red.*

1.1.3. The structure and organization of the photosystem I

The organization of the Lhc protein around the photosystems is different between PSII and PSI. Crystallographic model and single particle analysis revealed a single layer of Lhca proteins bound on one side of the core complex of plant PSI in order of Lhca1, Lhca4, Lhca2, Lhca3 (Fig. 6). Subunit PsaG is considered important for the anchoring of the Lhca antenna proteins to the PSI core (Ben-Shem et al. 2003).

In all conditions in which PSII is preferentially excited, part of the LHCII population moves to PSI to increase its antenna size, forming the PSI-LHCI-LHCII supercomplex (Lemeille and Rochaix 2010). The LHCII trimer binds on the opposite side of the Lhca's interacting with the PsaH subunit (Croce and van Amerongen 2013; Kouřil et al. 2005). However, this complex is very sensitive to most non-ionic detergents, but it is stable in digitonin (Kouřil et al. 2005). Excitation energy transfer from LHCII to PSI core is extremely fast, making LHCII a perfect light harvester for the system (Wientjes et al. 2013a).

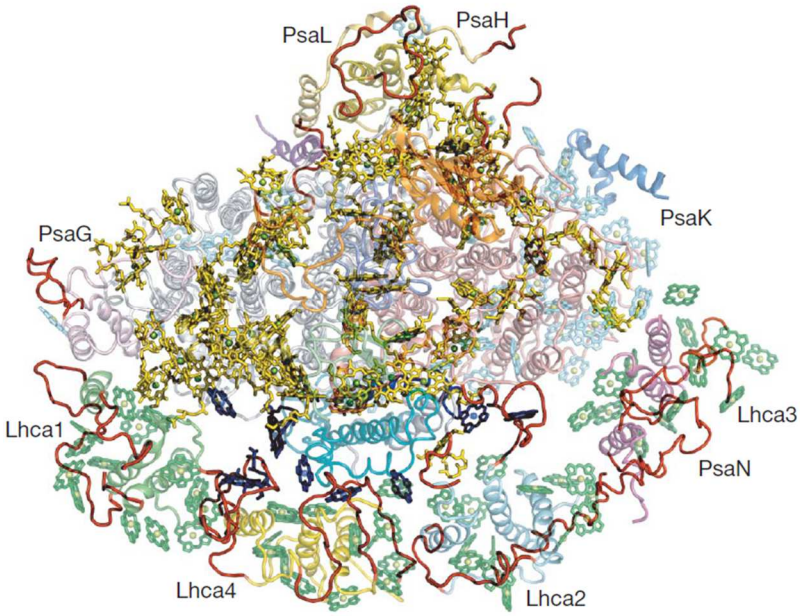

Fig. 6: *The structural model of plant photosystem I at 3.4A° resolution (adopted from (Amunts et al. 2007). View from the stroma of the structure of plant PSI. Chlorophylls with detected phytyl side chains, revealing the orientation of the Qx and Qy transition dipole moments, are yellow. The rest of the reaction centre chlorophylls are cyan, gap chlorophylls are blue and chlorophylls of LHCI are green. The positions of PsaG, H, K, L and N, as well as the various LHCI monomers, are indicated. Each individual subunit is coloured differently.*

1.2. Photoprotection mechanisms of the photosynthetic apparatus against photo-oxidative damage

Light reactions of photosynthesis are inevitably associated with production of potentially harmful reactive oxygen species (ROS). The oxidative stress is increased by unfavourable conditions either directly by excess photosynthetically active radiation, UV radiation and high temperatures, or indirectly by temperatures below optimum, drought or salinity. In most cases particularly PSII is a target of photooxidative damage (Pospíšil 2012; Ruban et al. 2012; Vass 2012).

Plants have evolved a comprehensive set of protective mechanisms that determine the resulting resistance and/or acclimation strategy to changing environmental conditions. Plants are capable to respond at different levels of organization: for example at the tissue level via optical screening by epidermal phenolics (Agati et al. 2011; Merzlyak et al. 2008; Štroch et al. 2008b), at the cellular level by chloroplast movements (Banas et al. 2012; Nauš

et al. 2008; Wada 2013) and regulation of chloroplast number (Oguchi et al. 2003), or at the molecular level by regulation of protein (Bailey et al. 2001; Garab 2014; Timperio et al. 2012) and lipid (Harwood 1998; Lepetit et al. 2012) composition of the thylakoid membranes. All these processes with very different dynamics on the timescale from seconds to weeks lead to lowering of ROS formation or the detoxification of already formed ROS (for example by accumulation of the direct antioxidants such as low-molecular compounds such as phenolics and Cars).

Among the prompt regulatory responses (on the timescale from seconds to minutes), which helps plants and algae to survive under rapidly changing light conditions, the so-called non-photochemical quenching of Chl *a* fluorescence (NPQ) (Demmig-Adams et al. 2014; Goss and Lepetit 2015; Niyogi and Truong 2013; Ruban 2016; Ruban et al. 2012) is a crucial one (Fig. 7). Mechanisms of NPQ processes that turn on and off rapidly (often called qE) differs in green algae, mosses and plants (Goss and Lepetit 2015; Niyogi and Truong 2013). According to a current concept the PsbS protein belonging to the family of LHC is important for NPQ in higher plants (Croce 2015). In lower plants (e.g. green algae, mosses) the stress-related LHC proteins (Lhcsr) overtake the role of PsbS in NPQ activation (Goss and Lepetit 2015; Niyogi and Truong 2013). In higher plants, qE process is triggered by acidification of the thylakoid lumen, which causes protonation of PsbS (Croce 2015) and its monomerization (Correa-Galvis et al. 2016). Moreover, low lumenal pH activates VDE converting violaxanthin into zeaxanthin via antheraxanthin (Jahns and Holzwarth 2012). Resulting structural rearrangement of PSII is responsible for functional disconnection of part of LHCII from PSII core and formation of quenching centres within detached major LHCII (quenching site Q1) or in the remaining PSII antenna (quenching site Q2) (Jahns and Holzwarth 2012; Johnson and Ruban 2011). Whether LHCII aggregates in the light adapted state contains M trimers only or also bind CP24 is still under debate.

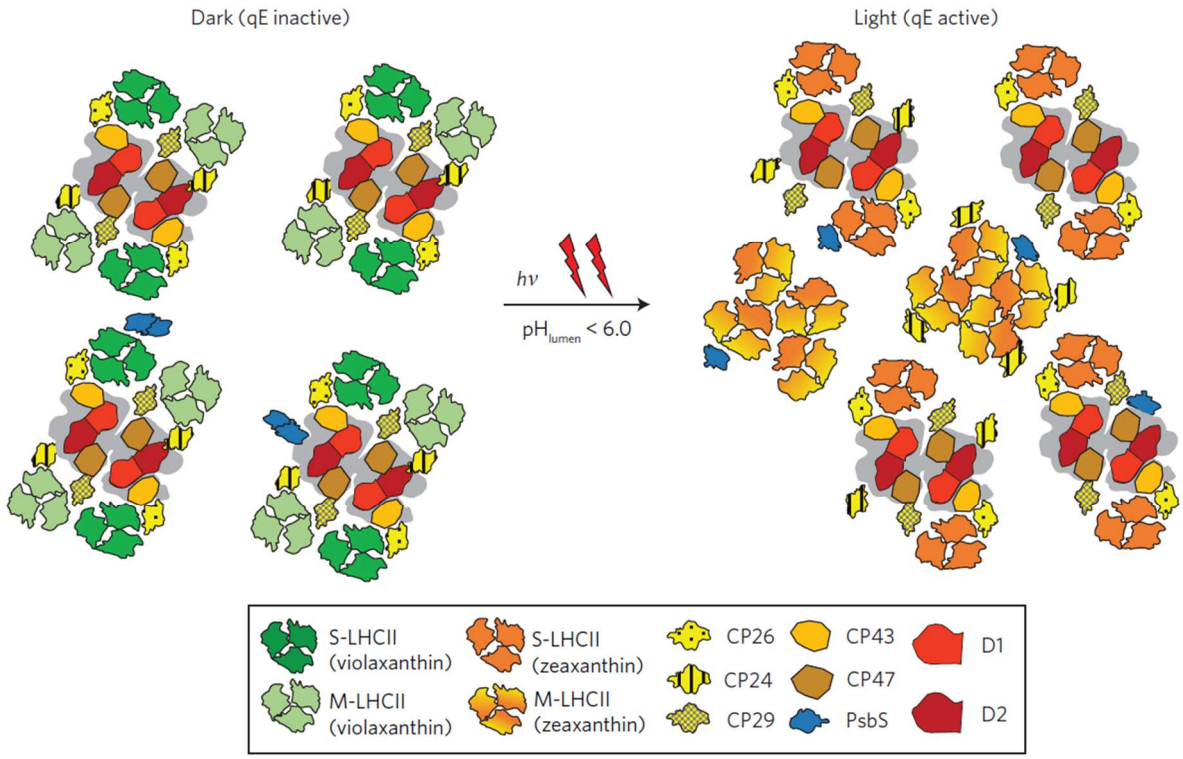

Fig. 7: *Model for PsbS-induced conformational changes in PSII–LHCII (adopted from (Correa-Galvis et al. 2016)). In the dark-adapted state, dimeric PsbS is supposed to interact with PSII–LHCII supercomplexes predominantly through the S LHCII trimers and probably also with the RC core (CP47/D2/CP43). Acidification of the lumen drives the monomerization of PsbS, which induces the detachment of trimeric LHCII from the PSII core through interaction of PsbS with LHCII M trimers. These PsbS induced conformational changes are accompanied by the activation of quenching at two sites: one in the detached and aggregated LHCII complexes (quenching site Q1) and one in the antenna proteins that remain bound to PSII (quenching site Q2). Two possible scenarios for LHCII aggregation in the light adapted state are shown, one containing M trimers only and the other also binding CP24. Other PsbS monomers might also interact through CP47 with the RC core. Green/grey colour of LHCII proteins indicates violaxanthin binding, orange/yellow colour zeaxanthin binding.*

Upon exposure to excess light, several other mechanisms are attributed to NPQ, except the most rapid component qE operating in the range of seconds to minutes. Slower component reflects the enhancement of energy dissipation due to the accumulation of zeaxanthin (qZ) through the xanthophyll cycle, which develops in the time range from 10 to 30 min at moderate light (ML)(similarly as qE). Under very high light (HL) at longer illumination time (>30 min) dominates photoinhibition quenching (qI) (Jahns and Holzwarth

2012). Also light-avoidance movements of the chloroplasts within the plant cell significantly contribute to slower component of NPQ (Dall'Osto et al. 2014). Under low light (LL), the state transition component of NPQ operates in the timeframe of a few minutes and reflects the dynamic allocation of part of LHCII either to PSII or to PSI (qT) (Goldschmidt-Clermont and Bassi 2015; Minagawa 2011; Tikkanen et al. 2011). State transitions operate particularly under LL and are replaced by other mechanisms such as qE under ML and HL. In higher plants, state transitions do not significantly contribute to NPQ, in contrast to the situation in green algae (Jahns and Holzwarth 2012).

1.2.1. Acclimation of photosynthetic apparatus to different light intensity

Regulatory responses of the photosynthetic apparatus on the timescale of days to weeks to natural light regimes, so-called long-term acclimation, rely mostly on two types of adjustment, i.e. modulation of the relative amount of LHCII and changes in the PSI/PSII ratio adjusting the balance of excitation of both photosystems. A number of acclimation responses have been described for various plant species grown under different light conditions.

At the turn of the millennium, particularly biochemical studies on amount of accumulated proteins and photosynthetic pigments were performed. Significant increase in the amount of cytochrome b_6f complex and the activity of ATP synthase has been reported for several species grown under HL (de la Torre and Burkey 1990). Considerably elevated levels of PSII reaction centres (RCs) in response to HL have been demonstrated for *Arabidopsis* (Bailey et al. 2001; Walters et al. 1999), pea (Evans 1987; Leong and Anderson 1984), and mustard (Wild et al. 1986). On the contrary, only slightly enhanced amounts of PSI RCs at HL were reported for *Arabidopsis* (Bailey et al. 2001) and pea (Leong and Anderson 1984), but a dramatic increase in PSI content was observed in thylakoid membranes of plants grown under very LL (Bailey et al. 2001). It has been known for decades that the ratio of LHCII to PSII is decreased under HL growth conditions (Anderson et al. 1995). More recently, changes in LHCII protein composition (Bailey et al. 2001; Kouřil et al. 2013) or even in their individual isoforms (Albanese et al. 2016; Timperio et al. 2012) were described for *Arabidopsis* acclimated to different light intensities. Reduction of LHCII size in HL plants has often been assessed indirectly by increased ratio of Chl *a*/*b*, for example in barley (de la Torre and Burkey 1990; Kurasová et al. 2002; Štroch et al. 2004), *Arabidopsis*

(Bailey et al. 2001; Kouřil et al. 2013), spinach (Lindahl et al. 1995), and pea (Leong and Anderson 1984). Furthermore, diminution of functional antenna size of PSII in HL-grown barley as compared with LL plants has been roughly assessed from the reduced ratio of the main Chl *b* and Chl *a* excitation bands in the Soret region of the 77 K fluorescence excitation spectra measured on leaf segments (Čajánek et al. 2002; Štroch et al. 2004) and by advanced methods based on Chl *a* fluorescence (Bielczynski et al. 2016; Wientjes et al. 2013b). Regarding changes in the composition of photosynthetic pigments, the Cars/Chls ratio increased in plants grown at HL conditions as well that was particularly due to relative increase VAZ pool (Bielczynski et al. 2016; Kurasová et al. 2002; Štroch et al. 2004). In consequence, the acclimation to HL results in enhanced capacity of NPQ, and enhanced convertibility of violaxanthin to zeaxanthin (Bugos et al. 1999; Demmig-Adams 1998; Kurasová et al. 2002; Štroch et al. 2004). Part of VAZ pool pigments (bigger part may be expected for HL plants in comparison with LL ones) is formed by non-protein bound xanthophylls in the lipid phase of the thylakoid membrane. Z in the lipid phase of the thylakoid membrane is linked to an important photoprotective function of Z independent from its role in qE (Havaux and Niyogi 1999) and serves as antioxidant, additive to the photoprotective function of tocopherol (Havaux et al. 2007).

In the last decade, the structural response of PSII-LHCII supercomplexes in the thylakoid membranes after acclimation to different light intensity has been characterized (Albanese et al. 2016; Bielczynski et al. 2016; Kouřil et al. 2013). Reduction of LHCII size under HL conditions was related to the decreased amount of large C2S2M2 PSII-LHCII supercomplexes, while acclimation to very LL had no influence on large supercomplexes in comparison with ML (Albanese et al. 2016; Kouřil et al. 2013). The structural modification of PSII supercomplexes at HL is accompanied by a specific reduction of antenna protein subunits Lhcb3, Lhcb6 and M-LHCII trimers bound to the PSII cores (Albanese et al. 2016; Kouřil et al. 2013), while the Lhcb4.3 isoform increased in PSII–LHCII supercomplex response to HL intensities. These results suggest that the Lhcb3, Lhcb4.3 and Lhcb6 antenna subunits are major players in modulation of the PSII antenna size upon long-term acclimation to HL. On the other hand, the amount of the “extra” LHCII was increased in LL membranes, whereas in HL membranes their amount remained at the same level as in ML plants. Furthermore, occurrence of semi-crystalline PSII arrays was strongly reduced in HL plants as compared to LL and ML plants, probably due to the increased structural heterogeneity of

PSII supercomplexes. Kouřil et al. (2013) found that the C2S2M2 supercomplexes in semi-crystalline arrays in LL plants were more densely packed than in HL or ML plants and suggested that the spacing between supercomplexes is important for efficient energy transfer between PSII under light-limiting conditions.

1.4.2. Thermal stability of photosystem II

As mentioned above, temperatures out of the range of optimum increase oxidative stress either directly such as in the case of high temperature stresses, or indirectly by cold stresses. Moreover, an elevated temperature can cause direct negative effects on photosynthetic assimilation of carbon dioxide. PSII is considered to be the most heat sensitive component of photosynthetic apparatus (Allakhverdiev et al. 2008; Zhang and Sharkey 2009). At the temperature from 42 °C to 48 °C the PSII donor side undergoes a disruption due to loss of oxygen evolution complex (Cramer et al. 1981; DelasRivas and Barber 1997). PSII acceptor side becomes gradually inactivated at temperatures above 40 °C by changed midpoint potential of the primary quinone acceptor Q_A (Pospíšil and Tyystjarvi 1999). The increasing permeability to protons can lead to dissipation of ΔpH and finally to loss of the thylakoid membranes integrity resulting in inability to maintain transmembrane electrochemical potential (Zhang et al. 2009). The disassembly of the chiral macrodomains occurs in the temperature range of 45 - 55 °C (Krumova et al. 2010; Varkonyi et al. 2009). At a temperature around 60 °C the PSII core denatures (Shi et al. 1998) and trimeric LHCII dissociate to its monomeric form (Dobrikova et al. 2003). Heat denaturation of LHCII monomers occurs at temperature between 70–80 °C (Lípová et al. 2010; Yang et al. 2006). The more stable PSI undergoes the major conformation transition at 60 °C to 70 °C, which is accompanied by the energetic disconnection of LHCI from PSI core, that denatures in a wide temperature interval 70–90 °C (Hu et al. 2004; Lípová et al. 2010). It should be noted that the mentioned denaturation temperatures of individual PPCs can be influenced by the type of temperature treatment or heating rate during linear heating (Krumova et al. 2005).

The analysis of temperature dependence of Chl *a* fluorescence parameters *in vivo* documented considerably different thermal stability of PSII function among plants species (Knight and Ackerly 2002), genotypes (Brestič et al. 2012) and its seasonal variations (Brestič et al. 2012; Froux et al. 2004). It has been proved that increased temperatures lead, in addition to adjustment of numerous photosynthetic processes and structures, to a relatively

fast increase of PSII thermal stability (Brestič et al. 2012; Ghouil et al. 2003). An improved thermal stability of PSII was also observed as a result of acclimation to other stress factors, e.g. drought (Epron 1997; Lu and Zhang 1999) and salinity (Chen et al. 2004; Wen et al. 2005). However, knowledge on the mechanisms that are responsible for the mentioned variability of PSII sensitivity to heat stress is still not complete and controversies remain.

The thermal stability of PSII can be increased by stable forms of PSII proteins as observed in the case of double mutation in PSII reaction centre protein D1 of mesophilic cyanobacterium (Dinamarca et al. 2011). More often the different thermal stability of PSII is attributed to lipid composition and/or the fatty acid composition of thylakoid membrane. Under conditions of heat stress changes in the ratio between the two major lipids, monogalactosyldiacylglycerol (MGDG) and digalactosyldiacylglycerol (DGDG) occur (Kalisch et al. 2016; Williams 1994), the chain length and the number of double bonds in FAs is affected (Harwood 1998). It is generally accepted that the thylakoid membrane lipids in higher plants respond to prolonged high temperature exposure with increased degree of fatty acid saturation (Gombos et al. 1994; Makarenko et al. 2014). On the contrary, studies on cyanobacterium Synechocystis suggest that thermal stability of PPCs does not depend on the lipid composition of the membranes (Laczko-Dobos and Szalontai 2009) or that lipid saturation *per se* is not a regulator of thermal stability (Nanjo et al. 2010). DGDG-deficient *Arabidopsis* mutant revealed lowered thermal stability of macrodomain organization of PPC in thylakoid membranes compared to wild type, and thus proved direct role of DGDG in the stabilization of thylakoid membranes at elevated temperatures (Krumova et al. 2010). Similarly, importance of DGDG in the enhanced thermal stability of LHCII trimers incorporated into liposomes was confirmed (Zhang et al. 2008). Heat shock proteins produced as a result of stress are important for protecting cells against high temperature and other stresses, as well as conferred heat tolerance to the photosynthetic electron transport chain in isolated chloroplasts (Allakhverdiev et al. 2008; Mathur et al. 2014).

1.5. Spectroscopy techniques for macro-organization of pigment-protein complexes in the thylakoid membrane

Low temperature steady-state Chl *a* fluorescence is one of the non-invasive tools to study the structural organization of thylakoids. This simple spectroscopic method is highly sensitive to the energy transfer between PPCs and to the aggregation of LHCII as well

(Horton et al. 1996). The 77 K steady-state emission spectrum of higher plant thylakoid membranes is characterized by three clearly recognizable bands, two of which, at wavelengths of 685 and 695 nm, are attributed to PSII, and third band at 735 nm to PSI (Van Grondelle et al. 1994). More detailed fluorescence studies have shown that the fluorescence bands at 685 nm (F685) and 695 nm (F695) correspond to two different PPCs of PSII, the core antenna complexes CP43 and CP47, respectively (Dekker et al. 1995). The shoulder at 680 nm (F680) was ascribed to the LHCII and presence of LHCII aggregates leads to the appearance of the major emission band at 700 nm (F700) (Ruban et al. 1997). Fluorescence emission of PSI consists of at least two bands, emitting mainly at 720 nm (F720) and at 735 nm (F735) attributed to PS I core and LHCI, respectively (Van Grondelle et al. 1994).

The presence of the strong pigment–pigment interactions in photosynthetic membranes and isolated PPCs enables use of non-invasive techniques of polarization spectroscopy, such as linear dichroism and circular dichroism (CD). CD spectroscopy is a non-invasive method suitable for investigation of pigment-pigment interaction even in as complex systems as intact cells *in vivo*. CD is the absorption difference of the left and right circularly polarized light at a given wavelength. CD signals originate from the chirality of the molecules or from asymmetric interactions of the molecules. In photosynthetic apparatus containing highly organized system of Chls, CD signals originate from molecular systems of different complexity (Garab and van Amerongen 2009).

Chiral molecules exhibit optical activity, called intrinsic CD. Chls as a planar ring-structured molecules have electric and magnetic dipole moments nearly perpendicular to each other, which results in weak CD signals. The band shapes of the intrinsic CD are identical with those of the absorption bands, their sign can be either positive or negative determining the handedness of the molecule. On grounds of symmetry of the pigment molecules the intrinsic CD signals in photosynthetic systems are weak, i.e. some 10^{-5} intensities per absorbance unit (Fig. 8).

In the case of excitonic interaction of two or more pigment molecules a conservative band structure can be observed. That means that positive and negative CD bands can be observed, the areas of which gives zero in the energy spectrum (Devoe 1965). This is called exciton-coupled CD signal or excitonic CD. In photosynthetic systems the excitonic CD signal is typically by an order of magnitude higher than the intrinsic CD signal of the same pigment molecules (Fig. 8). Excitonic CD is observed in PPCs or small Chl aggregates containing

pigments localized close to each other, which allows participating in short-range dipole-dipole interactions. Excitonic CD is often used for fingerprinting of isolated PPCs, because it provides information on pigment-pigment interactions in these complexes (Garab and van Amerongen 2009).

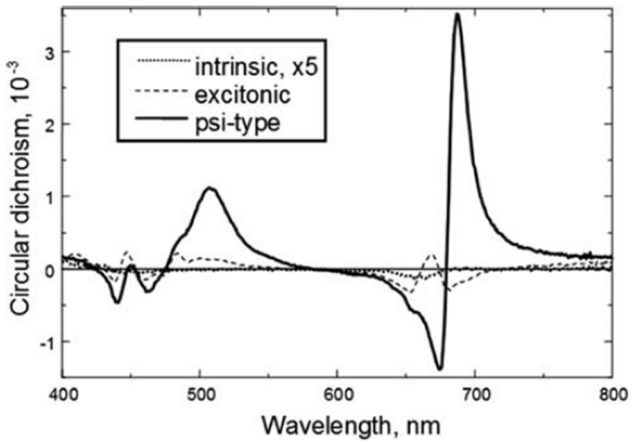

Fig. 8: *Circular dichroism spectra exhibited by the thylakoid pigments at different levels of organization (adopted from (Garab and van Amerongen 2009)). The pigment concentrations adjusted to 20 μg Chls/ml are identical in the three samples. The extract of photosynthetic pigments in 80% acetone yielding intrinsic CD (the signal is multiplied by a factor 5), pea thylakoid membranes suspended in low salt hypotonic medium dominated by the sum of the excitonic bands (unstacked thylakoids), and the same membranes suspended in isotonic medium in the presence of Mg ions (stacked thylakoids).*

In aggregates with sizes comparable with the wavelength of the visible light (hundreds of nanometres) and with high chromophore density, new anomalous CD bands with non-conservative band structure may be observed. That means that the intensity of the negative or positive component of a band-pair can vary independently from each other in the case of this type of CD. These signals are called Ψ (psi - polymer or salt-induced) type bands. Ψ-type CD can also be observed in non-absorbing regions, which originate from circular differential scattering and thus can provide useful information about the size of the aggregate (Garab et al. 1988). Measured CD signal is then composed of differential absorption (A_L-A_R) and differential light scattering (S_L-S_R) of the sample [CD = (A_L - A_R) + (S_L - S_R)]. The intensity of the Ψ-type bands depends on the extent of the long-range chiral order, the domain size and the direction of the chiral order (handedness) (Keller and Bustamante 1986). Photosynthetic pigments are able to form large chiral aggregates, so called chiral

macrodomains, exhibiting intense Ψ-type CD signals (Fig. 8) due to long-range chiral organization or macroorganization of pigments bound within PPCs, possibly extending the pigment interactions in the thylakoid membrane system (Garab 2014; Garab 2016; Garab and van Amerongen 2009).

The CD signals of thylakoid membranes of green plants are dominated by intense bands with anomalous shape at around (−)674 nm, and (+)690 and (+)506 nm and are accompanied by long tails outside the main absorbance bands. Detailed analyses on detached leaves and isolated thylakoid membranes of wild-type and mutant plants provide more specific information on the origin of the major Ψ-type CD bands, which are summarized in the following findings (Garab 2014; Garab 2016; Garab and van Amerongen 2009; Toth et al. 2016):

- The chiral macrodomains disassemble upon mild detergent treatments and chaotropic effects. Nevertheless, detergent and chaotropic effects on the CD signal can be prevented by pre-treatment of the thylakoid membrane with glutaraldehyde that cross-links the proteins. These confirm that long-range ordered protein domains organized using weak protein–protein interactions result in the intense Ψ-type CD bands of thylakoid membranes.
- It is evident that multilamellar organization of grana is conducive to the generation of Ψ-type CD. However, the well-developed grana do not automatically generate Ψ-type CD bands. The various *Arabidopsis* mutants with altered antenna composition exhibit drastically different CD spectra while they retain the same wild type like granum structure. Thus role of the granum ultrastructure in generating Ψ-type CD signals could be in the induction or stabilization of the macro-domain organization of PPCs in the thylakoid membrane and the fast unstacking of the grana triggers a gradual disassembly of protein macro-domains. However, the occurrence of the positive Ψ-type CD bands requires only a few stacked layers.
- The impact of the PPCs composition on their long-range order in the membrane plane has been demonstrated using various *Arabidopsis* mutants with altered antenna composition. Examined mutants containing distinct PSII supercomplex structures, which have been described earlier, reveal characteristic CD fingerprints (Fig. 9). This suggests that the main positive Ψ-type bands (+)690 depend on LHCII

contents of the thylakoid membranes. Further, the (+)506 nm band appears only in the presence of PSII–LHCII supercomplexes and does not depend on the xanthophyll composition of the membranes.

- The CD signatures of different wild-type leaves of dicotyledonous and monocotyledonous angiosperms are quite robust, characterized by very similar excitonic and Ψ-type CD bands. This suggests similar protein composition and macro-organization of PSII-LHCII supercomplexes in the granal thylakoid membranes.
- The chiral macrodomains of the photosynthetic membranes undergo gross (up to 80-90%) light induced reversible structural changes, which can be detected in the major Ψ-type CD bands. These light-induced changes are largely independent on the photochemical activity of the thylakoid membranes, although they are sensitive to the inhibitors of qE component of NPQ. In addition, the amplitude of light-induced CD changes exhibit linear correlation with the light intensity, even above the intensities that saturate the linear electron transport.
- Chiral macrodomains in isolated thylakoid membranes are also susceptible to elevated temperatures. This can be concluded from the decrease of the Ψ-type CD signals between 40 and 50 °C, while the excitonic CD signals persist even at 65-70 °C. These data reveal that the thermal stability of the chiral macrodomains is considerably lower than that of the PPCs. Thylakoid membranes preilluminated with strong actinic light exhibit even higher sensitivity to increased temperatures. In contrast, the excitonic interactions are essentially not affected by preillumination, suggesting that the majority of PPCs undergo no detectable light induced changes.

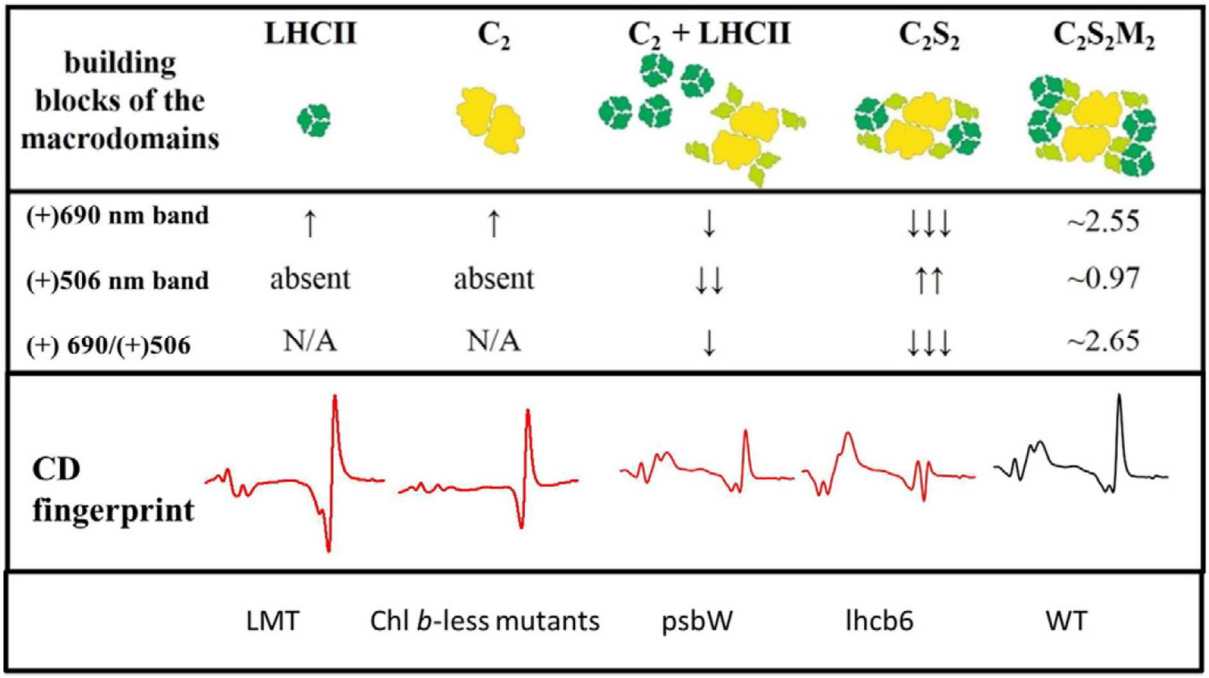

Fig. 9: *Protein constituents of supercomplexes that determine the circular dichroism fingerprint of the chiral macro-domains (adopted from (Toth et al. 2016)). The scheme shows the role of different protein components of PSII supercomplexes in the assembly of different macro-domains with different CD fingerprints. The up and down arrows indicate the enhancement and suppression, respectively, of the (+)690 nm or (+)506 nm Ψ-type CD bands or their ratio by the given component of the supercomplex, relative to C2S2M2 and the calculated band-intensity ratios for the given plant species; N/A: non-applicable.*

2. AIMS

During my PhD work, the following aims and goals were addressed:

I. To introduce CD spectroscopy at the Laboratory of spectral-optical methods at University of Ostrava in order to obtain technique that can provide information on the organization of PPCs in the thylakoid membranes, complementary to that obtained by low temperature Chl *a* fluorescence spectroscopy.

II. To demonstrate using spectroscopic techniques that isolation procedures of thylakoid membranes applied to *Arabidopsis*, barley leaves and especially spruce reflect the state of PPCs in intact leaves/needles.

III. To examine structural and functional stability of the PPCs in spruce thylakoid membranes by measuring their thermal stabilities and compare to model plants such as *Arabidopsis* or barley.

IV. To examine acclimation responses of pigment composition and PPCs organization in of thylakoid membranes to LL and HL, particularly in comparison with acclimation responses of model plants such as *Arabidopsis* and barley.

3. MATERIALS AND METHODS

In this section only the methods, results of which are directly shown in section 4 "Results and discussion", are described. Details on other methods can be found in attached manuscripts.

3.1.1. Sample preparation

3.1.1. Plant material and growth conditions

Arabidopsis (*Arabidopsis thaliana* L. cv. Columbia), spring barley (*Hordeum vulgare* L. cv. Bonus) and Norway spruce (*Picea abies* [L.] Karst.) were grown from seeds under controlled environmental conditions inside a HB 1014 growth chamber (Vötsch Industrietechnik, Balingen-Frommern, Germany) at photosynthetic photon flux density of 50 µmol photons m^{-2} s^{-1}, 20 °C, 65 % relative humidity and light/dark regime of 8/16 for *Arabidopsis* and 16/8 for barley and spruce. The middle segments of dark adapted primary leaves/needles of 11–13 week-old *Arabidopsis*, 1-week-old barley or 3–4 week-old spruce seedlings were used for measurements on the intact leaves/ needles and isolation of thylakoid membranes.

For purposes of the study of acclimation response in barley photosynthesis apparatus to different light intensities, barley seedlings were from seeds in growth chamber at 50, 300 and 1000 µmol photons m^{-2} s^{-1}, respectively termed LL, ML, and HL. Other growing conditions were the same as in the previous experiment with barley.

For purposes of the study of acclimation response in spruce photosynthesis apparatus to different light intensities, spruce seedlings were grown from seeds in growth chamber at 100 mmol photons m^{-2} s^{-1} for 17 days. Other growing conditions were the same as in the previous experiment with spruce. Afterwards parts of seedlings were acclimated to low (LL, 20 mmol photons m^{-2} s^{-1}) and high (HL, 800 mmol photons m^{-2} s^{-1}) lights for 10 days, whereas control plants continued to grow under original (normal, control, moderate) light ML. Other growing conditions were the same as in the previous experiment with spruce.

3.1.2. Isolation of thylakoid membranes

For the purposes of experiments concerning photosynthetic pigment composition changes and functional state of the thylakoid membranes from barley during the individual

steps of preparation and acclimation response in barley photosynthesis apparatus to different light intensities the modified method described by Ilík et al. (2002) was used. The leaf segments (12 g) were homogenized for 10 s in a grinding medium using *Ultra-Turrax T25* homogenizer (*IKA Labortechnik*, Staufen, Germany). The grinding medium contained 0.33 M sorbitol, 5 mM $MgCl_2$, 10 mM NaCl, 2 mM sodium ascorbate, and 50 mM Tricine-NaOH, pH 7.8. The homogenate was rapidly filtered through four layers of polyamide sieve *Uhelon 130T* (*Silk & Progress*, Brněnec, Czech Republic) with mesh width of 42 μm and the filtrate was centrifuged at 3,020 × *g* for 2.5 min (*Sigma 3K 30*, Osterode, Germany). The sedimented chloroplasts were osmotically lysed by suspending the pellet in a resuspension medium consisting of 5 mM $MgCl_2$, 10 mM NaCl, and 50 mM Tricine-NaOH, pH 7.8 (RES1 medium). The thylakoid membranes were obtained by a subsequent centrifugation at 20,000 × *g* for 6 min. The pellet was resuspended in a resuspension medium that contained 11.3 mM Tris, 87 mM glycine and 9% (v/v) glycerol (RES2 medium). The thylakoid membranes were solubilized with 20% (w/v) stock of decyl-β-D-maltosid (Dm). This surfactant and the RES2 membranes were mixed to obtain a final 2% concentration of the surfactant and Chls concentration of 1,250 μg ml^{-1}. The extract was centrifuged at 7,500 × *g* for 2.5 min to remove a colorless insoluble material and to obtain a green supernatant (denoted as Dm medium) that was also used for the measurements. All isolation steps were performed at 0–4°C under dim green light. Chls content of all suspensions was adjusted to 1,000 μg ml^{-1}.

For the purposes of experiments concerning the comparison of plant species studied, their thermal stability and acclimation response in spruce photosynthesis apparatus to different light intensities different method for thylakoid membrane preparation was used. Plant tissue was disintegrated using blender-type homogenizer Ultra-Turrax T25-18G (IKA, Staufen, Germany; 45 s at 18,000 rpm) in a homogenization medium (400 mM sucrose, 400 mM NaCl, 4 mM $MgCl_2$, BSA - 2 mg/ml, 5 mM ascorbic acid, 35 mM Hepes, pH = 7.2). Homogenate was filtrated through 8 layers of polyamide sieve Uhelon 130T (Silk and Progress, Moravská Chrastová, Czech Republic) of pore size 42 μm and centrifuged (3K30; Sigma Laborzentrifugen, Osterode am Harz, Germany) for 6 min at 5,000 *g*. Pellet was resuspended in medium I for disrupting the chloroplast envelope (150 mM NaCl, 8 mM $MgCl_2$, 1 mM Na_2-EDTA, 25 mM Hepes, pH = 7.5) and centrifuged for 10 min at 5,000 *g*. Removal of potential starch from pellet was performed by pellet resuspension in medium II

(400 mM sucrose, 15 mM NaCl, 5 mM $MgCl_2$, 50 mM Hepes, pH = 7.2) and by centrifugation for 3 min at 200 *g*. The resulting supernatant was again centrifuged (5 min at 5 000 *g*), final thylakoid pellet was suspended into a small aliquot of medium II and diluted to concentration of 1,000 µg Chls/ml. All isolation and centrifugation steps were performed at 0 °C according to Nosek (2012).

3.1.3. Clear native-polyacrylamide gel electrophoresis (CN-PAGE)

Separation of PPCs by CN-PAGE was carried out using 4 % (w/v) focusing and 4.5–11.5 % (w/v) linear gradient polyacrylamide gel (acrylamide:bis acrylamide; 30% T and 2.67% C) enabling well distinguished separation of large PPCs such as PSI and PSII-LHCII supercomplexes (Järvi et al. 2011). BisTris system of cathode and anode buffers (pH = 7.0) were used with addition of β-DM (0.02 % w/v) and anionic detergent sodium deoxycholate (0.05 % w/v) to cathode buffer. Electrophoresis was performed at 4 °C in dark at gradual increase of voltage from 75 to 200 V (Järvi et al. 2011) with total running time about 3.5 h. Images of gels containing separated PPCs were captured by ChemiDoc MP gel imager (Bio-Rad Laboratories, Hercules, CA, USA) in transmitting white light or Chl *a* fluorescence excited by blue light with CCD detection. Relative amounts of individual PPCs in heat-treated membranes in comparison with membranes at 20 °C were evaluated from one-dimensional densitograms calculated from the green gel images using the Matlab software procedure according to Ilík et al. (2002).

3.2. Measurements

3.2.1. Fluorescence spectroscopy

Chl *a* fluorescence spectra at 77 K were measured using an LS50B luminescence spectrofluorometer (Perkin-Elmer, Beaconsfield, United Kingdom) equipped with a custom-made Dewar-type optical cryostat. The Chl content was set to 5 µg/ml to avoid reabsorption (OD_{680} < 0.05 with optical pathlength of 0.1 cm). In experiment concerning the thylakoid membranes from barley during the individual steps of its preparation thylakoid membranes with 1,000 µg/ml Chl content diluted in membrane filter with defined pore size were used for measurement. The emission spectra were recorded at the preferential excitation of Chl *a* (436 nm) or Chl *b* (476 nm). The excitation spectra were measured at the wavelengths emission maxima. The emission spectra were measured with 5 and 2.5 nm slit widths of the

excitation and emission monochromators, respectively. The measurements of excitation spectra of the suspensions were carried out with 2.5 and 5 nm slit widths of the excitation and emission monochromators, respectively. The emission spectra were corrected for the spectral sensitivity of the detection system. The excitation spectra were automatically corrected for the output of the excitation source, efficiency of the excitation monochromator, and sensitivity of the reference photomultiplier.

3.2.2. Circular dichroism spectroscopy

CD spectra were recorded in the range of 400–750 nm with a J-815 spectropolarimeter (Jasco, Tokyo, Japan). The spectra were recorded in steps of 0.5 nm with an integration time of 1 s, a band-pass of 2 nm and scanning speed of 100 nm min^{-1}. For measuring of spectra on intact leaf samples detached leaves were placed in between the two detachable glass windows of an optical cell of 0.2 mm path length, and were measured at the distance of the sample from the photomultiplier of 5 cm. Stacked thylakoid membranes were prepared by resuspension of isolated membranes at a Chl content of 20 μg ml^{-1} in medium containing 50 mM Tricine (pH = 7.5), 0.4 M sorbitol, 5 mM KCl and 5 mM $MgCl_2$. In order to obtain unstacked thylakoids displaying no Ψ-type CD bands, the thylakoid membranes at the same Chl concentration were washed in 50 mM Tricine buffer supplemented with 5 mM MEDTA (pH 7.5) and were sonicated (GM 3100; Bandelin Electronic, Berlin, Germany) on ice for 300 s using 0.5 s duty cycle and output value of 25%. CD spectra of thylakoid membranes were recorded in the cell with optical pathlength of 1 cm.

The measurements of temperature-dependent changes of CD signal were performed in two different ways. For purposes of comparison with the heat-induced changes in the PSII function, the samples were sequentially thermostated in Peltier holder for 5 min at each temperature starting from 20 °C up to 70 °C. Measured temperature dependences of the CD bands or band pairs were fitted with a sigmoidal curve that resulted in estimation of transition temperatures (T_m). T_m marks the disassembly of the chiral macrodomains of the complexes (Cseh et al. 2000) and is defined as the temperature at which the intensity of the CD band is decreased to 50% of its value at 20 °C.

For purposes of comparison with CN-PAGE of heat-treated thylakoids, suspensions of prepared thylakoid membranes were doubly diluted with medium II to concentration of 500 µg Chls/ml and placed in Eppendorf tube into water baths to gain the temperature of membranes to 20, 32, 36, 40, 44, 48, 52, 56, and 60 °C for 15 min in a dark room. Then part of the sample was used for CD measurements as described in the paragraphs above and rest immediately frozen in liquid nitrogen and stored at 80 °C for CN-PAGE.

3.2.3. Measurement of photosystem II function

PSII function in heat-treated leaf/needles was monitored using potential yield of PSII photochemistry (F_V/F_M) measured by pulse amplitude-modulated fluorometer PAM 101–103 (Walz, Effeltrich, Germany). Needle or leaf samples were exposed to linear heating in the temperature-controlled measuring chamber equipped with optical lid for PAM fibre-optics and connected to temperature-controlled bath MC-4 (Julabo, Seelbach, Germany). The linear heating of the water-bath was set to speed of 1 °C min^{-1} within the temperature range 20–48 °C. During the heating regime the surface temperature of the sample was continuously monitored using a thermocouple. In order to avoid desiccation all samples were inserted into the measuring chamber on the water soaked foam during the measurement and pre-acclimated at 20 °C for 5 min in darkness before the heating. The saturation pulses (1 s time duration, 1400 µmol photons m^{-2} s^{-1} light intensity) applied at 20 °C and during heating with an increment of 2 °C (after approximately 2 min), were used for determination of maximum fluorescence in the dark-adapted states (F_M). Immediately before the application of saturation pulse minimum fluorescence in dark-adapted state (F_0) were taken and the maximum efficiency of PSII photochemistry (F_V/F_M) was calculated as $(F_M–F_0)/F_M$.

3.2.4. Determination of the chlorophyll content

The ratios of Chl *a* to Chl *b* (Chl *a*/*b*) and of total Cars to Chls (Cars/Chls) were estimated spectrophotometrically (UV/VIS 550, Unicam, Leeds, England) from the pigment extracts according to Lichtenthaler (1987). In the case of suspensions, the pigments were extracted in 80% acetone. Because the single extraction of pigments (mainly β-carotene) from leaves in aqueous acetone solvent is incomplete (Dunn et al. 2004; Thayer and Björkman 1992), we used triple acetone extraction (80:100:100%) of pigments from leaves.

3.2.5. Determination of the pigment composition by high performance liquid chromatography

The contents of the individual Cars (lutein, neoxanthin, β-carotene, and the pool of xanthophyll cycle pigments, *i.e.* violaxanthin + antheraxanthin + zeaxanthin) expressed on a Chls basis were estimated by the gradient reversed-phase high-performance liquid chromatography (*TSP Analytical*, USA) according to Färber and Jahns (1998) with a minor modification (Kurasová et al. 2003) that are described in details in previous study (Štroch et al. 2008a).

4. RESULTS AND DISCUSSION

4.1. Structure-functional state of thylakoid membranes

Isolation of chloroplasts, thylakoid membranes from plant tissues and following separation of individual PPCs by native gel electrophoresis or ultracentrifugation is necessary for most of biochemical and some spectroscopic studies of photosynthetic apparatus concerning adaptation or acclimation mechanisms to changing environmental conditions. The interpretation of findings obtained from native gel electrophoresis is based on the assumption that they reflect the state of PPCs in intact leaves. In this section, I summarize used isolation procedures of thylakoid membranes applied to *Arabidopsis*, barley and spruce leaves/needles by primarily spectroscopic monitoring of the structure-functional state of PPCs that indicate the above mentioned assumption.

4.1.1. Isolation of thylakoid membrane for native electrophoresis

In the first study, we examined changes in photosynthetic pigment composition and functional state of the thylakoid membranes from barley leaves grown under low irradiance during the individual steps of preparation of samples that are intended for a separation of PPCs by non-denaturing polyacrylamide gel electrophoresis. Functional state of the thylakoid membranes preparations was evaluated by a determination of F_V/F_M, by an analysis of excitation and emission spectra of Chl *a* fluorescence at 77 K and CD spectra. All measurements were done at three phases of preparation of the samples: (1) in the suspensions of osmotically-shocked broken chloroplasts (RES1), (2) thylakoid membranes in extraction buffer containing Tris, glycine and glycerol (RES2) and (3) thylakoid membranes solubilized with a detergent decyl-β-D-maltosid (Dm).

Pigment composition was not pronouncedly changed during all steps of preparation of the thylakoid membrane. In comparison with the intact leaves and thylakoid membranes resuspended in RES1 medium, F_V/F_M of the membranes resuspended in RES2 ones was reduced to 0.723±0.018 (from 0.826±0.002 and 0.815±0.004, respectively) and to values close to zero in solubilized membranes. In 77-K Chl fluorescence emission spectra, thylakoid membranes solubilization resulted in a pronounced emission band with the maximum around 680 nm corresponding to emission of LHCII trimers detached from PSII core after Dm treatment (Fig. 10A). In comparison with intact leaves, the broad Chl *b* and Cars excitation

band in the spectral region of 460-510 nm within PSII was slightly reduced in RES1, RES2 and more pronouncedly in Dm samples, which are comparable to those LHCII trimers (Fig. 10B). In addition, disassembly of PSI and PSII supercomplexes after solubilization of the thylakoid membranes is accompanied by loss of chiral macrodomains in the thylakoid membrane as indicated disappearance of Ψ-type CD signal in CD spectra (Fig. 11). It is valuable to note that chiral macrodomains were not affected by the isolation of thylakoid membranes (Fig. 11). These results indicate that thylakoid membranes from barley leaves affected the pigment composition, macrodomain organization of PPCs in the thylakoid membranes and the functional state of the PSII complexes only slightly. Despite a functional disconnection of LHCII from PSII antenna core in Dm-solubilized thylakoid membranes, energy transfer from Chl *b* and Cars to emission forms of Chl *a* within LHCII trimers remained effective.

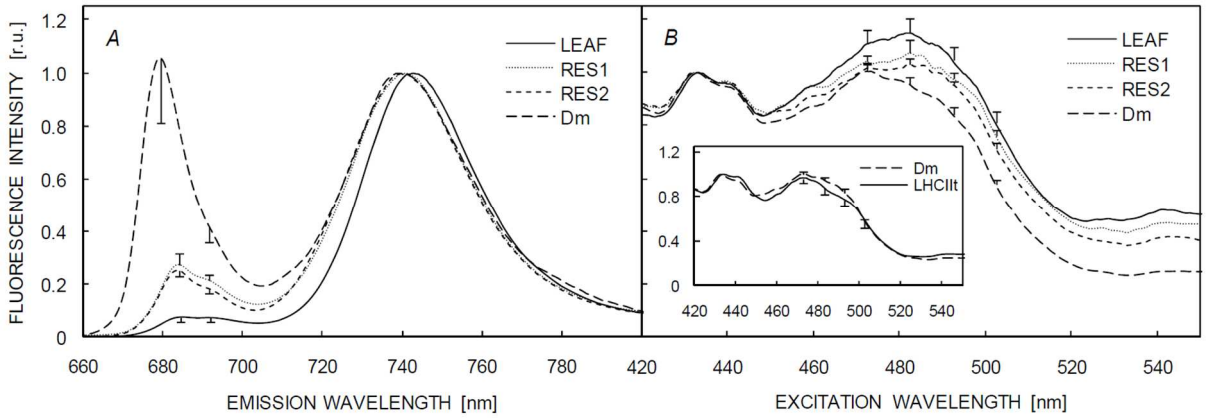

Fig. 10: *Chlorophyll a fluorescence emission (A) and excitation (B) spectra at 77 K of barley leaves and isolated thylakoid membranes suspended in RES1, RES2 and Dm media during the individual steps of the isolation procedure. The inset shows excitation spectra of Dm membranes and band containing LHCII trimers (LHCIIt) obtained by nondenaturing gel electrophoresis. The emission spectra were recorded at the excitation wavelength of 436 nm and normalized at the long wavelength maximum. The excitation spectra were measured at the emission wavelengths of 685 nm for leaves and the membranes and 681 nm for LHCIIt bands. The excitation spectra were normalized at the excitation maximum of chlorophyll a in the Soret region. The mean spectra from 6–12 samples are presented. Error bars indicate SD.*

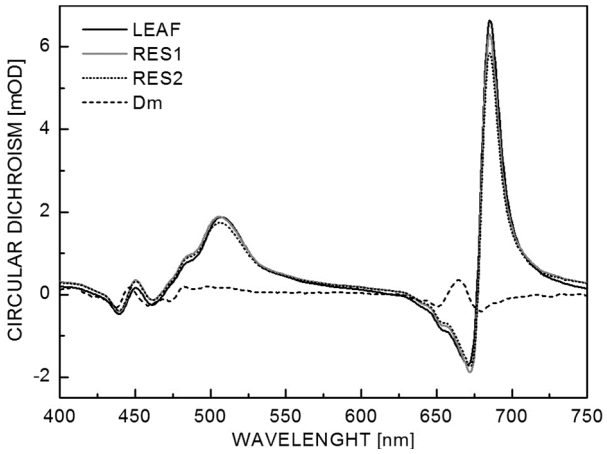

Fig. 11: *CD spectra of isolated thylakoid membranes of barley leaves and isolated thylakoid membranes suspended in RES1, RES2 and Dm media during the individual steps of the isolation procedure. The CD spectra were normalized to the absorbance at 678 nm. The spectra represent the means and SD of 3 samples.*

Similarly, isolation of photochemically active thylakoid membranes (or "broken chloroplasts") from one year old needles of Norway spruce was tested. Unfortunately, there were not conventional methods suitable for the isolation of highly active thylakoids for conifers, mainly for the following reasons. Firstly, highly fibrous character of needles complicates the isolation process due to difficulties of cells disruption without damaging the chloroplasts. And secondly, the high content of specific compounds (phenols, resin, tannin, etc.) that are released from the vacuole or other cell compartments of broken cells can cause either inhibition or degradation of some components of the photosynthetic electron-transport chain. Since previous isolation procedure used for barley (Attachment III; Karlický et al. 2010) did not provide highly active thylakoid membranes, we tested method specifically designed for conifers revealed moderately lower F_V/F_M than intact needles (about 0-12 %) and only slightly reduced Chl *b* and Cars bands in blue region of 77K Chl *a* fluorescence excitation spectra. Although the prepared thylakoid membranes seemed appropriate for the following experiments, this procedure reveals low yield of thylakoid suspension or poor solubilization under mild detergent condition, which complicates the separation of PPCs by native electrophoresis. For this reason we performed thylakoid membrane isolation from young spruce seedlings that proved to be convenient material for highly efficient preparation of photochemically active thylakoid membranes, sufficient yield of thylakoid suspension, and reasonable solubilization of PPCs under mild detergent

condition. In addition, utilization of young spruce seedlings allows the use of conventional methods from herbaceous plants as described above (Attachment III; Karlický et al. 2010) or similar (Nosek 2012), which was used in the following experiments.

4.1.2. Spectral characteristics of pigment-protein complexes *in vivo* and *in vitro* – the similarities and particularities among plant species

Low temperature fluorescence emission spectra and CD spectra of intact leaves/needles, thylakoid membranes and isolated PPCs reveal spectral characteristics of PPCs both, *in vivo* and *in vitro*, which are specific for different plant species. Some of these spectral properties are summarized in this section.

Fluorescence emission spectrum of intact spruce needles at 77 K was reported long before (Špunda et al. 1994). In this spectrum, PSII emission from spruce dominates about 692 nm in contrast to *Arabidopsis* and barley having roughly the same intensity of both, emission at 685 nm and 692 nm (Fig. 12A). However, this was originally explained by strongly suppressed fluorescence band around 685 nm in the case of spruce needles due to the fluorescence reabsorption effect (Špunda et al. 1994), which was consistent with the general concept assuming the similar structure of PSII for higher plants.

Using highly efficient preparation of photochemically active thylakoid membranes and separation of PPCs by CN-PAGE we showed that main signatures of fluorescence emission spectra on intact leaves/needles remains at the level of isolated thylakoids (removal of reabsorption) and PSII-LHCII and PSI-LHCI supercomplexes (Fig. 12), despite that reabsorption has significant contribution to the shape of the emission spectrum *in vivo*. Indeed, 77K fluorescence emission spectra of isolated PSII-LHCII supercomplexes from spruce peaked at around 692 nm compared to those of *Arabidopsis* and barley, which revealed maximum at wavelength of 685 nm (Fig. 12D). Secondly, variability of position of LHCI emission maxima observed in intact leaves (Fig. 12A; *Arabidopsis*: 732 nm, barley: 743 nm, spruce: 738 nm) is also manifested on isolated PSI-LHCI supercomplexes (Fig. 12E). Other PPCs including parts of PSII supecomplexes like core complex of PSII or LHCII monomers and trimers showed almost the same spectra in all studied species (e.g. LHCII trimers, (Attachment I; Karlický et al. 2016)).

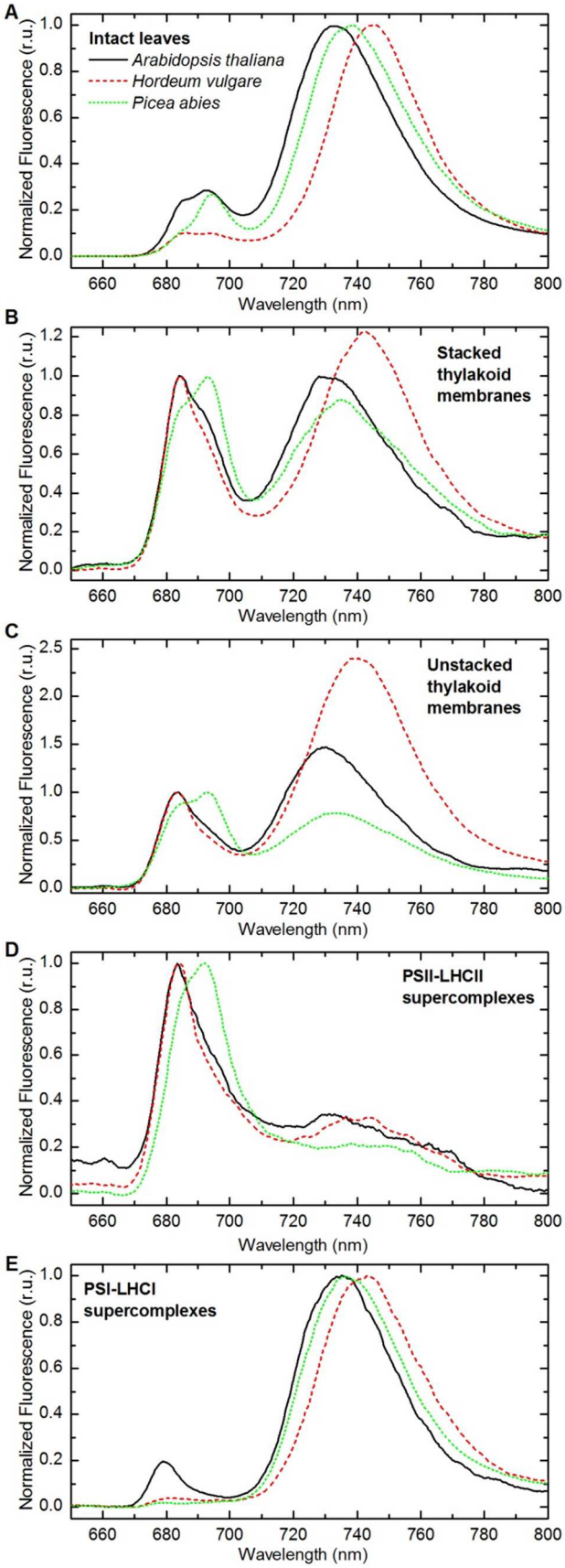
A
Intact leaves
Arabidopsis thaliana
Hordeum vulgare
Picea abies
B
Stacked thylakoid membranes
C
Unstacked thylakoid membranes
D
PSII-LHCII supercomplexes
E
PSI-LHCI supercomplexes
Normalized Fluorescence (r.u.)
Wavelength (nm)

Fig. 12: *Normalized 77 K fluorescence emission spectra of intact barley leaves/needles (A), stacked (B) and unstacked (C) thylakoid membranes (total chlorophylls concentration of 4 µg ml^{-1} for), PSII supercomplexes (D), and PSI supercomplexes (E) isolated from Arabidopsis (black line), barley (red line) and spruce (green line) grown under low light conditions (50 µmol m^{-2} s^{-1}). Samples were excited at wavelength of 436 nm (preferential excitation of chlorophyll a). Typical spectra from the three independent experiments are displayed.*

The CD spectra of thylakoid membranes isolated from *Arabidopsis*, barley and spruce revealed similar character as described previously (Krumova et al. 2010; Varkonyi et al. 2009). Nevertheless, amplitude of the main Ψ-type CD band of *Arabidopsis* and barley membranes was much higher in comparison with spruce ones (Fig. 13A), which indicates much smaller size of the chiral macrodomains (Garab et al. 1991; Garab and Mustardy 1999) or a different organization of PSII superomplexes (Kovacs et al. 2006) in thylakoid membranes of spruce than in those of *Arabidopsis* and barley. In contrast to stacked thylakoid membranes spruce thylakoids did not exhibit significant changes compared to *Arabidopsis* and barley in the CD originating from short-range interactions in unstacked thylakoid membranes, which indicated similar composition of PPCs in the thylakoid membranes (Fig. 13B).

Red shift of 77K Chl *a* fluorescence emission maximum of PSII supercomplexes from spruce, smaller macrodomain organization in spruce membranes and absence of electrophoretic band containing LHCII-CP29-CP24 complexes in spruce thylakoid membranes (Fig. 17) strongly indicate different structural organization of LHCII in spruce PSII supecomplexes as compared to those from *Arabidopsis* and barley. Indeed, the loss of both Lhcb6 (CP24) and Lhcb3 proteins in some gymnosperm genera such as Picea was described very recently (Kouřil et al. 2016). Absence of these proteins in spruce led to modified structural organization of LHCII in PSII superomplexes similar to that observed in PSII supercomplexes of *Chlamydomonas reinhardtii* (Kouřil et al. 2016). It is useful to note that CD spectra of spruce thylakoid membrane revealed similarities with those of *C. reinhardtii* as regards the spectrum shape and magnitude of Ψ-type CD bands (Toth et al. 2016).

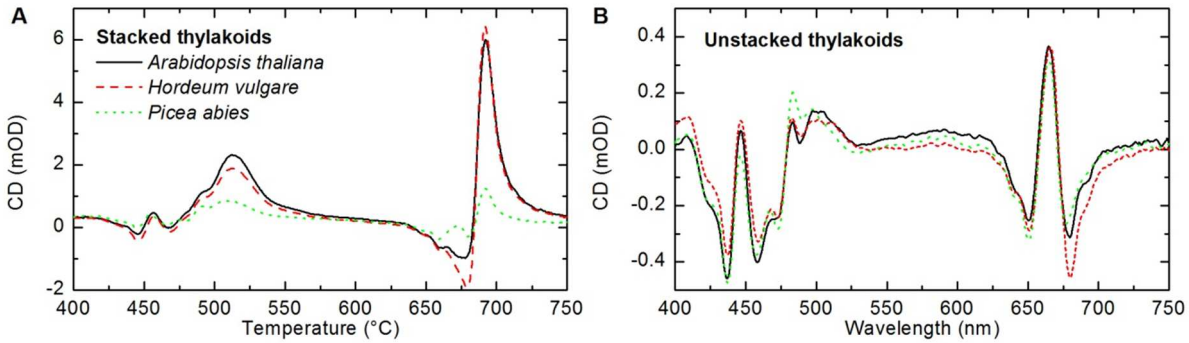

Fig. 13: *CD spectra of stacked (A) and unstacked (B) thylakoid membranes from Arabidopsis (solid black line), barley (dashed red line) and spruce (dotted green line). The CD spectra were normalized to the absorbance at 678 nm. The spectra represent the typical spectra from 4-5 independent experiments.*

4.2. Thermal stability of the thylakoid membranes from different species of higher plants

PPCs of photosynthetic apparatus in thylakoid membranes have dual requirement of structural stability: 1) to preserve the integrity of the membranes and the entire organelle, 2) to provide necessary flexibility to ensure the adaptability of the system that is evidently required in various steps of the multilevel regulatory system. The main objective of this work is to examine the structural and functional stability of the PPCs in spruce thylakoid membranes by measuring their thermal stabilities and compare to model plants such as *Arabidopsis* or barley. We have found that thermal stability of PSII photochemistry in spruce needles is higher than in other plants cultivated under the same temperatures. In addition, we studied whether higher thermal stability of PSII photochemistry found in spruce needles is accompanied with specific features of thylakoid membranes composition that can be related to the enhanced structural stability of PPCs in the thylakoid membranes.

4.2.1. Higher thermal stability of PSII photochemistry of spruce is accompanied by the maintenance of PSII macro-organization

Thermal stability of the PSII function was monitored via the measurement of the maximum quantum yield of PSII photochemistry (the parameter F_V/F_M) on intact leaves/needles exposed to linear heating. We found that F_V/F_M of *Arabidopsis* and barley leaves steeply decreased at 42 °C and almost complete PSII inactivation occurred at 46 °C. On the contrary, reduction of PSII photochemical activity was more gradual in needles of

spruce seedlings at temperatures above 40 °C and still F_V/F_M values about 0.5 were observed at 46 °C (Fig. 14A).

Structural stability of PPCs in the thylakoid membranes was examined by measuring their thermal stabilities. On the plot of the temperature dependence of the main Ψ-type CD band pair differences in the thermal stability of the macrodomain organization of the PPCs between plant species studied can be seen (Fig. 14B). The T_ms of the main Ψ-type CD in spruce membranes is higher by about 6 °C in comparison with the *Arabidopsis* and barley membranes (Fig. 14B). Similarly as heat induced inactivation of PSII photochemistry, also decreases of Ψ-type CD bands with increasing temperature were less steep for spruce membranes compared to *Arabidopsis* and barley ones. T_ms of Ψ-type CD bands or band pair are summarised in Table 1. T_m values observed in spruce were significantly higher in comparison with those observed in *Arabidopsis* and barley by about 6 °C in the case of Ψ-type CD in red spectral region and by about 4 °C for Ψ-type CD band in green spectral region.

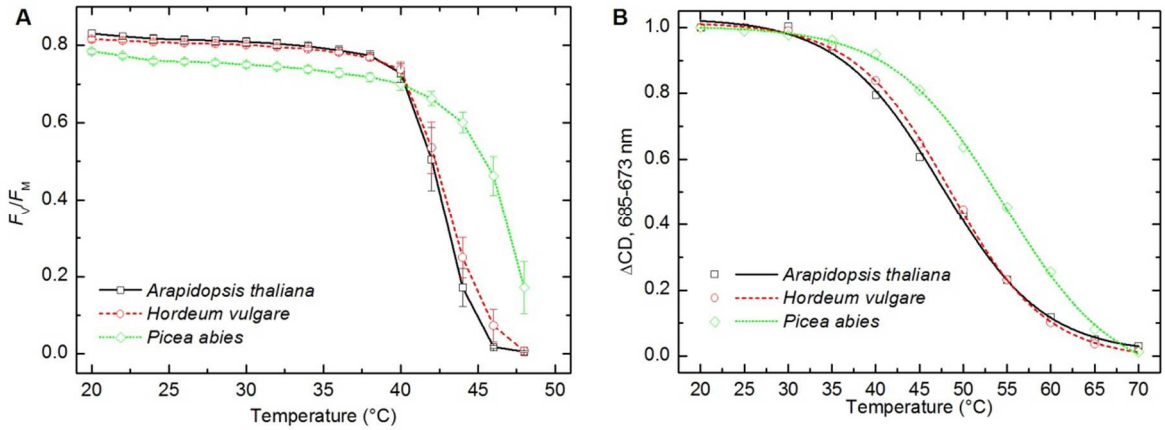

Fig. 14: *Temperature dependences of maximum efficiency of PSII photochemistry (F_V/F_M) measured on overnight dark-adapted Arabidopsis (black), barley leaves (red) and spruce needles (green)(A). Leaf or needle samples were exposed to linear heating of 1 °C min^{-1}. Mean values (points) and standard deviation (error bars) are presented (n = 5–6). Typical temperature dependences of the amplitude differences of the Ψ-type bands at around (+)685 nm and (–)673 nm of the Arabidopsis, barley and the spruce thylakoid membranes exposed to gradual heating (B). Data points from one representative series fitted with a sigmoidal curve resulting transition temperatures (T_m) of 47.8 °C, 47.6 °C and 54.7 °C for Arabidopsis, barley and spruce, resp. Mean values and standard deviation of T_m from six independent experiments are presented in Table 1.*

Table 1 Transition temperatures (T_m) of selected CD bands or band pairs for Arabidopsis, barley and spruce stacked and unstacked thylakoid membranes

CD signal (nm)	*Assignment*	*T_m (Arabidopsis) (°C)*	*T_m (Barley) (°C)*	*T_m (Spruce) (°C)*
685–730	Ψ-type	47.9 ± 2.8[a]	48.3 ± 2.2[a]	54.1 ± 1.4[b]
685–673	Ψ-type	47.5 ± 2.9[a]	47.9 ± 1.9[a]	54.3 ± 1.1[b]
505–550	Ψ-type	47.8 ± 2.2[a]	48.4 ± 1.2[a]	52.4 ± 1.2[b]
483–473	Excitonic (Chl *a*, LHCII trimers)	61.7 ± 0.4[a]	61.1 ± 0.2[a]	62.3 ± 0.7[a]
665–650	Excitonic (Chl *b*, LHCII)	70.0 ± 0.3[a]	67.4 ± 0.5[b]	74.4 ± 0.5[c]

The samples of thylakoid membranes were gradually heated in the range between 20 °C and 70 °C and between 20 °C and 80 °C for stacked and unstacked membranes, resp. The amplitudes for the individual bands were calculated from the difference in the intensity at specific wavelengths. T_m is defined as the temperature at which the intensity of the CD band is decreased to 50% of its value at 20 °C. T_m of Ψ-type CD bands or band pair were estimated from stacked thylakoid membranes and T_m of excitonic CD band pairs were calculated from unstacked ones. Mean values and standard deviations from five (n = 5) and four (n = 4) independent experiments are presented for stacked and unstacked membranes, resp. Data within a row followed by the same letter are not significantly different ($P > 0.05$).

In contrast to stacked thylakoid membranes, unstacked spruce membranes exhibited similar diminution of excitonic bands at elevated temperatures as *Arabidopsis* and barley ones. The excitonic CD band pair of (+)483 nm/(–)473 nm is specific for LHCII trimers and disappearance of this band pair indicates the monomerization of LHCII trimers, both in the thylakoid membranes and in the isolated LHCII (Garab et al. 2002; Yang et al. 2006). It can be clearly seen in Fig. 15A that the T_m of the LHCII trimers monomerization in the *Arabidopsis* and barley correspond well with that of spruce (Table 1). CD bands in red region at (–)650 nm, (+)665 nm and (–)680 nm are present in the CD spectra of both trimeric LHCII and monomeric LHCII (Yang et al. 2006). Therefore, temperature dependence of amplitude of (+)665 nm/(–)650 nm band pair indicates disintegration of LHCII monomers. It can be clearly seen in Fig. 15B that again the T_m of the LHCII monomers disintegration in the spruce membranes is higher by about 4 °C and 7 °C in comparison with *Arabidopsis* and barley ones, resp. (Table 1).

In order to quantify the relation between thermal stability of PSII photochemistry and PPC macro-organization also Tm for F_V/F_M [$T_m(F_V/F_M)$] were expressed by fitting temperature-dependent data with sigmoidal Boltzmann function. Although T_m for the temperature dependence of Ψ-type CD signal [$T_m(\Delta CD685\text{-}673)$] was always higher than T_m of F_V/F_M [$T_m(F_V/F_M)$], linear dependence of $T_m(F_V/F_M)$ on $T_m(T_m(\Delta CD685\text{-}673))$ clearly demonstrated connection between thermal stability of the PSII photochemistry and ability to maintain PSII macro-organization in the thylakoid membranes at elevated temperatures

(Fig. 16). In addition to higher thermal stability of PSII structure and function for spruce in comparison with *Arabidopsis* and barley grown at same light and temperature these data revealed also higher thermal stability of PSII structure and function of both mature spruce needles and 3-4 weeks old seedlings in comparison with early developmental stage (2 weeks old seedlings).

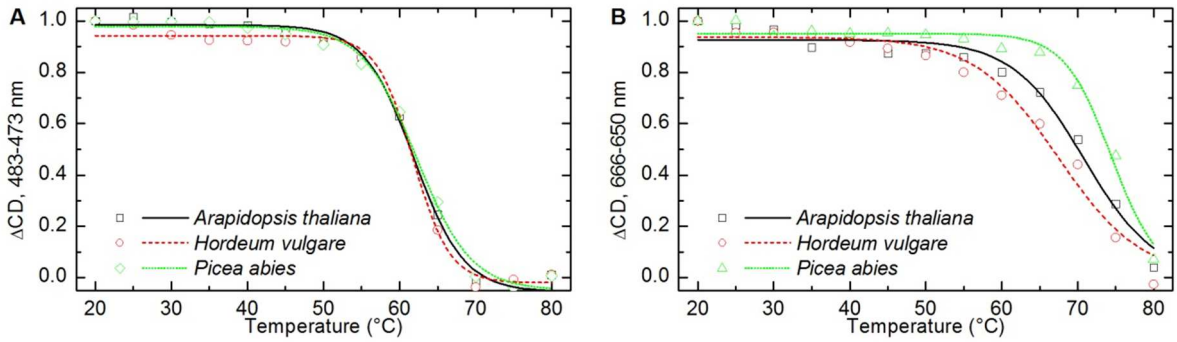

Fig. 15: *Typical temperature dependences of the amplitude differences of the excitonic bands at around (+)483 nm and (–)473 nm (D) and (+)666 nm and (–)650 nm (E) in the Arabidopsis (black), barley (red)and the spruce (green) membranes exposed to gradual heating. Data points from one representative series fitted with a sigmoidal curve resulting transition temperatures (T_m). Mean values and standard deviation of T_m from four independent experiments are presented in Table 1.*

It should be noted that despite of close correlation between the mentioned quantitative estimates of PSII thermal stability, T_m of Ψ-type CD was on average by 6 °C higher than T_m of F_V/F_M. Similarly, parameters derived from F_0 temperature curves (e.g. temperature of the 50% increase of fluorescence from F_0 to F_M levels - T_{50}) occur at considerably higher temperatures than T_m of F_V/F_M and are usually tightly correlated together (Froux et al. 2004; Knight and Ackerly 2002). As a matter of fact, the decrease in F_V/F_M upon increasing temperatures is initiated due to a decrease in F_M with no increase of F_0, which indicate mainly a reversible increase of thermal dissipation in PS II (Berry and Bjorkman 1980; Epron 1997) and the increase of F_0 at higher temperatures reflects an irreversible inactivation of PSII photochemistry due to reaction centre disorganization (Berry and Bjorkman 1980). Hence, analyses of correlations between parameters derived from F_0 temperature curves and Ψ-type CD during heating could contribute to elucidation of suggested connection between thermal stability of PSII photochemistry and PPC macro-organization in thylakoid membranes.

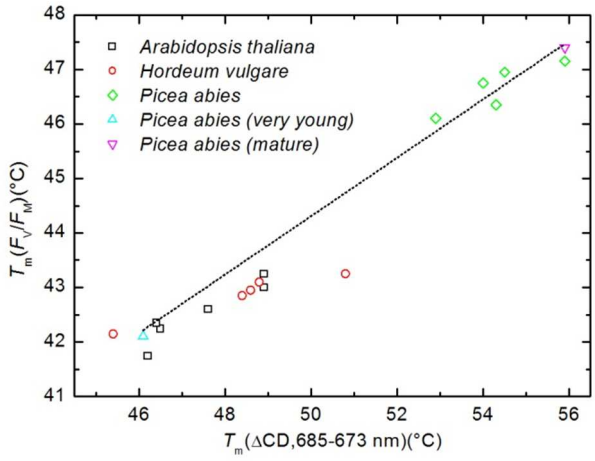

Fig. 16: *The dependence of transition temperature of PSII photochemistry (T_m (F_V/F_M)) on the transition temperature of amplitude differences of the main Ψ-type bands at around (+)685 nm and (–)673 nm (T_m (ΔCD, 685–673 nm)) estimated from sigmoidal fits of temperature dependence of F_V/F_M and ΔCD measured on samples exposed to gradual heating. Data points presenting independent cultivations of Arabidopsis (black squares) and barley plants (red circles) and spruce seedlings (green diamonds). The plot is supplemented by data of very young spruce seedlings (2-weeks old; light blue up triangle) and from mature needles of 4-year spruce trees (magenta down triangle).*

4.2.2 Higher thermal stability of PSII macro-organization of spruce is associated with the maintenance of PSII supercomplexes in the thylakoid membrane

We have also attempted to explain whether the observed enhanced thermal stability of spruce membranes is connected with increased structural stability of individual PPCs at elevated temperatures. Therefore, CD spectra measurements of thylakoid membranes pre-heated 15 minutes at given temperature were performed together with directly observation of thermal stability of individual PPCs of thylakoid membranes using CN-PAGE separation (fog. 17). Among the separated PPCs, only PSII supecomplexes revealed considerably higher thermal stability in spruce thylakoids as compared to *Arabidopsis* and barley ones (Figs. 17,18A). The most heat sensitive PSII supercomplexes disappeared in the temperature range from 40 °C to 52 °C (Figs. 17,18A), thus roughly at the same temperatures as the Ψ-type CD signal (Fig. 18B). The most abundant LHCII trimers started to decrease at the temperature of 52 °C till 56 °C similarly as excitonic CD signal. Therefore, these results indicate that enhanced thermal stability of macrodomain organization of spruce is associated with the

maintenance of PSII-LHCII supercomplexes in the thylakoid membrane, rather than with more stable LHCII trimers.

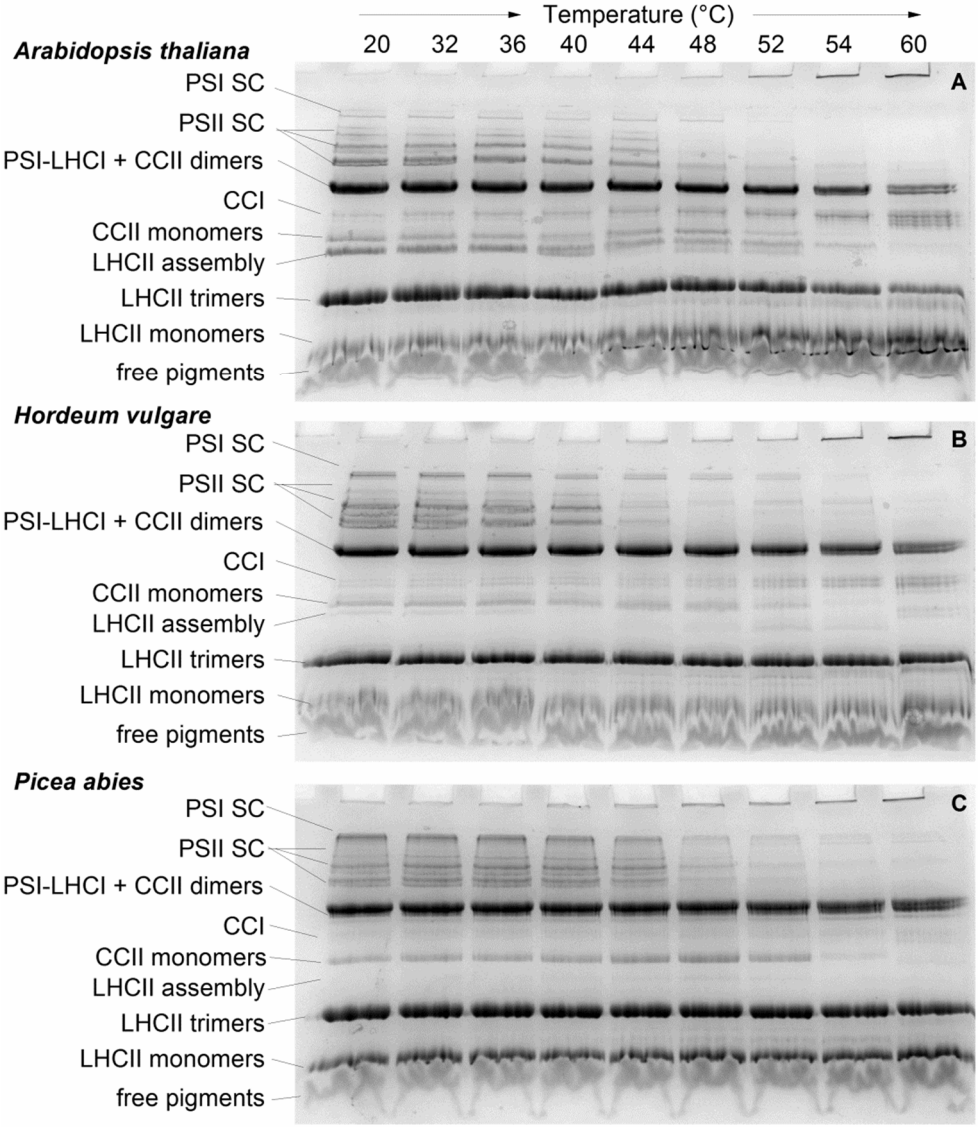

Fig. 17: *CN-PAGE separation of PPCs of thylakoid membranes from Arabidopsis (A), barley (B) and spruce (C) preheated to 20 - 60 °C for 15 minutes in the dark. Thylakoid membranes were solubilized using n-dodecyl-β-D-maltoside with detergent/chlorophyll ratio of 20:1 (Arabidopsis, barley) a 35:1 (spruce). Gel images were obtained as transmittance of white light using CCD camera ChemiDoc MP (BioRad). Typical electropherograms from the three independent experiments are displayed.*

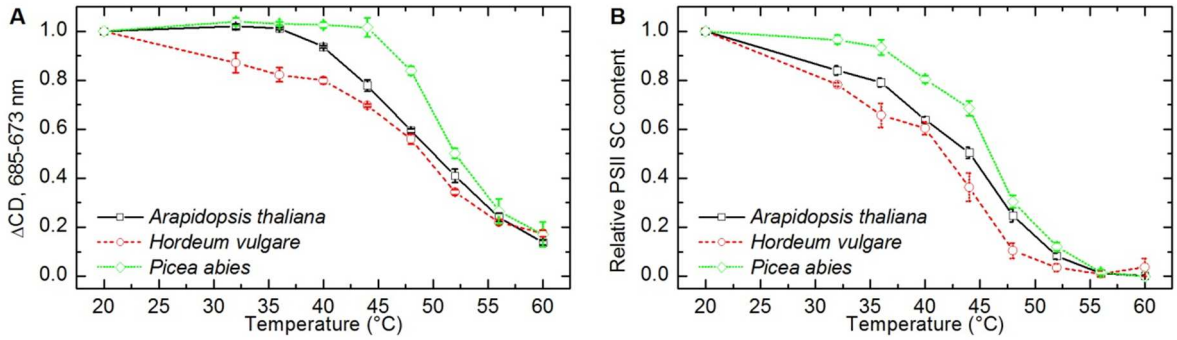

Fig. 18: *Temperature dependences of the amplitude differences of the main Ψ-type bands at around (+)685 nm and (–)673 nm of the Arabidopsis (black), barley (red) and the spruce (green) heat treated thylakoid membranes (A). Temperature dependences of the PSII supercomplexes stability determined from the green gel density profiles of same heat treated membranes (B). Temperatures experiments were carry out in the three independent experiments. Mean values (points) and standard deviations (error bars) from three independent experiments (n = 3) are displayed.*

Closer inspection of these analyses show the connection between the heat-induced decreases in the content PSII supercomplexes and macro-organization of PPCs in the thylakoid membranes that was assessed based on dependence of reduction of the amplitude differences of the main Ψ-type bands at around (+)685 nm and (–)673 nm on decrease in total content of PSII superomplexes in the heat treated thylakoid membranes (Fig. 19). This clearly non-linear dependence, with similarities for all plants species, revealed that 20% reduction of total content of PSII superomplexes in the heat treated thylakoid membranes did not cause significant change of Ψ-type CD signal. After disintegration of almost all PSII supercomplexes in thylakoid membranes by heat, Ψ-type CD signal was reduced to below 50% of the initial value. It is appropriate to note that LHCII-only domains also contribute to the Ψ-type CD signal (Garab et al. 1991; Garab and Mustardy 1999), which thermal stability cannot be determined by CN-PAGE, and could thus partially explain the observed residual Ψ-type CD signal after the disintegration of all PSII supercomplexes. Nevertheless, the fact that main part of PSII inactivation and reduction of PSII supercomplexes content occurs in a similar temperature range (40 – 46 °C) indicate that stability of PSII supercomplexes may be important for short-term resistance of photosynthetic apparatus against heat stress.

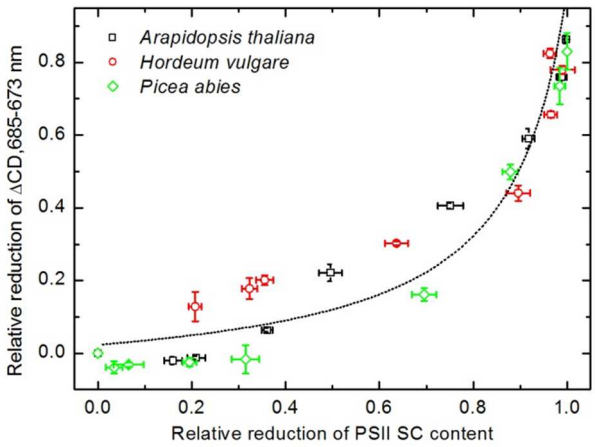

Fig. 19: *Dependence of heat induced reduction of the amplitude differences of the main Ψ-type bands at around (+)685 nm and (–)673 nm on the decrease in total content of PSII supercomplexes (SC) in the heat treated thylakoid membranes from Arabidopsis (black squares), barley (red circles) and spruce (green diamonds). Mean values (points) and standard deviations (error bars) from three independent experiments (n = 3) are displayed.*

Different composition of LHCII protein subunits and PSII-LHCII supercomplex structural organization (Kouřil et al. 2016) and thylakoid membrane lipids (Attachment I; Karlický et al. 2016) in spruce led us to propose factors that can affect the thermal stability of spruce thylakoid membranes.

- Different structure of the PSII supercomplexes from spruce resulting in smaller macrodomains, which may possess higher thermal stability itself.
- More free packing of PPCs that can be expected from higher fatty acids to Chl *a* ratio (Attachment I; Karlický et al. 2016) also could have the role in thermal stability of PSII. But as this ratio in spruce thylakoids was only by 10% higher than in *Arabidopsis* and barley we do not expect pronounced contribution of the higher lipid to protein ratio to the enhanced thermal stability of spruce PSII supercomplexes.
- Although, the relation of lipid desaturation and the thermal sensitivity of PSII is still unclear and data are contradictory (Allakhverdiev et al. 2008), increase in the degree of fatty acid saturation in lipids of spruce thylakoid membranes (Attachment I; Karlický et al. 2016) could be further factor responsible for the enhanced thermal stability of PSII.

- Moreover, considerably lower ratio of MGDG/DGDG in spruce thylakoid membranes can significantly affect membranes stability at higher temperatures (Krumova et al. 2010). Despite of lower MGDG/DGDG ratio in spruce thylakoids monomerization of LHCII trimers in *Arabidopsis*, barley and spruce occurred at the same temperature (T_m approximately 62 °C, Fig. 15A, Table 1) that is in agreement with Krumova et al. (2010). On the other hand, the thermal stability of LHCII monomers in spruce thylakoid membranes was significantly higher than in *Arabidopsis* and barley ones (Fig. 15B, Table 1).
- Possible role of interactions of LHCII and DGDG with FAs specific for gymnosperms (i.e. very long chain fatty acids, branched-17:0 fatty acid and Δ5-unsaturated fatty acids (Attachment I; Karlický et al. 2016; Moellering et al. 2009; Mongrand et al. 2001) on the thermal stability of LHCII proteins cannot be excluded.

Although we cannot distinguish between the contribution of these factors to resulting higher thermal stability of PSII function and structure in spruce thylakoid membranes, we suppose that different lipid-protein interaction together with different structure of PSII supercomplexes play a crucial role.

4.3. Long-term acclimation response of photosynthetic apparatus to different growth light intensity

Up to now it has been thought that protein composition of both photosystems is highly conserved among higher plants (Croce and van Amerongen 2011). Particularly the presence of Lhcb6 and Lhcb3 proteins has been determined as the characteristic evolutionary difference between the land plants and algae regarding the PSII protein composition, due to fact that *C. reinhardtii* is lacking both proteins (Ballottari et al. 2012). It has been proposed that absence of Lhcsr, involved in photoprotective ΔpH- and zeaxanthin-dependent energy dissipation in green algae such as *C. reinhardtii* (Koziol et al. 2007; Peers et al. 2009), and appearance of PsbS protein overtaking this function in higher plants is another evolutionary step from algae to land plants (Goss and Lepetit 2015; Niyogi and Truong 2013). Moreover, some evolutionary older land species, e.g. *Physcomitrella patens* retain both of these PSII regulatory proteins (Alboresi et al. 2010). Recently, the loss of both Lhcb6 (CP24) and Lhcb3 proteins was confirmed in some gymnosperm genera such as *Picea* (Kouřil et al. 2016), resulting in modified structural organization of LHCII trimers in PSII-LHCII

supercomplexes of spruce in comparison to *Arabidopsis*, but similar to that observed in *C. reinhardtii* (Kouřil et al. 2016). Further, possible presence of the Lhcsr protein together with PsbS in some species of *Pinaceae* family was outlined (Dittami et al. 2010; Kouřil et al. 2016). In addition, in comparison with *Arabidopsis* different composition of lipids and fatty acids is known in spruce thylakoids (Attachment I; Karlický et al. 2016) or generally in gymnosperms (Mongrand et al. 2001), again more similar to that observed in evolutionarily older organisms such as mosses, ferns or algae as well (Karunen 1990; Mongrand et al. 2001). All these findings indicate that spruce could possess a different mechanism of NPQ and long-term acclimation response to different growth light intensity than other land plants. The aim of this work was to examine acclimation responses of pigment composition and PPCs organization in thylakoid membranes to LL and HL, particularly in comparison with acclimation responses of model plants such as *Arabidopsis* and barley.

Earlier, we studied acclimation responses of barley grown at 50, 300 and 1000 µmol photons m^{-2} s^{-1} using biochemical and spectroscopical analyses of leaves and individual PPCs in order to contribute to elucidation of processes associated with regulation of functional size of PSII antenna *in vivo* (details in attachment IV). Gradual reduction of PSII antenna size was revealed in barley leaves grown under LL, ML and HL light intensities by Chl *a*/*b* ratio and the 77K fluorescence excitation spectra of PSII. The excitation spectra of individual PSII-LHCII supercomplexes and LHCII trimers, separated from thylakoids isolated from LL, ML and HL plants, revealed no reduction of the Chl *b* and Car excitation bands with increasing growth light, suggesting that variations in the functional antenna size originate from changes in the macro-organization and/or composition of PPCs of thylakoid membranes. CD spectra of intact barley leaves revealed gradual decline in the long-range chiral order of PPCs with increasing growth light intensities. Analysis of the composition of LHCII proteins separated by CN-PAGE corresponded to the gradually reduced amounts of trimers forming major LHCII subunits, Lhcb1 and Lhcb2, and particularly the LHCII subunits related to PSII M-trimers, Lhcb3 and Lhcb6, with enhanced growth light intensity. Overall, the acclimation to different growth light intensity in barley were similar as described in *Arabidopsis* (Bielczynski et al. 2016; Kouřil et al. 2013), indicating the same main features of acclimation to different growth light intensity in dicotyledons (represented by *Arabidopsis*) and monocotyledons (barley), for the first time studied from this point of view. In order to identify possible

peculiar HL responses in specific clades of monocotyledons or dicotyledons more detailed analysis would be needed.

In the following paragraphs I describe several interesting findings arising on the experiments with spruce seedlings. Norway spruce seedlings were grown from seeds in a growth chamber at 100 µmol photons m^{-2} s^{-1} (17 days). Afterwards parts of seedlings were acclimated to LL (20 µmol photons m^{-2} s^{-1}) and HL (800 µmol photons m^{-2} s^{-1}) lights for 10 days, whereas control plants continued to grow under original (normal) light (ML).

Firstly, modulability of the Chl *a*/*b* ratio and the amount of LHCII upon HL and LL acclimation is not a universal property of all land plants. This capability is lacking in bryophytes (Gerotto et al. 2011) and also in early diverging vascular plants, lycophytes (Ferroni et al. 2016). Previous study on mature spruce needles indicated that also photosynthetic apparatus of spruce could be unable to adjust light harvesting antennas during acclimation to different light intensity as determined by from Chl *a*/*b* ratios and fluorescence excitation spectra (Kurasová et al. 2003; Štroch et al. 2008a). Nevertheless, young spruce seedlings revealed increased Chl *a*/*b* ratio under HL (Table 2) indicating the ability to modulate the antenna size similarly as observed in different species of angiosperms (Bielczynski et al. 2016; Kouřil et al. 2013) (attachment IV). Likewise, decreases of Chl *b* and Cars excitation band (460-490 nm) in 77K fluorescence excitation spectra demonstrated reduced antenna size of both, PSII and PSI with increasing acclimation light intensity (Fig. 20A,B).

Table 2 Pigment analysis of plants grown under different light conditions.

Light intensity	LL	NL	HL
Chl *a* /*b*	2,59 ± 0,04^{a}	2,76 ± 0,05^{b}	3,03 ± 0,10^{c}
Car x + c/1000 Chl *a*	261,6 ± 4,7^{a}	265,3 ± 3,2^{a}	365,4 ± 15,4^{b}
L/1000 Chl *a*	108,1 ± 1,1^{a}	116,0 ± 7,5^{a}	189,1 ± 9,0^{b}
VAZ/1000 Chl *a*	25,7 ± 4,8^{a}	26,2 ± 4,6^{a}	44,0 ± 12,5^{b}
N/1000 Chl *a*	33,2 ± 0,7^{a}	35,8 ± 1,8^{a}	35,9 ± 1,7^{a}
α + β-Car/1000 Chl *a*	93,2 ± 1,6^{a}	95,3 ± 2,9^{a}	79,9 ± 5,1^{b}
α Car/β-Car	1,52 ± 0,05^{a}	1,31 ± 0,06^{b}	0,37 ± 0,05^{c}

Chlorophyll *a* /chlorophyll *b* (Chl *a* /*b*) and total carotenoids/Chl *a* (Car x + c/Chl *a*) ratios determined spectroscopically from 80% acetone needle extracts. The same extracts were used for the quantification by HPLC of the carotenoids per 1000 Chl *a*. The values represent the means SD of 6 determinations. Data within a row followed by the same letter are not significantly different (P > 0:05).L, lutein V, violaxanthin; A, antheraxanthin; Z, zeaxanthin; N, neoxanthin; α, β-Car, α, β - carotene.

Secondly, the higher Cars/Chls ratio in HL spruce seedlings in comparison with LL and ML ones was particularly due to relative increase of lutein and VAZ pool (Table 2). Acclimation response of Car composition to HL in spruce differs from *Arabidopsis* (Bielczynski et al. 2016) or barley (attachment IV), which revealed more pronounced increase of VAZ pool size and only slight changes of lutein content. Again, such increased amount of lutein was observed in evolutionarily earlier plant species such as algal species *C. reinhardtii* acclimated to HL, in which concomitant accumulation of lutein and Lhcsr3 is likely responsible for enhanced capacity of excess energy dissipation in HL acclimated cells (Bonente et al. 2012). Very recently, it was demonstrated that pH-dependent and zeaxanthin-independent reductive quenching mechanism is active in Lhcsr1 from *Physcomitrella patens*, which result in formation of lutein radical cation and Chl *a* radical anion (Pinnola et al. 2016). Acclimation response of Car composition of spruce suggests possible presence of the Lhcsr protein in spruce.

Thirdly, CD spectra of isolated thylakoid membranes demonstrated reduced macro-organisation of the PPCs in the thylakoid membranes under higher light intensities (Fig.20C). HL spruce seedlings revealed almost none Ψ-type CD signal (Fig.20C), that indicate disappearance of long-range ordered PSII-LHCII supercomplexes in the membrane plane in HL spruce. Similar response of reduced Ψ-type CD bands with increasing acclimation light intensities was observed in barley (attachment IV) although Ψ-type CD magnitudes were significantly greater than in spruce, under all light conditions (Fig. 21). Since Ψ-type CD signal originates from macrodomains consisting of the PSII-LHCII supercomplexes (the (+)685 and the (+)505 nm Ψ-type CD bands, Fig. 9) and LHCII-only domain (the (+)685 and the (−)674 nm Ψ-type CD bands, Fig. 9), main Ψ-type CD at (+)685 nm and (+)685/(+)505 Ψ-type CD ratio correlate with Chl *a*/*b* ratio, which roughly express LHCII/PSII core ratio (Toth et al. 2016) (Fig. 21). As seen in Fig. 21, this correlation is different for spruce and angiosperms species reflecting distinct structure of PSII-LHCII, building blocks of the long-range ordered domains.

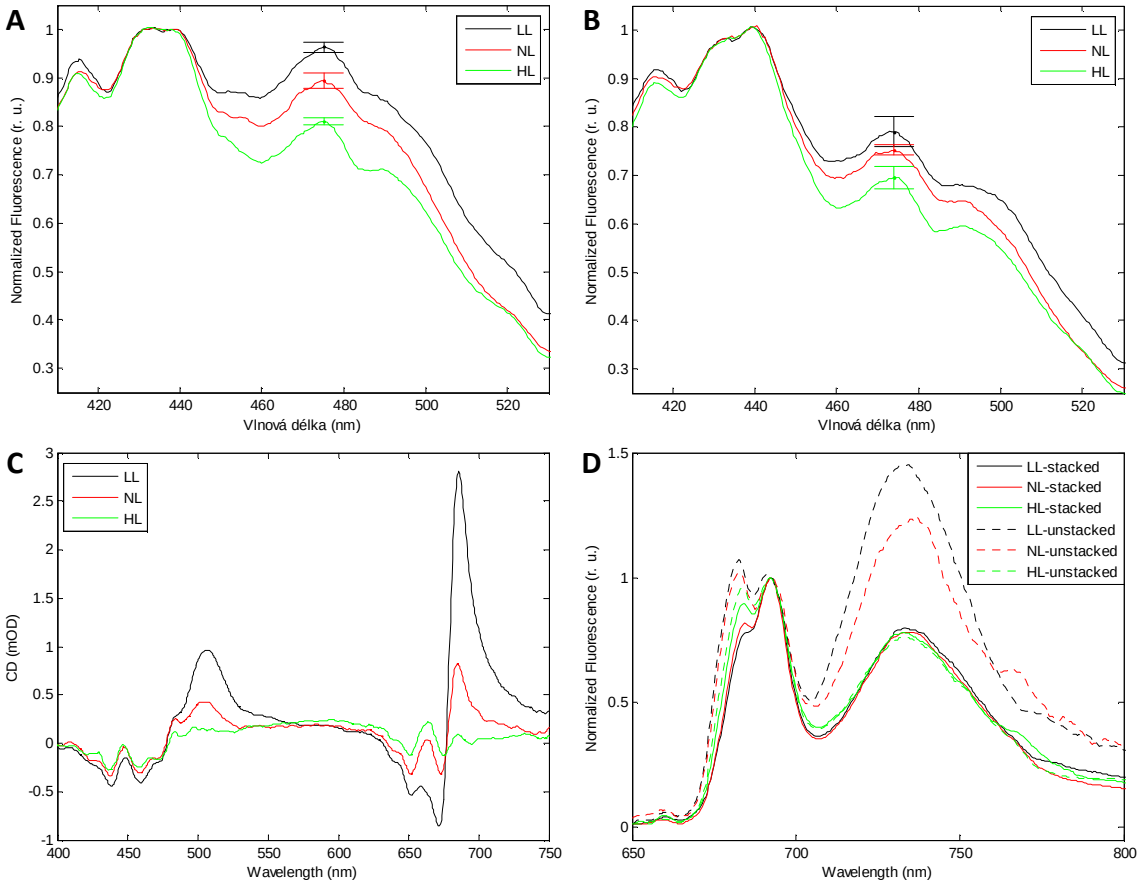

Fig. 20: *Normalized 77 K fluorescence excitation spectra of PSII (**A**) and PSI (**B**), room temperature circular dichroism spectra (**C**) and normalized 77 K fluorescence emission spectra (**D**) measured on stacked and unstacked (indicated in the legend) thylakoid membranes isolated from spruce seedlings acclimated to low (LL), normal (NL) and high (HL) intensity of light. Emission spectra were excited at wavelength of 476 nm and excitation spectra were collected at wavelength of 685 nm (PSII) and 735 nm (PSI). Average spectra and standard deviations from three independent experiments (n = 3) are presented.*

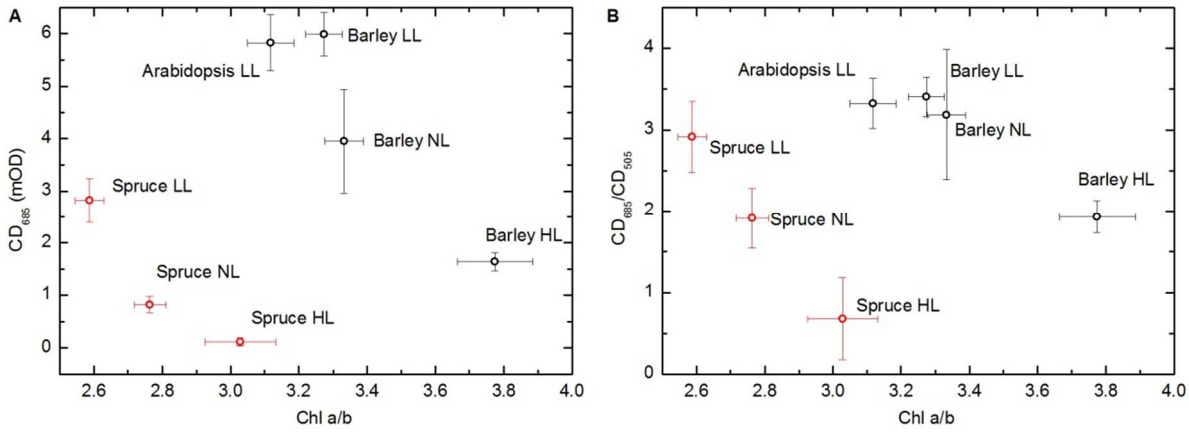

Fig. 21: *Correlation between the positive Ψ-type CD band and the Chl a/b ratios. Correlation of the amplitude of (+)685 with Chl a/b (A) and the correlation of the (+)685/(+)505 peak ratio with Chl a/b. The amplitudes of CD bands are normalized to the red maximum of the Chl a absorption band.*

Finally, in the presence of cations (NaCl and $MgCl_2$), LHCII is tightly connected with PSII in stacked grana regions (Kirchhoff et al. 2007), which resulted in high fluorescence emission from the PSII complexes (Fig. 20D). Depletion of cations in the buffer induced unstacking of the grana thylakoids accompanied by lateral disorganisation of PSII and LHCII (intermixing and randomization of the proteins, especially PSII, LHCII and PSI) and caused a spillover of excitation energy from LHCII to PSI (Kirchhoff et al. 2007) as indicated by increased fluorescence emission from the PSI complex (Fig. 20D). Almost identical 77K fluorescence emission spectra of HL spruce thylakoid membranes under stacked and unstacked conditions indicate very low segregation of PPCs in granal and lamellar thylakoids *in vivo*, under HL conditions.

5. CONCLUSIONS AND FUTURE PERSPECTIVES

I have investigated structure-functional characteristics of PPCs, and their macro-organization and stability in thylakoid membranes in three different species of higher plants, Norway spruce belonging to the gymnosperms and model plants from angiosperms, *Arabidopsis* thaliana and spring barley. Information on the molecular organization and their structural stabilities were obtained mainly from spectroscopic techniques, including circular dichroism spectroscopy and low temperature fluorescence, as well as from biochemical analyses.

The results of my work can be summarized as follows:

I. We showed that main specific signatures of low temperature fluorescence emission spectra on intact leaves/needles remain at the level of isolated thylakoids after removal of reabsorption and PSII-LHCII and PSI-LHCI supercomplexes. Low temperature fluorescence emission of PSII-LHCII supercomplexes from spruce peaked at around 692 nm compared to those of *Arabidopsis* and barley, which revealed maximum at wavelength of 685 nm.

II. Thylakoid membranes of spruce possess enhanced thermal stability of PSII photochemistry than in other plants (*Arabidopsis*, barley) cultivated under the same temperatures. Our data show that higher thermal stability of PSII photochemistry of spruce is accompanied by the maintenance of PSII macro-organization. In addition, clear-native polyacrylamide gel electrophoresis of preheated thylakoids demonstrated that higher thermal stability of PSII macro-organization of spruce is associated with the maintenance of PSII-LHCII supercomplexes in the membrane.

III. Photosynthetic apparatus of spruce revealed different long-term acclimation response to different growth light intensity than other higher plants such as barley (attachment 4) or *Arabidopsis*. In contrast to previous study on mature spruce needles (Kurasová et al. 2003; Štroch et al. 2008a), young spruce seedlings exhibit ability to adjust light harvesting antennas during acclimation to different light intensity, similarly as observed in other higher plants (Bielczynski et al. 2016; Kouřil et al. 2013) (attachment IV). The pronounced increase in lutein content in seedlings acclimated to HL differs from acclimation response of *Arabidopsis* (Bielczynski et al. 2016) or barley (attachment IV) characterized by only slight changes of lutein content.

In the following section I would like to address a few questions, work in progress and plans for the near future, which are not discussed or only marginally treated in the dissertation but nevertheless constitute important parts of work on this field:

I. During my research stay in Biological Research Centre in Szeged I have participated in experiments focused on signatures of oriented thylakoid membranes using anisotropic CD (attachment IV; Miloslavina et al. 2012). It was found that the anisotropic CD spectra of face- and edge-aligned stacked thylakoid membranes exhibit substantial differences in their Ψ-type CD bands. Also excitonic CD of unstacked thylakoid membranes revealed appreciable differences. Nevertheless, the theoretical approach has to be further developed in order to interconnect structural data with the spectral signatures. This might help to use the full potential of anisotropic CD to improve current understanding of Ψ-type CD in further studies.

II. Based on different structural organization of LHCII in spruce PSII-LHCII supercomplexes accompanied by red shift of 77K Chl *a* fluorescence emission maximum and smaller macrodomain organization in spruce membranes as compared to *Arabidopsis* and barley we started comparative spectroscopic experiments focusing on excitonic interactions and excitation energy transfer in PSII-LHCII supercomplexes of spruce and *Arabidopsis* (work is in progress).

III. Up till now long-term acclimation of spruce photosynthetic apparatus to different growth light intensity could not be studied biochemically on the level of PPCs using native electrophoresis due to difficulties with solubilization of thylakoid membranes from HL acclimated spruce seedlings. We found that this is caused by high contents of charged lipids, and that changes in the content of lipids and fatty acids play important role in long-term acclimation of spruce photosynthetic apparatus to different growth light intensity. Again the pronounced changes in lipid composition in spruce seedlings acclimated to HL correspond rather to the response of green algae thylakoids (*C. reinhardtii*) acclimated to HL than to that typically found in model higher plants

IV. As mentioned above, there are particular responses of spruce to HL including different acclimation strategy to HI, e.g. lutein accumulation indicating enhanced involvement of Lhcsr in photoprotective processes in spruce acclimated to HL and

extremely altered macro-organization of PPCs suggesting loss of typical spatial segregation of PSI and PSII in granal and or stromal membranes. Thus altered lipid and protein composition is related to several structure-functional particularities. This opens an attractive field of future research aimed at elucidation of structural and functional flexibility of thylakoid membranes related to different short- and long-term response of photosynthetic apparatus to changing environmental conditions. We plan an implementation of advanced biophysical methods such as small-angle neutron scattering, phosphorus 31 nuclear magnetic resonance spectroscopy, time-resolved fluorescence spectroscopy or anisotropic CD spectroscopy for further research in order to obtain additional information on the architecture of spruce thylakoid membranes and organization of PPCs, with focus on their flexibility.

6. ACKNOWLEDGEMENTS

I would like to thank to my supervisor Assoc. prof. RNDr. Vladimír Špunda CSc. for his great support in all aspects of my research carrier and his help in the theoretical and practical work during my PhD studies.

I would like to thank to my co-supervisor Prof. RNDr. Petr Ilík Ph.D. for supporting my work at Department of Biophysics in Olomouc.

I would like to thank to Assoc. prof. Dr. Otmar Urban Ph.D. to the possibility to perform part of my research work at the Global Change Research Institute CAS in Brno and his valuable guidance.

Special thanks to Dr. Győző Garab and Dr. Petar Lambrev, who supported me during my research stay in Szeged and gave me an excellent basis and advices regarding circular dichroism spectroscopy.

I would like to thank to all my colleagues in our research group in Ostrava, Olomouc and Brno for all the technical and personal help and for the fruitful discussions.

Last but not least I would like to express my warmest thanks to my wife and my family for their support during all my research carrier and encouragements.

This work was supported by Grants Agency of the Czech Republic (13-28093S/P501, 522-08-H003), the Grant Number LO1415 under the National Sustainability Program I (NPU I, Ministry of Education, Youth and Sports of CR) and Internal grant of Palacký University (PrF_2010_050)

7. REFERENCES

Agati G, Cerovic ZG, Pinelli P, Tattini M (2011) Light-induced accumulation of ortho-dihydroxylated flavonoids as non-destructively monitored by chlorophyll fluorescence excitation techniques. Environ Exp Bot 73:3-9 doi: 10.1016/j.envexpbot.2010.10.002

Albanese P, Manfredi M, Meneghesso A, Marengo E, Saracco G, Barber J, Morosinotto T, Pagliano C (2016) Dynamic reorganization of photosystem II supercomplexes in response to variations in light intensities. Biochim Biophys Acta 1857:1651-1660 doi: 10.1016/j.bbabio.2016.06.011

Alboresi A, Gerotto C, Giacometti GM, Bassi R, Morosinotto T (2010) Physcomitrella patens mutants affected on heat dissipation clarify the evolution of photoprotection mechanisms upon land colonization. Proc Natl Acad Sci U S A 107:11128-11133 doi: 10.1073/pnas.1002873107

Allakhverdiev SI, Kreslavski VD, Klimov VV, Los DA, Carpentier R, Mohanty P (2008) Heat stress: an overview of molecular responses in photosynthesis. Photosynth Res 98:541-550 doi: 10.1007/s11120-008-9331-0

Amunts A, Drory O, Nelson N (2007) The structure of a plant photosystem I supercomplex at 3.4 angstrom resolution. Nature 447:58-63 doi: 10.1038/nature05687

Anderson JM, Chow WS, Park YI (1995) The grand design of photosynthesis: Acclimation of the photosynthetic apparatus to environmental cues. Photosynth Res 46:129-139 doi: 10.1007/Bf00020423

Austin JR, 2nd, Staehelin LA (2011) Three-dimensional architecture of grana and stroma thylakoids of higher plants as determined by electron tomography. Plant Physiol 155:1601-1611 doi: 10.1104/pp.110.170647

Bailey S, Walters RG, Jansson S, Horton P (2001) Acclimation of Arabidopsis thaliana to the light environment: the existence of separate low light and high light responses. Planta 213:794-801 doi: 10.1007/s004250100556

Ballottari M, Girardon J, Dall'Osto L, Bassi R (2012) Evolution and functional properties of Photosystem II light harvesting complexes in eukaryotes. Biochim Biophys Acta-Bioenerg 1817:143-157 doi: 10.1016/j.bbabio.2011.06.005

Banas AK, Aggarwal C, Labuz J, Sztatelman O, Gabrys H (2012) Blue light signalling in chloroplast movements. J Exp Bot 63:1559-1574 doi: 10.1093/Jxb/Err429

Ben-Shem A, Frolow F, Nelson N (2003) Crystal structure of plant photosystem I. Nature 426:630-635 doi: 10.1038/nature02200

Berry J, Bjorkman O (1980) Photosynthetic Response and Adaptation to Temperature in Higher-Plants. Annu Rev Plant Phys 31:491-543 doi: 10.1146/annurev.pp.31.060180.002423

Bielczynski LW, Schansker G, Croce R (2016) Effect of Light Acclimation on the Organization of Photosystem II Super- and Sub-Complexes in Arabidopsis thaliana. Front Plant Sci 7:105 doi: 10.3389/fpls.2016.00105

Boekema EJ, van Breemen JFL, van Roon H, Dekker JP (2000) Arrangement of photosystem II supercomplexes in crystalline macrodomains within the thylakoid membrane of green plant chloroplasts. J Mol Biol 301:1123-1133 doi: 10.1006/jmbi.2000.4037

Boekema EJ, van Roon H, van Breemen JFL, Dekker JP (1999) Supramolecular organization of photosystem II and its light-harvesting antenna in partially solubilized photosystem II membranes. Eur J Biochem 266:444-452 doi: 10.1046/j.1432-1327.1999.00876.x

Bonente G, Pippa S, Castellano S, Bassi R, Ballottari M (2012) Acclimation of Chlamydomonas reinhardtii to Different Growth Irradiances. J Biol Chem 287:5833-5847 doi: 10.1074/jbc.M111.304279

Brestič M, Živčák M, Kalaji HM, Carpentier R, Allakhverdiev SI (2012) Photosystem II thermostability in situ: Environmentally induced acclimation and genotype-specific reactions in Triticum aestivum L. Plant Physiol Biochem 57:93-105 doi: 10.1016/j.plaphy.2012.05.012

Bugos RC, Chang SH, Yamamoto HY (1999) Developmental expression of violaxanthin de-epoxidase in leaves of tobacco growing under high and low light. Plant Physiol 121:207-213 doi: 10.1104/pp.121.1.207

Caffarri S, Kouřil R, Kereiche S, Boekema EJ, Croce R (2009) Functional architecture of higher plant photosystem II supercomplexes. Embo J 28:3052-3063 doi: 10.1038/emboj.2009.232

Caffarri S, Tibiletti T, Jennings RC, Santabarbara S (2014) A Comparison Between Plant Photosystem I and Photosystem II Architecture and Functioning. Curr Protein Pept Sc 15:296-331

Correa-Galvis V, Poschmann G, Melzer M, Stuhler K, Jahns P (2016) PsbS interactions involved in the activation of energy dissipation in Arabidopsis. Nat Plants 2:15225 doi: 10.1038/nplants.2015.225

Cramer WA, Whitmarsh J, Low PS (1981) Differential scanning calorimetry of chloroplast membranes: identification of an endothermic transition associated with the water-splitting complex of photosystem II. Biochemistry 20:157-162

Croce R (2015) PsbS is the plants' pick for sun protection. Nat Struct Mol Biol 22:650-652 doi: 10.1038/nsmb.3079

Croce R, van Amerongen H (2011) Light-harvesting and structural organization of Photosystem II: From individual complexes to thylakoid membrane. J Photochem Photobiol B-Biol 104:142-153 doi: 10.1016/j.jphotobiol.2011.02.015

Croce R, van Amerongen H (2013) Light-harvesting in photosystem I. Photosynth Res 116:153-166 doi: 10.1007/s11120-013-9838-x

Cseh Z, Rajagopal S, Tsonev T, Busheva M, Papp E, Garab G (2000) Thermooptic effect in chloroplast thylakoid membranes. Thermal and light stability of pigment arrays with different levels of structural complexity. Biochemistry 39:15250-15257 doi: 10.1021/Bi001600d

Čajánek M, Navrátil M, Kurasová I, Kalina J, Špunda V (2002) The development of antenna complexes of barley (Hordeum vulgare cv. Akcent) under different light conditions as judged from the analysis of 77 K chlorophyll a fluorescence spectra. Photosynth Res 74:121-133 doi: 10.1023/A:1020943107318

Dall'Osto L, Caffarri S, Bassi R (2005) A mechanism of nonphotochemical energy dissipation, independent from PsbS, revealed by a conformational change in the antenna protein CP26. Plant Cell 17:1217-1232 doi: 10.1105/tpc.104.030601

Dall'Osto L, Cazzaniga S, Wada M, Bassi R (2014) On the origin of a slowly reversible fluorescence decay component in the Arabidopsis npq4 mutant. Philos Trans R Soc Lond B Biol Sci 369:20130221 doi: 10.1098/rstb.2013.0221

de la Torre WR, Burkey KO (1990) Acclimation of Barley to Changes in Light-Intensity - Chlorophyll Organization. Photosynth Res 24:117-125 doi: 10.1007/BF00032592

Dekker JP, Boekema EJ (2005) Supramolecular organization of thylakoid membrane proteins in green plants. Biochim Biophys Acta-Bioenerg 1706:12-39 doi: 10.1016/j.bbabio.2004.09.009

Dekker JP, Hassoldt A, Pettersson A, vanRoon H, Groot ML, vanGrondelle R (1995) On the nature of the F695 and F685 emission of photosystem II. Photosynthesis: From Light to Biosphere, Vol I:53-56

DelasRivas J, Barber J (1997) Structure and thermal stability of photosystem II reaction centers studied by infrared spectroscopy. Biochemistry 36:8897-8903 doi: 10.1021/bi970684w

Demmig-Adams B (1998) Survey of thermal energy dissipation and pigment composition in sun and shade leaves. Plant Cell Physiol 39:474-482

Demmig-Adams B, Garab G, Adams III W, Govindjee (eds) (2014) Non-Photochemical Quenching and Energy Dissipation in Plants, Algae and Cyanobacteria. Advances in Photosynthesis and Respiration, vol 40. Springer Netherlands, Berlin; Heidelberg. doi:10.1007/978-94-017-9032-1

Devoe H (1965) Optical Properties of Molecular Aggregates .2. Classical Theory of Refraction Absorption and Optical Activity of Solutions and Crystals. J Chem Phys 43:3199-& doi: 10.1063/1.1697294

Dinamarca J, Shlyk-Kerner O, Kaftan D, Goldberg E, Dulebo A, Gidekel M, Gutierrez A, Scherz A (2011) Double mutation in photosystem II reaction centers and elevated CO2 grant thermotolerance to mesophilic cyanobacterium. PLoS One 6:e28389 doi: 10.1371/journal.pone.0028389

Dittami SM, Michel G, Collen J, Boyen C, Tonon T (2010) Chlorophyll-binding proteins revisited - a multigenic family of light-harvesting and stress proteins from a brown algal perspective. BMC Evol Biol 10 doi: 10.1186/1471-2148-10-365

Dobrikova AG, Varkonyi Z, Krumova SB, Kovacs L, Kostov GK, Todinova SJ, Busheva MC, Taneva SG, Garab G (2003) Structural Rearrangements in chloroplast thylakoid membranes revealed by differential scanning calorimetry and circular dichroism spectroscopy. Thermo-optic effect. Biochemistry 42:11272-11280 doi: 10.1021/bi034899j

Dunn JL, Turnbull JD, Robinson SA (2004) Comparison of solvent regimes for the extraction of photosynthetic pigments from leaves of higher plants. Funct Plant Biol 31:195-202 doi: 10.1071/Fp03162

Epron D (1997) Effects of drought on photosynthesis and on the thermotolerance of photosystem II in seedlings of cedar (Cedrus atlantica and C-libani). J Exp Bot 48:1835-1841 doi: 10.1093/jexbot/48.315.1835

Evans JR (1987) The Relationship between Electron-Transport Components and Photosynthetic Capacity in Pea Leaves Grown at Different Irradiances. Aust J Plant Physiol 14:157-170

Farber A, Jahns P (1998) The xanthophyll cycle of higher plants: influence of antenna size and membrane organization. Biochim Biophys Acta-Bioenerg 1363:47-58 doi: 10.1016/S0005-2728(97)00093-5

Ferroni L, Suorsa M, Aro EM, Baldisserotto C, Pancaldi S (2016) Light acclimation in the lycophyte Selaginella martensii depends on changes in the amount of photosystems and on the flexibility of the light-harvesting complex II antenna association with both photosystems. New Phytol doi: 10.1111/nph.13939

Froux F, Ducrey M, Epron D, Dreyer E (2004) Seasonal variations and acclimation potential of the thermostability of photochemistry in four Mediterranean conifers. Annals of Forest Science 61:235-241 doi: 10.1051/forest:2004016

Garab G (2014) Hierarchical organization and structural flexibility of thylakoid membranes. Biochim Biophys Acta-Bioenerg 1837:481-494 doi: 10.1016/j.bbabio.2013.12.003

Garab G (2016) Self-assembly and structural-functional flexibility of oxygenic photosynthetic machineries: personal perspectives. Photosynth Res 127:131-150 doi: 10.1007/s11120-015-0192-z

Garab G, Cseh Z, Kovacs L, Rajagopal S, Varkonyi Z, Wentworth M, Mustardy L, Der A, Ruban AV, Papp E, Holzenburg A, Horton P (2002) Light-induced trimer to monomer transition in the main light-harvesting antenna complex of plants: Thermo-optic mechanism. Biochemistry 41:15121-15129 doi: 10.1021/bi026157g

Garab G, Kieleczawa J, Sutherland JC, Bustamante C, Hind G (1991) Organization of Pigment Protein Complexes into Macrodomains in the Thylakoid Membranes of Wild-Type and Chlorophyll-B-Less Mutant of Barley as Revealed by Circular-Dichroism. Photochem Photobiol 54:273-281 doi: 10.1111/j.1751-1097.1991.tb02016.x

Garab G, Mustardy L (1999) Role of LHCII-containing macrodomains in the structure, function and dynamics of grana. Aust J Plant Physiol 26:649-658

Garab G, Ughy B, Goss R (2016) Role of MGDG and Non-bilayer Lipid Phases in the Structure and Dynamics of Chloroplast Thylakoid Membranes. Subcell Biochem 86:127-157 doi: 10.1007/978-3-319-25979-6_6

Garab G, van Amerongen H (2009) Linear dichroism and circular dichroism in photosynthesis research. Photosynth Res 101:135-146 doi: 10.1007/s11120-009-9424-4

Garab G, Wells S, Finzi L, Bustamante C (1988) Helically Organized Macroaggregates of Pigment Protein Complexes in Chloroplasts - Evidence from Circular Intensity Differential Scattering. Biochemistry 27:5839-5843 doi: 10.1021/bi00416a003

Gerotto C, Alboresi A, Giacometti GM, Bassi R, Morosinotto T (2011) Role of PSBS and LHCSR in Physcomitrella patens acclimation to high light and low temperature. Plant Cell Environ 34:922-932 doi: 10.1111/j.1365-3040.2011.02294.x

Ghouil H, Montpied P, Epron D, Ksontini M, Hanchi B, Dreyer E (2003) Thermal optima of photosynthetic functions and thermostability of photochemistry in cork oak seedlings. Tree Physiol 23:1031-1039

Goldschmidt-Clermont M, Bassi R (2015) Sharing light between two photosystems: mechanism of state transitions. Curr Opin Plant Biol 25:71-78 doi: 10.1016/j.pbi.2015.04.009

Gombos Z, Wada H, Hideg E, Murata N (1994) The Unsaturation of Membrane-Lipids Stabilizes Photosynthesis against Heat-Stress. Plant Physiol 104:563-567

Goss R, Lepetit B (2015) Biodiversity of NPQ. J Plant Physiol 172:13-32 doi: 10.1016/j.jplph.2014.03.004

Guskov A, Kern J, Gabdulkhakov A, Broser M, Zouni A, Saenger W (2009) Cyanobacterial photosystem II at 2.9-A resolution and the role of quinones, lipids, channels and chloride. Nat Struct Mol Biol 16:334-342 doi: 10.1038/nsmb.1559

Hankamer B, Morris E, Nield J, Gerle C, Barber J (2001) Three-dimensional structure of the photosystem II core dimer of higher plants determined by electron microscopy. J Struct Biol 135:262-269 doi: 10.1006/jsbi.2001.4405

Harwood JL (1998) Involvement of chloroplast lipids in the reaction of plants submitted to stress. In: Siegenthaler PA, Murata, N. (ed) Lipids in Photosynthesis: Structure,

Function and Genetics. Kluwer Academic Publishers, Dordrecht, The Netherlands, pp 290–300

Havaux M, Dall'Osto L, Bassi R (2007) Zeaxanthin has enhanced antioxidant capacity with respect to all other xanthophylls in Arabidopsis leaves and functions independent of binding to PSII antennae(1 C W). Plant Physiol 145:1506-1520 doi: 10.1104/pp.107.108480

Havaux M, Niyogi KK (1999) The violaxanthin cycle protects plants from photooxidative damage by more than one mechanism. Proc Natl Acad Sci U S A 96:8762-8767 doi: 10.1073/pnas.96.15.8762

Horton P, Ruban AV, Walters RG (1996) Regulation of light harvesting in green plants. Annu Rev Plant Phys 47:655-684 doi: 10.1146/annurev.arplant.47.1.655

Hu ZH, Xu YN, Jiang GZ, Kuang TY (2004) Degradation and inactivation of photosystem I complexes during linear heating. Plant Sci 166:1177-1183 doi: 10.1016/j.plantsci.2003.12.026

Chen HX, Li WJ, An SZ, Gao HY (2004) Characterization of PSII photochemistry and thermostability in salt-treated Rumex leaves. J Plant Physiol 161:257-264 doi: 10.1078/0176-1617-01231

Ilík P, Krchňák P, Tomek P, Nauš J (2002) 2-D gel densitometer for high-contrast and selective imaging of chlorophyll-containing protein complexes separated by non-denaturing polyacrylamide gel electrophoresis. J Biochem Biophys Methods 51:273-281 doi: 10.1016/S0165-022x(02)00029-5

Jahns P, Holzwarth AR (2012) The role of the xanthophyll cycle and of lutein in photoprotection of photosystem II. Biochim Biophys Acta-Bioenerg 1817:182-193 doi: 10.1016/j.bbabio.2011.04.012

Järvi S, Suorsa M, Paakkarinen V, Aro EM (2011) Optimized native gel systems for separation of thylakoid protein complexes: novel super- and mega-complexes. Biochem J 439:207-214 doi: 10.1042/bj20102155

Johnson MP (2016) Photosynthesis. Essays Biochem 60:255-273 doi: 10.1042/EBC20160016

Johnson MP, Ruban AV (2011) Restoration of Rapidly Reversible Photoprotective Energy Dissipation in the Absence of PsbS Protein by Enhanced Delta pH. J Biol Chem 286:19973-19981 doi: 10.1074/jbc.M111.237255

Kalisch B, Dörmann P, Hölzl G (2016) DGDG and Glycolipids in Plants and Algae. In: Nakamura Y, Li-Beisson Y (eds) Lipids in Plant and Algae Development. Springer International Publishing,

Karlický V, Kurasová I, Ptáčková B, Večeřová K, Urban O, Špunda V (2016) Enhanced thermal stability of the thylakoid membranes from spruce. A comparison with selected angiosperms. Photosynth Res 130:357-371 doi: 10.1007/s11120-016-0269-3

Karlický V, Podolinská J, Nadkanská L, Štroch M, Čajánek M, Špunda V (2010) Pigment composition and functional state of the thylakoid membranes during preparation of samples for pigment-protein complexes separation by nondenaturing gel electrophoresis. Photosynthetica 48:475-480 doi: 10.1007/s11099-010-0063-y

Karunen P (1990) Galactolipid fatty-fcids of bryophytes. Plant lipid biochemistry, structure and utilization:30-32

Keller D, Bustamante C (1986) Theory of the Interaction of Light with Large Inhomogeneous Molecular Aggregates .2. Psi-Type Circular-Dichroism. J Chem Phys 84:2972-2980 doi: 10.1063/1.450278

Kirchhoff H, Haase W, Haferkamp S, Schott T, Borinski M, Kubitscheck U, Rogner M (2007) Structural and functional self-organization of photosystem II in grana thylakoids. Biochim Biophys Acta-Bioenerg 1767:1180-1188 doi: 10.1016/j.bbabio.2007.05.009

Knight CA, Ackerly DD (2002) An ecological and evolutionary analysis of photosynthetic thermotolerance using the temperature-dependent increase in fluorescence. Oecologia 130:505-514 doi: 10.1007/s00442-001-0841-0

Kouřil R, Dekker JP, Boekema EJ (2012) Supramolecular organization of photosystem II in green plants. Biochim Biophys Acta-Bioenerg 1817:2-12 doi: 10.1016/j.bbabio.2011.05.024

Kouřil R, Nosek L, Bartoš J, Boekema EJ, Ilík P (2016) Evolutionary loss of light-harvesting proteins Lhcb6 and Lhcb3 in major land plant groups - break-up of current dogma. New Phytol 210:808-814 doi: 10.1111/nph.13947

Kouřil R, Wientjes E, Bultema JB, Croce R, Boekema EJ (2013) High-light vs. low-light: Effect of light acclimation on photosystem II composition and organization in Arabidopsis thaliana. Biochim Biophys Acta-Bioenerg 1827:411-419 doi: 10.1016/j.bbabio.2012.12.003

Kouřil R, Zygadlo A, Arteni AA, de Wit CD, Dekker JP, Jensen PE, Scheller HV, Boekema EJ (2005) Structural characterization of a complex of photosystem I and light-harvesting complex II of Arabidopsis thaliana. Biochemistry 44:10935-10940 doi: 10.1021/bi051097a

Kovacs L, Damkjaer J, Kereiche S, Ilioaia C, Ruban AV, Boekema EJ, Jansson S, Horton P (2006) Lack of the light-harvesting complex CP24 affects the structure and function of the grana membranes of higher plant chloroplasts. Plant Cell 18:3106-3120 doi: 10.1105/tpc.106.045641

Koziol AG, Borza T, Ishida K, Keeling P, Lee RW, Durnford DG (2007) Tracing the evolution of the light-harvesting antennae in chlorophyll a/b-containing organisms. Plant Physiol 143:1802-1816 doi: 10.1104/pp.106.092536

Krumova SB, Laptenok SP, Kovacs L, Toth T, van Hoek A, Garab G, van Amerongen H (2010) Digalactosyl-diacylglycerol-deficiency lowers the thermal stability of thylakoid membranes. Photosynth Res 105:229-242 doi: 10.1007/s11120-010-9581-5

Krumova SB, Todinova SJ, Busheva MC, Taneva SG (2005) Kinetic nature of the thermal destabilization of LHCII macroaggregates. J Photochem Photobiol B-Biol 78:165-170 doi: 10.1016/j.jphotobiol.2004.11.005

Kurasová I, Čajánek M, Kalina J, Urban O, Špunda V (2002) Characterization of acclimation of Hordeum vulgare to high irradiation based on different responses of photosynthetic activity and pigment composition. Photosynth Res 72:71-83

Kurasová I, Kalina J, Štroch M, Urban O, Špunda V (2003) Acclimation of two distinct plant species, spring barley and Norway spruce, to combined effect of various irradiance and CO2 concentration during cultivation in controlled environment. Photosynthetica 41:513-523

Laczko-Dobos H, Szalontai B (2009) Lipids, Proteins, and Their Interplay in the Dynamics of Temperature-Stressed Membranes of a Cyanobacterium, Synechocystis PCC 6803. Biochemistry 48:10120-10128 doi: 10.1021/bi9011034

Latowski D, Akerlund HE, Strzalka K (2004) Violaxanthin de-epoxidase, the xanthophyll cycle enzyme, requires lipid inverted hexagonal structures for its activity. Biochemistry 43:4417-4420 doi: 10.1021/bi049652g

Lemeille S, Rochaix JD (2010) State transitions at the crossroad of thylakoid signalling pathways. Photosynth Res 106:33-46 doi: 10.1007/s11120-010-9538-8

Leong TY, Anderson JM (1984) Adaptation of the Thylakoid Membranes of Pea-Chloroplasts to Light Intensities .2. Regulation of Electron-Transport Capacities, Electron Carriers, Coupling Factor (Cf1) Activity and Rates of Photosynthesis. Photosynth Res 5:117-128 doi: 10.1007/Bf00028525

Lepetit B, Goss R, Jakob T, Wilhelm C (2012) Molecular dynamics of the diatom thylakoid membrane under different light conditions. Photosynth Res 111:245-257 doi: 10.1007/s11120-011-9633-5

Lichtenthaler HK (1987) Chlorophylls and Carotenoids - Pigments of Photosynthetic Biomembranes. Method Enzymol 148:350-382

Lindahl M, Yang DH, Andersson B (1995) Regulatory Proteolysis of the Major Light-Harvesting Chlorophyll a/B Protein of Photosystem-Ii by a Light-Induced Membrane-Associated Enzymatic System. Eur J Biochem 231:503-509 doi: 10.1111/j.1432-1033.1995.tb20725.x

Lípová L, Krchňák P, Komenda J, Ilík P (2010) Heat-induced disassembly and degradation of chlorophyll-containing protein complexes in vivo. Biochim Biophys Acta-Bioenerg 1797:63-70 doi: 10.1016/j.bbabio.2009.08.001

Liu ZF, Yan HC, Wang KB, Kuang TY, Zhang JP, Gui LL, An XM, Chang WR (2004) Crystal structure of spinach major light-harvesting complex at 2.72 angstrom resolution. Nature 428:287-292 doi: 10.1038/nature02373

Loll B, Kern J, Saenger W, Zouni A, Biesiadka J (2005) Towards complete cofactor arrangement in the 3.0 A resolution structure of photosystem II. Nature 438:1040-1044 doi: 10.1038/nature04224

Lu CM, Zhang JH (1999) Effects of water stress on photosystem II photochemistry and its thermostability in wheat plants. J Exp Bot 50:1199-1206

Makarenko SP, Konenkina TA, Suvorova GG, Oskorbina MV (2014) Seasonal changes in the fatty acid composition of Pinus sylvestris needle lipids. Russ J Plant Physiol 61:119-123 doi: 10.1134/S1021443713050105

Mathur S, Agrawal D, Jajoo A (2014) Photosynthesis: Response to high temperature stress. J Photochem Photobiol B-Biol 137:116-126 doi: 10.1016/j.jphotobiol.2014.01.010

Merzlyak MN, Melo TB, Naqvi KR (2008) Effect of anthocyanins, carotenoids, and flavonols on chlorophyll fluorescence excitation spectra in apple fruit: signature analysis, assessment, modelling, and relevance to photoprotection. J Exp Bot 59:349-359 doi: 10.1093/jxb/erm316

Miloslavina Y, Lambrev PH, Javorfi T, Varkonyi Z, Karlický V, Wall JS, Hind G, Garab G (2012) Anisotropic circular dichroism signatures of oriented thylakoid membranes and lamellar aggregates of LHCII. Photosynth Res 111:29-39 doi: 10.1007/s11120-011-9664-y

Minagawa J (2011) State transitions-The molecular remodeling of photosynthetic supercomplexes that controls energy flow in the chloroplast. Biochim Biophys Acta-Bioenerg 1807:897-905 doi: 10.1016/j.bbabio.2010.11.005

Moellering ER, Miller R, Benning C (2009) Molecular Genetics of Lipid Metabolism in the Model Green Alga Chlamydomonas reinhardtii. In: Wada H, Murata N (eds) Lipids in Photosynthesis: Essential and Regulatory Functions. Springer Netherlands, Dordrecht, The Netherlands, pp 139–155

Mongrand S, Badoc A, Patouille B, Lacomblez C, Chavent M, Cassagne C, Bessoule JJ (2001) Taxonomy of gymnospermae: multivariate analyses of leaf fatty acid composition. Phytochemistry 58:101-115 doi: 10.1016/S0031-9422(01)00139-X

Mustardy L, Buttle K, Steinbach G, Garab G (2008) The three-dimensional network of the thylakoid membranes in plants: quasihelical model of the granum-stroma assembly. Plant Cell 20:2552-2557 doi: 10.1105/tpc.108.059147

Nanjo Y, Mizusawa N, Wada H, Slabas AR, Hayashi H, Nishiyama Y (2010) Synthesis of fatty acids de novo is required for photosynthetic acclimation of Synechocystis sp PCC 6803 to high temperature. Biochim Biophys Acta-Bioenerg 1797:1483-1490 doi: 10.1016/j.bbabio.2010.03.014

Nauš J, Rolencová M, Hlaváčková V (2008) Is chloroplast movement in tobacco plants influenced systemically after local illumination or burning stress? J Integr Plant Biol 50:1292-1299 doi: 10.1111/j.1744-7909.2008.00743.x

Nield J (2011) Schematic models for the major protein complexes involved in photosynthesis. http://macromol.sbcs.qmul.ac.uk/oldsite/psIIimages/oxygenicphotosynthmodel.html .

Niyogi KK, Truong TB (2013) Evolution of flexible non-photochemical quenching mechanisms that regulate light harvesting in oxygenic photosynthesis. Curr Opin Plant Biol 16:307-314 doi: 10.1016/j.pbi.2013.03.011

Nosek L (2012) Usage of 2D-CN/SDS-PAGE for determination of changes in pigment-protein complexes from thylakoid membranes of stressed plants. Masters thesis, Palacký University Olomouc

Oguchi R, Hikosaka K, Hirose T (2003) Does the photosynthetic light-acclimation need change in leaf anatomy? Plant Cell Environ 26:505-512

Olaya-Castro A, Scholes GD (2011) Energy transfer from Forster-Dexter theory to quantum coherent light-harvesting. Int Rev Phys Chem 30:49-77 doi: 10.1080/0144235x.2010.537060

Olive J, Vallon O (1991) Structural organization of the thylakoid membrane: freeze-fracture and immunocytochemical analysis. J Electron Microsc Tech 18:360-374 doi: 10.1002/jemt.1060180405

Pali T, Garab G, Horvath LI, Kota Z (2003) Functional significance of the lipid-protein interface in photosynthetic membranes. Cell Mol Life Sci 60:1591-1606 doi: 10.1007/s00018-003-3173-x

Pan XW, Li M, Wan T, Wang LF, Jia CJ, Hou ZQ, Zhao XL, Zhang JP, Chang WR (2011) Structural insights into energy regulation of light-harvesting complex CP29 from spinach. Nat Struct Mol Biol 18:309-U394 doi: 10.1038/nsmb.2008

Passarini F, Wientjes E, Hienerwadel R, Croce R (2009) Molecular Basis of Light Harvesting and Photoprotection in CP24: unique features of the most recent antenna complex. J Biol Chem 284:29536-29546 doi: 10.1074/jbc.M109.036376

Peers G, Truong TB, Ostendorf E, Busch A, Elrad D, Grossman AR, Hippler M, Niyogi KK (2009) An ancient light-harvesting protein is critical for the regulation of algal photosynthesis. Nature 462:518-U215 doi: 10.1038/nature08587

Pinnola A, Staleva-Musto H, Capaldi S, Ballottari M, Bassi R, Polívka T (2016) Electron transfer between carotenoid and chlorophyll contributes to quenching in the LHCSR1 protein from Physcomitrella patens. Biochim Biophys Acta 1857:1870-1878 doi: 10.1016/j.bbabio.2016.09.001

Pospíšil P (2012) Molecular mechanisms of production and scavenging of reactive oxygen species by photosystem II. Biochim Biophys Acta-Bioenerg 1817:218-231 doi: 10.1016/j.bbabio.2011.05.017

Pospíšil P, Tyystjarvi E (1999) Molecular mechanism of high-temperature-induced inhibition of acceptor side of Photosystem II. Photosynth Res 62:55-66 doi: 10.1023/A:1006369009170

Qin XC, Suga M, Kuang TY, Shen JR (2015) Structural basis for energy transfer pathways in the plant PSI-LHCI supercomplex. Science 348:989-995 doi: 10.1126/science.aab0214

Ruban AV (2016) Nonphotochemical Chlorophyll Fluorescence Quenching: Mechanism and Effectiveness in Protecting Plants from Photodamage. Plant Physiol 170:1903-1916 doi: 10.1104/pp.15.01935

Ruban AV, Calkoen F, Kwa SLS, vanGrondelle R, Horton P, Dekker JP (1997) Characterisation of LHC II in the aggregated state by linear and circular dichroism spectroscopy. Biochim Biophys Acta-Bioenerg 1321:61-70 doi: 10.1016/S0005-2728(97)00047-9

Ruban AV, Johnson MP (2015) Visualizing the dynamic structure of the plant photosynthetic membrane. Nat Plants 1:15161 doi: 10.1038/nplants.2015.161

Ruban AV, Johnson MP, Duffy CDP (2012) The photoprotective molecular switch in the photosystem II antenna. Biochim Biophys Acta-Bioenerg 1817:167-181 doi: 10.1016/j.bbabio.2011.04.007

Shi H, Xiong L, Yang KY, Tang CQ, Kuang TY, Zhao NM (1998) Protein secondary structure and conformational changes of photosystem II during heat denaturation studied by Fourier transform-infrared spectroscopy. J Mol Struct 446:137-147 doi: 10.1016/S0022-2860(98)00287-7

Scholes GD, Fleming GR, Olaya-Castro A, van Grondelle R (2011) Lessons from nature about solar light harvesting. Nat Chem 3:763-774 doi: 10.1038/nchem.1145

Simidjiev I, Barzda V, Mustardy L, Garab G (1998) Role of thylakoid lipids in the structural flexibility of lamellar aggregates of the isolated light-harvesting chlorophyll a/b complex of photosystem II. Biochemistry 37:4169-4173 doi: 10.1021/bi972726m

Simidjiev I, Stoylova S, Amenitsch H, Javorfi T, Mustardy L, Laggner P, Holzenburg A, Garab G (2000) Self-assembly of large, ordered lamellae from non-bilayer lipids and integral membrane proteins in vitro. Proc Natl Acad Sci U S A 97:1473-1476

Špunda V, Marek M, Kalina J, Kuropatwa R, Marková I, Mašláň M, Miklicová M, Nauš J (1994) Changes in the photosynthetic apparatus of juvenile Norway spruce (Picea abies L. Karst) induced by the first frost under field condition. 1. Universitas Ostraviensis, Acta Facultatis Rerum Naturalium, Physica - Chemia 141:37-52

Štroch M, Čajánek M, Kalina J, Špunda V (2004) Regulation of the excitation energy utilization in the photosynthetic apparatus of chlorina f2 barley mutant grown under different irradiances. J Photochem Photobiol B-Biol 75:41-50 doi: 10.1016/j.jphotobiol.2004.04.004

Štroch M, Kuldová K, Kalina J, Špunda V (2008a) Dynamics of the xanthophyll cycle and non-radiative dissipation of absorbed light energy during exposure of Norway spruce to high irradiance. J Plant Physiol 165:612-622 doi: 10.1016/j.jplph.2007.03.013

Štroch M, Lenk S, Navrátil M, Špunda V, Buschmann C (2008b) Epidermal UV-shielding and photosystem II adjustment in wild type and chlorina f2 mutant of barley during exposure to increased PAR and UV radiation. Environ Exp Bot 64:271-278 doi: 10.1016/j.envexpbot.2008.05.007

Thayer SS, Björkman O (1992) Carotenoid Distribution and Deepoxidation in Thylakoid Pigment-Protein Complexes from Cotton Leaves and Bundle-Sheath Cells of Maize. Photosynth Res 33:213-225 doi: 10.1007/Bf00030032

Tikkanen M, Grieco M, Aro EM (2011) Novel insights into plant light-harvesting complex II phosphorylation and 'state transitions'. Trends Plant Sci 16:126-131 doi: 10.1016/j.tplants.2010.11.006

Timperio AM, Gevi F, Ceci LR, Zolla L (2012) Acclimation to intense light implies changes at the level of trimeric subunits involved in the structural organization of the main light-harvesting complex of photosystem II (LHCII) and their isoforms. Plant Physiol Biochem 50:8-14 doi: 10.1016/j.plaphy.2011.09.015

Toth TN, Rai N, Solymosi K, Zsiros O, Schroder WP, Garab G, van Amerongen H, Horton P, Kovacs L (2016) Fingerprinting the macro-organisation of pigment-protein complexes in plant thylakoid membranes in vivo by circular-dichroism spectroscopy. Biochim Biophys Acta 1857:1479-1489 doi: 10.1016/j.bbabio.2016.04.287

Umena Y, Kawakami K, Shen JR, Kamiya N (2011) Crystal structure of oxygen-evolving photosystem II at a resolution of 1.9 A. Nature 473:55-60 doi: 10.1038/nature09913

van Amerongen H, Croce R (2013) Light harvesting in photosystem II. Photosynth Res 116:251-263 doi: 10.1007/s11120-013-9824-3

Van Grondelle R, Dekker JP, Gillbro T, Sundstrom V (1994) Energy-Transfer and Trapping in Photosynthesis. Biochim Biophys Acta-Bioenerg 1187:1-65 doi: 10.1016/0005-2728(94)90166-X

Varkonyi Z, Nagy G, Lambrev P, Kiss AZ, Szekely N, Rosta L, Garab G (2009) Effect of phosphorylation on the thermal and light stability of the thylakoid membranes. Photosynth Res 99:161-171 doi: 10.1007/s11120-008-9386-y

Vass I (2012) Molecular mechanisms of photodamage in the Photosystem II complex. Biochim Biophys Acta-Bioenerg 1817:209-217 doi: 10.1016/j.bbabio.2011.04.014

Wada M (2013) Chloroplast movement. Plant Sci 210:177-182 doi: 10.1016/j.plantsci.2013.05.016

Walters RG, Rogers JJM, Shephard F, Horton P (1999) Acclimation of Arabidopsis thaliana to the light environment: the role of photoreceptors. Planta 209:517-527 doi: 10.1007/s004250050756

Wen XG, Qiu NW, Lu QT, Lu CM (2005) Enhanced thermotolerance of photosystem II in salt-adapted plants of the halophyte Artemisia anethifolia. Planta 220:486-497 doi: 10.1007/s00425-004-1382-7

Wientjes E, van Amerongen H, Croce R (2013a) LHCII is an antenna of both photosystems after long-term acclimation. Biochim Biophys Acta-Bioenerg 1827:420-426 doi: 10.1016/j.bbabio.2012.12.009

Wientjes E, van Amerongen H, Croce R (2013b) Quantum yield of charge separation in photosystem II: functional effect of changes in the antenna size upon light acclimation. J Phys Chem B 117:11200-11208 doi: 10.1021/jp401663w

Wild A, Hopfner M, Ruhle W, Richter M (1986) Changes in the Stoichiometry of Photosystem-Ii Components as an Adaptive Response to Highlight and Low-Light Conditions during Growth. Z Naturforsch (C) 41:597-603

Williams WP (1994) The Role of Lipids in the Structure and Function of Photosynthetic Membranes. Prog Lipid Res 33:119-127

Williams WP (1998) The physical properties of thylakoid membrane lipids and their relation to photosynthesis. In: Siegenthaler PA, Murata N (eds) Advances in photosynthesis. Lipids in photosynthesis. Kluwer Academic Publishers, Dordrecht, pp pp 103–118

Yamamoto HY, Higashi RM (1978) Violaxanthin de-epoxidase. Lipid composition and substrate specificity. Arch Biochem Biophys 190:514-522 doi: 10.1016/0003-9861(78)90305-3

Yang CH, Boggasch S, Haase W, Paulsen H (2006) Thermal stability of trimeric light-harvesting chlorophyll a/b complex (LHCIIb) in liposomes of thylakoid lipids. Biochim Biophys Acta-Bioenerg 1757:1642-1648 doi: 10.1016/j.bbabio.2006.08.010

Zhang R, Cruz JA, Kramer DM, Magallanes-Lundback ME, Dellapenna D, Sharkey TD (2009) Moderate heat stress reduces the pH component of the transthylakoid proton motive force in light-adapted, intact tobacco leaves. Plant Cell Environ 32:1538-1547 doi: 10.1111/j.1365-3040.2009.02018.x

Zhang R, Sharkey TD (2009) Photosynthetic electron transport and proton flux under moderate heat stress. Photosynth Res 100:29-43 doi: 10.1007/s11120-009-9420-8

Zhang YJ, Liu C, Liu SA, Shen Y, Kuang TY, Yang CH (2008) Structural stability and properties of three isoforms of the major light-harvesting chlorophyll a/b complexes of photosystem II. Biochim Biophys Acta-Bioenerg 1777:479-487 doi: 10.1016/j.bbabio.2008.04.012

CURRICULUM VITAE

PERSONAL INFORMATIONS

Karlický Václav

Hlavní 1378, 739 11 Frýdlant nad Ostravicí

Vaclav.Karlicky@osu.cz

+420 597 092 156

Date of birth: 04/11/1982

Nationality: Czech

Education

- B.Sc.: University of Ostrava, Faculty of Science, Biophysics (2002-2005)

- M.Sc.: University of Ostrava, Faculty of Science, Biophysics (2005-2007)

- Ph.D.: Palacky University in Olomouc, Faculty of Science, Biophysics (2007- present)

Academic and professional appointments

2011-present: Department of Physics, Faculty of Science, University of Ostrava (Assistant professor)

2011-present: Global Change Research Centre ASCR (Junior Researcher)

Important research visits, fellowships

2011, 2013, 2016 - Laboratory of Photosynthetic Membranes, Institute of Plant Biology, Biological Research Centre, Hungarian Academy of Sciences, Szeged, Hungary, G. Garab and P.Lambrev, circular and linear dichroism of photosynthetic membranes

Fields of scientific interest

Study of response mechanisms of the assimilation apparatus of higher plants to short-term and long-term changes of light intensity and temperature, fluorescence and circular dichroism spectroscopy

Awards

1st place in young scientists competition, poster session, 8th International Conference "Ecophysiological aspects of plant responses to stress factors", September 16-19, 2009, Krakow, Poland

„Young Talents Award Certificate“ at international conference "Photosynthesis Research for Sustainability", July 24-30, 2011, Baku, Azerbaijan

„Best Poster Award Certificate“ at international conference "Photosynthesis Research for Sustainability", September 21-26, 2015, Colymbari, Crete, Greece

Short scientometry

Papers in the reviewed journal with impact factor 4

Papers in proceeding from conference – ISI Web of Science 2

Total number of citations: 12 (10 without self-citations)

H-index according ISI Web of Science: 2

ATTACHEMENTS

I. **Karlický, V.**, Kurasová, I., Ptáčková, B., Večeřová, K., Urban, O., Špunda, V. (2016) Enhanced thermal stability of the thylakoid membranes from spruce. A comparison with selected angiosperms. Photosynthesis Research: *First Online.* DOI: 10.1007/s11120-016-0269-3

II. Miloslavina, Y., Lambrev, P., Jávorfi, T., Várkonyi, Z., **Karlický, V.**, Wall, J., Hind, G., Garab, G. (2012) Anisotropic circular dichroism signatures of oriented thylakoid membranes and lamellar aggregates of LHCII. Photosynthesis Research 111:29-39. DOI: 10.1007/s11120-011-9664-y

III. **Karlický, V.**, Podolinská, J., Nadkanská, L., Štroch, M., Čajánek, M., Špunda, V. (2010) Pigment composition and functional state of the thylakoid membranes during preparation of samples for pigment-protein complexes separation by nondenaturing gel electrophoresis. Photosynthetica 48:475-480. DOI: 10.1007/s11099-010-0063-y

IV. **Karlický, V.**, Strouhal, O., Ilík, P., Štroch, M., Kurasová, I., Garab, G., Šebela, M., Špunda, V. The effect of growth light intensity on pigment-protein composition and efficiency of excitation energy transfer within photosystem II in barley leaves. Photosynthesis Research, s*ubmitted*

Photosynth Res
DOI 10.1007/s11120-016-0269-3

ORIGINAL ARTICLE

Enhanced thermal stability of the thylakoid membranes from spruce. A comparison with selected angiosperms

Václav Karlický[1,2] · Irena Kurasová[1,2] · Božena Ptáčková[1] · Kristýna Večeřová[2] · Otmar Urban[2] · Vladimír Špunda[1,2]

Received: 15 January 2016 / Accepted: 25 April 2016

Abstract Recently, we have found that thermal stability of photosystem II (PSII) photochemistry in spruce needles is higher than in other plants (barley, beech) cultivated under the same temperatures. In this work, temperature dependences of various characteristics of PSII organization were studied in order to obtain complex information on the thermal stability of PSII function and organization in spruce. Temperature dependency of circular dichroism spectra revealed by about 6 °C higher thermal stability of macrodomain organization in spruce thylakoid membranes in comparison with *Arabidopsis* and barley ones; however, thermal disintegration of light-harvesting complex of PSII did not significantly differ among the species studied. These results thus indicate that thermal stability of PSII macro-organization in spruce thylakoid membranes is enhanced to a similar extent as thermal stability of PSII photochemistry. Clear-native polyacrylamide gel electrophoresis of preheated thylakoids demonstrated that among the separated pigment–protein complexes, only PSII supercomplexes (SCs) revealed considerably higher thermal stability in spruce thylakoids as compared to *Arabidopsis* and barley ones. Hence we suggest that higher thermal stability of PSII macro-organization of spruce is influenced by the maintenance of PSII SCs in the thylakoid membrane. In addition, we discuss possible effects of different PSII organizations and lipid compositions on the thermal stability of spruce thylakoid membranes.

Keywords Norway spruce · Thermal stability · Circular dichroism · Photosystem II organization · Thylakoid membrane

Abbreviations

CD	Circular dichroism
CCII	Core complex of photosystem II
CN-PAGE	Clear-native polyacrylamide gel electrophoresis
DGDG	Digalactosyldiacylglycerol
FA	Fatty acid
Chl	Chlorophyll
LHCI	Light-harvesting complex of photosystem I
LHCII	Light-harvesting complex of photosystem II
MGDG	Monogalactosyldiacylglycerol
PPC	Pigment–protein complex
PSI	Photosystem I
PSII	Photosystem II
SC	Supercomplex
T_m	Transition temperature
Ψ	Polymer and salt induced

Introduction

The responses of photosynthetic reactions in higher plants to temperature increases have a crucial importance if we take into account both the global warming and the increasing frequency of extreme heat waves (Meehl and Tebaldi 2004). An elevated temperature can cause direct negative effects on photosynthetic assimilation of carbon dioxide. However,

✉ Václav Karlický
vaclav.karlicky@osu.cz

[1] Faculty of Science, Ostrava University, 30. dubna 22, 701 03 Ostrava 1, Czech Republic

[2] Global Change Research Institute CAS, Bělidla 986/4a, 603 00 Brno, Czech Republic

Published online: 06 May 2016

photosystem II (PSII) is considered as the most heat sensitive component (Allakhverdiev et al. 2008; Zhang and Sharkey 2009). At the temperature from 42 to 48 °C, the PSII donor side undergoes a disruption due to loss of oxygen evolution complex (Cramer et al. 1981; DelasRivas and Barber 1997). PSII acceptor side becomes gradually inactivated at temperatures above 40 °C by changed midpoint potential of the primary quinone acceptor Q_A (Pospíšil and Tyystjarvi 1999). The increasing permeability to protons can lead to dissipation of ΔpH and finally to loss of the thylakoid membranes integrity resulting in inability to maintain transmembrane electrochemical potential (Zhang et al. 2009). At a temperature around 60 °C, the PSII core denatures (Shi et al. 1998) and trimeric light-harvesting complex of PSII (LHCII) dissociates to its monomeric form (Dobrikova et al. 2003). Heat denaturation of LHCII monomers occurs at temperature between 70 and 80 °C (Lípová et al. 2010; Yang et al. 2006). The more stable photosystem I (PSI) undergoes the major conformation transition at 60–70 °C, which is accompanied by the energetic disconnection of light-harvesting complex of PSI (LHCI) from PSI core, whose denaturation was shown to take place in a wide temperature interval 70–90 °C (Hu et al. 2004; Lípová et al. 2010). It should be noted that the mentioned denaturation temperatures of individual pigment–protein complexes (PPCs) can be influenced by the type of temperature treatment or heating rate during linear heating (Krumova et al. 2005).

The analysis of temperature dependence of chlorophyll *a* (Chl *a*) fluorescence parameters in vivo documented considerably different thermal stabilities of PSII function among plants species (Knight and Ackerly 2002), genotypes (Brestič et al. 2012) and its seasonal variations (Brestič et al. 2012; Froux et al. 2004). It has been proved that increased temperatures lead, in addition to adjustment of numerous photosynthetic processes and structures, to a relatively fast increase of PSII thermal stability (Brestič et al. 2012; Ghouil et al. 2003). An improved thermal stability of PSII was also observed as a result of acclimation to other stress factors, e.g. drought (Epron 1997; Lu and Zhang 1999) and salinity (Chen et al. 2004; Wen et al. 2005). However, knowledge on the mechanisms that are responsible for the mentioned variability of PSII sensitivity to heat stress is still not complete and controversies remain.

The thermal stability of PSII can be increased by stable forms of PSII proteins as observed in the case of double mutation in PSII reaction centre protein D1 of mesophilic cyanobacterium (Dinamarca et al. 2011). More often the different thermal stabilities of PSII is attributed to lipid composition and/or the fatty acid (FA) composition of thylakoid membrane. Under conditions of heat stress, changes in the ratio between the two major lipids, monogalactosyldiacylglycerol (MGDG) and digalactosyldiacylglycerol (DGDG) occur (Williams 1994), and the chain length and the number of double bonds in FAs are affected (Harwood 1998). It is generally accepted that the thylakoid membrane lipids in higher plants respond to prolonged high-temperature exposure with increased degree of FA saturation (Gombos et al. 1994; Makarenko et al. 2014). On the contrary, studies on cyanobacterium *Synechocystis* suggest that thermal stability of PPCs does not depend on the lipid composition of the membranes (Laczko-Dobos and Szalontai 2009) or that lipid saturation per se is not a regulator of thermal stability (Nanjo et al. 2010). DGDG-deficient *Arabidopsis* mutant revealed lowered thermal stability of macrodomain organization of PPC in thylakoid membranes compared to wild type, and thus proved direct role of DGDG in the stabilization of thylakoid membranes at elevated temperatures (Krumova et al. 2010). Similarly, importance of DGDG in the stabilization of LHCII trimers incorporated into liposomes with different compositions of lipids was confirmed (Zhang et al. 2008).

Circular dichroism (CD) spectroscopy is a non-invasive method for an investigation of pigment–pigment interaction, even in such highly complex systems as intact leaves. Hierarchically organized systems of chromophores, such as thylakoid membranes, contain three types of signals of different physical origins. However, for the study of PPCs and their organization in the thylakoid membranes only the excitonic bands from short-range (nanometre scale) excitonic interactions between pigments within PPCs and high-intensity Ψ-type CD bands from long-range order (hundreds of nanometres) of the chromophores in chirally organized macroarrays are relevant (Garab and van Amerongen 2009). High temperature induced changes of CD spectra and their interpretation are helpful for studies of thermal stability of pigment–pigment interaction both in thylakoid membranes in vivo (Krumova et al. 2010; Varkonyi et al. 2009) and isolated LHCII in vitro (Yang et al. 2006; Zhang et al. 2008).

Recently, we have found that thermal stability of PSII photochemistry in spruce needles is higher than in other plants (barley, beech) cultivated under the same temperatures (Špunda et al. unpublished results). The main objective of this work is to elucidate whether higher thermal stability of PSII photochemistry found in spruce needles is accompanied with specific features of thylakoid membranes composition that can be related to enhanced stability of PSII complexes.

Materials and methods

Plant material and growth conditions

Arabidopsis (*Arabidopsis thaliana* L. cv. Columbia), spring barley (*Hordeum vulgare* L. cv. Bonus) and Norway spruce

(*Picea abies* [L.] Karst.) were grown from seeds under controlled environmental conditions inside a HB 1014 growth chamber (Vötsch Industrietechnik, Balingen-Frommern, Germany) at photosynthetic photon flux density of 50 μmol photons m^{-2} s^{-1}, 20 °C, 65 % relative humidity and light/dark regime of 8/16 for *Arabidopsis* and 16/8 for barley and spruce. The middle segments of dark-adapted primary leaves/needles of 11–13 week-old *Arabidopsis*, 1-week-old barley or 3–4 week-old spruce seedlings were used for measurements on the intact leaves/needles and isolation of thylakoid membranes.

Measurement of photosystem II function

PSII function in heat-treated leaf/needles was monitored using potential yield of PSII photochemistry (F_V/F_M) measured by pulse amplitude-modulated fluorometer PAM 101–103 (Walz, Effeltrich, Germany). Needle or leaf samples were exposed to linear heating in the temperature-controlled measuring chamber equipped with optical lid for PAM fibre-optics and connected to temperature-controlled bath MC-4 (JULABO, Seelbach, Germany). The linear heating of the water-bath was set to speed of 1 °C min^{-1} within the temperature range 20–48 °C. During the heating regime, the surface temperature of the sample was continuously monitored using a thermocouple. In order to avoid desiccation, all samples were inserted into the measuring chamber on the water soaked foam during the measurement and pre-acclimated at 20 °C for 5 min in darkness before the heating. The saturation pulses (1 s time duration, 1400 μmol photons m^{-2} s^{-1} light intensity) applied at 20 °C and during heating with an increment of 2 °C (after approximately 2 min) were used for determination of maximum fluorescence in the dark-adapted states (F_M). Immediately before the application of saturation pulse, minimum fluorescence in dark-adapted state (F_0) was taken and the maximum efficiency of PSII photochemistry (F_V/F_M) was calculated as $(F_M - F_0)/F_M$.

Isolation, thermal incubation and solubilization of the thylakoid membranes

Plant tissue was disintegrated using blender-type homogenizer Ultra-Turrax T25-18G (IKA, Staufen, Germany; 45 s at 18,000 rpm) in a homogenization medium (400 mM sucrose, 400 mM NaCl, 4 mM $MgCl_2$, BSA 2 mg ml^{-1}, 5 mM ascorbic acid, 35 mM HEPES, pH 7.2). Homogenate was filtrated through eight layers of polyamide sieve Uhelon 130T (Silk and Progress, Moravská Chrastová, Czech Republic) of pore size 42 μm and centrifuged (3K30, Sigma Laborzentrifugen, Osterode am Harz, Germany) for 6 min at 5000×*g*. Pellet was resuspended in medium I for disrupting the chloroplast envelope (150 mM NaCl, 8 mM $MgCl_2$, 1 mM Na_2–EDTA, 25 mM HEPES, pH 7.5) and centrifuged for 10 min at 5000×*g*. Removal of potential starch from pellet was performed by pellet resuspension in medium II (400 mM sucrose, 15 mM NaCl, 5 mM $MgCl_2$, 50 mM HEPES, pH 7.2) and by centrifugation for 3 min at 200×*g*. The resulting supernatant was again centrifuged (5 min at 5000×*g*), final thylakoid pellet was suspended into a small aliquot of medium II and diluted to concentration of 1000 μg total chlorophylls ml^{-1}. Chl content of thylakoids was estimated after extraction in 80 % acetone by UV/VIS 550 spectrophotometer (Unicam, Leeds, UK) according to Lichtenthaler (1987). All isolation and centrifugation steps were performed at 0 °C according to Nosek (2012).

Suspensions of prepared thylakoid membranes were doubly diluted with medium II and placed in Eppendorf tube into water baths to gain the temperature of membranes to 20, 32, 36, 40, 44, 48, 52, 56 and 60 °C for 15 min in a dark room and then immediately frozen in liquid nitrogen and stored at 80 °C. Thawed thylakoid membranes were solubilized for 5 min (barley, *Arabidopsis*) or 10 min (spruce) with 10 % (w/v) detergent *n*-dodecyl-β-D-maltoside (β-DM) to yield a ratio of detergent–total Chls of 35:1 (w/w) for spruce and 20:1 for barley and *Arabidopsis*. High-speed centrifugation (21,000×*g* for 10 min) was used to remove unsolubilized thylakoid membranes. The supernatant with thylakoid membranes (containing 15 μg of total Chls) was immediately loaded onto polyacrylamide gel.

Clear-native polyacrylamide gel electrophoresis (CN-PAGE)

Separation of PPCs by CN-PAGE was carried out using 4 % (w/v) focusing and 4.5–11.5 % (w/v) linear gradient polyacrylamide gel (acrylamide:bis acrylamide; 30 % T and 2.67 % C) enabling well-distinguished separation of large protein complexes such as PSI and PSII–LHCII supercomplexes (SCs; Järvi et al. 2011). Bis-Tris system of cathode and anode buffers (pH 7.0) were used with addition of β-DM (0.02 % w/v) and anionic detergent sodium deoxycholate (0.05 % w/v) to cathode buffer. Electrophoresis was performed at 4 °C in dark at gradual increase of voltage from 75 to 200 V (Järvi et al. 2011) with total running time about 3.5 h. Images of gels containing separated PPCs were captured by ChemiDoc MP gel imager (Bio-Rad Laboratories, Hercules, CA, USA) in transmitting white light or Chl *a* fluorescence excited by blue light with CCD detection. Relative amounts of individual PPCs in heat-treated membranes in comparison with membranes at 20 °C were evaluated from one-dimensional densitograms calculated from the green gel images using

the Matlab software procedure according to Ilík et al. (2002).

Chlorophyll *a* fluorescence spectra at 77 K

Chl *a* fluorescence spectra at 77 K were measured using a luminescence spectrofluorimeter LS50B (Perkin-Elmer, Beaconsfield, UK) equipped with the custom-made Dewar-type optical cryostat. The emission spectra were recorded at the preferential excitation of Chl *a* at 436 nm with 5 and 2.5 nm slit widths of excitation and emission monochromators, respectively. The emission spectra were corrected for the spectral sensitivity of the detection system.

CD spectroscopy

CD spectra were recorded in the range of 400–750 nm with a J-815 spectropolarimeter (JASCO, Tokyo, Japan). The spectra were recorded in steps of 0.5 nm with an integration time of 1 s, a band-pass of 2 nm and scanning speed of 100 nm min^{-1}. For measuring of spectra on intact leaf samples, detached leaves were placed in between the two detachable glass windows of an optical cell of 0.2 mm path length and were measured at the distance of the sample from the photomultiplier of 5 cm. Stacked thylakoid membranes were prepared by resuspension of isolated membranes at a Chl content of 20 μg ml^{-1} in medium containing 50 mM Tricine (pH 7.5), 0.4 M sorbitol, 5 mM KCl and 5 mM $MgCl_2$. In order to obtain unstacked thylakoids displaying no Ψ-type CD bands, the thylakoid membranes at the same Chl concentration were washed in 50 mM Tricine buffer supplemented with 5 mM EDTA (pH 7.5) and were sonicated (GM 3100, Bandelin Electronic, Berlin, Germany) on ice for 300 s using 0.5 s duty cycle and output value of 25 %. CD spectra of thylakoid membranes were recorded in the cell with optical path length of 1 cm.

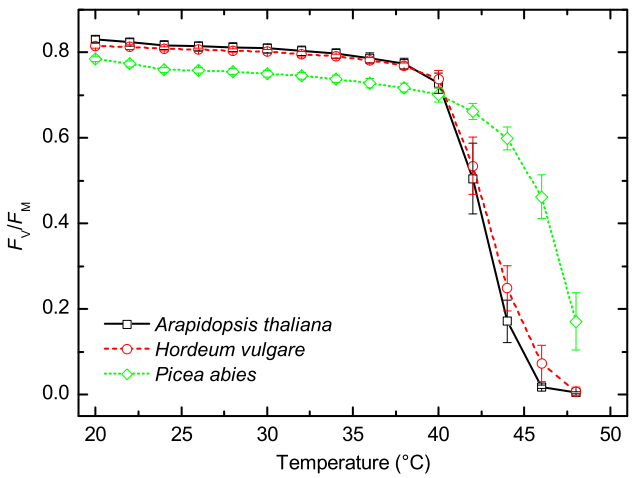

Fig. 1 Temperature dependences of maximum efficiency of PSII photochemistry (F_V/F_M) measured on overnight dark-adapted *Arabidopsis* (*black squares*), barley leaves (*red circles*) and spruce needles (*green diamonds*). Leaf or needle samples were exposed to linear heating of 1 °C min^{-1}. Mean values (*points*) and standard deviation (*error bars*) are presented ($n = 5$–6)

The measurements of temperature-dependent changes of CD signal were performed in two different ways. For purposes of comparison with the heat-induced changes in the PSII function, the samples were sequentially thermostated in Peltier holder for 5 min at each temperature starting from 20 up to 70 °C. Measured temperature dependences of the CD bands or band pairs were fitted with a sigmoidal curve that resulted in estimation of transition temperatures (T_m). T_m marks the disassembly of the chiral macrodomains of the complexes (Cseh et al. 2000) and is defined as the temperature at which the intensity of the CD band is decreased to 50 % of its value at 20 °C. For purposes of comparison with CN-PAGE of heat-treated thylakoids, samples were preheated as described in section Isolation, thermal incubation and solubilization of the thylakoid membranes and then resuspended and measured at room temperature.

Analysis of thylakoid lipids and their fatty acids

The thylakoid membranes were extracted using 1.5 ml of chloroform:methanol solution (2:1). The samples were heated at 60 °C for 30 min and lower phase (chloroform) was collected, the process was then repeated. In case of insufficient phase separation 1 ml 0.88 % potassium chloride was added. After collection of lower phases the samples were dried using nitrogen flow and dissolved in 1 ml of chloroform. Aliquots of samples were taken for determination of total lipid content in thylakoid membranes and the rest was applied to silica thin-layer chromatography and developed in chloroform:acetone:distilled H_2O (30:60:2) for the separation of MGDG and DGDG. The lipid bands corresponding to MGDG and DGDG fractions were visualized under UV light, scraped off and then extracted as mentioned before.

Extracts with addition of internal standard (non-adecanoic acid) were dried using nitrogen flow. The methyl derivates of FAs were prepared using 1 ml of 3 N methanolic HCl which was added to dried extract and then heated for 90 min at 60 °C. Subsequently, the samples were extracted three times with 2.5 ml of *n*-hexane and dried using nitrogen flow. Finally, extracts were dissolved in *n*-hexane and subjected to chromatographic analysis.

The analysis of FAs was performed by gas chromatography coupled with mass spectrometry (GC–MS) using a TSQ quantum XLS triple quadrupole (Thermo Fisher Scientific, Waltham, MA, USA) on a 30 m, 0.25 mm

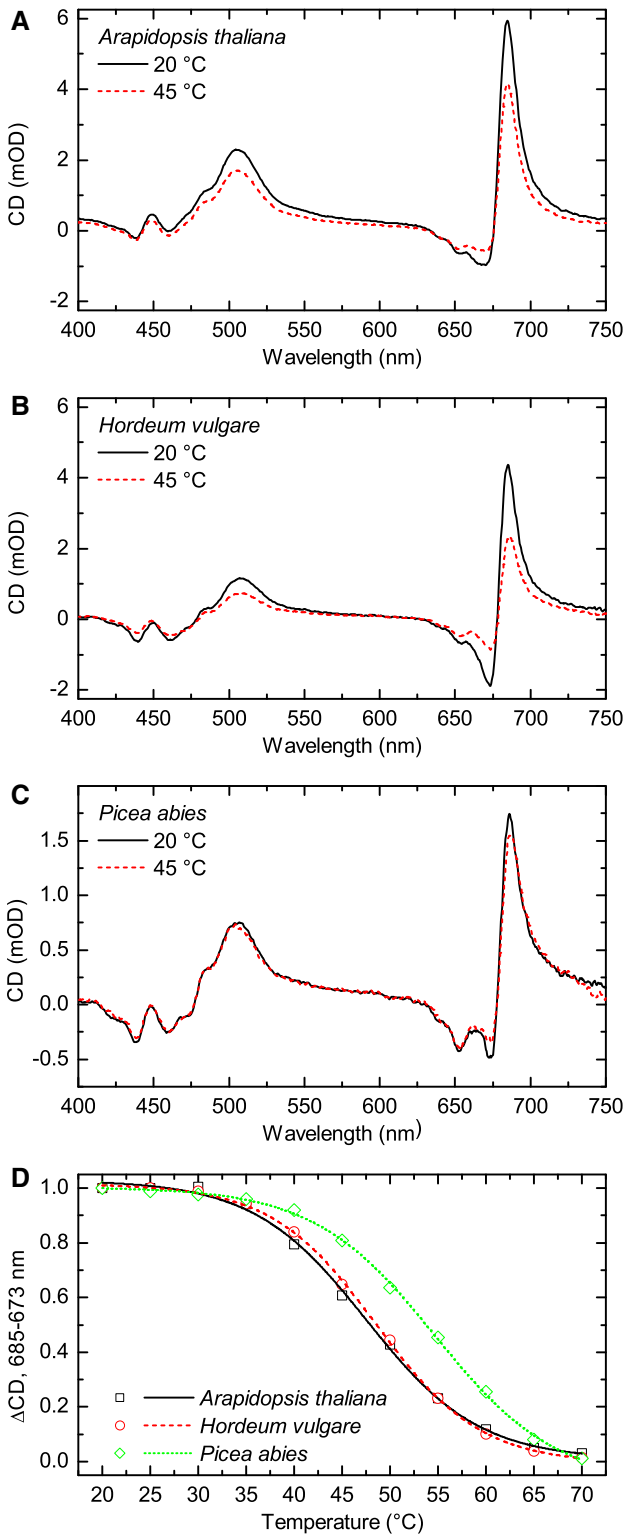

◀**Fig. 2** Typical CD spectra of stacked thylakoid membranes from *Arabidopsis* (**A**), barley (**B**) and spruce (**C**) measured at 20 °C (*solid black line*) and 45 °C (*dashed red line*). Typical temperature dependences of the amplitude differences of the main Ψ-type bands at around (+)685 nm and (−)673 nm (**D**) of the *Arabidopsis*, barley and the spruce thylakoid membranes exposed to gradual heating. *Data points* from one representative series fitted with a *sigmoidal curve* resulting transition temperatures (T_m) of 47.8, 47.6 and 54.7 °C for *Arabidopsis*, barley and spruce, respectively. Mean values and standard deviation of T_m from six independent experiments are presented in Table 1

(inside diameter), 0.25 µm column (ZB-5MS, Phenomenex, Torrance, CA, USA). Samples (1 µl) were injected in splitless mode. The inlet pressure of the carrier gas (helium) was 100 kPa at the initial oven temperature and its flow rate was 1.2 ml min^{-1}, the injection temperature was 250 °C. The temperature gradient of the oven began at 100 °C and increased to 150 °C at 10 °C min^{-1}, followed by increase of temperature to 260 °C at the rate 2.5 °C min^{-1}. The interface temperature was maintained at 250 °C. GC–MS (electrospray ionization 50 eV, ion source temperature 200 °C) was performed at full scan in range 50–450 *m/z* (scan time 0.15 s). The FAs were searched in the mass library which had been created from measurement of standards in full mode of GC–MS.

Statistical analysis

The statistical differences between the means were determined using a two-sample *F* test for variances followed by a Student's *t* test at the levels of significance of 0.05. Based on the results of the *F* test, the *t* test assuming either equal or unequal variances was used. All statistical tests were performed using the data analysis tools of *Microsoft Office Excel 2010*.

Results

The PSII function during linear heating

Thermal stability of the PSII function was monitored via the measurement of the maximum quantum yield of PSII photochemistry (the parameter F_V/F_M) on intact leaves/needles exposed to linear heating (see "Materials and methods" section). We found that F_V/F_M of *Arabidopsis* and barley leaves steeply decreased at 42 °C and almost complete PSII inactivation occurred at 46 °C. On the contrary, reduction of PSII photochemical activity was more gradual in needles of spruce seedlings at temperatures above 40 °C and still F_V/F_M values about 0.5 were observed at 46 °C (Fig. 1).

Circular dichroism spectra of stacked thylakoid membranes during gradual heating

The thermal stability of chiral macrodomains was estimated from Ψ-type CD signal on isolated thylakoid membranes exposed to gradual heating. The CD spectra of

Table 1 Transition temperatures (T_m) of selected CD bands or band pairs for *Arabidopsis*, barley and spruce stacked and unstacked thylakoid membranes

CD signal (nm)	Assignments	T_m (*Arabidopsis*, °C)	T_m (barley, °C)	T_m (spruce, °C)
685–730	Ψ-Type	47.9 ± 2.8[a]	48.3 ± 2.2[a]	54.1 ± 1.4[b]
685–673	Ψ-Type	47.5 ± 2.9[a]	47.9 ± 1.9[a]	54.3 ± 1.1[b]
505–550	Ψ-Type	47.8 ± 2.2[a]	48.4 ± 1.2[a]	52.4 ± 1.2[b]
483–473	Excitonic (Chl *a*, LHCII trimers)	61.7 ± 0.4[a]	61.1 ± 0.2[a]	62.3 ± 0.7[a]
665–650	Excitonic (Chl *b*, LHCII)	70.0 ± 0.3[a]	67.4 ± 0.5[b]	74.4 ± 0.5[c]

The samples of thylakoid membranes were gradually heated in the range between 20 and 70 °C and between 20 and 80 °C for stacked and unstacked membranes, respectively. The amplitudes for the individual bands were calculated from the difference in the intensity at specific wavelengths. T_m is defined as the temperature at which the intensity of the CD band is decreased to 50 % of its value at 20 °C. T_m of Ψ-type CD bands or band pair were estimated from stacked thylakoid membranes and T_m of excitonic CD band pairs were calculated from unstacked ones. Mean values and standard deviations from five ($n = 5$) and four ($n = 4$) independent experiments are presented for stacked and unstacked membranes, respectively. Data within a row followed by the same letter are not significantly different ($P > 0.05$)

thylakoid membranes isolated from *Arabidopsis*, barley and spruce revealed similar character as described previously on thylakoid membranes from various plant species of higher plants (Krumova et al. 2010; Varkonyi et al. 2009). The main CD bands at wavelength around (+)685 nm, (−)673 nm and (+)505 nm, which are of Ψ-type origin (Barzda et al. 1994; Dobrikova et al. 2003), and less intensive CD bands of excitonic origin at wavelength of (−)438 nm, (+)448 nm, (−)459 nm and (−)650 nm (Garab and van Amerongen 2009; Georgakopoulou et al. 2007) were present in all samples (Fig. 2A–C). Nevertheless, at the temperature of 20 °C, amplitude of the main Ψ-type CD band of *Arabidopsis* and barley membranes was more than double in comparison with spruce ones (Fig. 2A–C), which indicates much smaller size of the chiral macrodomains (Garab et al. 1991; Garab and Mustardy 1999) or a different organization of PSII SCs (Kovacs et al. 2006) in thylakoid membranes of spruce than in those of *Arabidopsis* and barley.

In the *Arabidopsis* and barley membranes, the Ψ-type signal was reduced considerably more by elevating the temperature to 45 °C (Fig. 2A, B) than in the spruce ones (Fig. 2C). This difference in the thermal stability of the macrodomain organization of the PPCs can be more clearly seen on the plot of the temperature dependence of the main Ψ-type CD band pair (Fig. 2D), when the T_m in spruce membranes is higher by about 6 °C in comparison with the *Arabidopsis* and barley membranes. Similarly as heat-induced inactivation of PSII photochemistry, also decreases of Ψ-type CD bands with increasing temperature were less steep for spruce membranes compared to *Arabidopsis* and barley ones. Transient temperatures of Ψ-type CD bands or band pair are summarized in Table 1. T_m values observed in spruce were significantly higher in comparison with those observed in *Arabidopsis* and barley by about 6 °C in the case of Ψ-type CD in red spectral region ($CD_{685–730}$, $CD_{685–673}$) and by about 4 °C for Ψ-type CD band in green spectral region ($CD_{505–550}$).

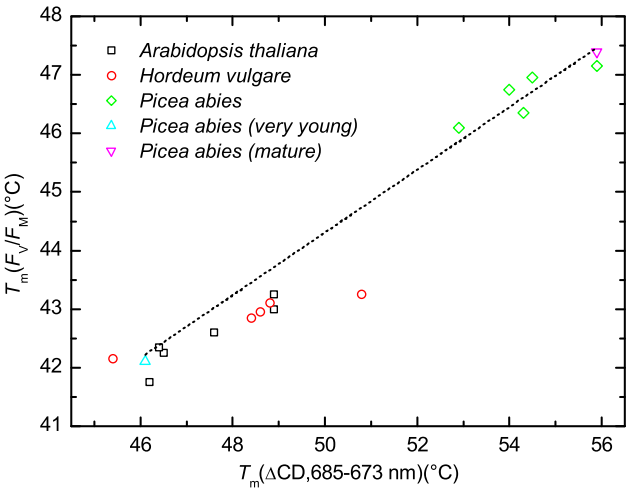

Fig. 3 The dependence of transition temperature of PSII photochemistry [$T_m(F_V/F_M)$] on the transition temperature of amplitude differences of the main Ψ-type bands at around (+)685 nm and (−)673 nm [T_m (ΔCD, 685–673 nm)] estimated from sigmoidal fits of temperature dependence of F_V/F_M and ΔCD measured on samples exposed to gradual heating. *Data points* presenting independent cultivations of *Arabidopsis* (*black squares*) and barley plants (*red circles*) and spruce seedlings (*green diamonds*). The *plot* is supplemented by data of very young spruce seedlings (2 week-old, *light blue up triangle*) and from mature needles of 4 year-old spruce trees (*magenta down triangle*). *Line* represents regression fit curve (linear, $y = 0.53x + 17.5$, $R^2 = 0.98$)

In order to quantify the relation between thermal stability of PSII photochemistry and PPC macro-organization, also T_m for F_V/F_M [$T_m(F_V/F_M)$] were expressed by fitting temperature-dependent data with sigmoidal Boltzmann function. Although T_m for the temperature dependence of Ψ-type CD signal [$T_m(\Delta CD_{685–673})$] was always higher than T_m of F_V/F_M [$T_m(F_V/F_M)$], linear dependence of $T_m(F_V/F_M)$ on T_m [$T_m(\Delta CD_{685–673})$] clearly demonstrated

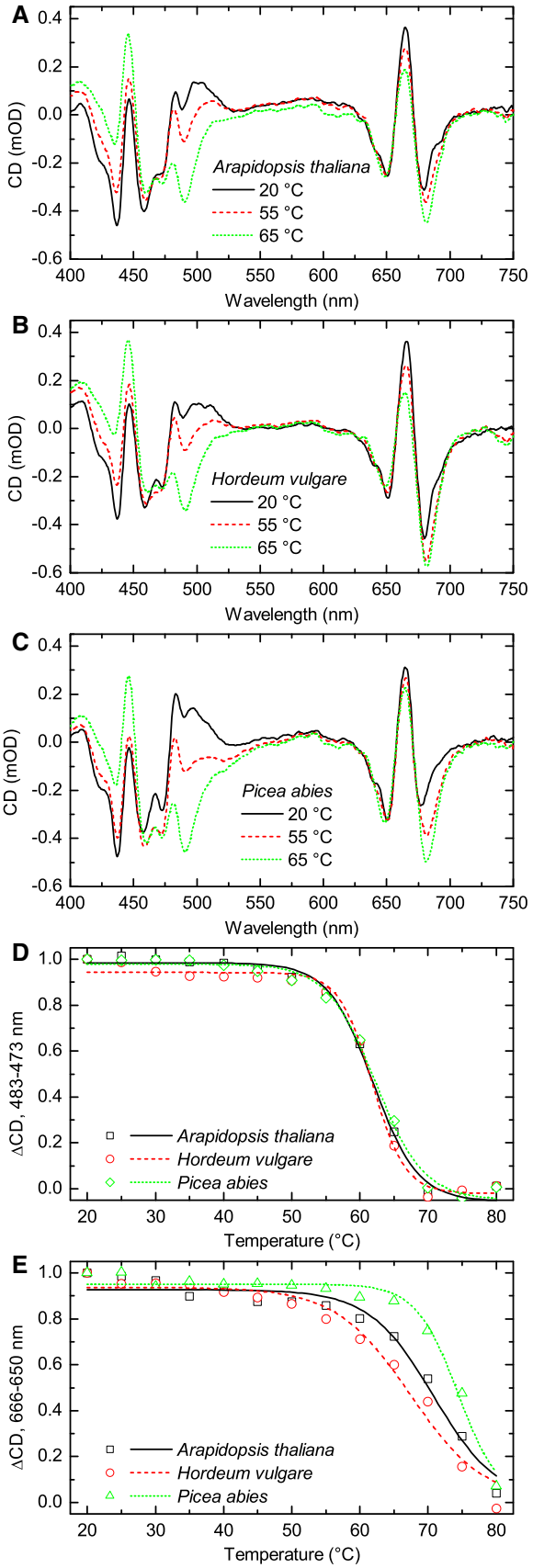

◀**Fig. 4** Typical CD spectra of unstacked thylakoid membranes from *Arabidopsis* (**A**), barley (**B**) and spruce (**C**) measured at 20 °C (*solid black line*), 55 °C (*dashed red line*) and 65 °C (*dotted green line*). Typical temperature dependences of the amplitude differences of the excitonic bands at around (+)483 nm and (−)473 nm (**D**) and (+)666 nm and (−)650 nm (**E**) in the *Arabidopsis*, barley and the spruce membranes exposed to gradual heating. *Data points* from one representative series fitted with a *sigmoidal curve* resulting transition temperatures (T_m). Mean values and standard deviation of T_m from four independent experiments are presented in Table 1

connection between thermal stability of the PSII photochemistry and ability to maintain PSII macro-organization in the thylakoid membranes at elevated temperatures (Fig. 3). In addition to higher thermal stability of PSII structure and function for spruce in comparison with *Arabidopsis* and barley grown at same light and temperature these data revealed also higher thermal stability of PSII structure and function of both mature spruce needles and 3–4 weeks-old seedlings in comparison with early developmental stage (2 week-old seedlings, Fig. 3).

Circular dichroism spectra of unstacked thylakoid membranes during gradual heating

A comparison of Fig. 4A–C revealed that spruce thylakoids did not exhibit significant changes compared to *Arabidopsis* and barley in the CD originating from short-range interactions in unstacked thylakoid membranes. For all the species studied, the CD spectra at 20 °C were almost identical in four independent isolations of thylakoid membranes (typical spectra, see Fig. 4, black curves). The CD signals under these conditions originate from short-range interactions inside individual PPC (Garab and van Amerongen 2009), predominantly from excitonic interactions inside LHCII as the most abundant PPC (Georgakopoulou et al. 2007; Lambrev et al. 2007).

In contrast to stacked thylakoid membranes, unstacked spruce membranes exhibited similar diminution of excitonic bands at elevated temperatures (Fig. 4C) as *Arabidopsis* and barley ones (Fig. 4A, B). Again, this heat-induced reduction of CD signal can be more clearly seen on the plot of the temperature dependence of the specific CD band pairs (Fig. 4D, E). The CD band pair of (+)483 nm/(−)473 nm is specific for LHCII trimers and the disappearance of this band pair indicates the monomerization of the LHCII trimers, both in the thylakoid membranes and in the isolated LHCII (Garab et al. 2002; Yang et al. 2006). It can be clearly seen in Fig. 4D that the T_m of the LHCII trimers monomerization in the *Arabidopsis* and barley correspond well with that of spruce (Table 1) and also with that determined earlier on different plant species

(Dobrikova et al. 2003; Krumova et al. 2010; Varkonyi et al. 2009). CD bands in red region at (−)650 nm, (+)665 nm and (−)680 nm are present in the CD spectra of both trimeric LHCII and monomeric LHCII (Yang et al. 2006). Therefore, temperature dependence of amplitude of (+)665 nm/(−)650 nm band pair indicates disintegration of LHCII monomers. It can be clearly seen in Fig. 4E that the T_m of the LHCII monomers disintegration in the spruce membranes is higher by about 4 and 7 °C in comparison with *Arabidopsis* and barley ones, respectively (Table 1).

Clear-native gel electrophoresis of heat-treated thylakoid membranes

Since the CD signal of unstacked thylakoid membranes reflects the sum of excitonic interaction of all PPCs in the thylakoid membranes, it contains mainly information about the thermal stability of the most abundant PPC, the LHCII. Therefore, thermal stability of individual PPCs of thylakoid membranes was observed directly using CN-PAGE of *Arabidopsis*, barley and spruce thylakoid membranes pre-heated 15 min at given temperature (see "Materials and methods" section). Electropherograms at the temperature of 20 °C of control plants revealed typical patterns of the thylakoid membranes protein complexes after solubilization with DM as previously described (Järvi et al. 2011). The separated PPCs of barley were identified using SDS-PAGE combined with immunoblotting in previous work (Lípová et al. 2010) and were confirmed by measuring the 77 K Chl *a* fluorescence spectra.

The relative contents of individual PPCs of control thylakoids (20 °C) isolated from spruce needles were slightly different in comparison with those of *Arabidopsis* and barley thylakoid membranes exposed to the same temperature (Fig. 5, first line). Firstly, spruce thylakoid membranes revealed completely missing LHCII–CP29–CP24 complexes in contrast to *Arabidopsis* and barley thylakoids (Fig. 5C). Secondly, PSI SCs band of spruce

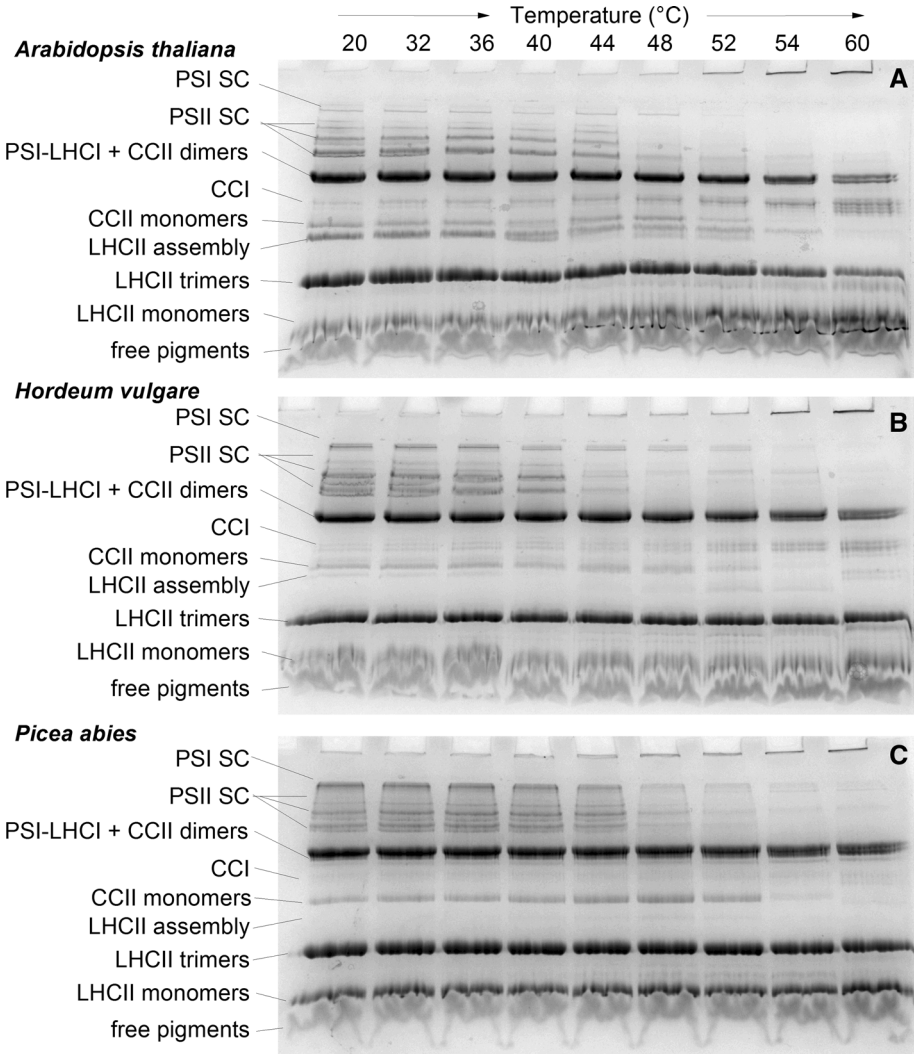

Fig. 5 CN-PAGE separation of PPCs of thylakoid membranes from *Arabidopsis* (**A**), barley (**B**) and spruce (**C**) preheated to 20–60 °C for 15 min in the dark. Thylakoid membranes were solubilized using *n*-dodecyl-β-D-maltoside with detergent/chlorophyll ratio of 20:1 (*Arabidopsis*, barley) a 35:1 (spruce). Gel images were obtained as transmittance of white light using CCD camera ChemiDoc MP (Bio-Rad Laboratories). Typical electropherograms from the three independent experiments are displayed

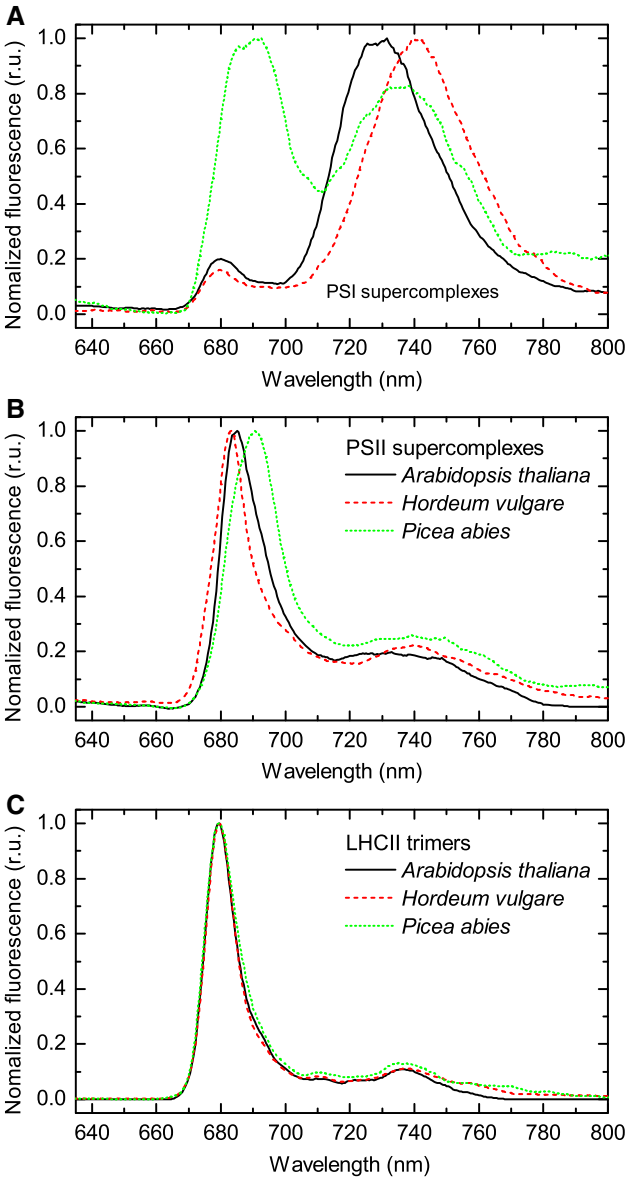

Fig. 6 Normalized 77 K fluorescence emission spectra of PSI supercomplexes (PSI SC) (**A**), PSII supercomplexes (PSII SC) (**B**) and LHCII trimers (**C**) isolated from *Arabidopsis* (*solid black line*), barley (*dashed red line*) and spruce (*dotted green line*). Samples were excited at wavelength of 436 nm (preferential excitation of chlorophyll *a*). Typical spectra from the three independent experiments are displayed

was much more contaminated by some PSII megacomplexes than *Arabidopsis* and barley as revealed by low-temperature fluorescence emission spectra (Fig. 6A). Thirdly, 77 K fluorescence emission spectra of PSII SCs from spruce peaked at around 695 nm compared to those of *Arabidopsis* and barley, which revealed maximum at wavelength of 685 nm (Fig. 6B). Other PPCs including parts of PSII SCs like core complex of PSII (CCII) or LHCII monomers and trimers showed almost the same spectra (e.g. LHCII trimers, see Fig. 6C). All these points suggested different macro-organizations of PSII SCs in thylakoid membranes of spruce than in those of *Arabidopsis* and barley.

Different thermal stabilities for individual PPCs were confirmed (Fig. 5). The PSII SC bands of *Arabidopsis* and barley decreased significantly above the temperature of 44 °C, the more heat stable PSI SCs band was vanished at the temperature over 52 °C. Further, at the temperature of 60 °C partial disintegration of PSI–LHCI and LHCII trimers were observed. Decreases in content of the above-mentioned PPCs were followed by increases of their degradation products. Therefore, the contents of PSII SCs proteins such as CCII dimers and monomers or LHCII assembly increased in heat-treated membranes in the temperature range from 32 to 52 °C, but at the temperature of 54 °C and higher also almost completely disappeared.

This difference in the thermal stability of chosen PPCs can be more clearly seen on the plot of the temperature dependence of their relative amount (Fig. 8). Thermal stability of PSII SCs from spruce was considerably higher than from *Arabidopsis* and barley as revealed from relative amount of all PSII SCs determined from the green gel density profiles of images estimated as intensity of Chl *a* fluorescence excited by blue light (Fig. 8C). The heat sensitivity of other PPCs from spruce did not differ significantly in comparison with those from *Arabidopsis* and barley (e.g. LHCII trimers, see Fig. 8D).

Circular dichroism spectra of heat-treated stacked thylakoid membranes

In order to reveal whether the observed decreases of the PSII SCs amount at elevated temperatures are connected with diminution of PPCs macro-organization, the CD spectra were measured in isolated thylakoid membranes exposed to the same heat treatments as those used for CN-PAGE separation of PPCs. In the spruce membranes, similarly as described for gradually heated membranes (Fig. 2), the chiral macrodomains were affected considerably less in membranes preheated at the temperature of 40 °C (Fig. 7C) than in the *Arabidopsis* and barley membranes exposed to the same heat treatment (Fig. 7A, B). Nevertheless, the temperature dependence of the Ψ-type CD band pairs showed far less sigmoidal signature, especially in the case of barley, not allowing satisfactory estimation of T_m by fitting a Boltzmann function. It can be clearly seen in Fig. 8A, that the thermal stability of macrodomains in spruce membranes was significantly higher than in *Arabidopsis* membranes. Barley membranes revealed substantial reduction of Ψ-type CD signal even at 32 °C. The thermal destabilization of different PPCs was monitored via the amplitudes of their corresponding

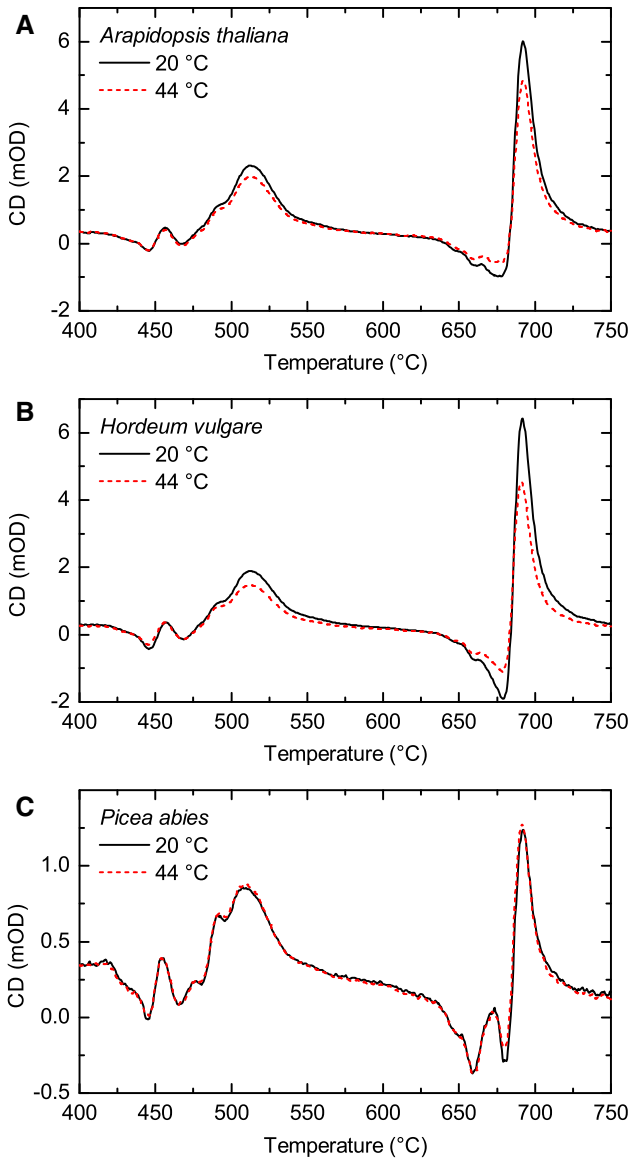

Fig. 7 CD spectra of thylakoid membranes from *Arabidopsis* (**A**), barley (**B**) and spruce (**C**) preheated at 20 °C (*solid black line*) and 44 °C (*dashed red line*) for 15 min in the dark. Spectra measured at room temperature were normalized to the absorbance at wavelength 678 nm. Typical spectra from three independent experiments are displayed

excitonic bands. On the contrary to Ψ-type CD signal, the Chl *a* excitonic bands at around 450 nm (Garab et al. 1991), determined as $CD_{448–438}$, exhibited the similar temperature dependence for *Arabidopsis*, barley and spruce and displayed at 60 °C still greater than 50 % signals in comparison to those measured at 20 °C (Fig. 8C).

Connection between the heat-induced decreases in the content PSII SCs and their macro-organization was assessed based on dependence of reduction of the amplitude differences of the main Ψ-type bands at around (+)685 nm and (−)673 nm on decrease in total content of PSII SCs in the heat-treated thylakoid membranes (Fig. 9). This clear non-linear dependence, with similarities for all plants species, revealed that 20 % reduction of total content of PSII SCs in the heat-treated thylakoid membranes did not cause significant change of Ψ-type CD signal. After disintegration of almost all PSII SCs in thylakoid membranes by heat, Ψ-type CD signal was reduced to below 50 % of the initial value.

Fatty acid composition of thylakoid membranes

Total content of FAs per Chls was by about 15 % higher in spruce thylakoid membranes than in *Arabidopsis* and barley (Table 2). *Arabidopsis* and barley thylakoid membranes contained similar distribution of saturated and mono-, di- and tri-unsaturated FAs. However, the content of tri-unsaturated FAs was by 10 % greater at the expense of the remaining FAs in barley membranes as compared to *Arabidopsis* ones, resulting in a doubled ratio of unsaturated–saturated FAs (Table 2). Thylakoid FAs from spruce revealed increased content of saturated and di-unsaturated FAs and decreases in mono- and tri-unsaturated FAs contents resulting in significantly reduced ratio of unsaturated–saturated FAs (Table 2). Spruce thylakoid membranes contained some unique FAs in comparison with *Arabidopsis* and barley (data not shown). These are represented by high contents of short ($C < 16$) and very long ($C > 18$) chain FAs, branched-17:0 FA (also called 14-methylpalmitic acid) and Δ5-unsaturated FAs. As found previously, these FAs are characteristic for mosses, ferns and gymnosperms (Karunen 1991; Mongrand et al. 2001), and angiosperms (with a few exceptions) have lost the ability to synthesize these FAs.

The FA composition of the two main thylakoid lipids MGDG and DGDG from all species studied was determined (data not shown). Between thylakoid membranes of spruce and those of *Arabidopsis* and barley the difference appeared when the amount of both of the galactolipids was calculated from that of each FA determined by GC. In spruce, the MGDG/DGDG ratio was lower by 30 % or almost by 50 % in comparison with MGDG/DGDG ratios determined in *Arabidopsis* and barley, respectively (Table 2). This result is in the line with finding that gymnosperms may possess much lower MGDG/DGDG ratio than angiosperm (Mongrand et al. 2001).

Discussion

Herein, structural attributes of PSII related to unusually high thermal stability of PSII photochemistry observed in spruce needles have been studied. To this end, we used comparison of spruce thylakoids with both *Arabidopsis* and

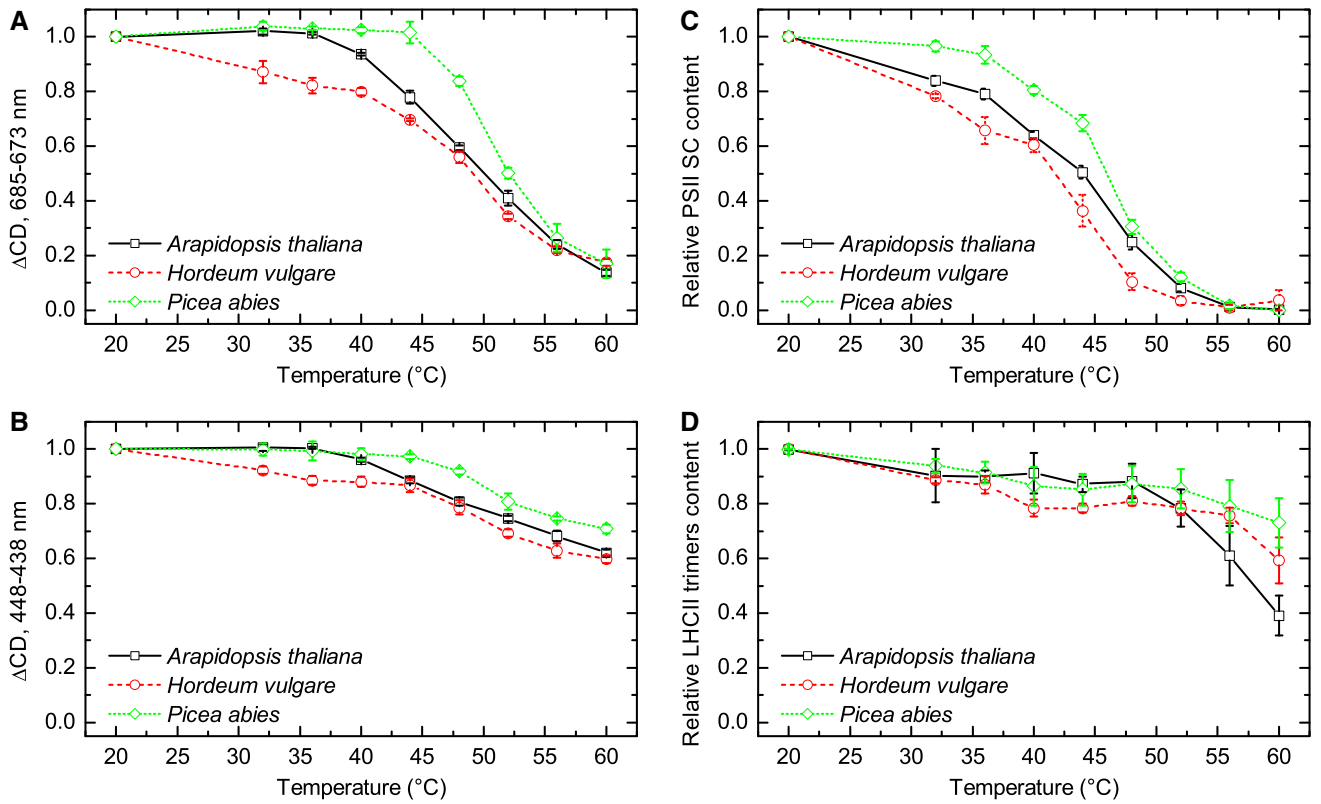

Fig. 8 Temperature dependences of the amplitude differences of the main Ψ-type bands at around (+)685 nm and (−)673 nm (**A**) and excitonic bands at around (+)448 nm and (−)438 nm (**B**) of the *Arabidopsis* (*black squares*), barley (*red circles*) and the spruce (*green diamonds*) heat-treated thylakoid membranes. Temperature dependences of the PSII supercomplexes (PSII SC) (**C**) and LHCII trimers (**D**) stability determined from the *green* gel density profiles of same heat-treated membranes. Temperatures experiments were carried out in the three independent experiments. Mean values (*points*) and standard deviations (*error bars*) from three independent experiments ($n = 3$) are displayed

barley ones, and measured different biophysical and biochemical parameters such as CD of both stacked und unstacked thylakoid membranes, decreases in content of PPCs using native gel electrophoresis of heat-treated thylakoid membranes as well as the FA composition of studied thylakoid membranes.

Higher thermal stability of PSII photochemistry of spruce is accompanied by the maintenance of PSII macro-organization

Ψ-Type CD bands of spruce thylakoid membranes had significantly higher T_m than *Arabidopsis* and barley ones (Fig. 2D; Table 1), while T_m values of LHCII trimer specific excitonic band pair were not different (Fig. 4D; Table 1). These results indicate that spruce thylakoid membranes have considerable higher thermal stability of chiral macro-organization of PPCs, but thermal destabilization of LHCII trimers itself remained the same in comparison with *Arabidopsis* and barely thylakoids, as also documented by CN-PAGE of heat-treated thylakoid membranes (Figs. 5, 8C, D).

Comparison of temperature dependences of F_V/F_M (Fig. 1) and Ψ-type CD (Fig. 2D) of all the three plant species studied clearly demonstrated that F_V/F_M started to decrease sharply after decline of Ψ-type amplitude to approximately 80 % of its value at 20 °C and complete PSII inactivation is caused by a drop of Ψ-type signal roughly below 60 %. These results indicate that stability of PSII macro-organization in different plant species quantitatively correlates with thermal stability of PSII photochemistry in intact needles/leaves and therefore is connected to the maintenance of photochemical activity under high temperature stress. Also linear dependency of T_m of F_V/F_M on the T_m of Ψ-type CD measured in several independent experiments for all the three studied plants or even for spruce needles in different developmental stages (Fig. 3) supports the connection between thermal stability of PSII photochemistry and PPC macro-organization. It should be noted that despite of close correlation between

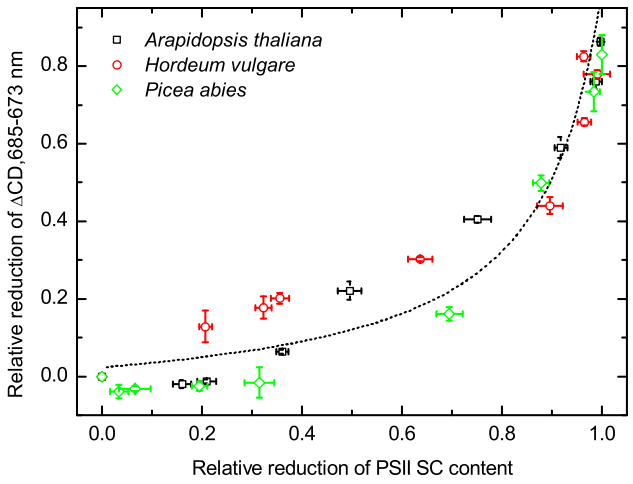

Fig. 9 Dependence of heat-induced reduction of the amplitude differences of the main Ψ-type bands at around (+)685 nm and (−)673 nm on the decrease in total content of PSII SCs in the heat-treated thylakoid membranes from *Arabidopsis* (*black squares*), barley (*red circles*) and spruce (*green diamonds*). Mean values (*points*) and standard deviations (*error bars*) from three independent experiments ($n = 3$) are displayed. *Line* represents regression fit curve [rational, $y = 1 - (1.097 \cdot (1 - x))/(0.124 + (1 - x))$, $R^2 = 0.92$]

the mentioned quantitative estimates of PSII thermal stability, T_m of Ψ-type CD was on average by 6 °C higher than T_m of F_V/F_M. Similarly, parameters derived from F_0 temperature curves (e.g. temperature of the 50 % increase of fluorescence from F_0 to F_M levels: T_{50}) occur at considerably higher temperatures than T_m of F_V/F_M and are usually tightly correlated together (Froux et al. 2004; Knight and Ackerly 2002). As a matter of fact, the decrease in F_V/F_M upon increasing temperatures is initiated due to a decrease in F_M with no increase of F_0, which indicate mainly a reversible increase of thermal dissipation in PSII (Berry and Björkman 1980; Epron 1997) and the increase of F_0 at higher temperatures reflects an irreversible inactivation of PSII photochemistry due to reaction centre disorganization (Berry and Björkman 1980). Hence, analyses of correlations between parameters derived from F_0 temperature curves and Ψ-type CD during heating could contribute to elucidation of suggested connection between thermal stability of PSII photochemistry and PPC macro-organization in thylakoid membranes.

It is valuable to note that heat sensitivity of the macrodomains was not affected by the isolation of thylakoid membranes. *Arabidopsis* and barley leaves exhibited similar T_m of both Ψ-type and excitonic CD bands or band pairs (e.g. $T_{m\ 685–730}$: 47.7 ± 1.6 and 47.5 ± 1.9 °C, respectively, mean value ± standard deviation, $n = 6$) as those measured using isolated thylakoid membranes (Table 1). Unfortunately, it was not possible to measure CD signal of spruce needles in vivo due to their structure and small size. Nevertheless, it is evident that information about thermal stability of both excitonic interactions between pigments within PPCs and Ψ-type CD bands from long-range ordered chromophores are equivalent on the levels of intact leaves and isolated thylakoid membranes.

Higher thermal stability of PSII macro-organization of spruce is associated with the maintenance of PSII supercomplexes in the thylakoid membrane

CN-PAGE of heat-treated thylakoid membranes revealed composition of PPCs in spruce thylakoid membranes (Fig. 5). Although the composition of PPCs in spruce membranes did not differ pronouncedly from that of *Arabidopsis* and barley, both absence of LHCII–CP29–CP24 complexes in spruce thylakoid membranes (Fig. 5) and 10 nm red shift of 77 K Chl *a* fluorescence emission maximum of PSII SCs from spruce (Fig. 6B) strongly indicate different structural organizations of LHCII in spruce PSII SCs as compared to those from *Arabidopsis* and barley. These results, together with smaller macrodomain organization in spruce membranes in comparison with *Arabidopsis* and barley, indicated by Ψ-type CD

Table 2 Fatty acid composition of thylakoid membranes in *Arabidopsis*, barley and spruce

		Arabidopsis	Barley	Spruce
Total FA content	μg mg^{-1} Chls	706 ± 50[a]	712 ± 20[a]	823 ± 25[b]
Saturated FA	%	8.0 ± 0.9[a]	4.0 ± 0.4[b]	13.0 ± 0.8[c]
Mono-unsaturated FA	%	6.6 ± 1.1[a]	2.3 ± 1.2[b]	0.3 ± 0.1[c]
Di-unsaturated FA	%	4.0 ± 0.3[a]	2.3 ± 0.2[b]	18.7 ± 0.6[c]
Tri-unsaturated FA	%	81.4 ± 1.4[a]	91.4 ± 1.5[b]	67.9 ± 0.8[c]
Unsaturated/saturated FA ratio		11.6 ± 1.4[a]	24.0 ± 2.6[b]	7.1 ± 0.6[c]
MGDG/DGDG		2.30 ± 0.36[a]	3.07 ± 0.11[b]	1.62 ± 0.23[c]

Total content of fatty acids (FAs) per chlorophylls (μg mg^{-1} Chl *a*), ratio of saturated, mono-, di- and tri-unsaturated FA–total FA content (%), ratio of unsaturated–saturated FA and ratio of FA contained in MGDG and DGDG determined by GC–MS were estimated in thylakoid membranes isolated from *Arabidopsis*, barley and spruce. The values represent the mean values and standard deviations from three independent experiments ($n = 3$). Data within a row followed by the same letter are not significantly different ($P > 0.05$)

signal of stacked thylakoid membranes (Figs. 2, 7) support absence of CP24 protein in spruce PSII, as the lack of the CP24 in *Arabidopsis* mutant koLhcb6 strongly reduces the macrodomain organization (Ψ-type CD signal) (Kovacs et al. 2006). Indeed, the loss of both Lhcb6 (CP24) and Lhcb3 proteins in some gymnosperm genera such as *Picea* was described very recently (Kouřil et al. 2016). Absence of these proteins in spruce led to modified structural organization of LHCII in PSII SCs similar to that observed in PSII SCs of *Chlamydomonas reinhardtii* (Kouřil et al. 2016).

Further, CN-PAGE of heat-treated thylakoid membranes revealed thermal stabilities of separated PPCs (Fig. 5). Among the separated PPCs, only PSII SCs revealed considerably higher thermal stability in spruce thylakoids as compared to *Arabidopsis* and barley ones (Figs. 5, 8C, D). The most heat sensitive PSII SCs disappeared in the temperature range from 40 to 52 °C (Figs. 5, 8C), thus roughly at the same temperatures as the Ψ-type CD signal (Fig. 8A). The most abundant LHCII trimers started to decrease at the temperature of 52 °C till 56 °C similarly as excitonic CD signal (Fig. 8B, D). Therefore, these results indicate that enhanced thermal stability of macrodomain organization of spruce is associated with the maintenance of PSII SCs in the thylakoid membrane, rather than with more stable LHCII trimers. The connection between the amount of PSII SCs and size of PPC macro-organization is further supported by dependence of the main Ψ-type CD bands reduction on decrease in total content of PSII SCs in the thylakoid membranes preheated to temperatures ranging from 20 to 60 °C (Fig. 9). At moderate reductions of PSII SCs, the Ψ-type band revealed approximately linear correlation with PSII SCs content, but at lower PSII SCs amount (below 10 % of that contained in membranes preheated to 20 °C), still almost 50 % of the Ψ-type CD amplitude observed in membranes preheated to 20 °C can be observed. It is appropriate to note that LHCII-only domains also contribute to the Ψ-type CD signal (Garab et al. 1991; Garab and Mustardy 1999), whose thermal stability cannot be determined by CN-PAGE, and could thus partially explain the observed residual Ψ-type CD signal after the disintegration of all PSII SCs. Nevertheless, the fact that main part of PSII inactivation and reduction of PSII SCs content occurs in a similar temperature range (40–46 °C) indicate that stability of PSII SCs may be important for short-term resistance of photosynthetic apparatus against heat stress.

Potential factors affecting the thermal stability of thylakoid membranes from spruce

Several possible factors determining the higher thermal stability of the PSII macro-organization of spruce thylakoid membranes can be proposed based on the presented results. As revealed by CD spectroscopy and CN-PAGE of heat-treated membranes, different structures of the PSII SCs from spruce result in smaller macrodomains, which may possess higher thermal stability itself. In addition to specific PSII structure, we have found several specific features of lipid composition in spruce thylakoids that can contribute to thermal stability.

More free packing of PPCs that can be expected from higher FA–Chl *a* ratio (Table 2) also could have the role in thermal stability of PSII. But as this ratio in spruce thylakoids was only by 10 % higher than in *Arabidopsis* and barley, we do not expect pronounced contribution of the higher lipid–protein ratio to the enhanced thermal stability of spruce PSII SCs. Although the relation of lipid desaturation and the thermal sensitivity of PSII is still unclear and data are contradictory (Allakhverdiev et al. 2008), increase in the degree of FA saturation in lipids of spruce thylakoid membranes (Table 2) could be further factor responsible for the enhanced thermal stability of PSII. Moreover, considerably lower ratio of MGDG/DGDG in spruce thylakoid membranes can significantly affect membranes stability at higher temperatures (Krumova et al. 2010). In addition, destabilization of LHCII trimers was not affected by DGDG content as concluded from the same temperature dependence of LHCII trimers disassembly in wild-type *Arabidopsis* and its DGDG-deficient mutant thylakoid membranes (Krumova et al. 2010). Despite lower MGDG/DGDG ratio in spruce thylakoids, monomerization of LHCII trimers in *Arabidopsis*, barley and spruce occurred at the same temperature (T_m approximately 62 °C, Fig. 4D; Table 1) which is in agreement with Krumova et al. (2010). On the other hand, the thermal stability of LHCII monomers in spruce thylakoid membranes was significantly higher than in *Arabidopsis* and barley ones (Fig. 4E; Table 1). DGDG was resolved in the crystal structure of major LHCII (Liu et al. 2004; Yan et al. 2007). Therefore, possible role of interactions of LHCII and DGDG with FAs specific for gymnosperms (e.g. Δ5-unsaturated FAs) (Moellering et al. 2009; Mongrand et al. 2001) on the thermal stability of LHCII proteins cannot be excluded.

Although we cannot distinguish between the contribution of these factors to resulting higher thermal stability of PSII function and structure in spruce thylakoid membranes, we suppose that different lipid–protein interactions together with different structures of PSII SCs play a crucial role.

Acknowledgments This work was supported by Grant Agency of the Czech Republic No. 13-28093S/P501. VK, IK, KV and OU were supported by Grant Number LO1415 and VŠ was supported by Grant Number LO1208 under the National Sustainability Program I (NPU I, Ministry of Education, Youth and Sports of CR).

References

Allakhverdiev SI, Kreslavski VD, Klimov VV, Los DA, Carpentier R, Mohanty P (2008) Heat stress: an overview of molecular responses in photosynthesis. Photosynth Res 98:541–550. doi:10.1007/s11120-008-9331-0

Barzda V, Mustardy L, Garab G (1994) Size dependency of circular-dichroism in macroaggregates of photosynthetic pigment–protein complexes. Biochemistry 33:10837–10841. doi:10.1021/bi00201a034

Berry J, Björkman O (1980) Photosynthetic response and adaptation to temperature in higher-plants. Annu Rev Plant Physiol 31:491–543. doi:10.1146/annurev.pp.31.060180.002423

Brestič M, Živčák M, Kalaji HM, Carpentier R, Allakhverdiev SI (2012) Photosystem II thermostability in situ: environmentally induced acclimation and genotype-specific reactions in *Triticum aestivum* L. Plant Physiol Biochem 57:93–105. doi:10.1016/j.plaphy.2012.05.012

Chen HX, Li WJ, An SZ, Gao HY (2004) Characterization of PSII photochemistry and thermostability in salt-treated *Rumex* leaves. J Plant Physiol 161:257–264. doi:10.1078/0176-1617-01231

Cramer WA, Whitmarsh J, Low PS (1981) Differential scanning calorimetry of chloroplast membranes: identification of an endothermic transition associated with the water-splitting complex of photosystem II. Biochemistry 20:157–162

Cseh Z, Rajagopal S, Tsonev T, Busheva M, Papp E, Garab G (2000) Thermooptic effect in chloroplast thylakoid membranes. Thermal and light stability of pigment arrays with different levels of structural complexity. Biochemistry 39:15250–15257. doi:10.1021/Bi001600d

DelasRivas J, Barber J (1997) Structure and thermal stability of photosystem II reaction centers studied by infrared spectroscopy. Biochemistry 36:8897–8903. doi:10.1021/bi970684w

Dinamarca J et al (2011) Double mutation in photosystem II reaction centers and elevated CO_2 grant thermotolerance to mesophilic cyanobacterium. PLoS One 6:e28389. doi:10.1371/journal.pone.0028389

Dobrikova AG et al (2003) Structural rearrangements in chloroplast thylakoid membranes revealed by differential scanning calorimetry and circular dichroism spectroscopy. Thermo-optic effect. Biochemistry 42:11272–11280. doi:10.1021/bi034899j

Epron D (1997) Effects of drought on photosynthesis and on the thermotolerance of photosystem II in seedlings of cedar (*Cedrus atlantica* and *C. libani*). J Exp Bot 48:1835–1841. doi:10.1093/jexbot/48.315.1835

Froux F, Ducrey M, Epron D, Dreyer E (2004) Seasonal variations and acclimation potential of the thermostability of photochemistry in four Mediterranean conifers. Ann For Sci 61:235–241. doi:10.1051/forest:2004016

Garab G, Mustardy L (1999) Role of LHCII-containing macrodomains in the structure, function and dynamics of grana. Aust J Plant Physiol 26:649–658

Garab G, van Amerongen H (2009) Linear dichroism and circular dichroism in photosynthesis research. Photosynth Res 101:135–146. doi:10.1007/s11120-009-9424-4

Garab G, Kieleczawa J, Sutherland JC, Bustamante C, Hind G (1991) Organization of pigment protein complexes into macrodomains in the thylakoid membranes of wild-type and chlorophyll-*b*-less mutant of barley as revealed by circular-dichroism. Photochem Photobiol 54:273–281. doi:10.1111/j.1751-1097.1991.tb02016.x

Garab G et al (2002) Light-induced trimer to monomer transition in the main light-harvesting antenna complex of plants: thermo-optic mechanism. Biochemistry 41:15121–15129. doi:10.1021/bi026157g

Georgakopoulou S, van der Zwan G, Bassi R, van Grondelle R, van Amerongen H, Croce R (2007) Understanding the changes in the circular dichroism of light harvesting complex II upon varying its pigment composition and organization. Biochemistry 46:4745–4754. doi:10.1021/bi062031y

Ghouil H, Montpied P, Epron D, Ksontini M, Hanchi B, Dreyer E (2003) Thermal optima of photosynthetic functions and thermostability of photochemistry in cork oak seedlings. Tree Physiol 23:1031–1039

Gombos Z, Wada H, Hideg E, Murata N (1994) The unsaturation of membrane-lipids stabilizes photosynthesis against heat-stress. Plant Physiol 104:563–567

Harwood JL (1998) Involvement of chloroplast lipids in the reaction of plants submitted to stress. In: Siegenthaler PA, Murata N (eds) Lipids in photosynthesis: structure, function and genetics. Kluwer Academic Publishers, Dordrecht, pp 290–300

Hu ZH, Xu YN, Jiang GZ, Kuang TY (2004) Degradation and inactivation of photosystem I complexes during linear heating. Plant Sci 166:1177–1183. doi:10.1016/j.plantsci.2003.12.026

Ilík P, Krchňák P, Tomek P, Nauš J (2002) 2-D gel densitometer for high-contrast and selective imaging of chlorophyll-containing protein complexes separated by non-denaturing polyacrylamide gel electrophoresis. J Biochem Biophys Methods 51:273–281. doi:10.1016/S0165-022x(02)00029-5

Järvi S, Suorsa M, Paakkarinen V, Aro EM (2011) Optimized native gel systems for separation of thylakoid protein complexes: novel super- and mega-complexes. Biochem J 439:207–214. doi:10.1042/bj20102155

Karunen P (1991) Galactolipid fatty-acids of bryophytes. In: Quinn PJ, Harwood JL (eds) Plant lipid biochemistry, structure and utilization. Proceedings of the 9th international symposium plant lipids. Portland Press, London, pp 30–32

Knight CA, Ackerly DD (2002) An ecological and evolutionary analysis of photosynthetic thermotolerance using the temperature-dependent increase in fluorescence. Oecologia 130:505–514. doi:10.1007/s00442-001-0841-0

Kouřil R, Nosek L, Bartoš J, Boekema EJ, Ilík P (2016) Evolutionary loss of light-harvesting proteins Lhcb6 and Lhcb3 in major land plant groups—break-up of current dogma. N Phytol. doi:10.1111/nph.13947

Kovacs L et al (2006) Lack of the light-harvesting complex CP24 affects the structure and function of the grana membranes of higher plant chloroplasts. Plant Cell 18:3106–3120. doi:10.1105/tpc.106.045641

Krumova SB, Todinova SJ, Busheva MC, Taneva SG (2005) Kinetic nature of the thermal destabilization of LHCII macroaggregates. J Photochem Photobiol B 78:165–170. doi:10.1016/j.jphotobiol.2004.11.005

Krumova SB, Laptenok SP, Kovacs L, Toth T, van Hoek A, Garab G, van Amerongen H (2010) Digalactosyl-diacylglycerol-deficiency lowers the thermal stability of thylakoid membranes. Photosynth Res 105:229–242. doi:10.1007/s11120-010-9581-5

Laczko-Dobos H, Szalontai B (2009) Lipids, proteins, and their interplay in the dynamics of temperature-stressed membranes of a cyanobacterium, *Synechocystis* PCC 6803. Biochemistry 48:10120–10128. doi:10.1021/bi9011034

Lambrev PH, Varkonyi Z, Krumova S, Kovacs L, Miloslavina Y, Holzwarth AR, Garab G (2007) Importance of trimer–trimer interactions for the native state of the plant light-harvesting complex II. In: International conference on photosynthesis in the post genomic era—structure and function of photosystems, Pushchino, Russia, 20–26 August 2007. Elsevier Science Bv, Amsterdam, p 847–853. doi:10.1016/j.bbabio.2007.01.010

Lichtenthaler HK (1987) Chlorophylls and carotenoids—pigments of photosynthetic biomembranes. Method Enzymol 148:350–382

Lípová L, Krchňák P, Komenda J, Ilík P (2010) Heat-induced disassembly and degradation of chlorophyll-containing protein complexes in vivo. Biochim Biophys Acta Bioenerg 1797:63–70. doi:10.1016/j.bbabio.2009.08.001

Liu ZF et al (2004) Crystal structure of spinach major light-harvesting complex at 2.72 angstrom resolution. Nature 428:287–292. doi:10.1038/nature02373

Lu CM, Zhang JH (1999) Effects of water stress on photosystem II photochemistry and its thermostability in wheat plants. J Exp Bot 50:1199–1206

Makarenko SP, Konenkina TA, Suvorova GG, Oskorbina MV (2014) Seasonal changes in the fatty acid composition of *Pinus sylvestris* needle lipids. Russ J Plant Physiol 61:119–123. doi:10.1134/S1021443713050105

Meehl GA, Tebaldi C (2004) More intense, more frequent, and longer lasting heat waves in the 21st century. Science 305:994–997. doi:10.1126/science.1098704

Moellering ER, Miller R, Benning C (2009) Molecular genetics of lipid metabolism in the model green alga *Chlamydomonas reinhardtii*. In: Wada H, Murata N (eds) Lipids in photosynthesis: essential and regulatory functions. Springer Netherlands, Dordrecht, pp 139–155

Mongrand S, Badoc A, Patouille B, Lacomblez C, Chavent M, Cassagne C, Bessoule JJ (2001) Taxonomy of gymnospermae: multivariate analyses of leaf fatty acid composition. Phytochemistry 58:101–115. doi:10.1016/S0031-9422(01)00139-X

Nanjo Y, Mizusawa N, Wada H, Slabas AR, Hayashi H, Nishiyama Y (2010) Synthesis of fatty acids de novo is required for photosynthetic acclimation of *Synechocystis* sp. PCC 6803 to high temperature. Biochim Biophys Acta Bioenerg 1797:1483–1490. doi:10.1016/j.bbabio.2010.03.014

Nosek L (2012) Usage of 2D-CN/SDS-PAGE for determination of changes in pigment–protein complexes from thylakoid membranes of stressed plants. Masters Thesis, Palacky University, Olomouc

Pospíšil P, Tyystjarvi E (1999) Molecular mechanism of high-temperature-induced inhibition of acceptor side of Photosystem II. Photosynth Res 62:55–66. doi:10.1023/A:1006369009170

Shi H, Xiong L, Yang KY, Tang CQ, Kuang TY, Zhao NM (1998) Protein secondary structure and conformational changes of photosystem II during heat denaturation studied by Fourier transform-infrared spectroscopy. J Mol Struct 446:137–147. doi:10.1016/S0022-2860(98)00287-7

Varkonyi Z, Nagy G, Lambrev P, Kiss AZ, Szekely N, Rosta L, Garab G (2009) Effect of phosphorylation on the thermal and light stability of the thylakoid membranes. Photosynth Res 99:161–171. doi:10.1007/s11120-008-9386-y

Wen XG, Qiu NW, Lu QT, Lu CM (2005) Enhanced thermotolerance of photosystem II in salt-adapted plants of the halophyte *Artemisia anethifolia*. Planta 220:486–497. doi:10.1007/s00425-004-1382-7

Williams WP (1994) The role of lipids in the structure and function of photosynthetic membranes. Prog Lipid Res 33:119–127

Yan HC, Zhang PF, Wang C, Liu ZF, Chang WR (2007) Two lutein molecules in LHCII have different conformations and functions: insights into the molecular mechanism of thermal dissipation in plants. Biochem Biophys Res Commun 355:457–463. doi:10.1016/j.bbrc.2007.01.172

Yang CH, Boggasch S, Haase W, Paulsen H (2006) Thermal stability of trimeric light-harvesting chlorophyll *a*/*b* complex (LHCIIb) in liposomes of thylakoid lipids. Biochim Biophys Acta Bioenerg 1757:1642–1648. doi:10.1016/j.bbabio.2006.08.010

Zhang R, Sharkey TD (2009) Photosynthetic electron transport and proton flux under moderate heat stress. Photosynth Res 100:29–43. doi:10.1007/s11120-009-9420-8

Zhang YJ, Liu C, Liu SA, Shen Y, Kuang TY, Yang CH (2008) Structural stability and properties of three isoforms of the major light-harvesting chlorophyll *a*/*b* complexes of photosystem II. Biochim Biophys Acta Bioenerg 1777:479–487. doi:10.1016/j.bbabio.2008.04.012

Zhang R, Cruz JA, Kramer DM, Magallanes-Lundback ME, Dellapenna D, Sharkey TD (2009) Moderate heat stress reduces the pH component of the transthylakoid proton motive force in light-adapted, intact tobacco leaves. Plant Cell Environ 32:1538–1547. doi:10.1111/j.1365-3040.2009.02018.x

Photosynth Res (2012) 111:29–39
DOI 10.1007/s11120-011-9664-y

REGULAR PAPER

Anisotropic circular dichroism signatures of oriented thylakoid membranes and lamellar aggregates of LHCII

Yuliya Miloslavina · Petar H. Lambrev · Tamás Jávorfi · Zsuzsanna Várkonyi · Václav Karlický · Joseph S. Wall · Geoffrey Hind · Győző Garab

Received: 4 February 2011 / Accepted: 27 May 2011 / Published online: 12 June 2011

Abstract In photosynthesis research, circular dichroism (CD) spectroscopy is an indispensable tool to probe molecular architecture at virtually all levels of structural complexity. At the molecular level, the chirality of the molecule results in intrinsic CD; pigment–pigment interactions in protein complexes and small aggregates can give rise to excitonic CD bands, while "psi-type" CD signals originate from large, densely packed chiral aggregates. It has been well established that anisotropic CD (ACD), measured on samples with defined non-random orientation relative to the propagation of the measuring beam, carries specific information on the architecture of molecules or molecular macroassemblies. However, ACD is usually combined with linear dichroism and can be distorted by instrumental imperfections, which given the strong anisotropic nature of photosynthetic membranes and complexes, might be the reason why ACD is rarely studied in photosynthesis research. In this study, we present ACD spectra, corrected for linear dichroism, of isolated intact thylakoid membranes of granal chloroplasts, washed unstacked thylakoid membranes, photosystem II (PSII) membranes (BBY particles), grana patches, and tightly stacked lamellar macroaggregates of the main light-harvesting complex of PSII (LHCII). We show that the ACD spectra of face- and edge-aligned stacked thylakoid membranes and LHCII lamellae exhibit profound differences in their psi-type CD bands. Marked differences are also seen in the excitonic CD of BBY and washed thylakoid membranes. Magnetic CD (MCD) spectra on random and aligned samples, and the largely invariable nature of the MCD spectra, despite dramatic variations in the measured isotropic and anisotropic CD, testify that ACD can be measured without substantial distortions and thus employed to extract detailed information on the (supra)molecular organization of photosynthetic complexes. An example is provided showing the ability of CD data to indicate such an organization, leading to the discovery of a novel crystalline structure in macroaggregates of LHCII.

Keywords Anisotropic circular dichroism · Magnetic circular dichroism · Psi-type circular dichroism · Thylakoid membranes · Grana patches · Light-harvesting complexes

Abbreviations

ACD	Anisotropic circular dichroism
BBY	Photosystem II-enriched grana membrane fragments, isolated according to Berthold, Babcock and Yocum
CD	Circular dichroism
CD_{exc}	Excitonic circular dichroism
CD_{ψ}	Psi-type circular dichroism
Chl	Chlorophyll
LD	Linear dichroism
LHCII	Light-harvesting complex of Photosystem II
MCD	Magnetic circular dichroism
PSI, PSII	Photosystem I, II
STEM	Scanning transmission electron microscopy

Y. Miloslavina · P. H. Lambrev · Z. Várkonyi · V. Karlický · G. Garab (✉)
Institute of Plant Biology, Biological Research Center, Hungarian Academy of Sciences, P.O. Box 521, 6701 Szeged, Hungary
e-mail: gyozo@brc.hu

T. Jávorfi
Diamond Light Source Ltd., Diamond House, Harwell Science and Innovation Campus, Chilton, Didcot OX11 0DE, UK

J. S. Wall · G. Hind
Biology Department, Brookhaven National Laboratory, Upton, NY, USA

Introduction

Photosynthetic membranes and isolated complexes, despite their remarkable diversity, exhibit strongly anisotropic and chiral pigment organization. This originates in the reaction center complexes as well as the antenna-reaction center super complexes. The presence of the strong pigment–pigment interactions in these systems makes the use of non-invasive, polarization spectroscopy techniques, such as linear dichroism (LD) and circular dichroism (CD), a valuable tool in elucidating their molecular architecture. The theoretical background, technical approaches and applicability of these methods in photosynthesis research have been covered in a number of books and review articles (Bloemendal and van Grondelle 1993; Clayton 1980; Garab 1996; Garab and van Amerongen 2009; Hofrichter and Eaton 1976; Johansson and Lindblom 1980; Norden et al. 1992; Pearlstein 1991; van Amerongen and Struve 1995; van Amerongen et al. 2000). As chirality can occur at different levels of structural complexity of the pigment system, CD spectroscopy can provide information on different levels of hierarchically organized assemblies (Garab and van Amerongen 2009). In most photosynthetic systems, CD signals arising from short-range intermolecular interactions are superimposed on those arising from molecular asymmetries. In densely packed aggregates with dimensions commensurate with the wavelength of visible light, an additional CD signal is superimposed on the spectrum, which arises from long-range chiral order of the chromophores.

The intrinsic CD (CD_i) signals of photosynthetic pigments are very weak because of the symmetry of the pigment molecules. CD_i bands can also be induced by the protein environment of symmetric or planar molecules, such as carotenoids and chlorophylls, which thus can exhibit large CD_i-type signals (Büchel and Garab 1997; Cogdell and Scheer 1985; Frank et al. 1989). CD induced by strong external magnetic field with the field vector oriented parallel to the direction of light propagation, i.e., magnetic CD (MCD) can be considered as a special case of CD_i because its band shape is identical with the absorbance of the molecule exhibiting the positive or negative MCD band; MCD can also take the shape of the first derivative of the absorbance band (Sutherland 1978; Sutherland and Holmquist 1980). MCD spectroscopy is valuable for detecting weak or "hidden" electronic transitions and is particularly strong in porphyrins (Sutherland 1978). In this article, we show that it can be used as a specific spectroscopic marker—an internal standard in highly organized samples.

Excitonic CD (CD_{exc}) signals, arising from pigment–pigment interactions in pigment-protein complexes and small aggregates, are most easily recognized by their split conservative band structure, i.e., when plotted on an energy scale, the positive and negative bands exhibit equal areas. CD_{exc} is sensitive even to minor perturbations in the structure or in molecular environments, such as the effects of single mutations (Croce et al. 2004; Morosinotto et al. 2003) or the removing of complexes from their native environments (Lambrev et al. 2007). Hence, CD_{exc} is often used for fingerprinting isolated native and reconstituted complexes (Yang et al. 2008). A noteworthy property of CD_{exc} is that its magnitude, in addition to the strength of the dipole–dipole interactions, depends largely on the mutual orientation of the participating pigment molecules. This property, as will be discussed below, is of interest with regard to the inherent anisotropic architecture of photosynthetic membranes and (super) complexes.

Psi-type (psi: polymer- or salt-induced) CD (CD_ψ) arises from interactions of light with large chirally organized inhomogeneous molecular aggregates containing a high density of intensely interacting chromophores. Such features are abundant in viruses, nuclei, chromosomes, and different protein aggregates (Keller and Bustamante 1986; Tinoco et al. 1987). In photosynthesis, chiral macrodomains have been identified in granal thylakoid membranes and lamellar aggregates of LHCII. These macroassemblies exhibit psi-type features: large, anomalously shaped bands, accompanied by long tails outside the principal absorbance bands, which originate from differential scattering of left and right circularly polarized beams (Garab et al. 1988a, c). Genetic modifications, such as knock-out of specific antenna components can also affect the macroorganization of the complexes, which in turn is reflected in the CD spectra (Kovacs et al. 2006). CD_ψ readily monitors structural reorganizations in granal thylakoid membranes, which are very flexible and sensitive to environmental changes and can undergo light-induced reversible reorganizations driven by fast local thermal transients due to the dissipation of excess excitation (Barzda et al. 1996; Garab et al. 1988b; Istokovics et al. 1997). Structurally flexible chiral macrodomains have also been shown to be present in different algal cells (Büchel and Garab 1997; Goss et al. 2000; Szabó et al. 2008). Hence, CD_ψ is a sensitive tool to monitor the structure and structural dynamics in highly organized membrane systems in vivo. However, the nature of CD_ψ is extremely complex and is not well understood.

In contrast to CD, which is conventionally measured in an isotropic phase, that is, on randomly oriented complexes and membranes, LD can only be measured with non-random (anisotropic) orientation of the sample. It is well known, however, that CD also depends on the propagation direction of light with respect to the chiral molecule or oriented anisotropic phase (Schellman and Jensen 1987). The CD measured on molecules with fixed orientation, termed anisotropic CD (ACD), reveals additional, independent information about the system under investigation

that is not available in the isotropic CD (CD_{iso}) spectrum (Kuball 2002; Kuball et al. 1993, 2005; Kuball and Höfer 2000a, b). ACD of oriented molecules can yield information about their molecular configuration and chirality. ACD can also be employed to study chiral anisotropic phases, i.e., phases with superstructural chirality, which may be composed of chiral or achiral molecules. Despite these unique features of ACD, it has been rarely applied to studies of anisotropic photosynthetic systems. This might be due to a concern that ACD is possibly distorted by LD contributions, since LD is much more intense than CD. Contributions from LD, and from spurious ACD signals arising from instrumental artifacts, must be carefully assessed and corrected.

In this article, we have measured CD on oriented samples of differing complexity and corrected the spectra for LD contributions. By using MCD, as a distinctive, internally inducible CD signal, we show that our ACD spectra are essentially free of artifacts, and thus can be used for the characterization of molecular (macro) organizations. Our data show that CD_{ψ} spectra of lamellar macroaggregates of LHCII in stacked thylakoid membranes exhibit strong orientation dependency. By observing ACD, the lateral and inter-lamellar components of CD_{ψ} can be separated. Likewise, the CD of osmotically disrupted thylakoid membranes and PSII membrane fragments, which lack CD_{ψ}, are also found to be orientation-dependent, possibly allowing resolution of pigment–pigment interactions in the native membranes. An intense CD signal can be seen in aggregates of the delipidated LHCII-prompted study of this system using scanning transmission electron microscopy (STEM). A novel form of two-dimensional LHCII aggregate was visualized, and this is proposed to be the source of the intense CD signal. A preliminary description of this structure is reported.

Materials and methods

Thylakoid membranes

Thylakoid membranes (broken chloroplasts) and LHCII trimers from spinach were isolated as in Lambrev et al. (2007). Unstacked and osmotically disrupted thylakoid membranes were prepared by washing three times with 20 mM tricine buffer (pH 7.5). Tightly stacked lamellar macroaggregates of LHCII (type IV) were isolated as described by Simidjiev et al. (1997).

PSII-enriched grana membranes (BBY)

These were prepared from freshly isolated thylakoid membranes according to the procedure described by Völker et al. (1985) with some modifications. Thylakoid membranes were resuspended to 3 mg/ml chlorophyll concentration in stacking buffer containing 2 mM MES((pH 6.3), 5 mM $MgCl_2$, and 15 mM NaCl; after 45 min incubation on ice half the volume of 10% Triton X-100 was added to ensure a 1:10 Chl:detergent ratio. The samples were incubated on ice in the dark for 30 min, then the digested samples were diluted with stacking buffer and centrifuged at 30,000*g* for 30 min. The pellet was resuspended in stacking medium and spun down at 5,000*g* for 5 min to remove the unsolubilized material. The supernatant was centrifuged at 30,000*g* for 30 min, and the sedimented grana membrane fraction was resuspended in a buffer containing 20 mM tricine (pH 7.5), 5 mM $MgCl_2$, 5 mM NaCl, and 0.4 M sorbitol.

Grana patches were isolated from market spinach according to the procedure described by Morosinotto et al. (2010). Solubilization was done with 0.6% α-DM.

Circular dichroism and linear dichroism

CD and LD spectra were registered with a JASCO 815 dichrograph. Orientation of samples for LD and ACD measurements was achieved either by magnetic field or by gel-squeezing (see below). Magnetic alignment was used for the membranes and membrane-like particles (lamellar aggregates), which tend to orient themselves with their planes perpendicularly to the field. The poles of the NdFeB permanent magnets were oriented either along or perpendicularly to the excitation beam, hence, the membranes were oriented perpendicularly or parallel to the beam, respectively. The former orientation is referred to as face-aligned and the latter as edge-aligned (see Fig. 1). LD was measured in edge-aligned position; it vanishes for the face-aligned membranes. Magnetic field strength was ~0.6 T.

In the face-aligned position, the magnetic field induces MCD, so that the measured CD signal is the sum of ACD and MCD. These two contributions to the CD spectra are easily distinguished by reversing the magnetic field direction (polarity):

$$\mathrm{ACD} = \frac{1}{2}(\mathrm{CD}_{\mathrm{N}\rightarrow\mathrm{S}} + \mathrm{CD}_{\mathrm{S}\rightarrow\mathrm{N}})$$

$$\mathrm{MCD} = \frac{1}{2}(\mathrm{CD}_{\mathrm{N}\rightarrow\mathrm{S}} - \mathrm{CD}_{\mathrm{S}\rightarrow\mathrm{N}})$$

where $CD_{S\rightarrow N}$ and $CD_{N\rightarrow S}$ denote CD measured at reversed polarities of the magnet.

The measured CD signal, especially in edge-aligned orientation, can be distorted by the linear anisotropy of the sample (Disch and Sverdlik 1969), which can give rise to LD if the circular polarization of the beam is imperfect. LD of the sample can also couple with the inherent

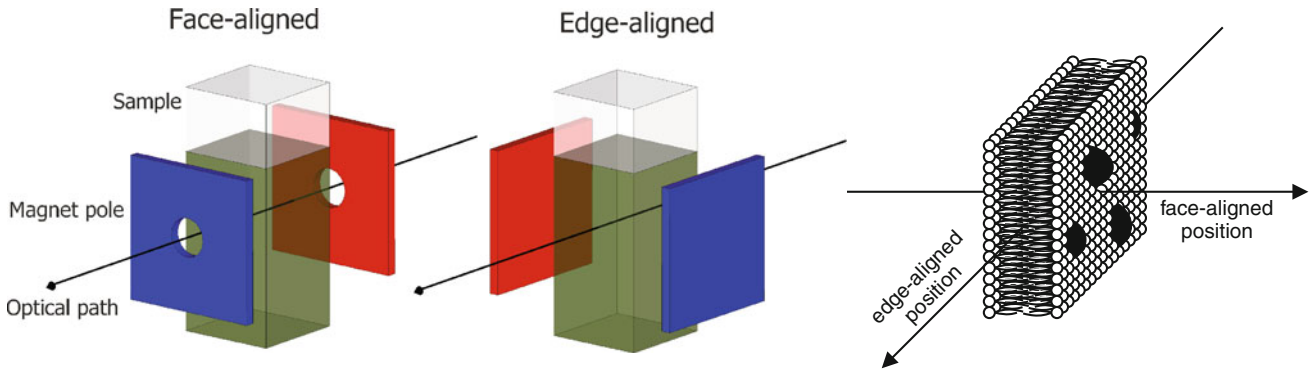

Fig. 1 Schematic view of the magnetic alignment of membranes for ACD measurement. In face-aligned orientation, the magnetic field is parallel to the measuring beam, in edge-aligned—perpendicular. The membranes in the external magnetic field are aligned preferentially with their planes perpendicular to the field vector, and thus show either their face or edge to the measuring beam

birefringence of the instrument itself to give spurious CD (Davidsson et al. 1980; Schellman and Jensen 1987). To correct for such distortions, the sample was rotated about the optical axis, and measurements were taken in two orthogonal positions—horizontal and vertical. Because rotation of the sample by 90° inverses the sign of LD, the arithmetic mean of the CD measured in the horizontal and vertical position is free from LD artifacts (Tunis-Schneider and Maestre 1970):

$$\mathrm{ACD} = \frac{1}{2}(\mathrm{CD}_{\mathrm{horiz.}} + \mathrm{CD}_{\mathrm{vert.}})$$

Washed, unstacked thylakoids, membrane fragments, and solubilized complexes do not align in a magnetic field and were oriented by gel-squeezing instead (Abdourakhmanov et al. 1979). Samples were trapped in 5% acrylamide:bis-acrylamide (30:1), polymerized with 0.2% ammonium persulfate, and 0.2% *N*,*N*,*N*′,*N*′-tetramethylethylene-diamine (TEMED). The gels were pressed in one direction to 60% of their length. The gels were placed in the dichrograph so that the excitation beam traversed the pressed side (face-aligned) or the stretched side (edge-aligned).

Scanning transmission electron microscopy

LHCII preparations were suspended in tricine buffer (pH 7.5) to chlorophyll concentration of 20–50 μg/ml and applied to carbon-coated grids, which were briefly washed in 20 mM ammonium acetate. The grids were frozen in liquid nitrogen and vacuum-dehydrated at −100°C. Images were analyzed using PCMass32 (available at ftp.stem.bnl.gov) to obtain mean mass per unit area (M/A). Mass values were referenced to the M/A for tobacco mosaic virus deposited on the same grid. Particle spacings were also analyzed using PCMass32.

Results and discussion

Isotropic circular dichroism

The well-known CD spectrum of intact, stacked thylakoid membranes in suspension (Barzda et al. 1996; Garab et al. 1988a) is characterized by strong psi-type bands in the blue and red region (Fig. 2a), which originate from the chiral macrodomains in the grana (Barzda et al. 1994; Garab et al. 1988a). CD_{ψ} is always accompanied by circular differential scattering (CDS) visible as long tail outside the principal absorption bands. After osmotic disruption of the granal macroorganization of the thylakoid membranes, the psi-type features are completely removed, and the spectra are dominated by excitonic CD bands arising from pigment–pigment interactions inside the pigment-protein complexes or their small aggregates (Barzda et al. 1996; Garab et al. 1991). The $\mathrm{CD}_{\mathrm{exc}}$ spectra of these membranes are very similar to the spectra of PSII-enriched (BBY) membrane fragments and grana patches (Fig. 2b), which are also stacked membranes but lack psi-type features. This demonstrates that the observation of CD_{ψ} requires more than simple pairing of membrane layers; a distinct 3D-ordered macroorganization must be present, to which the CD_{ψ} is very sensitive (Garab 1996; Keller and Bustamante 1986).

Strong CD_{ψ} can be generated not only in the native grana but also in isolated LHCII, which also can form chirally ordered lamellar macroaggregates (Simidjiev et al. 1997). In LHCII macroaggregates with long-range chiral order, large psi-type bands are superimposed on the excitonic bands (Fig. 3a). The illustration of this long-range LHCII order is shown in Fig. 3b obtained by STEM. Earlier, it has been thoroughly documented that psi-type CD is associated with large, densely packed aggregates (e.g. Keller and Bustamante 1986; Barzda et al. 1994). To our knowledge, this is the first demonstration that psi-type CD originates

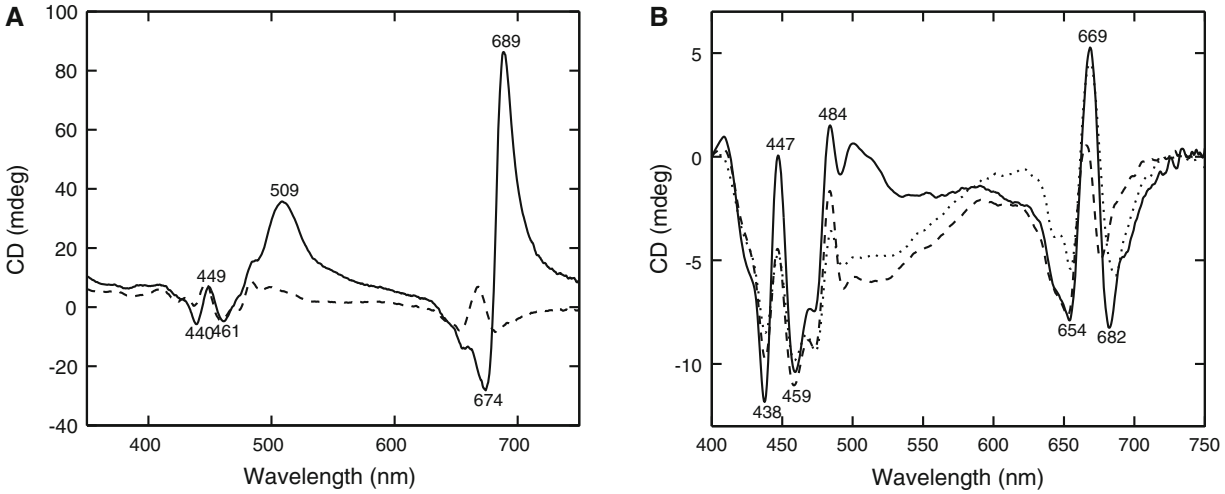

Fig. 2 CD spectra of thylakoid membranes, PSII-enriched (BBY) membranes, and isolated grana patches. **a** CD spectra of intact, stacked chloroplast thylakoid membranes (*solid line*), and thylakoid membranes (*dashed line*) washed in tricine buffer without sorbitol and cation supplements. **b** CD spectra of washed thylakoids (*solid line*), BBY particles (*dashed line*), and grana patches (*dotted line*)

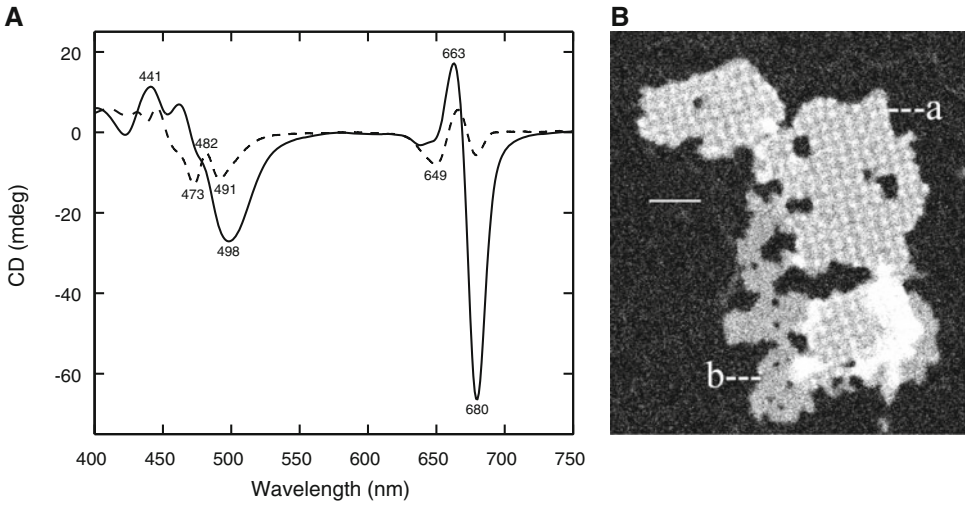

Fig. 3 **a** CD spectra of tightly stacked (type IV) lamellar macroaggregates of LHCII with long-range chiral order (*solid line*) and of LHCII trimers solubilized with *β*-DM (*dashed line*). **b** STEM image of unstained LHCII macroaggregate. Regions with (a) and without (b) particles are seen. Using PCMass32 software, mean particle spacing within rows was found to be 128 ± 3 Å, and the particle mass was estimated at 118 ± 7 kDa. Size marker: 500 Å

from ordered arrays of proteins, in this case light harvesting pigment-protein complexes. It represents an unstained image of a novel 2D-crystalline structure of LHCII macroaggregates: a rhombic, almost square array of particles with a mean repeat distance of ∼128 Å. The mass per unit area within the rhombic array was found to be ∼36 Da/Å^2 in contrast to a mean density of ∼29 Da/Å^2 in the adjoining featureless membrane. If the assumption is made that the particles lie on a patch of this membrane, the particle mass is measured to be 118 ± 7 kDa equivalent to a single LHCII trimer. Hence, we propose that the lamellar aggregates containing rhombic arrays of trimers are associated with large psi-type bands in the CD spectra of LHCII.

An interesting effect is observed comparing the CD of LHCII macroaggregates and the native chloroplast membrane—the CD spectra are remarkably similar but with opposite sign, as if comparing enantiomeric compounds, or comparing molecules with *syn* and *anti* configuration. While an exact explanation of this phenomenon is not given, we speculate that it may arise from the lateral arrangement of the LHCII complexes—in the native membrane, the trimeric complexes have the same orientation with respect to the lipid layer but in crystalline aggregates the trimers have alternating up-down orientations (Kühlbrandt et al. 1983; Standfuss et al. 2005). In line with the effects observed in thylakoid membranes, disruption of the macroorganization of LHCII eliminates the CD_{ψ}, and the much weaker CD_{exc} bands are revealed in detergent-solubilized LHCII trimers (Simidjiev et al. 1997).

Magnetic circular dichroism

In this study, we recorded MCD spectra by a simple procedure, viz. by subtracting two CD spectra measured in

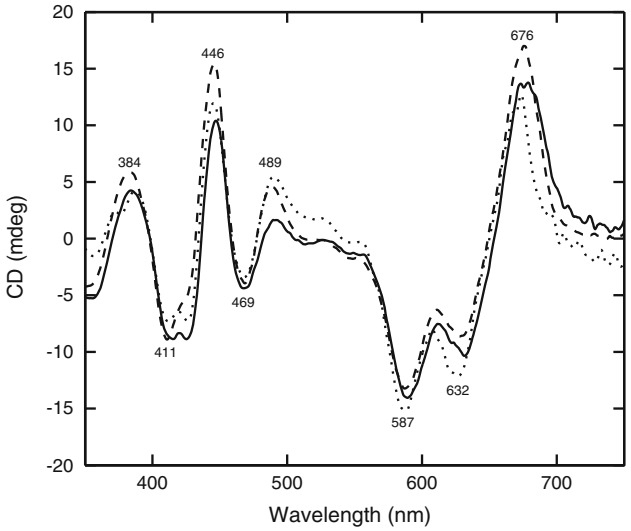

Fig. 4 Magnetic CD spectra of intact and washed thylakoid membranes and PSII-enriched (BBY) membranes (*solid*, *dashed* and *dotted lines*, respectively)

magnetic field with reverse direction. In this way, the inherent CD, even though might be much larger in intensity than the MCD, is completely eliminated while all other parameters remain unchanged. The MCD spectra of granal and osmotically disrupted thylakoids, as well as of PSII particles were virtually identical (Fig. 4), despite the drastic differences in their macroorganization and hence in their CD spectra (cf. Fig. 2). The magnetically induced orientation of the sample had very little effect on the MCD spectrum either. This was confirmed by measuring MCD spectra from samples that had been previously trapped in PAA gel to prevent their magnetic alignment (not shown) and comparing with the MCD spectra recorded in the random suspension. Insignificant differences between the MCD spectra of the aligned and randomly oriented membranes were found, e.g., at 490 nm but generally the spectra were nearly identical. Thus, MCD is essentially not affected by the supramolecular organization of the complexes, the orientation of the sample relative to the optical path, or by other optical effects like circular differential scattering. The fact that MCD was identical in samples with and without CD_{ψ} gives us confidence in the merit of the psi-type CD signal as a valuable indicator of the macroorganization because it shows that the CD measurement is free from artifacts due to scattering, etc. (see also Garab et al. 1988a). Thus, MCD spectra can serve as good "internal reference" for calibrating the results of CD measurements comparing samples with altered supramolecular structure, and hence different CD. Furthermore, although the CD of the photosynthetic complexes is a superposition of signals given rise by Chls and carotenoids (in the blue region), MCD is specific to Chls only and reveals weak Chl transitions with very small absorbance—the Chl Q_x bands at 580–630 nm (Sutherland and Holmquist 1980).

Anisotropic circular dichroism

ACD spectra, i.e., CD spectra recorded on spatially aligned samples with defined orientation of the pigment transition dipoles relative to the excitation path, are shown in Figs. 5 and 6. ACD allows us to differentiate between the

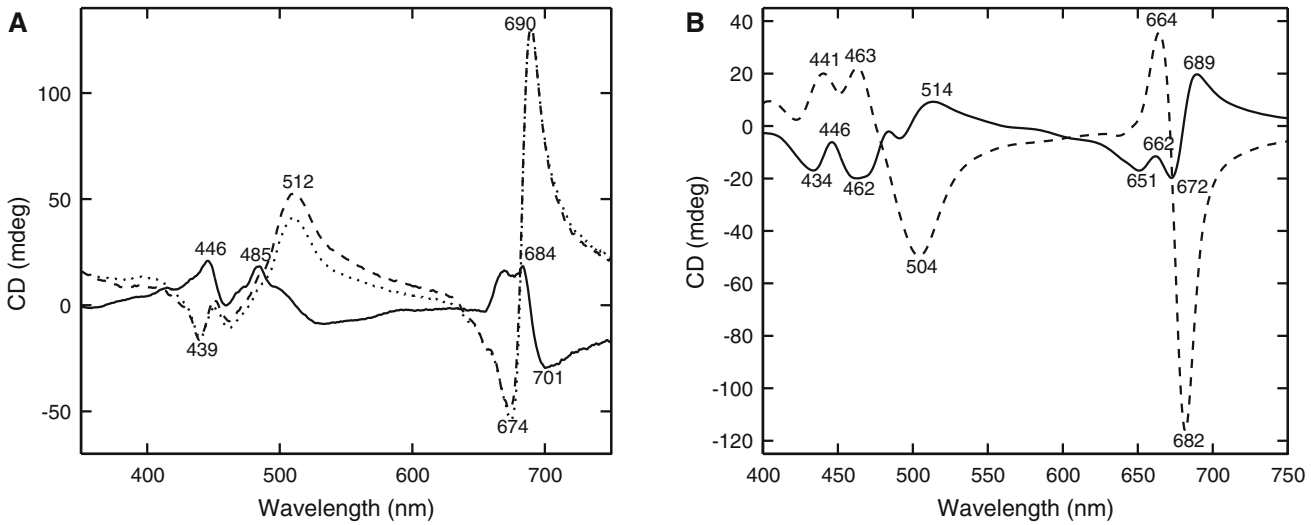

Fig. 5 **a** ACD spectra of intact thylakoid membranes in face-aligned orientation (*solid line*), and in edge-aligned orientation, either directly measured (*dotted line*) or calculated as $CD_{edge} = \frac{1}{2}(3CD_{random} - CD_{face})$ (*dashed line*). The membranes were oriented in solution by external magnetic field (~0.6 T). The edge-aligned spectrum, measured in a different optical cell, is additionally corrected by subtracting a straight baseline such that the two spectra cross each other at 350 nm and 750 nm. **b** ACD spectrum of magnetically aligned lamellar macroaggregates of LHCII with long-range chiral order in face- and edge-aligned orientation (*solid* and *dashed line*, respectively)

perpendicular (face-aligned) and parallel (edge-aligned) orientation of the sample to the beam. The face-aligned CD reveals structural features and interactions which primarily originate from transition dipole moments lying in the membrane plane (in-plane organization). In contrast, transition dipole moments lying along the normal to the membrane plane will preferentially contribute to the edge-aligned CD, which, for multilamellar systems reveals features and interactions between membrane sheets (inter-lamellar organization, Fig. 1).

The total CD in randomly oriented samples (isotropic CD) is the sum of the contributions from the different anisotropic CD components (Kuball et al. 1993, 2005):

$$\mathrm{CD_{iso}} = \frac{1}{3}\left(\mathrm{ACD}_x + \mathrm{ACD}_y + \mathrm{ACD}_z\right)$$

In the case of membrane disks, if the z-axis is defined as normal to the membrane plane, then in face-aligned orientation the z-axis is parallel to the optical path, hence $\mathrm{CD_{face}} = \mathrm{ACD}_z$ (in reality the measureable $\mathrm{CD_{face}}$ is a linear combination of all ACD components with weighting factors depending on the orientation distribution). In edge-aligned orientation, since there is a rotational symmetry (C_∞) about the z-axis, the measured CD will be composed of both the ACD_x and ACD_y components:

$$\mathrm{CD_{edge}} = \frac{1}{2}\left(\mathrm{ACD}_x + \mathrm{ACD}_y\right)$$

The isotropic CD is then

$$\mathrm{CD_{iso}} = \frac{1}{3}\left(\mathrm{CD_{face}} + 2\mathrm{CD_{edge}}\right)$$

It follows that, for uniaxial samples, it is sufficient to measure the CD in isotropic and only one of the oriented positions, while the other can be calculated (Kuball et al. 1993, 2005):

$$\mathrm{CD_{edge}} = \frac{1}{2}\left(3\mathrm{CD_{iso}} - \mathrm{CD_{face}}\right)$$

We stress that in any practical scenario the sample orientation is not perfectly uniform, hence the ACD components are not completely resolved in the measured $\mathrm{CD_{face}}$ and $\mathrm{CD_{edge}}$ spectra. The contribution of each ACD component can be calculated if the orientation distribution (mosaic spread) is known. For qualitative comparison and assignment of the spectral bands to one or the other ACD component, this is not necessary.

To validate the calculation of $\mathrm{CD_{edge}}$, the spectra derived as above were compared with the actually measured spectra from samples in edge-aligned orientation. The experimentally measured $\mathrm{CD_{edge}}$ matched quite well the calculated one (Fig. 5a), using $\mathrm{CD_{iso}}$ and $\mathrm{CD_{face}}$. This is noteworthy because the face-aligned and edge-aligned membranes differ basically in almost all relevant optical properties: LD is maximum with edge-aligned orientation and minimum (vanishes) for the face-aligned position (Breton and Vermeglio 1982); significant differences have been shown between selective polarized light-scattering spectra of the two orientations (Swenberg and Geacintov 1976); also birefringence is maximum for the edge-aligned position while very small for face-aligned chloroplasts (Garab et al. 2005; Steinbach et al. 2005). Hence, the fact that the above correlation between the ACD components and $\mathrm{CD_{iso}}$ holds true in the experiments, which nevertheless must be carefully executed, shows that despite the high complexity of the sample, exhibiting strong LD, birefringence, and differential scattering signals and possible imperfections in the optical system, ACD can be measured without significant distortions. Further confidence is given by the fact that the MCD spectrum of the random sample (Fig. 4) and the spectra of two orientations (data not shown, cf. Garab et al. 1988a), were almost identical, despite the large differences in the spectral shapes in the absence of external magnetic field.

A comparison of $\mathrm{CD_{edge}}$ and $\mathrm{CD_{face}}$ shows dramatic differences. Most notable is the sign inversion of the CD in the tails of the main psi-type bands (512 nm, 690 nm) but also the inverted sign at some of the CD extrema (439 nm, 674 nm) (Fig. 5a). The same effect was found previously in oriented chloroplasts in face-aligned position (Garab et al. 1988a). This sign-inversion might be explained by the complex angular dependence of circular intensity differential scattering, which is associated with psi-type signals and exhibits lobes with alternating signs (Garab et al. 1988c). The bands in the blue region of the CD spectra from edge-aligned orientation were found at (−)439, (+)450, (−)463, and (+)512 nm, whereas in the face-aligned spectra the peaks were located at (+)446, (−)460, (+)485, and (−)530 nm. In the Chl-Q_y region the edge-aligned chloroplasts showed a (−)674, (+)690 nm band pair and the face-aligned sample had peaks at (+)670, (−)677, (+)684, and (−)701 nm (Fig. 5a). It is evident that the edge-aligned component takes the major part in shaping the $\mathrm{CD_{iso}}$, whereas the face-aligned component is only expressed as smaller shoulders (Fig. 2a).

Figure 5b shows the CD of magnetically oriented lamellar macroaggregates of LHCII having long-range chiral order. The CD_ψ measured in the edge- and face-aligned position changed sign in the same fashion as in stacked granal thylakoid membranes and the edge-aligned spectrum determined to a large extent the isotropic CD. The lack of a sufficiently developed theoretical model for CD_ψ allows only a qualitative description of these results, but we propose that ordered LHCII macroaggregates or crystals are an excellent experimental model system to develop such a theory. For the same reasons, solubilized LHCII trimers which lack long-range order and CD_ψ could be a starting point to gain understanding of the orientation

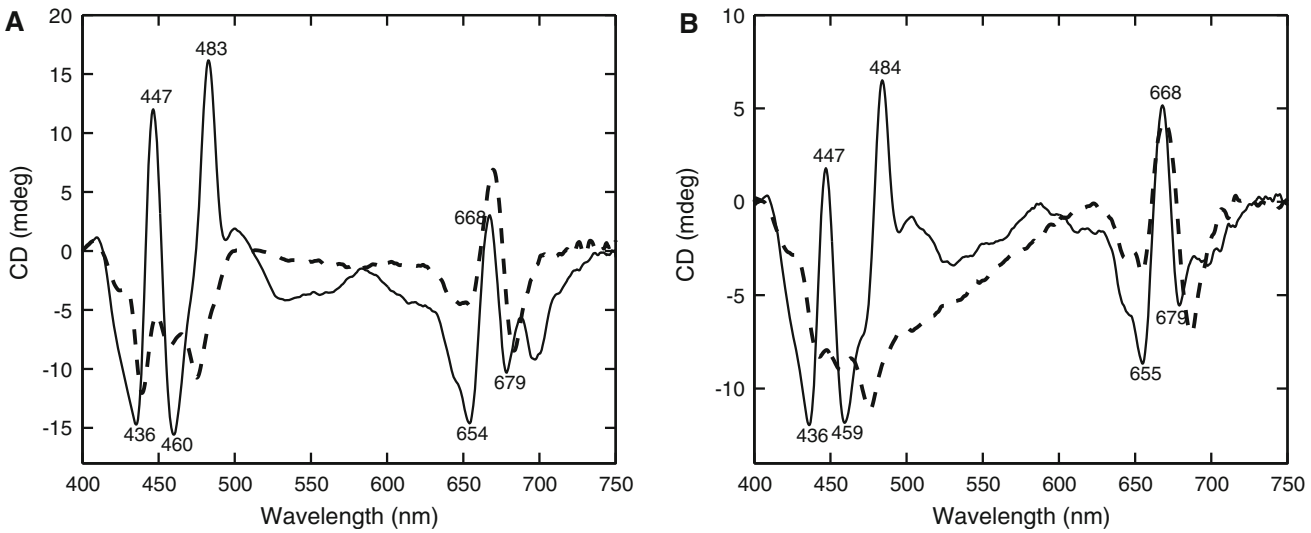

Fig. 6 CD spectra of washed thylakoid membranes (**a**) and grana patches (**b**) in face-aligned and edge-aligned orientation (*solid* and *dashed*, respectively). Samples were oriented by gel squeezing and measured in face-aligned position. The edge-aligned spectra were calculated as $CD_{edge} = \frac{1}{2}(3CD_{random} - CD_{face})$

dependence of the CD_{exc}, shown here for unstacked native thylakoid membranes. Though, the native membranes are still rather complex and structurally not completely understood, it is already possible to model the CD of individual LHCII complexes based on the crystal structures (Liu et al. 2004; Standfuss et al. 2005) and the models of Chl excitonic interactions (Novoderezhkin et al. 2005). Such model calculations on LHCII (by Georgakopoulou et al. 2007) have reproduced the main spectral features of trimeric and monomeric forms, as well as alterations due to pigment mutations. However, before attempting to model ACD of LHCII trimers, the experimental spectra must be obtained. So far, we have not been able to achieve sufficient degree of orientation of solubilized trimers to determine their ACD spectra. There are various technical approaches that could help to reach this goal. One way would be to incorporate LHCII in proteoliposomes (Moya et al. 2001; Yang et al. 2006) with appropriate dimensions that could be easily oriented.

Not only was the CD_{ψ} but also the CD_{exc} significantly affected by sample orientation. Figure 6 shows the spectra of gel-aligned unstacked thylakoid membranes and grana patches, where the long-range order structures are dismantled, and hence CD_{ψ} is absent. With the available technical equipment, it was only possible to obtain undistorted spectra from these samples in the face-aligned orientation. Because the CD is much smaller in amplitude (compared to samples with CD_{ψ}), measurement in edge-aligned orientation is prone to severe LD and birefringence artifacts, which are difficult to eliminate completely. The edge-aligned spectra could be extracted from the isotropic and the face-aligned spectra and are plotted in Fig. 6. There were marked differences in the spectra of oriented particles compared with the isotropic CD spectra (cf. Fig. 2b). Some of the bands in the isotropic CD could be clearly assigned to originate from one of the ACD components. In particular, the face-aligned component gave rise to the (+)447 nm, (−)460, and (+)483 nm bands. The edge-aligned component, on the other hand, accounted for the appearance of the (−)475 nm band, which is a characteristic fingerprint of the trimeric LHCII (Hobe et al. 1994). The same discrimination was valid in the sample types that contained no CD_{ψ}—washed, unstacked thylakoid membranes, BBY particles (not shown) and grana patches, which had in general very similar spectra (Fig. 6b). Another common feature of these samples was a band in the Q_x region of the face-aligned spectra, at 587 nm.

The unique presence of certain CD_{exc} bands in either face- or edge-aligned orientation can be understood, in the first approximation, by the fact that electronic transition dipole moments which are oriented nearly parallel to the propagation direction of light do not contribute to the absorbance and thus the measured CD. Hence, bands appearing in face-aligned orientation may be ascribed to chromophores (or excitonically coupled chromophore groups) with transition dipole moments preferentially lying in the membrane plane. Conversely, bands appearing in edge-aligned orientation may be ascribed to chromophores with transition dipole moments mostly perpendicular to the membrane plane. A precise quantitative treatment would be possible only based on the exact structure and excitonic interactions in the system.

A notable effect was found also in the Q_y region, especially in the red-most part. The isotropic CD has one

broad negative band at (−)682 nm with a small shoulder at 696 nm (Fig. 2b). In the face-aligned orientation this band was split with two well-resolved negative peaks at (−)679 nm and (−)697 nm in washed, unstacked thylakoids. It is interesting to observe a clear CD_{exc} band around 700 nm, significantly red-shifted from the bulk absorption of Chl. These data do not give exact information on the location of the pigment site, whether it is in the antennae or the photosystem core but the band appears to be associated with Photosystem I since it is substantially reduced in PSII-enriched membranes (BBY and grana patches). Further experiments are necessary to identify the responsible pigments.

In general, the bands in the CD_{exc} spectra of the oriented samples were sharper and better resolved. It is noteworthy that the peak positions did not match the isotropic CD bands. The ACD thus provides more detailed and specific information and more readily reveals the true excitonic transitions, whereas the CD of an isotropic suspension, which is a superposition of the anisotropic CD from all directions, carries less specific information.

Conclusions

With this study, we demonstrate the prospect of well known but otherwise unexploited techniques CD of oriented particles and MCD to be used as an additional non-invasive spectroscopy tool in photosynthesis research, providing new independent and specific information on the (macro)molecular architecture of pigment (macro)assemblies. Oriented CD may discriminate between lateral (in-plane) and inter-lamellar structural orders in membranes and lamellar aggregates. The narrow, highly resolved spectral features potentially allow identification of specific pigments and pigment interactions if the structure of the building units (pigment-proteins) is known, information which is nowadays available for many complexes.

MCD gives selective and specific structural information about the pigments and is also sensitive to weak electronic transitions which are difficult to observe in the absorption spectra. It can be used as an internal standard; its invariance, despite the dramatic variations in the spectral shapes in the ACD or CD spectra of samples with different macroorganizations, testifies that the spectra of granal thylakoid membranes and tightly stacked, lamellar aggregates of LHCII are largely void of artifacts. To exploit the full potential of ACD, the theoretical approach has to be further developed to link structural data with the spectral signatures. Eventually, this will improve our understanding of psi-type CD and its dynamic features in photosynthetic systems and in biology in general.

We provide an example of the valuable contribution CD spectroscopy can make toward the study of photosynthetic systems. An unusually intense CD signature led to an exploration by scanning transmission electron microscopy of isolated lamellar aggregates of LHCII. A novel 2D crystalline form of LHCII was discovered and is briefly described in this article. Its further characterization, being beyond the scope of the present study, will be provided elsewhere.

Acknowledgments This study was supported by the EC Marie Curie Training Network (ITN) "HARVEST" (No. 238017) and the Hungarian Scientific Research Fund, OTKA/NKTH CNK 80345 to G.G. and GOP-1.1.2-07/1-2008-0007 to P.L. The authors thank Hans-Georg Kuball for his helpful advice, László Kovács for the preparation of BBY and LHCII, Beth Lin for the STEM sample preparation and Martha Simon for the STEM operation. US-NIH and US-DOE provided financial support to the STEM Facility. GH received support from US-DOE, Office of Basic Energy Sciences, Division of Energy Biosciences.

References

Abdourakhmanov IA, Ganago AO, Erokhin YE, Solovev AA, Chugunov VA (1979) Orientation and linear dichroism of the reaction centers from *Rhodopseudomonas-sphaeroides* R-26. Biochem Biophys Acta 546:183–186

Barzda V, Mustárdy L, Garab G (1994) Size dependency of circular dichroism in macroaggregates of photosynthetic pigment–protein complexes. Biochemistry 33:10837–10841

Barzda V, Istokovics A, Simidjiev I, Garab G (1996) Structural flexibility of chiral macroaggregates of light-harvesting chlorophyll *a/b* pigment–protein complexes. Light-induced reversible structural changes associated with energy dissipation. Biochemistry 35:8981–8985

Bloemendal M, van Grondelle R (1993) Linear-dichroism spectroscopy for the study of structural-properties of proteins. Mol Biol Rep 18:49–69

Breton J, Vermeglio A (1982) Orientation of photosynthetic pigments in vivo. In: Govindjee R (ed) Photosynthesis. 1: energy conversion by plants and bacteria. Academic Press, New York, pp 153–194

Büchel C, Garab G (1997) Organization of the pigment molecules in the chlorophyll *a/c* light-harvesting complex of *Pleurochloris meiringensis* (xanthophyceae). Characterization with circular dichroism and absorbance spectroscopy. J Photochem Photobiol B 37:118–124

Clayton RK (1980) Photosynthesis: physical mechanism and chemical patterns. Cambridge University Press, Cambridge

Cogdell RJ, Scheer H (1985) Circular dichroism of light-harvesting complexes from purple photosynthetic bacteria. Photochem Photobiol 42:669–678

Croce R, Morosinotto T, Ihalainen JA, Chojnicka A, Breton J, Dekker JP, van Grondelle R, Bassi R (2004) Origin of the 701-nm fluorescence emission of the Lhca2 subunit of higher plant photosystem I. J Biol Chem 279:48543–48549

Davidsson A, Nordén B, Seth S (1980) Measurement of oriented circular dichroism. Chem Phys Lett 70:313–316

Disch RL, Sverdlik DI (1969) Apparent circular dichroism of oriented systems. Anal Chem 41:82–86

Frank HA, Violette CA, Taremi SS, Budil DE (1989) Linear dichroism of single crystals of the reaction center from

Rhodobacter sphaeroides wild type strain 2.4.1. Photosynth Res 21:107–116
Garab G (1996) Linear and circular dichroism. In: Amesz J, Hoff AJ (eds) Biophysical techniques in photosynthesis. Kluwer, Dordrecht, pp 11–40
Garab G, van Amerongen H (2009) Linear dichroism and circular dichroism in photosynthesis research. Photosynth Res 101: 135–146
Garab G, Faludi-Daniel A, Sutherland JC, Hind G (1988a) Macroorganization of chlorophyll *a/b* light-harvesting complex in thylakoids and aggregates: information from circular differential scattering. Biochemistry 27:2425–2430
Garab G, Leegood RC, Walker DA, Sutherland JC, Hind G (1988b) Reversible changes in macroorganization of the light-harvesting chlorophyll *a/b* pigment protein complex detected by circular-dichroism. Biochemistry 27:2430–2434
Garab G, Wells S, Finzi L, Bustamante C (1988c) Helically organized macroaggregates of pigment protein complexes in chloroplasts—evidence from circular intensity differential scattering. Biochemistry 27:5839–5843
Garab G, Kieleczawa J, Sutherland JC, Bustamante C, Hind G (1991) Organization of pigment-protein complexes into macrodomains in the thylakoid membranes of wild-type and chlorophyll b-less mutant of barley as revealed by circular dichroism. Photochem Photobiol 54:273–281
Garab G, Galajda P, Pomozi I, Finzi L, Praznovszky T, Ormos P, van Amerongen H (2005) Alignment of biological microparticles by a polarized laser beam. Eur Biophys J Biophys Lett 34:335–343
Georgakopoulou S, van der Zwan G, Bassi R, van Grondelle R, van Amerongen H, Croce R (2007) Understanding the changes in the circular dichroism of light harvesting complex II upon varying its pigment composition and organization. Biochemistry 46: 4745–4754
Goss R, Wilhelm C, Garab G (2000) Organization of the pigment molecules in the chlorophyll a/b/c containing alga *Mantoniella squamata* (Prasinophyceae) studied by means of absorption, circular and linear dichroism spectroscopy. Biochim Biophys Acta 1457:190–199
Hobe S, Prytulla S, Kühlbrandt W, Paulsen H (1994) Trimerization and crystallization of reconstituted light-harvesting chlorophyll a/b complex. Embo J 13:3423–3429
Hofrichter J, Eaton WA (1976) Linear dichroism of biological chromophores. Ann Rev Biophys Bioeng 5:511–560
Istokovics A, Simidjiev I, Lajko F, Garab G (1997) Characterization of the light induced reversible changes in the chiral macroorganization of the chromophores in chloroplast thylakoid membranes. Temperature dependence and effect of inhibitors. Photosynth Res 54:45–53
Johansson LBA, Lindblom G (1980) Orientation and mobility of molecules in membranes studied by polarized light spectroscopy. Quart Rev Biophys 13:63–118
Keller D, Bustamante C (1986) Theory of the interaction of light with large inhomogeneous molecular aggregates. II. Psi-type circular dichroism. J Chem Phys 84:2972–2980
Kovacs L, Damkjaer J, Kereïche S, Ilioaia C, Ruban AV, Boekema EJ, Jansson S, Horton P (2006) Lack of the light-harvesting complex CP24 affects the structure and function of the grana membranes of higher plant chloroplasts. Plant Cell 18:3106–3120
Kuball HG (2002) CD and ACD spectroscopy on anisotropic samples: Chirality of oriented molecules and anisotropic phases—a critical analysis. Enantiomer 7:197–205
Kuball HG, Höfer T (2000a) Chirality and circular dichroism of oriented molecules and anisotropic phases. Chirality 12:278–286
Kuball HG, Höfer T (2000b) Circular dichroism of oriented molecules. In: Berova N, Nakanishi K, Woody RW (eds) Circular dichroism: principles and applications. Wiley-VCH, New York, pp 133–157
Kuball HG, Sieber G, Neubrech S, Schultheis B, Schonhofer A (1993) Circular-dichroism of oriented molecules—magnetic dipole and electric quadrupole contribution to the ACD of chirally substituted diaminoanthraquinones. Chem Phys 169:335–350
Kuball HG, Dorr E, Höfer T, Turk O (2005) Exciton chirality method. Oriented molecules—anisotropic phases. Monatshefte fur Chemie 136:289–324
Kühlbrandt W, Thaler T, Wehrli E (1983) The structure of membrane crystals of the light-harvesting chlorophyll a/b protein complex. J Cell Biol 96:1414–1424
Lambrev P, Várkonyi Z, Krumova S, Kovács L, Miloslavina Y, Holzwarth AR, Garab G (2007) Importance of trimer–trimer interactions for the native state of the plant light-harvesting complex II. Biochim Biophys Acta 1767:847–853
Liu Z, Yan H, Wang K, Kuang T, Zhang J, Gui L, An X, Chang W (2004) Crystal structure of spinach major light-harvesting complex at 2.72 angstrom resolution. Nature 428:287–292
Morosinotto T, Breton J, Bassi R, Croce R (2003) The nature of a chlorophyll ligand in Lhca proteins determines the far red fluorescence emission typical of photosystem I. J Biol Chem 278:49223–49229
Morosinotto T, Segalla A, Giacometti GM, Bassi R (2010) Purification of structurally intact grana from plants thylakoids membranes. J Bioenerg Biomembr 42:37–45
Moya I, Silvestri M, Vallon O, Cinque G, Bassi R (2001) Time-resolved fluorescence analysis of the photosystem II antenna proteins in detergent micelles and liposomes. Biochem 40: 12552–12561
Norden B, Kubista M, Kurucsev T (1992) Linear dichroism spectroscopy of nucleic-acids. Quart Rev Biophys 25:51–170
Novoderezhkin VI, Palacios MA, van Amerongen H, van Grondelle R (2005) Excitation dynamics in the LHCII complex of higher plants: modeling based on the 2.72 angstrom crystal structure. J Phys Chem B 109:10493–10504
Pearlstein RM (1991) Theoretical interpretation of antenna spectra. In: Scheer H (ed) Chlorophylls. CRC Press, New York, pp 1047–1078
Schellman J, Jensen HP (1987) Optical spectroscopy of oriented molecules. Chem Rev 87:1359–1399
Simidjiev I, Barzda V, Mustárdy L, Garab G (1997) Isolation of lamellar aggregates of the light-harvesting chlorophyll *a/b* protein complex of photosystem II with long-range chiral order and structural flexibility. Anal Biochem 250:169–175
Standfuss J, van Scheltinga ACT, Lamborghini M, Kühlbrandt W (2005) Mechanisms of photoprotection and nonphotochemical quenching in pea light-harvesting complex at 2.5A resolution. EMBO J 24:919–928
Steinbach G, Besson F, Pomozi I, Garab G (2005) Differential polarization laser scanning microscopy: biological applications. Proc SPIE 5969:59692C
Sutherland JC (1978) The magnetic optical activity of porphyrins. The porphyrins. Academic Press, New York, pp 225–248
Sutherland JC, Holmquist B (1980) Magnetic circular dichroism of biological molecules. Ann Rev Biophys Bioeng 9:293–326
Swenberg CE, Geacintov NE (1976) Selective light scattering from oriented photosynthetic membranes. In: Birks JB (ed) Excited states in biology. Wiley, London, pp 288–300
Szabó M, Lepetit B, Goss R, Wihelm C, Mustárdy L, Garab G (2008) Structurally flexible macro-organization of the pigment-protein complexes of the diatom *Phaeodactylum tricornutum*. Photosynth Res 95:237–245
Tinoco I, Mickols W, Maestre MF, Bustamante C (1987) Absorption, scattering, and imaging of biomolecular structures with polarized-light. Annu Rev Biophys Biophys Chem 16:319–349

Tunis-Schneider MJ, Maestre MF (1970) Circular dichroism spectra of oriented and unoriented deoxyribonucleic acid films—a preliminary study. J Mol Biol 52:521–541

van Amerongen H, Struve WS (1995) Polarized optical spectroscopy of chromoproteins. In: Sauer K (ed) Methods in enzymology vol. 246 biochemical spectroscopy. Academic Press, San Diego, pp 259–283

van Amerongen H, Valkunas L, van Grondelle R (2000) Photosynthetic excitons. World Scientific, Singapore

Völker S, Ono T, Inoue Y, Renger G (1985) Effect of trypsin on PS-II particles—correlation between Hill-activity, Mn-abundance and peptide pattern. Biochim Biophys Acta 806:25–34

Yang C, Boggasch S, Haase W, Paulsen H (2006) Thermal stability of trimeric light-harvesting chlorophyll *a/b* complex (LHCIIb) in liposomes of thylakoid lipids. Biochim Biophys Acta 1757: 1642–1648

Yang C, Lambrev P, Chen Z, Jávorfi T, Kiss AZ, Paulsen H, Garab G (2008) The negatively charged amino acids in the lumenal loop influence the pigment binding and conformation of the major light-harvesting chlorophyll a/b complex of photosystem II. Biochim Biophys Acta 1777:1463–1470

PHOTOSYNTHETICA 48 (3): 475-480, 2010

BRIEF COMMUNICATION

Pigment composition and functional state of the thylakoid membranes during preparation of samples for pigment-protein complexes separation by nondenaturing gel electrophoresis

V. KARLICKÝ[*,**], J. PODOLINSKÁ[**], L. NADKANSKÁ[**], M. ŠTROCH[**,+], M. ČAJÁNEK[**], and V. ŠPUNDA[**]

Laboratory of Biophysics, Faculty of Science, Palacký University, tř. Svobody 26, CZ-771 46 Olomouc, Czech Republic[*]
Department of Physics, Faculty of Science, Ostrava University, 30. dubna 22, CZ-701 03 Ostrava 1, Czech Republic[**]

Abstract

The present study was conducted to examine changes in photosynthetic pigment composition and functional state of the thylakoid membranes during the individual steps of preparation of samples that are intended for a separation of pigment-protein complexes by nondenaturing polyacrylamide gel electrophoresis. The thylakoid membranes were isolated from barley leaves (*Hordeum vulgare* L.) grown under low irradiance (50 μmol m^{-2} s^{-1}). Functional state of the thylakoid membrane preparations was evaluated by determination of the maximal photochemical efficiency of photosystem (PS) II (F_V/F_M) and by analysis of excitation and emission spectra of chlorophyll *a* (Chl *a*) fluorescence at 77 K. All measurements were done at three phases of preparation of the samples: (*1*) in the suspensions of osmotically-shocked broken chloroplasts, (*2*) thylakoid membranes in extraction buffer containing Tris, glycine, and glycerol and (*3*) thylakoid membranes solubilized with a detergent decyl-β-D-maltosid. F_V/F_M was reduced from 0.815 in the first step to 0.723 in the second step and to values close to zero in solubilized membranes. Pigment composition was not pronouncedly changed during preparation of the thylakoid membrane samples. Isolation of thylakoid membranes affected the efficiency of excitation energy transfer within PSII complexes only slightly. Emission and excitation fluorescence spectra of the solubilized membranes resemble spectra of trimers of PSII light-harvesting complexes (LHCII). Despite a disrupted excitation energy transfer from LHCII to PSII antenna core in solubilized membranes, energy transfer from Chl *b* and carotenoids to emission forms of Chl *a* within LHCII trimers remained effective.

Additional key words: 77-K chlorophyll fluorescence spectra; *Hordeum vulgare*; photochemical efficiency; polyacrylamide gel electrophoresis; thylakoid membranes isolation.

Nondenaturing polyacrylamide gel electrophoresis is an important biochemical method of the photosynthesis research providing a deeper insight into the structure-function characteristics of the photosynthetic apparatus at the level of pigment-binding protein complexes (PPCs) of the thylakoid membranes. Separated PPCs can be used for the subsequent analyses in order to study *e.g.* pigment composition of the individual complexes (Thayer and Björkman 1992, Lee and Thornber 1995), assembly of the light-harvesting complexes of PSII during greening of the intermittent light-grown plants (Dreyfuss and Thornber 1994) or regulation of PSII antenna size and PSI/PSII ratio in plants acclimated to different environmental conditions (Ferraro *et al.* 2003, Ballottari *et al.* 2007).

The interpretation of findings obtained from native

Received 16 December 2009, *accepted* 25 May 2010.
[+]Corresponding author; fax: +420 59 709 21 59, e-mail: michal.stroch@osu.cz
Abbreviations: Cars – carotenoids; Chl – chlorophyll; Dm – decyl-β-D-maltosid; F_V/F_M – maximal photochemical efficiency of photosystem II; LHCII – light-harvesting complexes of photosystem II; PPCs – pigment-protein complexes; PSI and PSII – photosystem I and II; RES1 and RES2 – resuspension medium 1 and 2; VAZ – the pool of xanthophyll cycle pigments (violaxanthin + antheraxanthin + zeaxanthin).
Acknowledgements: We thank B. Piskořová for technical assistance. This work was supported by the Grant Agency of Czech Republic (522/07/P246), Ministry of Education, Youth and Sports of the Czech Republic (MSM 6198959215) and by the Palacky University (student project PrF_2010_050).

gel electrophoresis is based on the assumption that they reflect the state of PPCs in intact leaves. However, little is known how preparation of the thylakoid membrane samples that are loaded onto a polyacrylamide gel affects pigment composition and the functional state of the thylakoid membranes and the individual PPCs. Generally, preparation of the samples to perform electrophoretic separation of PPCs consists of three basic steps. Firstly, after homogenization of the leaf tissue, filtration and subsequent centrifugation, the sedimented chloroplasts are osmotically shocked to rupture chloroplast envelope membranes. Secondly, the thylakoid membranes obtained by further centrifugation are suspended in an extraction buffer containing Tris, glycine, and glycerol (Peter and Thornber 1991). Tris and glycine are compounds of the electrode buffer used during electrophoresis and glycerol is used to keep samples at the bottom of the well in gel so that samples do not undergo convective mixing with the electrode buffer (Shi and Jackowski 1998). In the last third step the thylakoid membranes are solubilized using a suitable detergent in order to release PPCs from the membranes without a disruption of pigment-protein interactions.

Besides changes caused by the electrophoretic fractionation of PPCs itself, like release of pigments from their binding sites (Lee and Thornber 1995), changes occurred during preparation of the thylakoid membranes should be taken into account as well. The objective of the present study was to examine changes in pigment composition and the structure-functional state of the thylakoid membranes during the individual steps of sample preparation for separation of PPCs by nondenaturing polyacrylamide gel electrophoresis. The structure-functional state of the thylakoid membrane preparations was evaluated by determination of the maximal photochemical efficiency of PSII (F_V/F_M) and by the analysis of excitation and emission spectra of chlorophyll *a* (Chl *a*) fluorescence at 77 K.

Spring barley (*Hordeum vulgare* L. cv. Bonus) was grown from seeds under controlled environment conditions inside a growth chamber (*BioLine VB1014*, *Vötsch*, Germany) at the photosynthetic photon flux density of 50 μmol m^{-2} s^{-1}, 20°C, 65% relative air humidity and 16/8 h day/night regime. The middle segments of 8-day-old primary leaves were used for both measurements on the intact leaves and isolation of the thylakoid membranes.

Barley leaves were harvested for isolation of the thylakoid membranes after 2 h of dark period. The modified method described by Ilík *et al.* (2002) was used. The leaf segments (12 g) were homogenized for 10 s in a grinding medium using *Ultra-Turrax T25* homogenizer (*IKA Labortechnik*, Staufen, Germany). The grinding medium contained 0.33 M sorbitol, 5 mM $MgCl_2$, 10 mM NaCl, 2 mM sodium ascorbate, and 50 mM Tricine-NaOH, pH 7.8. The homogenate was rapidly filtered through four layers of polyamide sieve *Uhelon 130T* (*Silk & Progress*, Brněnec, Czech Republic) with mesh width of 42 μm and the filtrate was centrifuged at 3,020 × *g* for 2.5 min (*Sigma 3K 30*, Osterode, Germany). The sedimented chloroplasts were osmotically lysed by suspending the pellet in a resuspension medium consisting of 5 mM $MgCl_2$, 10 mM NaCl, and 50 mM Tricine-NaOH, pH 7.8 (denoted as RES1 medium). At this point of isolation procedure, the part of suspension was taken for the measurements. Such samples were denoted as RES1 samples. The thylakoid membranes were obtained by a subsequent centrifugation at 20,000 × *g* for 6 min. The pellet was resuspended in a resuspension medium that contained 11.3 mM Tris, 87 mM glycine and 9% (v/v) glycerol (denoted as RES2 medium). Again, the part of thylakoid membranes resuspended in RES2 medium used for the measurements were correspondingly denoted as RES2 samples. The remaining thylakoid membranes were solubilized with 20% (w/v) stock of decyl-β-D-maltosid (Dm). This surfactant and the RES2 membranes were mixed to obtain a final 2% concentration of the surfactant and Chl (*a*+*b*) concentration of 1,250 μg ml^{-1}. The extract was centrifuged at 7,500 × *g* for 2.5 min to remove a colorless insoluble material and to obtain a green supernatant (denoted as Dm medium) that was also used for the measurements. All isolation steps were performed at 0–4°C under dim green light. Immediately after preparation of each of the suspensions of thylakoid membranes that were kept in darkness on ice, the samples for pigment analysis and the measurements of F_V/F_M and Chl *a* fluorescence spectra at 77 K were taken. Chl (*a*+*b*) content of all suspensions was adjusted to 1,000 μg ml^{-1}. The results of six independent isolation procedures are presented. As a control, the intact leaves after 2 h of dark adaptation were used for the measurements.

The ratios of Chl *a* to Chl *b* (Chl *a*/*b*) and of total chlorophylls to total carotenoids [Chl (*a*+*b*)/Car (x+c)] were estimated spectrophotometrically (*UV/VIS 550, Unicam*, England) from the pigment extracts according to Lichtenthaler (1987). In the case of suspensions, the pigments were extracted in 80% acetone. Because the single extraction of pigments (mainly β-carotene) from leaves in aqueous acetone solvent is incomplete (Thayer and Björkman 1992, Dunn *et al.* 2004), we used triple acetone extraction (80:100:100%) of pigments from leaves. The contents of the individual carotenoids (lutein, neoxanthin, β-carotene, and the pool of xanthophyll cycle pigments, *i.e.* violaxanthin + antheraxanthin + zeaxanthin) expressed on a Chl (*a*+*b*) basis were estimated by the gradient reversed-phase high-performance liquid chromatography (*TSP Analytical*, USA) according to Färber and Jahns (1998) with a minor modification (Kurasová *et al.* 2003). The details are described in our previous study (Štroch *et al.* 2008).

Chl *a* fluorescence spectra at 77 K were measured using a luminiscence spectrophotometer *LS50B* (*Perkin–Elmer*, UK) equipped with the custom-made Dewar-type

optical cryostat. The emission spectra were recorded at the excitation wavelength of 436 nm (preferential excitation of Chl *a*) and the excitation spectra were measured at the emission wavelength of 685 nm (preferentially PSII emission). The emission spectra of the thylakoid membrane suspensions were measured with 5- and 2.5-nm slit widths of excitation and emission monochromators, respectively. The measurements of excitation spectra of the suspensions were carried out with 2.5- and 5-nm slit widths of excitation and emission monochromators, respectively. All measurements with the leaves were done with 5-nm slit widths of both monochromators. The emission spectra were corrected for the spectral sensitivity of the detection system. The excitation spectra were automatically corrected for the output of excitation source, the efficiency of excitation monochromator and the sensitivity of reference photomultiplier.

F_V/F_M $[(F_M–F_0)/F_M]$ was determined using a pulse amplitude-modulated fluorometer (*PAM 101/103, Walz*, Effeltrich, Germany) equipped with the emitter-detector unit *ED-101BL* employing a blue light-emitting diode as a source of excitation light with the maximum at the wavelength of 461 nm (Štroch *et al.* 2005). The fluorescence emission was detected above 660 nm. F_0 was obtained upon excitation with a weak measuring light modulated at 1.6 kHz that did not induce any significant variable fluorescence. For F_M determinations, the saturating "white-light" pulses of 0.8-s and 1-s duration were triggered using a *KL 1500* halogen lamp (*Schott*, Mainz, Germany) for the intact leaves and thylakoid membrane suspensions, respectively. The different length of saturating pulses was needed for correct estimation of F_M. The incident photosynthetic photon flux density of the applied pulses was approximately 5,000 μmol m^{-2} s^{-1}.

The statistical differences between the means were determined using a two-sample *F*-test for variances followed by a Student's *t*-test at three levels of significance (0.001, 0.01, and 0.05). Based on the results of the *F*-test, the *t*-test assuming either equal or unequal variances was used. All statistical tests were performed using the data analysis tools of *Microsoft Office Excel 2007*.

F_V/F_M of the thylakoid membranes suspended in RES1 medium after the first centrifugation was 0.815 ± 0.004, documenting a successful isolation procedure in the first phase of preparation of the thylakoid membranes. Nevertheless, F_V/F_M was slightly but significantly reduced from 0.826 ± 0.002 in the intact leaves (P<0.001). Despite this decrease of F_V/F_M, PSII in the isolated membranes can be considered to be still in a fully functional state. After the second centrifugation and subsequent resuspension of the sedimented thylakoid membranes in RES2 medium, F_V/F_M decreased by 11% to the value of 0.723 ± 0.018. This moderate impairment of PSII functional state was expected, as the physico-chemical properties of RES2 medium did not correspond to conditions needed to maintain an optimum functional state of the thylakoid membranes (Leegood and Malkin 1986). RES2 medium contained Tris, glycine, and glycerol, the compounds necessary for a subsequent PPCs separation by a native gel electrophoresis (Peter and Thornber 1991, Ilík *et al.* 2002). After solubilization of the membranes with decyl-maltosid, PSI and PSII supercomplexes underwent disassembly that resulted in a very low F_V/F_M in the range of 0.0 to 0.1 (data not shown).

Chl *a*/*b* showed a decreasing trend during the individual steps of thylakoid membranes isolation (Fig. 1*A*). The suspension of membranes in Dm medium exhibited a slight but statistically significant decrease of Chl *a*/*b* by 3.5% in comparison with the pigment extracts from intact leaves (P<0.01). This indicates that Chl *a* content diminished more than that of Chl *b*. Chl (*a*+*b*)/Car (x+c) was quite stable during individual steps of the thylakoid membrane preparation (Fig. 1*B*). The ratios of the individual carotenoids to Chl (*a*+*b*) also showed no pronounced changes during preparation of the thylakoid membranes (Fig. 1*C–F*). Thus, our data showed that pigment composition was not pronouncedly changed during preparation of the thylakoid membrane samples that are loaded onto a polyacrylamide gel in order to perform the electrophoretic separation of PPCs in a native state. While Cars content was not significantly altered, one could expect a slight loss of Chl *a*, especially during solubilization of the thylakoid membranes. It can be due to a partial loss of stromal thylakoids that break more easily during centrifugation and cannot be pelleted. Therefore, a loss of stromal thylakoids with much higher Chl *a/b* in comparison with grana thylakoids (Quiles *et al*. 1999) can result in decrease of Chl *a/b* in RES2 suspensions (Fig. 1*A*). In addition, decreased Chl *a/b* in Dm samples can be explained by the fact that efficiency of solubilization never reaches 100% and PSI with higher Chl *a/b* is the least solubilizable complex.

The maximum of 77-K Chl fluorescence emission originating from light-harvesting complexes of PSI (LHCI) in the thylakoid membrane suspensions was shifted from 743 nm observed in leaves towards shorter wavelengths by 3–4 nm (Fig. 2*A*). PSII emission bands with the maxima around 684 and 692 nm were significantly higher for the thylakoid membrane samples than for intact leaves. Higher PSII emission (relative to PSI emission band) together with the shift of far-red Chl fluorescence maximum to shorter wavelengths is a characteristic effect of decreased reabsorption of the emitted Chl fluorescence in the suspensions (Buschmann 2007). Thylakoid membranes suspended in RES1 medium showed slightly higher PSII emission as compared to RES2 membranes (significantly only at the maximum of 692 nm, P<0.01). Solubilization of the membranes resulted in a pronounced PSII emission band with the maximum at 679 nm (Fig. 2*A*). Andreeva *et al.* (2009) observed the maximum at 679 nm in isolated LHCII trimers. Other authors reported the maximum near

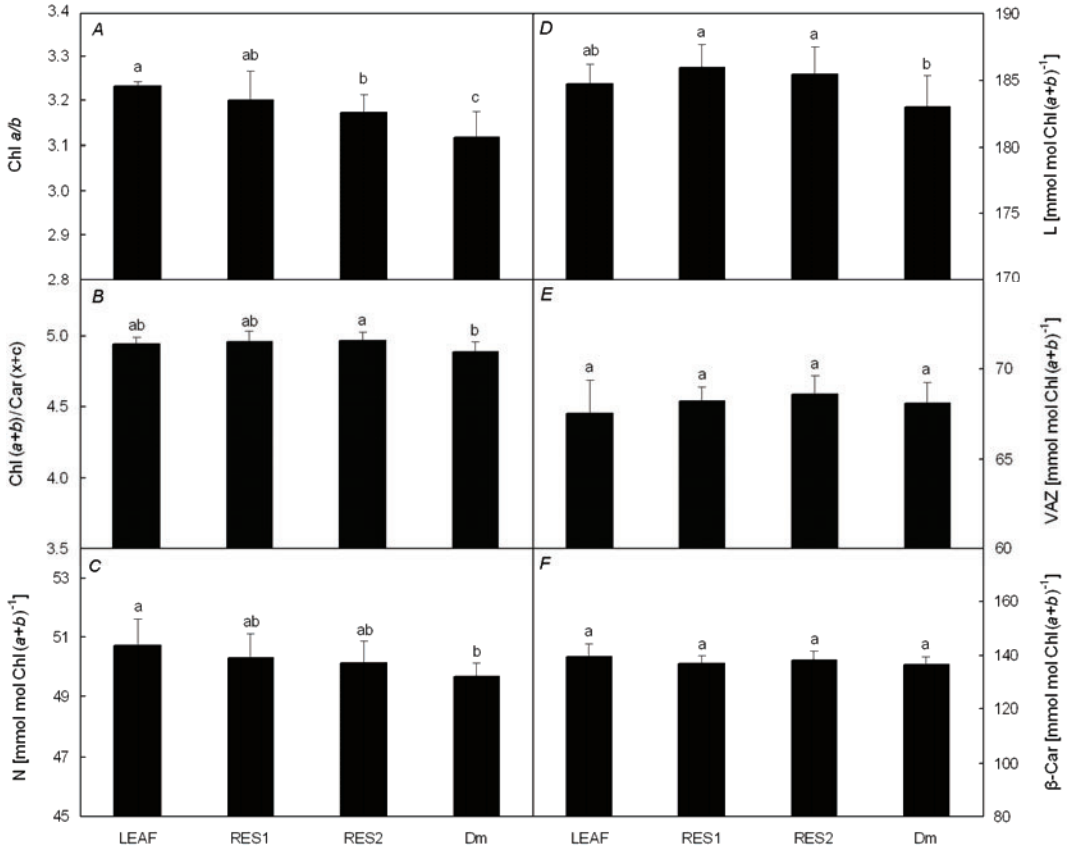

Fig. 1. *A*: The ratio of chlorophyll *a* to chlorophyll *b* (Chl *a/b*), *B*: the ratio of total chlorophylls to total carotenoids [Chl (*a*+*b*)/ Car (x+c)], *C*: the content of neoxanthin (N), *D*: lutein (L), *E*: xanthophyll cycle pigments (VAZ) and *F*: β-carotene (β-Car) expressed on Chl (*a*+*b*) basis. The pigment contents were determined in the extracts from *H. vulgare* leaves and isolated thylakoid membranes suspended in RES1, RES2 and Dm media during the individual steps of isolation procedure. Data followed by the same letter indicate non-significant difference (P>0.05; Student's t-test). $n = 6 \pm$ SD.

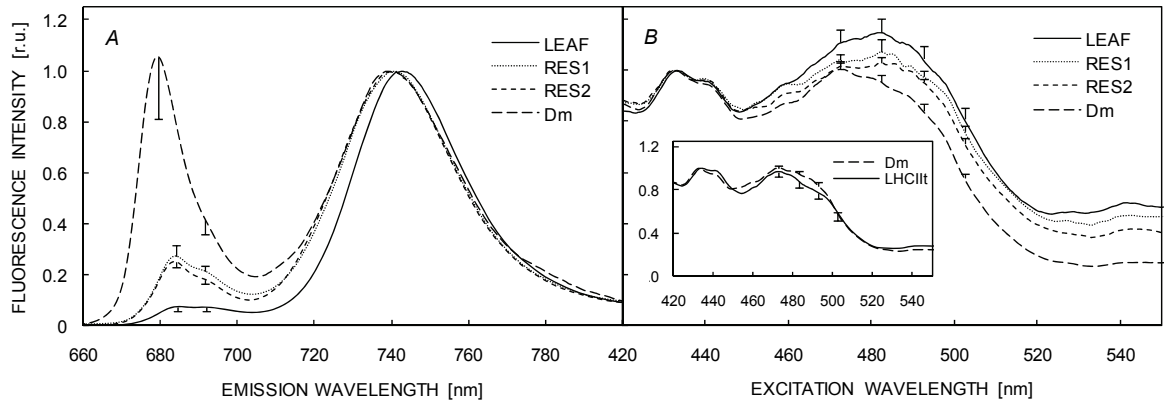

Fig. 2. *A*: Chlorophyll *a* fluorescence emission and *B*: excitation spectra at 77 K of *H. vulgare* leaves and isolated thylakoid membranes suspended in RES1, RES2 and Dm media during the individual steps of the isolation procedure. The *inset* shows excitation spectra of Dm membranes and band containing LHCII trimers (LHCIIt) obtained by nondenaturing gel electrophoresis according to Ilík *et al.* (2002). The emission spectra were recorded at the excitation wavelength of 436 nm and normalized at the long-wavelength maximum. The excitation spectra were measured at the emission wavelengths of 685 nm for leaves and the membranes and 681 nm for LHCIIt bands. The excitation spectra were normalized at the excitation maximum of chlorophyll *a* in the Soret region. The mean spectra from 6–12 samples are presented. *Error bars* indicate SD.

680 nm in LHCII trimers isolated after solubilization with Dm (Hemelrijk *et al.* 1992, Ruban *et al.* 1997). Thus, PSII emission band in Dm samples corresponds to emission from LHCII trimers that were detached from PSII core after Dm treatment. Pronounced emission of LHCII trimers indicates a disrupted excitation energy transfer to PSII antenna core, that can contribute to a strong F_V/F_M reduction.

In 77-K Chl fluorescence excitation spectra detected at PSII emission, the characteristic main excitation maximum of Chl *a* was observed at 433 nm for all samples (Fig. 2*B*). The broad Chl *b* and Cars excitation band in the spectral region of 460–510 nm with the maximum around 482 nm was detected for intact leaves, RES1 and RES2 samples. The maximum of this heterogeneous excitation band was shifted to 472 nm in Dm suspensions due to reduced contribution of excitation bands at longer wavelengths. The shape of excitation spectrum of solubilized thylakoid membranes was very similar to that of a band containing LHCII trimers obtained by nondenaturing gel electrophoresis (see *inset* of Fig. 2*B*).

The relative efficiency of excitation energy transfer from Chl *b* and Cars to the Chl *a* forms emitting PSII fluorescence can be estimated from the magnitude of Chl *b* and Cars excitation band relative to the excitation maximum of Chl *a* (Čajánek *et al.* 2002). In comparison with intact leaves, the efficiency of excitation energy transfer within PSII was slightly reduced in RES1, RES2 and more pronouncedly in Dm samples (Fig. 2*B*). Slightly decreased Chl *b* and Cars excitation band in RES2 suspensions relative to RES1 samples was accompanied by reduced F_V/F_M. However, it should be noted that the high efficiency of excitation energy transfer from Cars to Chl *a* emission forms at PSII is not a prerequisite for optimum F_V/F_M. The *chlorina f2* mutant of barley with impaired assembly of LHCII possesses almost the same PSII photochemical efficiency as the wild type barley, in spite of extremely low efficiency of excitation energy transfer from Cars to the PSII Chl *a* emission forms (Štroch *et al.* 2004). On the contrary to RES1 and RES2 samples, Cars excitation bands in the long-wavelength region (above 480 nm) were mainly reduced in Dm samples. As mentioned, in solubilized thylakoid membranes the PSII Chl *a* fluorescence was emitted from the LHCII trimers due to the disconnection of the excitation energy transfer to the PSII core. Thus, the reduction of the Cars bands can reflect either the lower content of the xanthophyll cycle pigments as compared to the inner LHCII complexes (Bassi *et al.* 1993) or the slightly decreased efficiency of excitation energy transfer from the xanthophylls to the fluorescing forms of Chl *a* within solubilized LHCII complex. In addition, a lower content of lutein (Fig. 1*D*) and decrease of light scattering that affects the excitation spectrum from about 450 up to 550 nm (Naqvi *et al.* 1997) can contribute to decreased Chl *b* and Cars excitation band in Dm samples.

Thus, in our study the isolation of thylakoid membranes from barley leaves affected the pigment composition and the functional state of the PSII complexes only slightly. Despite a disrupted excitation energy transfer from LHCII to PSII antenna core in Dm-solubilized thylakoid membranes, energy transfer from Chl *b* and Cars to emission forms of Chl *a* within LHCII trimers remained effective.

References

Andreeva, A., Abarova, S., Stoitchkova, K., Busheva, M.: Model for fluorescence quenching in light harvesting complex II in different aggregation states. – Eur. Biophys. J. **38**: 199-208, 2009.

Ballottari, M., Dall´Osto, L., Morosinotto, T., Bassi, R.: Contrasting behavior of higher plant photosystem I and II antenna systems during acclimation. – J. Biol. Chem. **282**: 8947-8958, 2007.

Bassi, R., Pineau, B., Dainese, P., Marquardt, J.: Carotenoid-binding proteins of photosystem II. – Eur. J. Biochem. **212**: 297-303, 1993.

Buschmann, C.: Variability and application of the chlorophyll fluorescence emission ratio red/far red of leaves. – Photosynth. Res. **92**: 261-271, 2007.

Čajánek, M., Navrátil, M., Kurasová, I., Kalina, J., Špunda, V.: The development of antenna complexes of barley (*Hordeum vulgare* cv. Akcent) under different light conditions as judged from the analysis of 77 K chlorophyll *a* fluorescence spectra. – Photosynth. Res. **74**: 121-133, 2002.

Dreyfuss, B.W., Thornber, J.P.: Assembly of the light-harvesting complexes (LHCs) of photosystem II - monomeric LHC IIB complexes are intermediates in the formation of oligomeric LHC IIB complexes. – Plant Physiol. **106**: 829-839, 1994.

Dunn, J.L., Turnbull, J.D., Robinson, S.A.: Comparison of solvent regimes for the extraction of photosynthetic pigments from leaves of higher plants. – Funct. Plant Biol. **31**: 195-202, 2004.

Färber, A., Jahns, P.: The xanthophyll cycle of higher plants: influence of antenna size and membrane organization. – Biochim. Biophys. Acta **1363**: 47-58, 1998.

Ferraro, F., Castagna, A., Soldatini, G.F., Ranieri, A.: Tomato (*Lycopersicon esculentum* M.) T3238*FER* and T3238*fer* genotypes. Influence of different iron concentrations on thylakoid pigment and protein composition. – Plant Sci. **164**: 783-792, 2003.

Hemelrijk, P.W., Kwa, S.L.S., van Grondelle, R., Dekker, J.P.: Spectroscopic properties of LHC-II, the main light-harvesting chlorophyll *a/b* protein complex from chloroplast membranes. – Biochim. Biophys. Acta **1098**: 159-166, 1992.

Ilík, P., Krchňák, P., Tomek, P., Nauš, J.: 2-D gel densitometer for high-contrast and selective imaging of chlorophyll-containing protein complexes separated by non-denaturing polyacrylamide gel electrophoresis. – J. Biochem. Biophys.

Methods **51**: 273-281, 2002.

Kurasová, I., Kalina, J., Urban, O., Štroch, M., Špunda, V.: Acclimation of two distinct plant species, spring barley and Norway spruce, to combined effect of various irradiance and CO_2 concentration during cultivation in controlled environment. – Photosynthetica **41**: 513-523, 2003.

Lee, A.L.C., Thornber, J.P.: Analysis of the pigment stoichiometry of pigment-protein complexes from barley (*Hordeum vulgare*) - the xanthophyll cycle intermediates occur mainly in the light-harvesting complexes of photosystem I and photosystem II. – Plant Physiol. **107**: 565-574, 1995.

Leegood, R.C., Malkin, R.: Isolation of sub-cellular photosynthetic systems. – In: Hipkins, M.F., Baker, N.R. (ed.): Photosynthesis Energy Transduction: a Practical Approach. Pp. 9-26. IRL Press, Oxford 1986.

Lichtenthaler, H.K.: Chlorophylls and carotenoids: pigments of photosynthetic biomembranes. – In: Colowick, S.P., Kaplan, N.O. (ed.): Methods in Enzymology 148. Pp. 350-382. Academic Press, San Diego – New York – Berkeley – Boston – London – Sydney – Tokyo – Toronto 1987.

Naqvi, K.R., Melø, T.B., Raju, B.B., Jávorfi, T., Garab, G.: Comparison of the absorption spectra of trimers and aggregates of chlorophyll *a/b* light-harvesting complex LHC II. – Spectrochim. Acta A **53**: 1925-1936, 1997.

Peter, G.F., Thornber, J.P.: Biochemical composition and organization of higher plant photosystem II light-harvesting pigment-proteins. – J. Biol. Chem. **266**: 16745-16754, 1991.

Quiles, M.J., García, A., Cuello, J.: Localization of the chloroplast NAD(P)H dehydrogenase complex in stroma thylakoids from barley. – Plant Sci. **146**: 17-25, 1999.

Ruban, A.V., Calkoen, F., Kwa, S.L.S., van Grondelle, R., Horton, P., Dekker, J.P.: Characterisation of LHC II in the aggregated state by linear and circular dichroism spectroscopy. – Biochim. Biophys. Acta **1321**: 61-70, 1997.

Shi, Q., Jackowski, G.: One-dimensional polyacrylamide gel electrophoresis. – In: Hames, B.D. (ed.): Gel Electrophoresis of Proteins. Pp. 1-52. Oxford University Press, Oxford – New York – Tokyo 1998.

Štroch, M., Čajánek, M., Kalina, J., Špunda, V.: Regulation of the excitation energy utilization in the photosynthetic apparatus of *chlorina f2* barley mutant grown under different irradiances. – J. Photochem. Photobiol. B: Biol. **75**: 41-50, 2004.

Štroch, M., Podolinská, J., Navrátil, M., Špunda, V.: Effects of different excitation and detection spectral regions on room temperature chlorophyll *a* fluorescence parameters. – Photosynthetica **43**: 411-416, 2005.

Štroch, M., Kuldová, K., Kalina, J., Špunda, V.: Dynamics of the xanthophyll cycle and non-radiative dissipation of absorbed light energy during exposure of Norway spruce to high irradiance. – J. Plant Physiol. **165**: 612-622, 2008.

Thayer, S.S., Björkman, O.: Carotenoid distribution and deepoxidation in thylakoid pigment-protein complexes from cotton leaves and bundle-sheath cells of maize. – Photosynth. Res. **33**: 213-225, 1992.

Title:

The effect of growth light intensity on pigment-protein composition and efficiency of excitation energy transfer within photosystem II in barley leaves

Authors:

Václav Karlický[1,2,4] • Ondřej Strouhal[2,3] • Petr Ilík[2] • Michal Štroch[1,4] • Irena Kurasová[1,4] • Győző Garab[1,5] • Marek Šebela[3] • Vladimír Špunda[1,4]

Affiliation:

[1] Faculty of Science, Ostrava University, 30. dubna 22, CZ-701 03 Ostrava 1, Czech Republic

[2] Department of Biophysics, Centre of the Region Haná for Biotechnological and Agricultural Research, Faculty of Science, Palacký University, Šlechtitelů 27, 783 71 Olomouc, Czech Republic

[3] Department of Protein Biochemistry and Proteomics, Centre of the Region Haná for Biotechnological and Agricultural Research, Faculty of Science, Palacký University, Šlechtitelů 27, 783 71 Olomouc, Czech Republic

[4] Global Change Research Institute CAS, Bělidla 986/4a, 603 00 Brno, Czech Republic

[5]Hungarian Academy of Sciences, Biological Research Centre, Institute of Plant Biology, Temesvári krt. 62, 6726 Szeged, Hungary

Corresponding Author:

Vladimír Špunda

Department of Physics, Faculty of Science, Ostrava University

Chittussiho 10, CZ-710 00 Ostrava – Slezská Ostrava, Czech Republic

Email: Vladimir.Spunda@osu.cz

Keywords Photosystem II supercomplex · Light-harvesting complex II · 77 K chlorophyll fluorescence spectra · native electrophoresis · *Hordeum vulgare*

Acknowledgements This work was supported by the Grant Agency of the Czech Republic, grant number 13-28093S/P501; and by COST CZ programme, grant number LD14005 from the Ministry of Education, Youth and Sports of the Czech Republic. Václav Karlický and Irena Kurasová were supported by the grant LO1415, Michal

Štroch and Vladimír Špunda by the grant LO1208 and Marek Šebela was supported by the grant LO1204 under the National Sustainability Program I (Ministry of Education, Youth and Sports of the Czech Republic). Győző Garab was supported by a grant of the Moravian–Silesian Region, grant number 01211/2016/RRC; partial support from NKFIH-OTKA (K112688) is also acknowledged.

Abbreviations:

CCI - core complex of photosystem I

CCII - core complex of photosystem II

CD - Circular dichroism

Chl - Chlorophyll

CN-PAGE - clear-native polyacrylamide gel electrophoresis

EET - excitation energy transfer

Fv/Fm - maximum quantum yield of photosystem II photochemistry

Deriphat-PAGE - Deriphat polyacrylamide gel electrophoresis

HL - high light

LHCI - light-harvesting complex I

LHCII - light-harvesting complex II

LL - low light

ML - medium light

PAR - photosynthetic active radiation

PPC - pigment-protein complex

PSI - photosystem I

PSII - photosystem II

RC - reaction centre

VAZ - xanthophyll cycle pigments

Abstract Biochemical and spectroscopical analyses of leaves and individual pigment-protein complexes (PPCs) from barley leaves grown at 50 (LL), 300 (ML) and 1000 (HL) μmol photons m^{-2} s^{-1} were performed in order to contribute to elucidation of processes associated with regulation of functional size of photosystem II (PSII) antenna in vivo. The 77 K fluorescence excitation spectra of PSII revealed that the functional size of PSII

antenna in vivo is reduced gradually in barley leaves grown under LL, ML and HL light intensities. The excitation spectra of individual PSII supercomplexes and the main light harvesting proteins, LHCIIs, separated from thylakoids isolated from LL, ML and HL plants, revealed no reduction of the chlorophyll *b* and carotenoid excitation bands with increasing growth light, suggesting that variations in the functional antenna size originate from changes in the macro-organization and/or composition of protein complexes of thylakoid membranes. Indeed, circular dichroism spectra of intact barley leaves revealed gradual decline in the long-range chiral order of LHCII and PSII pigment-protein complexes with increasing growth light intensities. Analysis of the composition of LHCII proteins in pigment protein complexes separated by clear-native polyacrylamide gel electrophoresis corresponded to the gradually reduced amounts of PSII supercomplexes containing M-trimers with enhanced growth light intensity.

Introduction

Under natural conditions photosynthetic organisms are frequently exposed to fluctuations in their environment, especially in the quantity of incident photosynthetically active radiation (PAR). A common feature of comprehensive acclimatory responses to different light conditions is to optimize the utilization of light in photosynthetic reactions and mitigate the photooxidative damage to the components of thylakoid membranes, particularly photosystem II (PSII) (Horton et al. 2008; Ruban et al. 2012). Responses of plants to altered PAR can occur at various levels, such as at the whole organism level by leaf movements and leaf deposits (Koller 1990), at the tissue level via optical screening by epidermal phenolics (Agati et al. 2011; Merzlyak et al. 2008; Štroch et al. 2008b), at the cellular level by chloroplast movements and regulation of chloroplast number (Banas et al. 2012; Naus et al. 2008), or at the molecular level by regulating composition and/or macro-organization of pigment-protein complexes (PPCs) and other components of the photosynthetic apparatus (Albanese et al. 2016; Bailey et al. 2001; Ballottari et al. 2007; Bielczynski et al. 2016; Caffarri et al. 2005; Garab 2014; Ruban and Johnson 2015; Timperio et al. 2012).

The regulation and acclimation of PSII structure and function at high light (HL) are the most crucial and have been studied intensively during the past few decades (Ruban et al. 2012). In particular, qE, the energy-dependent component of non-photochemical quenching, the main, fast regulatory response (on the timescale of seconds to minutes) of plants exposed to HL conditions, has been shown to enable harmless dissipation of excess excitation energy within PSII into heat (Baker 2008; Correa-Galvis et al. 2016; Lambrev et al. 2012; Muller et al. 2001; Ruban 2016; Ware et al. 2015). This process is triggered by acidification of the thylakoid lumen, which causes protonation of PsbS protein (Correa-Galvis et al. 2016; Croce 2015; Li et al. 2004) and activates violaxanthin de-epoxidase converting violaxanthin into zeaxanthin via antheraxanthin (Demmig-Adams 1998; Garab et al. 2016; Ruban et al. 2012). The resulting structural rearrangement of PSII is responsible for functional disconnection of a part of the PSII light-harvesting complex (LHCII) from the PSII core and formation of quenching centres within detached major LHCII or in the remaining PSII antenna (Betterle et al. 2009; Jahns and Holzwarth 2012; Johnson et al. 2011; Ruban 2016).

A number of acclimation responses (on the timescale of days to weeks) have been described for various plant species grown under different light conditions. Significant increase in the amount of cytochrome b6f complex and the activity of ATP synthase has been reported for several species grown under HL (de la Torre and Burkey 1990). Considerably elevated levels of PSII reaction centres (RCs) in response to HL have been demonstrated for *Arabidopsis* (Bailey et al. 2001; Walters et al. 1999), pea (Evans 1987; Leong and Anderson

1984), and mustard (Wild et al. 1986). On the contrary, only slightly enhanced amounts of photosystem I (PSI) RCs at HL were reported for *Arabidopsis* (Bailey et al. 2001) and pea (Leong and Anderson 1984), but a dramatic increase in PSI content was observed in thylakoid membranes of plants grown under very low light (LL) (Bailey et al. 2001).

The acclimation of PSII to HL results in down-regulation of light harvesting and enhanced capacity of non-photochemical quenching, at least a relative increase in the xanthophyll cycle pigment pool, and enhanced convertibility of violaxanthin to zeaxanthin (Bugos et al. 1999; Demmig-Adams 1998; Kurasová et al. 2002; Štroch et al. 2004). It has been known for decades that the ratio of LHCII to PSII is decreased under HL growth conditions (Anderson et al. 1995). More recently, changes in LHCII protein composition (Bailey et al. 2001; Kouřil et al. 2013) or even in their individual isoforms (Albanese et al. 2016; Timperio et al. 2012) were described for *Arabidopsis* acclimated to different light intensities. Reduction of LHCII size in HL plants has often been assessed indirectly by increased ratio of chlorophyll *a* to chlorophyll *b* (Chl *a*/*b*), for example in barley (de la Torre and Burkey 1990; Kurasová et al. 2002; Štroch et al. 2004), *Arabidopsis* (Bailey et al. 2001; Kouřil et al. 2013), spinach (Lindahl et al. 1995), and pea (Leong and Anderson 1984). Furthermore, diminution of functional antenna size of PSII in HL-grown barley as compared with LL plants has been assessed from the reduced ratio of the main Chl *b* and Chl *a* excitation bands in the Soret region of the 77 K fluorescence excitation spectra measured on leaf segments (Čajánek et al. 2002; Štroch et al. 2004) and by other methods based on Chl *a* fluorescence (Bielczynski et al. 2016; Wientjes et al. 2013).

In recent years, development of cryo-electron tomography has enabled improvements in knowledge on the structure of PSII and the architecture of grana membranes, including acclimatory response to different light intensity (Croce and van Amerongen 2011; Kouřil et al. 2012; Kouřil et al. 2013; Wei et al. 2016). A variable number of LHCII proteins can be bound to dimeric PSII core complexes (containing the PPCs D1, D2, CP43 and CP47), thereby forming different PSII–LHCII supercomplexes (Dekker and Boekema 2005). The largest supercomplex purified to date (denoted as C2S2M2) (Caffarri et al. (2009) contains a dimeric core associated with two copies of each of the monomeric complexes CP29 (Lhcb4), CP26 (Lhcb5), and CP24 (Lhcb6) and four LHCII trimers (Boekema et al. 1999; Kouřil et al. 2012; van Amerongen and Croce 2013). Two LHCII trimers, firmly bound on the Lhcb5 sides (S-trimers), are composed of the products of the *lhcb1* and *lhcb2* genes (Hankamer et al. 2001), while two others, moderately bound on the sides of Lhcb4 and Lhcb6 (M-trimers), contain also the product of the Lhcb3 gene (Boekema et al. 1999; Kouřil et al. 2012; van Amerongen and Croce 2013). In addition to the LHCII trimers associated within the supercomplexes, there also are extra trimers the

locations of which are still unknown (van Amerongen and Croce 2013). Most of these extra LHCII trimers denoted as L-trimers (loosely bound) should be connected to PSII (Ruban and Johnson 2015; van Amerongen and Croce 2013) and some of them might be located in the LHCII-only domains (Boekema et al. 2000).

The structural response of PSII supercomplex of *Arabidopsis* thylakoid membranes after acclimation to different light intensity has been characterized (Albanese et al. 2016; Bielczynski et al. 2016; Kouřil et al. 2013). HL conditions (800–1100 μmol photons m^{-2} s^{-1}) led to reduction in the antenna size of PSII and in the amount of large C2S2M2 PSII supercomplexes, while acclimation to very low light (20 μmol photons m^{-2} s^{-1}) had no influence on large supercomplexes in comparison with control medium light (ML, 100 μmol photons m^{-2} s^{-1}) (Kouřil et al. 2013). On the other hand, the amount of the "extra" LHCII was increased in LL membranes, whereas in HL membranes the amount remained at the same level as in ML plants. Furthermore, occurrence of semi-crystalline PSII arrays was strongly reduced in HL plants as compared to LL and ML plants, probably due to the increased structural heterogeneity of PSII supercomplexes. Kouřil et al. (2013) found that the C2S2M2 supercomplexes in semi-crystalline arrays in LL plants were more densely packed than in HL or ML plants and suggested that the spacing between supercomplexes is important for efficient energy transfer between PSII under light-limiting conditions.

Previous studies focused on PSII proteins composition and PSII structural changes upon acclimation to HL were mostly carried out on dicotyledons such as *Arabidopsis* (Bielczynski et al. 2016; Kouřil et al. 2013), pea (Albanese et al. 2016), and spinach (Bailey et al. 2004). For these plants, antenna subunits Lhcb3, Lhcb6 and dicotyledon-specific Lhcb4.3 (Klimmek et al. 2006) play a major role in modulation of the PSII antenna size upon long-term acclimation to increased light intensity (Albanese et al. 2016). To the best of our knowledge, no information on PSII protein composition and PSII structural changes is available for monocotyledons such as barley. We attempted to elucidate whether the reduction in functional LHCII size induced by acclimation to HL observed in vivo by measurement of 77 K excitation spectra of Chl *a* for PSII is caused exclusively by the aforementioned diminution (structural modifications) of PSII supercomplexes or whether excitation energy transfer (EET) efficiency within PSII supercomplexes and/or within individual PSII PPCs, especially LHCII trimers, is also decreased. Therefore, we have focused on deeper analysis of the 77 K Chl *a* excitation spectra of individual PSII PPCs and the PSII supercomplexes separated from barley plants acclimated at different growth PAR intensities. We undertook to characterize changes on the level of PSII organization in order to clarify whether the acclimation of barley to HL is related to the reorganization of PSII supercomplexes or rather to EET regulation within individual PSII supercomplexes occurring at various levels of growth light.

Materials and methods

Plant material and growth conditions

Seedlings of wild-type barley (*Hordeum vulgare* L. cv. Bonus) were grown under controlled environment conditions in a growth chamber (HB 1014, Bioline-Heraeus, Germany) at three photosynthetic photon flux densities: 50, 300 and 1000 μmol photons m^{-2} s^{-1}, respectively termed low light (LL), medium light (ML), and high light (HL). Other growing conditions were as follows: temperature at a constant 20 °C, relative humidity 65%, and 16/8 h light/dark regime. The middle segments of primary leaves from 8-days-old plants which had been adapted to darkness for 2 h were used for measurements both on the intact leaves and on isolated thylakoid membranes.

Isolation of the thylakoid membranes

Thylakoid membranes were isolated as presented by Ilík et al. (2002) with modifications as described by Karlický et al. (2010). The leaf segments (12 g) were homogenized in a grinding medium using an Ultra-Turrax T25 homogenizer (IKA Labortechnik, Staufen, Germany). The grinding medium contained 0.33 M sorbitol, 5 mM $MgCl_2$, 10 mM NaCl, 2 mM sodium ascorbate, and 50 mM Tricine-NaOH (pH 7.8). The homogenate was rapidly filtered through four layers of Uhelon 130T polyamide sieve (Silk & Progress, Brněnec, Czech Republic) with mesh width of 42 μm and the filtrate was centrifuged at 3020 g for 2.5 min (Sigma 3K 30, Osterode, Germany). The sedimented chloroplasts were osmotically lysed by suspending the pellet in a resuspension medium consisting of 5 mM $MgCl_2$, 10 mM NaCl, and 50 mM Tricine-NaOH (pH 7.8). The highly active thylakoid membranes with maximum quantum yield of photosystem II photochemistry (Fv/Fm) of around 0.82, determined with the aid of a PAM 101–103 pulse amplitude-modulated fluorometer (Walz, Effeltrich, Germany), were obtained by a subsequent centrifugation at 20 000 g for 6 min. The pellet was resuspended in a resuspension medium containing 11.3 mM Tris, 87 mM glycine, and 9% (v/v) glycerol to the final concentration of 1 mg chlorophyll/ml. The chlorophyll content was determined spectrophotometrically in 80% acetone according to Lichtenthaler (1987). All isolation steps were performed at 0–4 °C under dim green light. Immediately after preparation of each suspension of thylakoid membranes, the suspension was frozen in liquid nitrogen and then stored at –80 °C.

Deriphat-PAGE

We used native Deriphat-PAGE for separating LHCII trimers and monomers and PSII core complexes. The thylakoid membranes of LL and HL plants were solubilized with 20% (w/v) stock of decyl-β-D-maltoside to obtain a final 2% concentration of the surfactant (final 1:16 (w/w) ratio of chlorophyll to detergent). Solubilized thylakoid membranes were centrifuged at 7000 g for 2.5 min to eliminate insoluble particles and consequently green supernatant was applied to gel. Non-denaturing polyacrylamide gel electrophoresis (SE 660, Hoefer, USA) of PPC was performed as described by Peter and Thornber (1991) with modifications by Lípová et al. (2010). Pieces were cut from the gel for the photosynthetic pigment content estimation and measurement of 77 K chl *a* fluorescence spectra.

CN-PAGE

For mild isolation of supercomplexes, we used 10% n-dodecyl β-D-maltoside (w/v) with a final 1:10 or 1:20 (w/w) ratio of chlorophyll to detergent. The treated membranes of LL, ML and HL plants were centrifuged at 22 000 g for 10 min. The supernatant was loaded into wells of the 4–8% gradient polyacrylamide gel and covered by the upper buffer: 50 mM tricine, 15 mM Bis-Tris/HCl (pH 7), 1.4 mM deoxycholate and 600 μM n-dodecyl β-D-maltoside (Wittig et al. 2007). Electrophoresis was performed at 4 °C with linearly increasing voltage from 60 V to 500 V during 100 min. Densitograms were evaluated from the electrophoretograms illuminated with 670 nm using 2-D gel densitometer lights according to Ilík et al. (2002). The gel pieces were cut from the first dimension for measurement of 77 K Chl *a* fluorescence spectra.

SDS-PAGE

After separation of thylakoid membranes to first dimension by CN-PAGE we cut the strips from the gel and incubated them in denaturing buffer containing 30 mM dithiothreitol. The strips were put onto the 12–20% gradient SDS-PAGE. The second dimension was performed at 22 °C with linearly increasing voltage from 40 V up to 300 V during 11 h. The gel was stained by Coomassie blue according to Peng et al. (2009).

Matrix-assisted laser desorption/ionization time-of-flight mass spectrometry

The gel pieces were cut from SDS gel for the mass spectrometry analysis. The proteins inside the gel were reduced by 10 mM dithiothreitol, alkylated by 55 mM iodoacetamide, and in-gel digested overnight by modified trypsin (Šebela et al. 2006). Peptides were analyzed by MALDI-TOF MS and the results were compared with the NCBInr database.

Photosynthetic pigment analysis

Photosynthetic pigment content of leaves was estimated spectrophotometrically (UV/VIS 550, Unicam, England) from the pigment extracts in 80% acetone as described by Lichtenthaler (1987) with the modification of triple acetone extraction explained by Karlický et al. (2010). In addition, the leaves' photosynthetic carotenoid content was determined using gradient reversed-phase high-performance liquid chromatography (HPLC; TSP Analytical, USA) (Farber and Jahns 1998; Kurasová et al. 2003; Štroch et al. 2008a).

Chl a fluorescence spectra at 77 K

Chl *a* fluorescence spectra at 77 K were measured using an LS50B luminescence spectrofluorometer (Perkin-Elmer, United Kingdom) equipped with a custom-made Dewar-type optical cryostat, similarly as described previously by (Karlický et al. 2016). The emission spectra were recorded at the preferential excitation of Chl *a* (436 nm). The excitation spectra were measured at the emission wavelengths 685 nm, for intact leaves, PSII supercomplexes, and PSII core complexes, and 680 nm, for LHCII trimers and monomers. The emission spectra were measured with 5 and 2.5 nm slit widths of the excitation and emission monochromators, respectively. The measurements of excitation spectra of the suspensions were carried out with 2.5 and 5 nm slit widths of the excitation and emission monochromators, respectively. The emission spectra were corrected for the spectral sensitivity of the detection system. The excitation spectra were automatically corrected for the output of the excitation source, efficiency of the excitation monochromator, and sensitivity of the reference photomultiplier.

Circular dichroism spectroscopy

Circular dichroism (CD) spectra of intact leaves were recorded in the range of 400–750 nm at room temperature using a J-815 spectropolarimeter (Jasco, Tokyo, Japan). Detached leaves were placed between two glass windows and measured with 5 cm distance of the sample from the photomultiplier. The spectra were recorded in steps of 0.5 nm with an integration time of 1 s, band-pass of 2 nm, and scanning speed of 100 nm min^{-1}.

Statistical analysis

The statistical differences between the means were determined using a two-sample *F*-test for variances followed by Student's *t*-test at the 0.05 significance level. Based on the results of the *F*-test, the *t*-test assuming either equal or unequal variances was used.

Results

Photosynthetic pigment content and spectral analysis of intact leaves

Acclimation to HL led to increase in the Chl *a*/*b* ratio from values of about 3.3 for LL and ML plants to 3.8 for HL samples (Table 1). In comparison with LL- and ML-grown plants, the ratio of chlorophylls to total carotenoids (Chl/Car) was reduced by 27% for HL leaves. Such increase in Chl *a*/*b* and decline in Chl/Car have been shown to be consistent with pronounced decrease in the size of PSII light-harvesting antenna (Anderson 1986; Kurasová et al. 2002; Leong and Anderson 1984; Štroch et al. 2008a).

Regarding the contents of individual carotenoids, we found that plants grown under all three light conditions contained similar amounts of neoxanthin relative to Chl *a*, and only a slight reduction in lutein content was observed for ML plants as compared to barley grown under other growth lights (Table 1). Among carotenoids, the most sensitive to HL were xanthophyll cycle pigments (VAZ). In comparison with LL plants, the content of VAZ per Chl *a* was only slightly increased in ML plants (by 7%) but was approximately doubled in HL plants. The epoxidation of Z and A back to V in darkness was slowed for HL plants, as a part of the VAZ pool remaining in the de-epoxidized state increased by approximately 50% compared to that in ML and LL plants. The β-carotene content on a Chl *a* basis increased gradually by 13% for ML and 23% for HL in comparison with LL plants. Since β-carotene is located predominantly in the core complexes of both PSII and PSI (Bassi et al. 1993), an increased β-car/Chl *a* ratio indicates an increased ratio of core complexes to light-harvesting complexes. The lutein/VAZ ratio decreased gradually with growing light intensity from the value of 2.4 for LL plants by 11% and 51% for ML and HL plants, respectively.

Barley grown under low light intensity displayed similar 77 K Chl *a* fluorescence emission spectra as had been reported previously (Štroch et al. 2004). Typical maxima of emission at 685, 693, and 743 nm correspond to the emission from chlorophyll proteins of PSII core antennae (CP43 and CP47) and from LHCI, respectively (Dekker et al. 1995; Komura et al. 2006; van Dorssen et al. 1987). Emission from PSII relative to PSI emission increased gradually with increasing growth light intensity (0.10, 0.14 and 0.20 for LL, ML and HL, respectively; Fig. 1A). This, together with the reduced peripheral antenna size of PSII in HL, reflected by alterations in the pigment composition (Table 1), strongly suggest a decreased PSII to PSI ratio in LL leaves.

The 77 K excitation spectra of PSII emission measured on the leaves of LL, ML and HL plants were used to estimate the relative efficiency of EET within PSII. The excitation bands of Chl *b* and carotenoids form a broad band in the spectral region of 460–510 nm. Upon acclimation to increasing growth light, plants exhibited the typical relative decrease in Chl *b* and carotenoid excitation bands by 10% for ML and 17% for HL in comparison with LL plants (Fig. 1B), as was similarly observed previously by (Štroch et al. 2004).

The CD spectra of intact barley leaves grown under different growth light intensities are presented in Fig. 2. The (-)650 nm band, which originates from excitonic interactions of Chl *b* in monomeric and trimeric LHCII (Georgakopoulou et al. 2007), were present in all samples. Also, the Chl *a* CD signals around 440 nm (Garab et al. 1991) were not affected significantly by growth light intensity. In contrast, the intensities of the Ψ-type CD bands at wavelengths around (+)688, (–)670 and (+)510 nm were substantially reduced with increasing growth light intensity (Fig. 2). It had been demonstrated earlier (reviewed by Garab 2014; Garab and van Amerongen 2009) that these CD signals are determined by the long-range organization of the PPCs, in particular LHCII (Garab et al. 1991) and PSII-supercomplexes (Kovacs et al. 2006). The reduced intensity of the main, positive Ψ-type CD bands in leaves grown under ML and HL conditions appears to be correlated with the LHCII content of the thylakoid membranes, in good agreement with recent findings of Toth et al. (2016). Variations in the spectral region between 460 and 480 nm can be assigned to changes in LHCII trimers (Garab et al. 2002), suggesting reduction of LHCII trimers in ML and HL plants relative to LL.

Deriphat-PAGE analysis of PPC composition and function in plants acclimated to LL and HL

According to previous studies (Ilík et al. 2002; Lípová et al. 2010), individual bands obtained from electrophoretograms could be attributed to PSI-LHCI + CCII dimer, CCI, CCII monomer, RC-CP47, LHCII trimers, CP43, LHCII monomers, and free pigments. In agreement with previous studies (Anderson 1986; Bailey et al. 2001), HL thylakoid membranes exhibited higher ratios of PSII core complexes to LHCII and of LHCII monomers to trimers (data not shown).

In order to explain the causes of reduction in EET efficiency within PSII in intact leaves of HL plants, we focused on estimating relative EET efficiency within individual PPCs. Emission maxima of LHCII trimers and monomers at wavelength 680 nm and those of PSII core complexes around 685 nm supported the band identification as suggested above (Fig. 3A). Comparison of excitation spectra of individual PPCs clearly revealed high efficiency of EET from Chl *b* and xanthophylls to Chl *a* within LHCII trimers and monomers and characteristic excitation bands of β-carotene at 469 and 497 nm in CCII dimers and monomers, RC-CP47, and

CP43 (Fig. 3B, Alfonso et al. 1994). The excitation spectra of all PSII core complexes revealed no significant differences between LL and HL plants (Fig. 3C, D). On the contrary, excitation spectra of HL trimers and monomers revealed slightly but significantly higher excitation bands of Chl *b* and xanthophylls in comparison with LL samples (Fig. 3E, F), which could originate from the modulation of the LHCII protein composition (see Table 2) and the differences in lipid environment of the LHCIIs, as shown by (Janik et al. 2013).

CN-PAGE analysis of PPC composition

Relative quantification of individual LHCII proteins per CP47 (see the Fig. S1) confirmed that the separated supercomplexes I–IV could correspond to $C_2S_2M_2$ (supercomplex I), C_2S_2M (supercomplex II), C_2S_2 (supercomplex III), and C_2S (supercomplex IV) supercomplexes described previously (Caffarri et al. 2009). Regarding acclimation to growth light intensity, the protein compositions of PSII supercomplexes I–IV separated from LL, ML, and HL plants revealed no significant differences (data not shown). We have shown, however, that HL plants have a reduced amount of PSII supercomplexes in comparison with ML plants, and in particular the contents of supercomplex I and supercomplex II (Fig. 4). Also under LL the content of all PSII supercomplexes was lowered in comparison with that in ML plants, probably due to the increasing amount of extra LHCII (Boekema et al. 1999; Kouřil et al. 2013) or increasing PSI/PSII ratio, as also suggested by the 77K fluorescence emission spectra of leaves (Fig. 1).

The quantitative analysis of the chosen proteins from two-dimensional CN/SDS-PAGE of LL, ML and HL thylakoid membranes (Fig. 5), presented relative to the content of CP47, confirmed the findings as described above (Table 2). The amount of Lhcb3 and Lhcb6 involved in the formation of M-trimer containing PSII supercomplexes was lowered by almost 30% in HL plants as compared to ML plants, whereas the amount of Lhcb1+2 bound within all trimers was reduced to a considerably lesser extent. On the contrary, in LL plants the relative contents of Lhcb1+2, Lhcb3, and Lhcb6 were approximately 30% higher in comparison with ML plants. Qualitatively, the same information was obtained from the ratio of PSII SCI+SCII to PSII SCI+SCII+SCIII+SCIV (SC standing for supercomplex), which was slightly lower in HL plants than in ML plants but more pronouncedly higher in LL plants. Moreover, the part of CP47 bound in PSII supercomplexes was the highest in ML plants, slightly reduced in LL plants, but considerably reduced in HL plants. Finally, as compared to ML plants the ratio of PSI to PSII was slightly reduced in HL plants but considerably enhanced in LL plants.

Fluorescence emission spectra of individual PPCs isolated by CN-PAGE revealed emission maxima at 685 nm, whereas in LHCII trimers and monomers emission maxima were shifted to 680 nm (Fig. 6A). Thus, the shapes of emission spectra correspond well with previous results (Dekker et al. 1995; Ruban et al. 1997) and with the identification of PSII supercomplexes and LHCII trimers and monomers by SDS-PAGE and mass spectrometry (Fig. S1A). Fluorescence excitation spectra of PSII supercomplexes I–IV revealed gradual reduction in Chl *b* and carotenoids excitation bands in the spectral range of 460–490 nm (Fig. 6B), which corresponds with the decreasing amount of bound LHCII trimers from supercomplex I to supercomplex IV estimated by SDS-PAGE analyses (Fig. S1B).

Fluorescence excitation spectra of various PSII supercomplexes clearly revealed that the EET from Chl *b* and carotenoids within individual isolated PSII PPCs was not reduced in HL-acclimated plants (Fig. 6C–E). In the case of LHCII trimers (Fig. 6F, G), the slightly increased Chl *b* and carotenoids excitation bands in HL plants as compared to LL and ML specimens are in proper accordance with the fluorescence excitation spectra of LHCII trimers (and monomers) isolated by Deriphat-PAGE (Fig. 3E, F).

4. Discussion

Pigment composition and fluorescence emission and excitation spectra of intact leaves of LL and HL plants correspond well with the findings from previous studies on barley grown under different light conditions (Bailey et al. 2001; Kurasová et al. 2002; Štroch et al. 2004) (Fig. 1, Table 1). In the mentioned studies, the data clearly show that diminution of the functional size of PSII antenna is associated with a greater capacity for energy-dependent component of non-photochemical quenching, due to enhanced VAZ pool and facilitated the conversion of V to Z. This may serve to mitigate PSII over-reduction in plants acclimated to HL, thus ensuring efficient protection against progressive photo-oxidative damage to PSII.

Reduction of LHCII in plants grown under HL, as indicated by increased Chl *a*/*b* ratio and diminished functional antennae size of PSII, observed in fluorescence excitation spectra of HL intact leaves, was in accordance with the decreased ratio of LHCII to PSII core contents in HL plants in comparison with ML plants as revealed by CN-PAGE. On the other hand, the increased ratio of LHCII to PSII core contents in LL plants as compared to ML plants corresponds with the enlarged functional antennae size of PSII observed in fluorescence excitation spectra of LL intact leaves but not with the Chl *a*/*b* ratio. This can likely be due to the fact that Chl *a*/*b* estimated on leaves is markedly influenced by PSI (which was found to be enhanced in LL plants; see below) with high Chl *a*/*b* ratio and thus serves really only as a rough indicator of PSII antenna size.

Furthermore, HL plants typically exhibited a decrease in the Chl/Car ratio in comparison with ML plants (Table 1) caused by a decrease in relative content of PSI (Table 2) having higher Chl/Car ratio than PSII (Caffarri et al. 2014), and by a possible increase of unbound carotenoids. The almost unchanged lutein and neoxanthin contents are in accordance with previous results observed on acclimation of many plant species to light environments (Demmig-Adams 1998; Kurasová et al. 2002). Therefore, the decrease in Chl/Car ratio observed in HL plants is caused by an increase in β-car content and mainly in VAZ pigment content (Table 1). An increased β-car/Chl *a* ratio is consistent with the higher ratio of PSII core complexes to LHCII revealed by Deriphat-PAGE and CN-PAGE (Table 2).The ratio of core complexes to light-harvesting complexes can be qualitatively assessed based on the ratio of β-car to xanthophylls (Demmig-Adams 1998). As expected, this ratio was increased for ML plants as compared to LL plants (from 0.43 to 0.49), which is associated with LHC reduction. On the other hand, the similar β-car/xanthophylls ratios for LL and HL plants may be attributed to the substantial amount of VAZ pigment unbound in LHCs (Garab et al. 2016; Havaux and Niyogi 1999). Similarly, the ratio of LHCII major to minor complexes can be roughly determined as lutein/VAZ because minor LHCIIs have significantly lower lutein/VAZ ratio (Caffarri et al. 2014). The reduction in the LHCII trimers/monomers ratio observed by Deriphat-PAGE was implied by the considerably lower lutein/VAZ ratio (1.2) as compared with LL and ML plants (2.4 and 2.2) (Table 1).

It is noteworthy that while changes in fluorescence excitation spectra of intact leaves seem gradual with increasing acclimative light intensity (Fig. 1) ML plants revealed pigment composition very similar (except for β-carotene and lutein/VAZ ratio) to that of LL plants and which was in contrast to that of HL plants (Table 1). Similarly, a nonlinear response of Chl *a*/*b* ratio to varying growth light intensity has been shown for *Arabidopsis thaliana* (Bailey et al. 2001). As mentioned above, the decline in the Chl *a*/*b* ratio in PSII caused by a reduction of LHCII was compensated by a dramatic increase in the content of PSI, which has a higher Chl *a*/*b* ratio than does PSII. A reduction in the ratio of PSI to PSII with increasing growth light intensity was suggested by the 77 K Chl *a* fluorescence emission spectra of intact leaves (Fig. 1) and was confirmed by two-dimensional CN/SDS-PAGE. Similarly, the Chl/Car ratio remained at the same level in LL plants as compared to ML plants due to an increase in the content of PSI and possible decrease in unbound carotenoids that was compensated by an increase of LHCII (Table 2).

Major LHCII is the most abundant PPC, and that is why LHCII largely determines the shape of fluorescence excitation spectra of PSII in intact leaves and thylakoid membranes. The acclimation of plants to HL results in reduced efficiency of EET from carotenoids and Chl *b* within PSII in vivo (Fig. 1B), whereas the

EET from Chl *b* and carotenoids within individual LHCII trimers and monomers isolated by Deriphat-PAGE remains unaffected (or rather slightly increased) in HL-acclimated plants (Fig. 3E, F; Fig. 6F, G). Thus, our results indicate that HL-acclimation changes in functional size of PSII antenna in vivo in vivo are caused by different organization of PSII rather than by xanthophylls composition or other changes in LHCII monomers and trimers. Moreover, since the EET from Chl *b* and carotenoids within individual PSII supercomplexes isolated by CN-PAGE also remains unaffected (or even slightly increased) in HL-acclimated plants (Fig. 6C–E), we suggest that observed down-regulation of PSII antenna size in vivo at HL-acclimated plants is caused by different amounts of individual PSII supercomplexes and associated altered macro-organization of PSII supercomplexes, rather than by inner reorganization of LHCII in PSII supercomplexes.

Analysis of two-dimensional CN/SDS-PAGE revealed almost 25% or 50% reduction of Lhcb3 and Lhcb6 proteins in HL-acclimated plants (Table 2), indicating a one-quarter or one-half reduction of M-trimers in HL plants in comparison with ML and LL plants, respectively. This can be associated with an approximately 10% reduction of Lhcb1 and Lhcb2 proteins (which comprise two-thirds of M-trimers) in HL plants as compared to ML plants and a more than 33% reduction of Lhcb1 and Lhcb2 proteins in comparison with LL plants caused probably by reduction of the extra LHCII pool (Table 2). These results are quantitatively consistent with those obtained for *Arabidopsis* (Kouřil et al. 2013). ML barley, grown under 300 μmol photons m^{-2} s^{-1}, had partly reduced M-trimers, while M-trimers of ML plants of *Arabidopsis* grown at lower light intensity, 100 μmol photons m^{-2} s^{-1}, remained unaffected in comparison with LL plants. Furthermore, down-regulation of M-trimers should lead to a reduction of PSII–LHCII supercomplexes as observed in *Arabidopsis* by Kouřil et al. (2013). Densitograms of HL plants have shown in vitro a reduced ratio of larger PSII supercomplexes containing M-trimers to smaller PSII supercomplexes without M-trimers in comparison with LL plants (Fig. 4). This may be due to a reduced ratio of larger to smaller PSII supercomplexes in HL plants in vivo or reduced stability of PSII supercomplexes in thylakoid membranes of HL plants. We are aware, in the light of our current results of barley PPCs separation using mild-detergent CN-PAGE, that the amounts of larger PSII supercomplexes presented in Fig. 5 have been underestimated, as these supercomplexes were partly disassembled during separation procedure. However, the quantification of the individual Lhcb proteins presented in Table 2, did not account only for the amounts of Lhcbs in the bands corresponding to PSII supercomplexes, but their amounts were integrated through all the separated bands, including LHCII trimers and monomers. Thus, progressive decrease of Lhcb3 and Lhcb6 proteins in comparison to other Lhcb proteins, observed upon increasing light intensity (Table 2), indicates that reduction of the proportion of larger PSII supercomplexes is with high probability a real

acclimative response of PSII to high light, as this estimate does not depend on the degree of disassembly of these supercomplexes during CN-PAGE separation. Moreover, it also supports that the changes in relative amounts of individual PSII supercomplexes among LL, ML and HL plants observed from the densitograms of CN-PAGE gels (Fig. 4) are qualitatively reliable.

This finding on the different contents of various sizes of PSII is well in line with CD spectra on intact leaves. As shown on an *Arabidopsis* mutant, Lhcb6-deficient plants with a complete absence of larger PSII supercomplexes ($C_2S_2M_2$) and forming only smaller PSII supercomplexes (C_2S_2, which are deficient in the LHCII M-trimers) exhibit a major change in the macro-organization of PSII within membranes (Kovacs et al. 2006). Similarly, reduction of both Lhcb3 and Lhcb6 proteins in ML and HL plants was accompanied by a decrease in the macro-organization of PPC within membranes of these plants observed via CD spectroscopy in comparison with LL (Fig. 2). Lack of Lhcb6 also reduces connectivity between PSIIs (Kovacs et al. 2006). Therefore, decreased macro-organization of PSII within ML and HL membranes could result in a reduction of EET efficiency from LHCII to RC of PSII in these membranes compared to LL specimens.

References

Agati G, Cerovic ZG, Pinelli P, Tattini M (2011) Light-induced accumulation of ortho-dihydroxylated flavonoids as non-destructively monitored by chlorophyll fluorescence excitation techniques. Environ Exp Bot 73:3-9 doi: 10.1016/j.envexpbot.2010.10.002

Albanese P, Manfredi M, Meneghesso A, Marengo E, Saracco G, Barber J, Morosinotto T, Pagliano C (2016) Dynamic reorganization of photosystem II supercomplexes in response to variations in light intensities. Biochim Biophys Acta 1857:1651-1660 doi: 10.1016/j.bbabio.2016.06.011

Alfonso M, Montoya G, Cases R, Rodriguez R, Picorel R (1994) Core Antenna Complexes, Cp43 and Cp47, of Higher-Plant Photosystem-Ii - Spectral Properties, Pigment Stoichiometry, and Amino-Acid-Composition. Biochemistry 33:10494-10500 doi: 10.1021/bi00200a034

Anderson JM (1986) Photoregulation of the Composition, Function, and Structure of Thylakoid Membranes. Annu Rev Plant Phys 37:93-136 doi: 10.1146/annurev.pp.37.060186.000521

Anderson JM, Chow WS, Park YI (1995) The grand design of photosynthesis: Acclimation of the photosynthetic apparatus to environmental cues. Photosynth Res 46:129-139 doi: 10.1007/Bf00020423

Bailey S, Horton P, Walters RG (2004) Acclimation of Arabidopsis thaliana to the light environment: the relationship between photosynthetic function and chloroplast composition. Planta 218:793-802 doi: 10.1007/s00425-003-1158-5

Bailey S, Walters RG, Jansson S, Horton P (2001) Acclimation of Arabidopsis thaliana to the light environment: the existence of separate low light and high light responses. Planta 213:794-801 doi: 10.1007/s004250100556

Baker NR (2008) Chlorophyll fluorescence: A probe of photosynthesis in vivo. Annual Review of Plant Biology 59:89-113 doi: 10.1146/annurev.arplant.59.032607.092759

Ballottari M, Dall'Osto L, Morosinotto T, Bassi R (2007) Contrasting behavior of higher plant photosystem I and II antenna systems during acclimation. J Biol Chem 282:8947-8958 doi: 10.1074/jbc.M606417200

Banas AK, Aggarwal C, Labuz J, Sztatelman O, Gabrys H (2012) Blue light signalling in chloroplast movements. J Exp Bot 63:1559-1574 doi: 10.1093/Jxb/Err429

Bassi R, Pineau B, Dainese P, Marquardt J (1993) Carotenoid-Binding Proteins of Photosystem-II. European Journal of Biochemistry 212:297-303 doi: 10.1111/j.1432-1033.1993.tb17662.x

Betterle N, Ballottari M, Zorzan S, de Bianchi S, Cazzaniga S, Dall'Osto L, Morosinotto T, Bassi R (2009) Light-induced Dissociation of an Antenna Hetero-oligomer Is Needed for Non-photochemical Quenching Induction. J Biol Chem 284:15255-15266 doi: 10.1074/jbc.M808625200

Bielczynski LW, Schansker G, Croce R (2016) Effect of Light Acclimation on the Organization of Photosystem II Super- and Sub-Complexes in Arabidopsis thaliana. Front Plant Sci 7:105 doi: 10.3389/fpls.2016.00105

Boekema EJ, van Breemen JFL, van Roon H, Dekker JP (2000) Arrangement of photosystem II supercomplexes in crystalline macrodomains within the thylakoid membrane of green plant chloroplasts. Journal of Molecular Biology 301:1123-1133 doi: 10.1006/jmbi.2000.4037

Boekema EJ, van Roon H, van Breemen JFL, Dekker JP (1999) Supramolecular organization of photosystem II and its light-harvesting antenna in partially solubilized photosystem II membranes. European Journal of Biochemistry 266:444-452 doi: 10.1046/j.1432-1327.1999.00876.x

Bugos RC, Chang SH, Yamamoto HY (1999) Developmental expression of violaxanthin de-epoxidase in leaves of tobacco growing under high and low light. Plant Physiology 121:207-213 doi: Doi 10.1104/Pp.121.1.207

Caffarri S, Frigerio S, Olivieri E, Righetti PG, Bassi R (2005) Differential accumulation of Lhcb gene products in thylakoid membranes of Zea mays plants grown under contrasting light and temperature conditions. Proteomics 5:758-768 doi: 10.1002/pmic.200402008

Caffarri S, Kouřil R, Kereiche S, Boekema EJ, Croce R (2009) Functional architecture of higher plant photosystem II supercomplexes. Embo J 28:3052-3063 doi: 10.1038/emboj.2009.232

Caffarri S, Tibiletti T, Jennings RC, Santabarbara S (2014) A Comparison Between Plant Photosystem I and Photosystem II Architecture and Functioning. Curr Protein Pept Sc 15:296-331

Correa-Galvis V, Poschmann G, Melzer M, Stuhler K, Jahns P (2016) PsbS interactions involved in the activation of energy dissipation in Arabidopsis. Nat Plants 2:15225 doi: 10.1038/nplants.2015.225

Croce R (2015) PsbS is the plants' pick for sun protection. Nat Struct Mol Biol 22:650-652 doi: 10.1038/nsmb.3079

Croce R, van Amerongen H (2011) Light-harvesting and structural organization of Photosystem II: From individual complexes to thylakoid membrane. J Photochem Photobiol B-Biol 104:142-153 doi: 10.1016/j.jphotobiol.2011.02.015

Čajánek M, Navrátil M, Kurasová I, Kalina J, Špunda V (2002) The development of antenna complexes of barley (Hordeum vulgare cv. Akcent) under different light conditions as judged from the analysis of 77 K chlorophyll a fluorescence spectra. Photosynth Res 74:121-133 doi: 10.1023/A:1020943107318

de la Torre WR, Burkey KO (1990) Acclimation of Barley to Changes in Light-Intensity - Chlorophyll Organization. Photosynth Res 24:117-125 doi: 10.1007/BF00032592

Dekker JP, Boekema EJ (2005) Supramolecular organization of thylakoid membrane proteins in green plants. Biochim Biophys Acta-Bioenerg 1706:12-39 doi: 10.1016/j.bbabio.2004.09.009

Dekker JP, Hassoldt A, Pettersson A, van Roon H, Groot ML, van Grondelle R (1995) On the nature of the F695 and F685 emission of photosystem II. Photosynthesis: From Light to Biosphere, Vol I:53-56

Demmig-Adams B (1998) Survey of thermal energy dissipation and pigment composition in sun and shade leaves. Plant Cell Physiol 39:474-482

Evans JR (1987) The Relationship between Electron-Transport Components and Photosynthetic Capacity in Pea Leaves Grown at Different Irradiances. Aust J Plant Physiol 14:157-170

Farber A, Jahns P (1998) The xanthophyll cycle of higher plants: influence of antenna size and membrane organization. Biochim Biophys Acta-Bioenerg 1363:47-58 doi: 10.1016/S0005-2728(97)00093-5

Garab G (2014) Hierarchical organization and structural flexibility of thylakoid membranes. Biochim Biophys Acta-Bioenerg 1837:481-494 doi: 10.1016/j.bbabio.2013.12.003

Garab G (2016) Self-assembly and structural-functional flexibility of oxygenic photosynthetic machineries: personal perspectives. Photosynth Res 127:131-150 doi: 10.1007/s11120-015-0192-z

Garab G, Cseh Z, Kovacs L, Rajagopal S, Varkonyi Z, Wentworth M, Mustardy L, Der A, Ruban AV, Papp E, Holzenburg A, Horton P (2002) Light-induced trimer to monomer transition in the main light-harvesting antenna complex of plants: Thermo-optic mechanism. Biochemistry 41:15121-15129 doi: 10.1021/bi026157g

Garab G, Kieleczawa J, Sutherland JC, Bustamante C, Hind G (1991) Organization of Pigment Protein Complexes into Macrodomains in the Thylakoid Membranes of Wild-Type and Chlorophyll-B-Less Mutant of Barley as Revealed by Circular-Dichroism. Photochemistry and Photobiology 54:273-281 doi: DOI 10.1111/j.1751-1097.1991.tb02016.x

Garab G, Ughly B, Goss R (2016) Role of MGDG and Non-bilayer Lipid Phases in the Structure and Dynamics of Chloroplast Thylakoid Membranes. In: Nakamura Y, Li-Beisson Y (eds) Lipids in Plant and Algae Development. Springer International Publishing. doi:10.1007/978-3-319-25979-6

Garab G, van Amerongen H (2009) Linear dichroism and circular dichroism in photosynthesis research. Photosynth Res 101:135-146 doi: 10.1007/s11120-009-9424-4

Georgakopoulou S, van der Zwan G, Bassi R, van Grondelle R, van Amerongen H, Croce R (2007) Understanding the changes in the circular dichroism of light harvesting complex II upon varying its pigment composition and organization. Biochemistry 46:4745-4754 doi: 10.1021/bi062031y

Hankamer B, Morris E, Nield J, Gerle C, Barber J (2001) Three-dimensional structure of the photosystem II core dimer of higher plants determined by electron microscopy. J Struct Biol 135:262-269 doi: 10.1006/jsbi.2001.4405

Havaux M, Niyogi KK (1999) The violaxanthin cycle protects plants from photooxidative damage by more than one mechanism. Proc Natl Acad Sci U S A 96:8762-8767 doi: 10.1073/pnas.96.15.8762

Horton P, Johnson MP, Perez-Bueno ML, Kiss AZ, Ruban AV (2008) Photosynthetic acclimation: Does the dynamic structure and macro-organisation of photosystem II in higher plant grana membranes regulate light harvesting states? Febs Journal 275:1069-1079 doi: 10.1111/j.1742-4658.2008.06263.x

Ilík P, Krchňák P, Tomek P, Nauš J (2002) 2-D gel densitometer for high-contrast and selective imaging of chlorophyll-containing protein complexes separated by non-denaturing polyacrylamide gel electrophoresis. Journal of Biochemical and Biophysical Methods 51:273-281 doi: 10.1016/S0165-022x(02)00029-5

Jahns P, Holzwarth AR (2012) The role of the xanthophyll cycle and of lutein in photoprotection of photosystem II. Biochim Biophys Acta-Bioenerg 1817:182-193 doi: 10.1016/j.bbabio.2011.04.012

Janik E, Bednarska J, Zubik M, Puzio M, Luchowski R, Grudzinski W, Mazur R, Garstka M, Maksymiec W, Kulik A, Dietler G, Gruszecki WI (2013) Molecular Architecture of Plant Thylakoids under Physiological and Light Stress Conditions: A Study of Lipid-Light-Harvesting Complex II Model Membranes. Plant Cell 25:2155-2170 doi: 10.1105/tpc.113.113076

Johnson MP, Goral TK, Duffy CDP, Brain APR, Mullineaux CW, Ruban AV (2011) Photoprotective Energy Dissipation Involves the Reorganization of Photosystem II Light-Harvesting Complexes in the Grana Membranes of Spinach Chloroplasts. Plant Cell 23:1468-1479 doi: 10.1105/tpc.110.081646

Karlický V, Kurasová I, Ptáčková B, Večeřová K, Urban O, Špunda V (2016) Enhanced thermal stability of the thylakoid membranes from spruce. A comparison with selected angiosperms. Photosynth Res 130:357-371 doi: 10.1007/s11120-016-0269-3

Karlický V, Podolinská J, Nadkanská L, Štroch M, Čajánek M, Špunda V (2010) Pigment composition and functional state of the thylakoid membranes during preparation of samples for pigment-protein

complexes separation by nondenaturing gel electrophoresis. Photosynthetica 48:475-480 doi: 10.1007/s11099-010-0063-y

Klimmek F, Sjodin A, Noutsos C, Leister D, Jansson S (2006) Abundantly and rarely expressed Lhc protein genes exhibit distinct regulation patterns in plants. Plant Physiology 140:793-804 doi: 10.1104/pp.105.073304

Koller D (1990) Light-Driven Leaf Movements. Plant Cell Environ 13:615-632 doi: 10.1111/j.1365-3040.1990.tb01079.x

Komura M, Shibata Y, Itoh S (2006) A new fluorescence band F689 in photosystem II revealed by picosecond analysis at 4-77 K: Function of two terminal energy sinks F689 and F695 in PSII. Biochim Biophys Acta-Bioenerg 1757:1657-1668 doi: 10.1016/j.bbabio.2006.09.007

Kouřil R, Dekker JP, Boekema EJ (2012) Supramolecular organization of photosystem II in green plants. Biochim Biophys Acta-Bioenerg 1817:2-12 doi: 10.1016/j.bbabio.2011.05.024

Kouřil R, Wientjes E, Bultema JB, Croce R, Boekema EJ (2013) High-light vs. low-light: Effect of light acclimation on photosystem II composition and organization in Arabidopsis thaliana. Biochim Biophys Acta-Bioenerg 1827:411-419 doi: 10.1016/j.bbabio.2012.12.003

Kovacs L, Damkjaer J, Kereiche S, Ilioaia C, Ruban AV, Boekema EJ, Jansson S, Horton P (2006) Lack of the light-harvesting complex CP24 affects the structure and function of the grana membranes of higher plant chloroplasts. Plant Cell 18:3106-3120 doi: 10.1105/tpc.106.045641

Kurasová I, Čajánek M, Kalina J, Urban O, Špunda V (2002) Characterization of acclimation of Hordeum vulgare to high irradiation based on different responses of photosynthetic activity and pigment composition. Photosynth Res 72:71-83

Kurasová I, Kalina J, Štroch M, Urban O, Špunda V (2003) Acclimation of two distinct plant species, spring barley and Norway spruce, to combined effect of various irradiance and CO2 concentration during cultivation in controlled environment. Photosynthetica 41:513-523

Lambrev PH, Miloslavina Y, Jahns P, Holzwarth AR (2012) On the relationship between non-photochemical quenching and photoprotection of Photosystem II. Biochim Biophys Acta-Bioenerg 1817:760-769 doi: 10.1016/j.bbabio.2012.02.002

Leong TY, Anderson JM (1984) Adaptation of the Thylakoid Membranes of Pea-Chloroplasts to Light Intensities .2. Regulation of Electron-Transport Capacities, Electron Carriers, Coupling Factor (Cf1) Activity and Rates of Photosynthesis. Photosynth Res 5:117-128 doi: 10.1007/Bf00028525

Li XP, Gilmore AM, Caffarri S, Bassi R, Golan T, Kramer D, Niyogi KK (2004) Regulation of photosynthetic light harvesting involves intrathylakoid lumen pH sensing by the PsbS protein. J Biol Chem 279:22866-22874 doi: 10.1074/jbc.M402461200

Lichtenthaler HK (1987) Chlorophylls and Carotenoids - Pigments of Photosynthetic Biomembranes. Method Enzymol 148:350-382

Lindahl M, Yang DH, Andersson B (1995) Regulatory Proteolysis of the Major Light-Harvesting Chlorophyll a/B Protein of Photosystem-Ii by a Light-Induced Membrane-Associated Enzymatic System. European Journal of Biochemistry 231:503-509 doi: 10.1111/j.1432-1033.1995.tb20725.x

Lípová L, Krchňák P, Komenda J, Ilík P (2010) Heat-induced disassembly and degradation of chlorophyll-containing protein complexes in vivo. Biochim Biophys Acta-Bioenerg 1797:63-70 doi: 10.1016/j.bbabio.2009.08.001

Merzlyak MN, Melo TB, Naqvi KR (2008) Effect of anthocyanins, carotenoids, and flavonols on chlorophyll fluorescence excitation spectra in apple fruit: signature analysis, assessment, modelling, and relevance to photoprotection. J Exp Bot 59:349-359 doi: 10.1093/jxb/erm316

Muller P, Li XP, Niyogi KK (2001) Non-photochemical quenching. A response to excess light energy. Plant Physiology 125:1558-1566 doi: 10.1104/pp.125.4.1558

Naus J, Rolencova M, Hlavackova V (2008) Is chloroplast movement in tobacco plants influenced systemically after local illumination or burning stress? J Integr Plant Biol 50:1292-1299 doi: 10.1111/j.1744-7909.2008.00743.x

Peng LW, Fukao Y, Fujiwara M, Takami T, Shikanai T (2009) Efficient Operation of NAD(P)H Dehydrogenase Requires Supercomplex Formation with Photosystem I via Minor LHCI in Arabidopsis. Plant Cell 21:3623-3640 doi: 10.1105/tpc.109.068791

Peter GF, Thornber JP (1991) Biochemical-Composition and Organization of Higher-Plant Photosystem-Ii Light-Harvesting Pigment-Proteins. J Biol Chem 266:16745-16754

Ruban AV (2016) Nonphotochemical Chlorophyll Fluorescence Quenching: Mechanism and Effectiveness in Protecting Plants from Photodamage. Plant Physiol 170:1903-1916 doi: 10.1104/pp.15.01935

Ruban AV, Calkoen F, Kwa SLS, vanGrondelle R, Horton P, Dekker JP (1997) Characterisation of LHC II in the aggregated state by linear and circular dichroism spectroscopy. Biochim Biophys Acta-Bioenerg 1321:61-70 doi: 10.1016/S0005-2728(97)00047-9

Ruban AV, Johnson MP (2015) Visualizing the dynamic structure of the plant photosynthetic membrane. Nat Plants 1:15161 doi: 10.1038/nplants.2015.161

Ruban AV, Johnson MP, Duffy CDP (2012) The photoprotective molecular switch in the photosystem II antenna. Biochim Biophys Acta-Bioenerg 1817:167-181 doi: 10.1016/j.bbabio.2011.04.007

Šebela M, Štosová T, Havliš J, Wielsch N, Thomas H, Zdráhal Z, Shevchenko A (2006) Thermostable trypsin conjugates for high-throughput proteomics: synthesis and performance evaluation. Proteomics 6:2959-2963 doi: 10.1002/pmic.200500576

Štroch M, Čajánek M, Kalina J, Špunda V (2004) Regulation of the excitation energy utilization in the photosynthetic apparatus of chlorina f2 barley mutant grown under different irradiances. J Photochem Photobiol B-Biol 75:41-50 doi: 10.1016/j.jphotobiol.2004.04.004

Štroch M, Kuldová K, Kalina J, Špunda V (2008a) Dynamics of the xanthophyll cycle and non-radiative dissipation of absorbed light energy during exposure of Norway spruce to high irradiance. J Plant Physiol 165:612-622 doi: 10.1016/j.jplph.2007.03.013

Štroch M, Lenk S, Navrátil M, Špunda V, Buschmann C (2008b) Epidermal UV-shielding and photosystem II adjustment in wild type and chlorina f2 mutant of barley during exposure to increased PAR and UV radiation. Environ Exp Bot 64:271-278 doi: 10.1016/j.envexpbot.2008.05.007

Timperio AM, Gevi F, Ceci LR, Zolla L (2012) Acclimation to intense light implies changes at the level of trimeric subunits involved in the structural organization of the main light-harvesting complex of photosystem II (LHCII) and their isoforms. Plant Physiol Biochem 50:8-14 doi: 10.1016/j.plaphy.2011.09.015

Toth TN, Rai N, Solymosi K, Zsiros O, Schroder WP, Garab G, van Amerongen H, Horton P, Kovacs L (2016) Fingerprinting the macro-organisation of pigment-protein complexes in plant thylakoid membranes in vivo by circular-dichroism spectroscopy. Biochim Biophys Acta 1857:1479-1489 doi: 10.1016/j.bbabio.2016.04.287

van Amerongen H, Croce R (2013) Light harvesting in photosystem II. Photosynth Res 116:251-263 doi: 10.1007/s11120-013-9824-3

van Dorssen RJ, Breton J, Plijter JJ, Satoh K, van Gorkom HJ, Amesz J (1987) Spectroscopic Properties of the Reaction Center and of the 47kda Chlorophyll Protein of Photosystem-Ii. Biochim Biophys Acta 893:267-274 doi: 10.1016/0005-2728(87)90048-X

Walters RG, Rogers JJM, Shephard F, Horton P (1999) Acclimation of Arabidopsis thaliana to the light environment: the role of photoreceptors. Planta 209:517-527 doi: 10.1007/s004250050756

Ware MA, Belgio E, Ruban AV (2015) Photoprotective capacity of non-photochemical quenching in plants acclimated to different light intensities. Photosynth Res 126:261-274 doi: 10.1007/s11120-015-0102-4

Wei X, Su X, Cao P, Liu X, Chang W, Li M, Zhang X, Liu Z (2016) Structure of spinach photosystem II-LHCII supercomplex at 3.2 A resolution. Nature 534:69-74 doi: 10.1038/nature18020

Wientjes E, van Amerongen H, Croce R (2013) Quantum yield of charge separation in photosystem II: functional effect of changes in the antenna size upon light acclimation. The journal of physical chemistry B 117:11200-11208 doi: 10.1021/jp401663w

Wild A, Hopfner M, Ruhle W, Richter M (1986) Changes in the Stoichiometry of Photosystem-Ii Components as an Adaptive Response to Highlight and Low-Light Conditions during Growth. Zeitschrift Fur Naturforschung C-a Journal of Biosciences 41:597-603

Wittig I, Carrozzo R, Santorelli FM, Schagger H (2007) Functional assays in high-resolution clear native gels to quantify mitochondrial complexes in human biopsies and cell lines. Electrophoresis 28:3811-3820 doi: DOI 10.1002/elps.200700367

Tables

Table 1 Pigment contents and carotenoid composition of wild-type barley plants grown at low light (LL: 50 μmol photons m^{-2} s^{-1}), medium light (ML: 300 μmol photons m^{-2} s^{-1}), and high light (HL: 1000 μmol photons m^{-2} s^{-1}).

	LL	ML	HL
Chl *a* (mg m^{-2})	179.1 ± 12.9^{a}	255.4 ± 21.3^{b}	191.2 ± 15.0^{a}
Chl *b* (mg m^{-2})	54.7 ± 4.1^{a}	76.6 ± 5.3^{b}	50.7 ± 4.2^{a}
Car (mg m^{-2})	51.2 ± 3.2^{a}	72.6 ± 6.5^{b}	72.5 ± 4.4^{b}
Chl *a*/*b*	3.27 ± 0.05^{a}	3.33 ± 0.06^{a}	3.77 ± 0.11^{b}
Chl/Car	4.56 ± 0.15^{a}	4.58 ± 0.06^{a}	3.33 ± 0.08^{b}
Neoxanthin	50.4 ± 0.5^{a}	50.2 ± 1.8^{a}	49.5 ± 1.3^{a}
Lutein	200.5 ± 8.1^{a}	189.0 ± 9.5^{b}	201.6 ± 6.6^{a}
β-carotene	142.1 ± 2.9^{a}	160.1 ± 7.0^{b}	175.2 ± 3.8^{c}
V+A+Z	82.6 ± 4.2^{a}	87.7 ± 4.4^{a}	168.0 ± 5.1^{b}
(Z +A)/(V+A+Z) [%]	3.3 ± 0.5^{a}	5.2 ± 0.7^{b}	13.3 ± 4.4^{c}
Lutein/(V+A+Z)	2.43 ± 0.08^{a}	2.16 ± 0.05^{b}	1.20 ± 0.06^{c}

Chlorophyll *a* (Chl *a*), chlorophyll *b* (Chl *b*), and total carotenoids (Car) contents per leaf area. The Chl *a*/*b*, Chl/Car ratios determined spectrophotometrically, carotenoid contents (mmol per mol Chl *a*) and ratios and the conversion state of xanthophyll cycle [(Z+A)/(V+A+Z)] by HPLC were estimated on 2 h darkness-adapted plants. The values report the means and SD from 6 determinations. Values within a row followed by the same superscript do not differ significantly ($P > 0.05$). V, violaxanthin; A, antheraxanthin; Z, zeaxanthin.

Table 2 Quantification of chosen protein from two-dimensional CN/SDS-PAGE analysis of thylakoid protein complexes of barley grown at low (LL) and high (HL) light relative to medium light (ML), changes in percentage (based on data in Fig. 5).

	LL	HL
PsaA/B	+38	–14
Lhcb1+2	+32	–11
Lhcb3	+26	–25
Lhcb6	+28	–29
$CP47_{SC}$	–7	–34
$CP47_{SC\ I+II}/CP47_{SC}$	+19	–11

Content of PSI core proteins PsaA/B; LHCII proteins Lhcb1+2, Lhcb3 and Lhcb6; and PSII core protein CP47 bound in PSII supercomplexes $CP47_{SC}$ were estimated relative to the amount of the PSII core (CP47) and were normalized to the polypeptide content on the ML plants. The ratio of $CP47_{SCI+II}/CP47_{SC}$ expresses representation of PSII supercomplexes I and II containing Lhcb3 and Lhcb6 in all PSII supercomplexes. Results are presented as the difference from ML plants in percentage terms. Typical results from 3 replicates are presented.

Figure Legends

Fig. 1 Normalized 77 K Chl *a* fluorescence spectra of intact barley leaves grown at low (LL), medium (ML), and high (HL) light. Emission spectra (**A**) were excited at wavelength of 436 nm (preferential excitation of Chl *a*) and excitation spectra for PSII emission (**B**) were detected at wavelengths of 685 nm. The spectra and error bars represent the means and SD of 6 samples.

Fig. 2 CD spectra of intact barley leaves grown at low (LL), medium (ML) and high (HL) light. The CD spectra were normalized to the absorbance at 678 nm. The numbers on the graph indicate the wavelength positions, in nanometers, of selected peaks. The spectra and error bars represent the means and SD of 6 samples.

Fig. 3 Normalized 77 K Chl a fluorescence spectra of PPCs isolated by Deriphat-PAGE from barley leaves grown at low (LL) and high (HL) light. (**A**) Emission spectra of PSII PPCs from LL plants. (**B**) Comparison of excitation spectra of PSII PPCs from LL plants. (**C–F**) Excitation spectra of individual PPCs (marked in legends) separated from LL and HL plants. The excitation wavelength of emission spectra was at 436 nm (preferential excitation of Chl *a*) and excitation spectra were detected at wavelengths of emission maxima, which means 680 and 685 nm for LHCII trimers and monomers and PSII core complexes, respectively. Excitation spectra were normalized to the excitation maximum of Chl *a* in the Soret region at wavelength of 440 nm. The spectra and error bars represent the means and SD of at least 6 samples.

Fig. 4 (**A**) Example of CN-PAGE electrophoretograms with separated PPCs from barley thylakoid membranes isolated from barley grown at low (LL), medium (ML), and high (HL) light. The lines represent the sample scanned in white transmitting light. 12 μl of thylakoid membranes with concentration of 1 mg chlorophyll/ml and a final 1:20 (w/w) ratio of chlorophyll to detergent were used for all samples. (**B**) Densitograms evaluated from the electrophoretograms obtained in monochromatic 670 nm light. Typical densitograms from 3 replicates are presented.

Fig. 5 An example of two-dimensional CN/SDS-PAGE analysis of thylakoid protein complexes of barley grown at low (LL), medium (ML) and high (HL) light. Excised lanes from CN-PAGE (Fig. 4A) were denatured, placed on the top of the SDS gel, electrophoresed on 12–20% (w/v) polyacrylamide gel, and stained with Coomassie brilliant blue.

Fig. 6 Normalized 77 K Chl a fluorescence spectra of PPCs isolated by CN-PAGE from barley leaves grown at low (LL), medium (ML), and high (HL) light. (**A**) Emission spectra of PPCs from LL plants. (**B**) Comparison of excitation spectra of PSII supercomplexes from LL plants. (**C–G**) Comparison of excitation spectra of PSII supercomplexes and LHCII trimers and monomers isolated from plants grown at light intensities indicated in legends. The excitation wavelength of emission spectra was at 436 nm (preferential excitation of Chl *a*) and excitation spectra were detected at wavelengths of emission maxima, which means 680 nm for LHCII trimers and monomers and 685 nm for PSII supercomplexes. The spectra show typical values from 3 samples.

Fig. S1 (**A**) Example of two-dimensional CN/SDS-PAGE of LL barley thylakoid membranes with indicated proteins identified by MALDI-TOF MS (PsaA/B: PSI core proteins; CP47, CP43: core antenna complexes of PSII; OEE1: oxygen-evolving enhancer protein 1; D1, D2: PSII core protein; lhcb1–6: LHCII proteins). In the first dimension, thylakoid membranes were incubated with n-dodecyl β-D-maltoside with a final 1:20 ratio of chlorophyll to detergent. (**B**) Densitograms of PSII supercomplexes evaluated from Coomassie blue stained two-dimensional CN/SDS-PAGE displayed on Fig. 5A after normalization on the content of the core antenna CP47. In comparison with supercomplex IV, the Lhcb1,2,3/CP47 ratio is 2.03, 2.75, and 3.91 times higher in supercomplexes III, II and I, respectively. The amounts of Lhcb3 and Lhcb6 proteins per CP47 are considerable only in supercomplexes II and I, and the latter contained approximately double the amounts of both Lhcb3 and Lhcb6. Typical densitograms from 4 replicates are presented.

Fig. 1

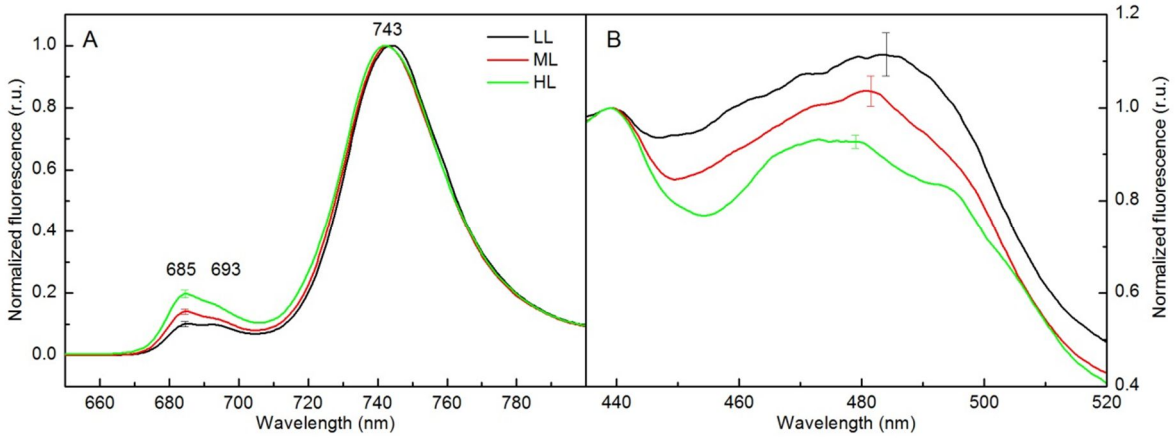
A
B
LL
ML
HL
743
685
693
Normalized fluorescence (r.u.)
Wavelength (nm)
660
680
700
720
740
760
780
440
460
480
500
520
0.0
0.2
0.4
0.6
0.8
1.0
1.2

Fig. 2

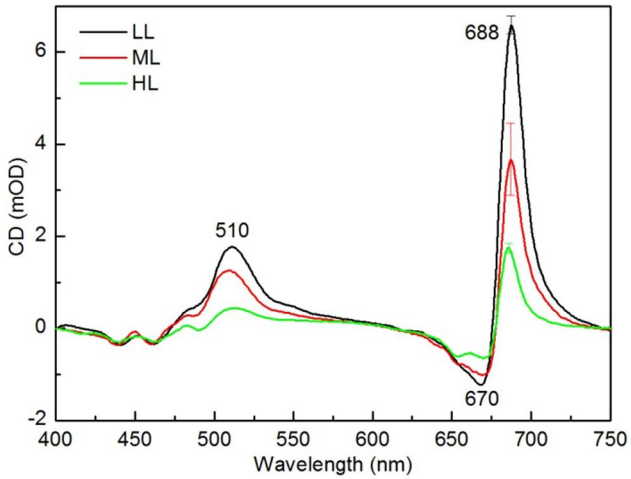
LL
ML
HL
688
510
670
CD (mOD)
Wavelength (nm)
400
450
500
550
600
650
700
750
-2
0
2
4
6

Fig. 3

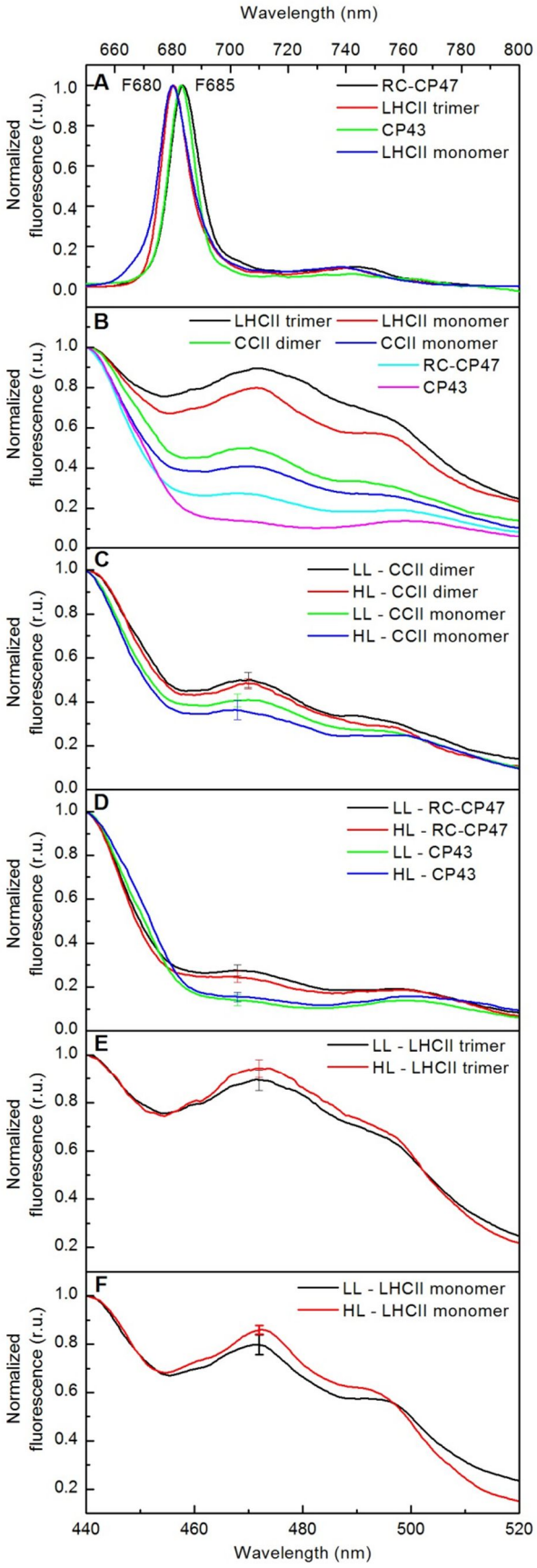
Wavelength (nm)
660
680
700
720
740
760
780
800
A
F680
F685
RC-CP47
LHCII trimer
CP43
LHCII monomer
B
LHCII trimer
LHCII monomer
CCII dimer
CCII monomer
RC-CP47
CP43
C
LL - CCII dimer
HL - CCII dimer
LL - CCII monomer
HL - CCII monomer
D
LL - RC-CP47
HL - RC-CP47
LL - CP43
HL - CP43
E
LL - LHCII trimer
HL - LHCII trimer
F
LL - LHCII monomer
HL - LHCII monomer
Normalized fluorescence (r.u.)
0.0
0.2
0.4
0.6
0.8
1.0
440
460
480
500
520
Wavelength (nm)

Fig. 4

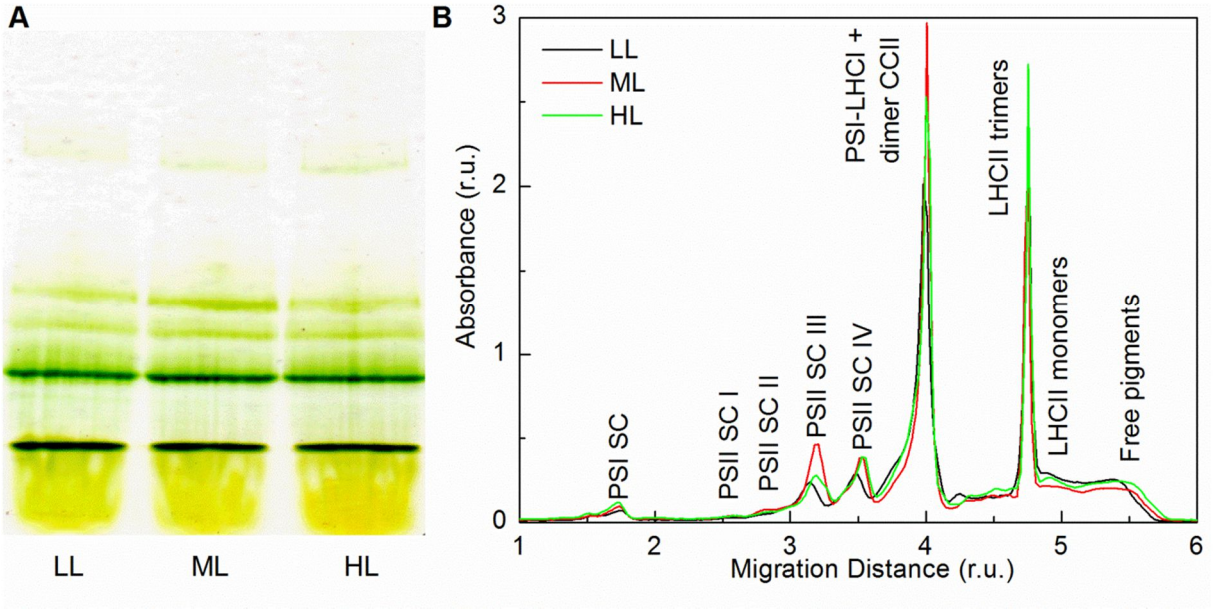
A
LL
ML
HL
B
LL
ML
HL
Absorbance (r.u.)
Migration Distance (r.u.)
PSI SC
PSII SC I
PSII SC II
PSII SC III
PSII SC IV
PSI-LHCI + dimer CCII
LHCII trimers
LHCII monomers
Free pigments

Fig. 5

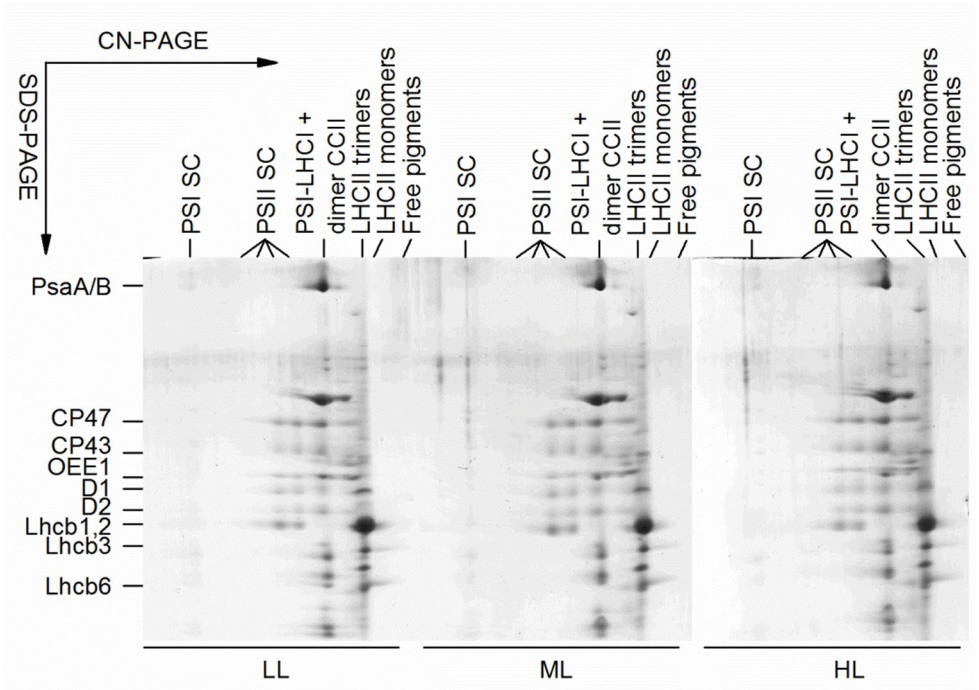
CN-PAGE
SDS-PAGE
PSI SC
PSII SC
PSI-LHCI + dimer CCII
LHCII trimers
LHCII monomers
Free pigments
PsaA/B
CP47
CP43
OEE1
D1
D2
Lhcb1,2
Lhcb3
Lhcb6
LL
ML
HL

Fig. 6

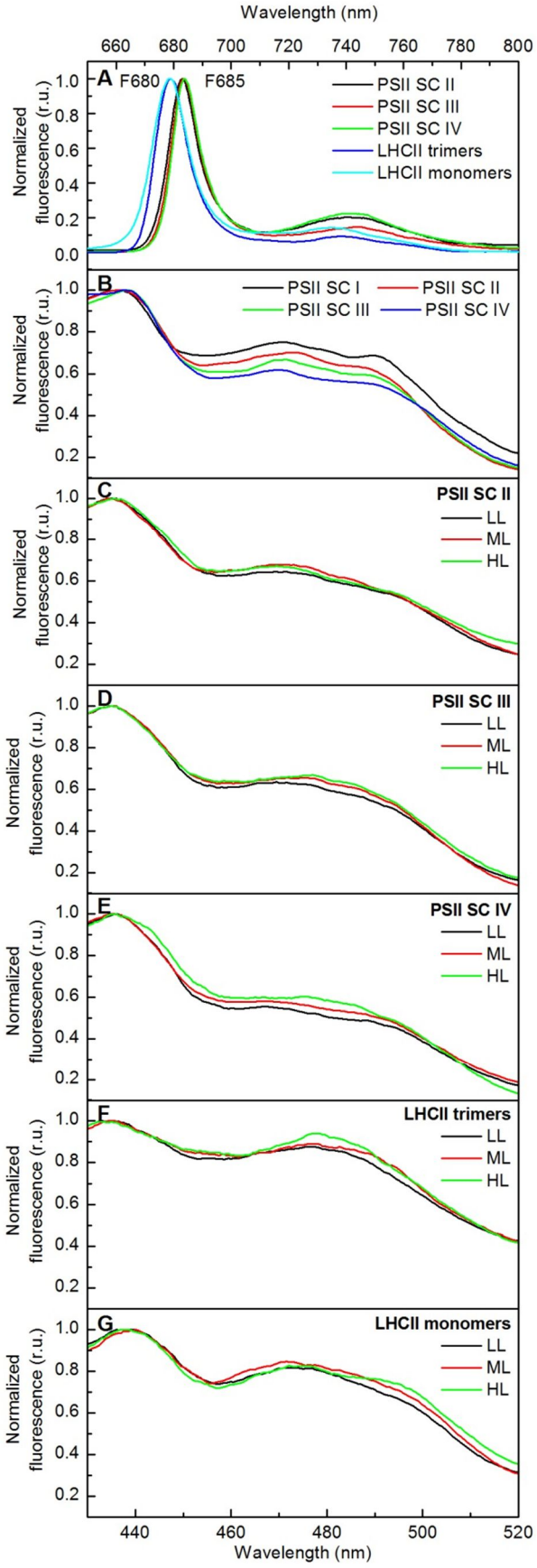
Wavelength (nm)
660
680
700
720
740
760
780
800
A
F680
F685
PSII SC II
PSII SC III
PSII SC IV
LHCII trimers
LHCII monomers
B
PSII SC I
PSII SC II
PSII SC III
PSII SC IV
C
PSII SC II
D
PSII SC III
E
PSII SC IV
F
LHCII trimers
G
LHCII monomers
LL
ML
HL
Normalized fluorescence (r.u.)
0.0
0.2
0.4
0.6
0.8
1.0
440
460
480
500
520
Wavelength (nm)

Fig. S1

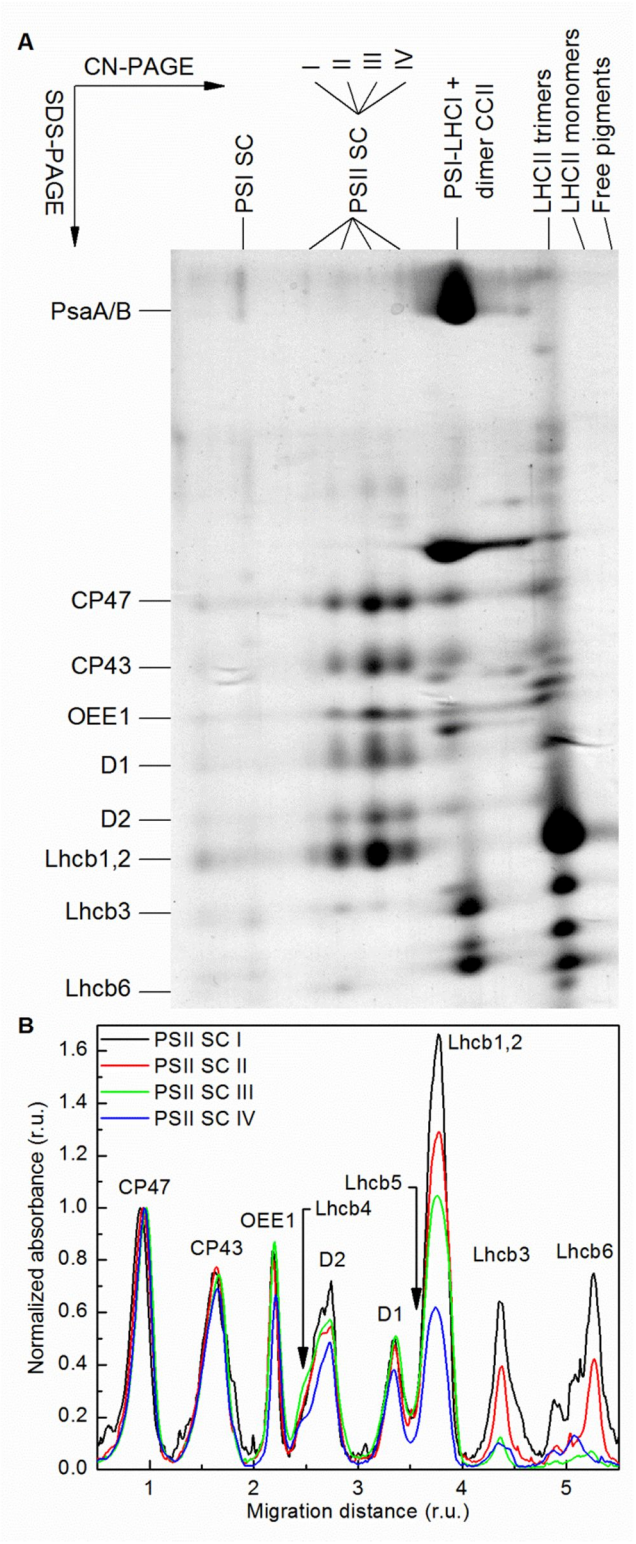
A
CN-PAGE
SDS-PAGE
I
II
III
IV
PSI SC
PSII SC
PSI-LHCI + dimer CCII
LHCII trimers
LHCII monomers
Free pigments
PsaA/B
CP47
CP43
OEE1
D1
D2
Lhcb1,2
Lhcb3
Lhcb6
B
PSII SC I
PSII SC II
PSII SC III
PSII SC IV
Normalized absorbance (r.u.)
Migration distance (r.u.)
CP47
CP43
OEE1
Lhcb4
Lhcb5
D2
D1
Lhcb1,2
Lhcb3
Lhcb6

UNIVERZITA PALACKÉHO V OLOMOUCI

Přírodovědecká fakulta

Katedra biofyziky

ve spolupráci s

OSTRAVSKÁ UNIVERZITA

Přírodovědecká fakulta

Katedra fyziky

Autoreferát disertační práce

SPECTRAL CHARACTERISTICS OF PHOTOSYNTHETIC PIGMENTS AND THEIR RELATION TO STRUCTURE-FUNCTIONAL ASPECTS OF PIGMENT-PROTEIN COMPLEXES *IN VIVO* AND *IN VITRO*

Spektrální charakteristiky fotosyntetických pigmentů a jejich vztah ke strukturně-funkčním aspektům pigment-proteinových komplexů *in vivo* a *in vitro*

Autor práce: Mgr. Václav Karlický

Studijní program: P1703/Fyzika

Studijní obor: Biofyzika

Školitel: Doc. RNDr. Vladimír Špunda, CSc.

Olomouc 2017

Uchazeč: Mgr. Václav Karlický

Katedra biofyziky

Přírodovědecká fakulta, Univerzita Palackého v Olomouci

&

Katedra fyziky

Přírodovědecká fakulta, Ostravská univerzita

Školitel: Doc. RNDr. Vladimír Špunda, CSc.

Katedra fyziky

Přírodovědecká fakulta, Ostravská univerzita

Oponenti: prof. RNDr. Tomáš Polívka, Ph.D.

Ústav fyziky a biofyziky

Přírodovědecká fakulta, Jihočeská univerzita v Českých Budějovicích

RNDr. Roman Kouřil, Ph.D.

Katedra biofyziky

Přírodovědecká fakulta, Univerzita Palackého v Olomouci

Místo a termín obhajoby: 10. března 2017 v 11 hodin

Seminární místnost Centra regionu Haná pro biotechnologický a zemědělský výzkum, budova F2, Šlechtitelů 27, 771 46 Olomouc

Místo, kde bude možné se s disertační prací a posudky alespoň 14 dnů před vykonáním obhajoby seznámit: Studijní oddělení Přírodovědecké fakulty Univerzity Palackého v Olomouci

BIBLIOGRAPHICAL IDENTIFICATION

Name of the author: Václav Karlický

Title of the doctoral thesis: Spectral characteristics of photosynthetic pigments and their relation to structure-functional aspects of pigment-protein complexes *in vivo* and *in vitro*

Study program: P1703/ Physics

Degree program field: Biophysics

Year of defense: 2017

Supervisor: Doc. RNDr. Vladimír Špunda, CSc.

Co-supervisor: prof. RNDr. Petr Ilík, Ph.D.

Number of pages: 140 (76 without attachments)

Number of attachments: 4

Annotation: In this thesis, spectral characteristics of Norway spruce photosynthetic apparatus are studied using circular dichroism and low temperature fluorescence spectroscopy and compare to those of model plants Arabidopsis thaliana and spring barley. Main goal of this thesis was to obtain new information about the pigment-protein complexes of spruce, their supramolecular organization and stability in the thylakoid membranes.

Keywords: Norway spruce; Spring barley; *Arabidopsis thaliana*; Fluorescence spectra; Circular dichroism; Photosystem II organization; Thylakoid membrane; Thermal stability

BIBLIOGRAFICKÉ IDENTIFIKAČNÍ ÚDAJE

Jméno autora: Václav Karlický

Název doktorské práce: Spektrální charakteristiky fotosyntetických pigmentů a jejich vztah ke strukturně-funkčním aspektům pigment-proteinových komplexů *in vivo* a *in vitro*

Studijní program: P1703/Fyzika

Studijní obor: Biofyzika

Rok obhajoby: 2017

Školitel: Doc. RNDr. Vladimír Špunda, CSc.

Konzultant: prof. RNDr. Petr Ilík, Ph.D.

Počet stran: 140 (76 bez příloh)

Počet příloh: 4

Anotace: V této práci jsou studovány spektrální charakteristiky fotosyntetického aparátu smrku ztepilého pomocí spektroskopie cirkulárního dichroismu a nízkoteplotní fluorescenční spektroskopie a porovnány vůči vybraným modelovým rostlinám (huseníček rolní, ječmen jarní). Hlavním cílem této práce bylo získat informace o pigment-proteinových komplexech smrku, jejich makro-organizaci a stabilitě v thylakoidní membráně.

Klíčová slova: Smrk ztepilý; Ječmen jarní; Arabidopsis thaliana; Fluorescenční spektra; Cirkulární dichroismus; Organizace fotosystému II; Thylakoidní membrána; Teplotní stabilita

CONTENT

ABSTRAKT

In this thesis, spectral characteristics of Norway spruce photosynthetic apparatus were studied using circular dichroism and low temperature fluorescence spectroscopy and compared to those of model plants *Arabidopsis thaliana* and spring barley. Main goal of this thesis was to obtain new information about the pigment-protein complexes of spruce, their supramolecular organization and stability in the thylakoid membranes. Red shift of 77K chlorophyll *a* fluorescence emission maximum of isolated PSII-LHCII supercomplexes and smaller macrodomain organization of pigment-protein complexes were confirmed in spruce membranes in comparison with *Arabidopsis* and barley, which can be related to recently described, different structure of spruce PSII-LHCII supercomplexes. It was shown that main signatures of low temperature fluorescence emission of isolated PSII-LHCII and also PSI-LHCI supercomplexes remain distinguishable in 77K chlorophyll *a* fluorescence emission spectra of isolated thylakoids and even intact leaves/needles, indicating that they reflect native state of those pigment-protein complexes. Further, thylakoid membranes of spruce revealed enhanced thermal stability PSII photochemistry than *Arabidopsis* and barley cultivated under the same temperatures. We have proved that higher thermal stability of PSII photochemistry of spruce is accompanied by the maintenance of PSII macro-organization and stability of PSII-LHCII supercomplexes at elevated temperatures. Finally, we documented the specific long-term acclimation response to different growth light intensity in spruce photosynthetic apparatus, in comparison with other higher plants such as *Arabidopsis* or barley. Similarly as observed in *Arabidopsis* and barley, young spruce seedlings exhibited ability to adjust light harvesting antennas during acclimation to different light intensity, but the pronounced increase in lutein content in seedlings acclimated to high light is not typical for other higher plants, but rather for algae (e.g. *Chlamydomonas reinhardtii*). This work thus contributes to the knowledge of the specific aspects of the Norway spruce photosynthetic apparatus and its unusual short- and long-term responses to different environmental conditions.

SOUHRN

V této práci byly studovány spektrální charakteristiky fotosyntetického aparátu smrku ztepilého pomocí spektroskopie cirkulárního dichroismu a nízkoteplotní fluorescenční spektroskopie a porovnány vůči vybraným modelovým rostlinám (huseníček rolní, ječmen jarní). Hlavním cílem této práce bylo získat informace o pigment-proteinových komplexech smrku, jejich makro-organizaci a stabilitě v thylakoidní membráně. U superkomplexu PSII-LHCII smrku při 77 K byl potvrzen posun emisního maxima fluorescence chlorofylu *a* k delším vlnovým délkám a menší makro-organizace pigment-proteinových komplexů v thylakoidních membránách ve srovnání s huseníčkem a ječmenem. Toto je pravděpodobně způsobeno díky odlišné struktuře PSII-LHCII superkomplexů smrku, jež byla nedávno popsána. Dále jsme prokázali, že hlavní rysy nízkoteplotní emise fluorescence chlorofylu *a* izolovaných superkomplexů PSII-LHCII, ale i PSI-LHCI zůstávají patrné nejen v nízkoteplotních emisních spektrech fluorescence chlorofylu *a* izolovaných thylakoidních membrán, ale i intaktních listů či jehlic, což ukazuje, že odráží nativní stav těchto pigment-proteinových komplexů. Navíc thylakoidní membrány smrku vykázaly zvýšenou teplotní stabilitu fotochemie PSII ve srovnání s rostlinami huseníčku a ječmene, které byly pěstovány při stejných teplotách. Prokázali jsme, že vyšší teplotní stabilita fotochemie PSII u smrku je doprovázena schopností udržet makro-organizaci PSII a stabilitu superkomplexů PSII-LHCII při zvýšených teplotách. Rovněž jsme prokázali, že fotosyntetický aparát smrku má odlišnou aklimační odezvu na různé intenzity světla než ostatní druhy vyšších rostlin jako huseníček či ječmen. Podobně jak bylo pozorováno u huseníčku a ječmene, semenáčky smrku vykazovaly schopnost přizpůsobit světlosběrné antény během aklimace na různé intenzity světla, nicméně výrazný nárůst obsahu luteinu semenáčků smrku aklimovanch na vysokou intenzitu světla není typické pro vyšší rostliny, ale spíše řasy (např. *Chlamydomonas reinhardtii*). Tato práce přispívá ke znalostem specifických aspekty fotosyntetického aparátu smrku ztepilého a jeho neobvyklé krátkodobé i dlouhodobé odezvy na různé environmentální odezvy.

LIST OF PUBLICATIONS

Published:

1) *Karlický, V., Podolinská, J., Nadkanská, L., Štroch, M., Čajánek, M., Špunda, V. (2010) Pigment composition and functional state of the thylakoid membranes during preparation of samples for pigment-protein complexes separation by nondenaturing gel electrophoresis. Photosynthetica 48: 475-480
2) *Miloslavina, Y., Lambrev, P.H., Jávorfi, T., Várkonyi, Z., Karlický, V., Wall, J.S., Hind, G., Garab, G (2012) Anisotropic circular dichroism signatures of oriented thylakoid membranes and lamellar aggregates of LHCII. Photosynthesis Research 111: 29-39
3) Štroch, M., Materová, Z., Vrábl, D., Karlický, V., Šigut, L., Nezval, J., Špunda, V. (2015) Protective effect of UV-A radiation during acclimation of the photosynthetic apparatus to UV-B treatment. Plant Physiology and Biochemistry 96: 90-96
4) *Karlický, V., Kurasová, I., Ptáčková, B., Večeřová, K., Urban, O., Špunda, V. (2016) Enhanced thermal stability of the thylakoid membranes from spruce. A comparison with selected angiosperms. Photosynthesis Research 130: 357-371

Submitted:

5) *Karlický, V., Strouhal, O., Ilík, P., Štroch, M., Kurasová, I., Garab, G., Šebela, M., Špunda, V. The effect of growth light intensity on pigment-protein composition and efficiency of excitation energy transfer within photosystem II in barley leaves. Photosynthesis Research
6) VI. Materová, Z., Sobotka, R., Zdvihalová, B., Oravec, M., Nezval, J., Karlický, V., Vrábl, D., Štroch, M., Špunda, V. Monochromatic green light induces an aberrant accumulation of geranylgeranyl-chlorophyll in plants. Plant Physiology and Biochemistry

Peer-reviewed conference papers (ISI Web of Science):

7) Karlický, V., Kurasová, I., Špunda, V. (2015) The thermostability of photosystem II photochemistry is related to maintenance of thylakoid membranes organization. Global Change: A Complex Challenge: 142-145
8) Kurasová, I., Svrčinová, K., Karlický, V., Špunda, V. (2015) CN-PAGE as a tool for separating pigment-protein complexes and studying their thermal stability in spruce and barley thylakoid membranes. Global Change: A Complex Challenge: 146-149

Peer-reviewed conference papers:

9) Karlický, V., Nezval, J., Štroch, M., Špunda, V. (2013) Response of epidermal blue-green fluorescence emission from Barley leaves to UV radiation stress. Global Change and Resilience: From Impacts to Responses: Proceedings of the 3rd annual Global Change and Resilience Conference, ISBN 978-80-904351-8-6

*These publications are the basis of the present Ph.D. thesis

ABBREVIATIONS

Car – Carotenoid; CD – Circular dichroism; CN-PAGE – Clear-native polyacrylamide gel electrophoresis; DGDG – Digalactosyldiacylglycerol; Chl – Chlorophyll; F_V/F_M – maximum efficiency of PSII photochemistry; HL – High light; Lhc – Light-harvesting complex; Lhca (LHCI) – Light-harvesting complex of PSI; Lhcb – Light-harvesting complex of PSII; LHCII – Major light-harvesting complex of PSII; Lhcb4 (CP29), Lhcb5 (CP26), Lhcb6 (CP24) – Minor light-harvesting complex of PSII; Lhcsr – stress-related LHC protein; LL – Low light; MGDG – Monogalactosyldiacylglycerol; ML – Moderate light; NPQ – Non-photochemical quenching of chlorophyll *a* fluorescence ; PPC – Pigment-protein complex; PSI – Photosystem I; PSII – Photosystem II; ROS – Reactive oxygen species; T_m – Transition temperature; VDE – Violaxanthin de-epoxidase; Ψ – Polymer and salt induced

1 INTRODUCTION

1.1. General introduction

Nowadays, one of the main scientific challenges is solution of problems related to the rapidly increasing energy consumption of humankind. Fossil fuels cannot be maintained in the long term perspective as a prevailing producer of the global energy due to the rapid decrease of its resources and increasing atmospheric carbon dioxide concentration. Therefore, scientific studies on the utilization of renewable resources became important. Amongst various energy resources, solar energy has a special role, because light energy reaching the Earth's surface is many times greater than the needs of world's energy. In the Biosphere, efficient collection, utilization and storage of solar energy through conversion to chemical energy is performed by photosynthetic organisms. Photosynthesis is the biochemical process in plants, algae and certain bacteria that serves as the energy input for the current life of terrestrial and aquatic organisms and it regulates the oxygen concentration and carbon dioxide in the atmosphere. On the basis of this natural process, a substantial contribution to industrial energy production can originate from modified photosynthetic organisms or artificial devices converting solar energy.

Moreover, the plants are exposed to extremely different climatic conditions, such as irradiances or temperatures that undergo considerable changes in very diverse time scales. As sessile organisms plants have to evolve highly sophisticated acclimation responses during evolution to allow survival under these environmental conditions. There is still a lack of information on diversity of photosynthetic apparatus, particularly if the importance of individual regulatory mechanisms that control the resistance of plants to environmental stresses and influence different acclimation strategies among different plant species is taken into account. In this work, we focused on higher plants, which form a large group of plants as regards the plant species, but relatively narrow group from the viewpoint of evolutionary history. Nevertheless, there are still differences in architecture and composition of photosynthetic apparatus components among land plant families and probably also in acclimation responses to environmental stresses.

This thesis is related to specific structural and functional aspects of photosynthetic apparatus of Norway spruce belonging to the *Pinaceae* family of gymnosperms, which were always less studied than angiosperms.

1.2. Thylakoid membrane of the chloroplast

The photosynthetic processes of higher plants and eukaryotic algae occur in an organelle, called the chloroplast. Evolutionary, the chloroplast became a plant cell organelle through an endosymbiotic event, during which a non-photosynthesizing eukaryotic organism engulfed a cyanobacterium. The chloroplasts contain the thylakoid membranes, the multilamellar lipid bilayer membrane assembly located in the aqueous matrix called stroma. Carbon fixation, the 'dark reactions', happen in the stroma, while thylakoid membranes are the site for the 'light reactions' of photosynthesis, and thus have a crucial role in the primary steps of photosynthesis. The thylakoid membranes separate two aqueous phases (the stroma and the lumen) and incorporate almost all components of the photosynthetic electron transfer pathway, including main protein complexes photosystem II (PSII), the cytochrome b6/f complex, photosystem I (PSI) and the ATP-synthase. Further, between PSII and cytochrome b6/f and between cytochrome b6/f and PSI the mobile plastoquinone and small water-soluble protein plastocyanin serve as electron carriers. These components have specific role in the photosynthetic electron transport or in the energy conversion.

The matrix of thylakoid membranes is composed of specific lipid classes (monogalactosyl-diacylglycerol - MGDG, digalactosyl-diacylglycerol - DGDG, sulfoquinosyl-diacylglycerol - SQDQ and phosphatidyl-glycerol - PG) forming the bulk lipid phase, interface with protein complexes and filling their cavities (Garab et al. 2016). Although for each of the thylakoid lipids a specific role in the assembly and functioning of both photosystems in thylakoid membrane has been identified (Pali et

al. 2003), MGDG, the most abundant thylakoid lipid, constituting about half of total thylakoid lipids in most higher plants, has a specially complex role. Although, MGDG belongs to the class of non-bilayer (or non-lamella-forming) lipids, which do not self-assemble into bilayers in aqueous media (Williams 1998), it has been shown that the non-bilayer lipid MGDG can be forced into a bilayer structure upon its association with the most abundant membrane protein, the light-harvesting complex of PSII (LHCII) (Simidjiev et al. 1998; Simidjiev et al. 2000). Role of MGDG in the operation of the xanthophyll cycle has been well established showing that the functioning of violaxanthin de-epoxidase (VDE) requires the presence of MGDG for its activity (Yamamoto and Higashi 1978) and the presence of non-bilayer lipid phases (Latowski et al. 2004). MGDG form a lipid shield around LHCII and free xanthophylls and thus avoid the formation of aggregates of hydrophobic xanthophyll cycle pigments in an aqueous medium so that they become accessible to the VDE. On the other hand, DGDG plays an important role in the stability and activity of PSII and PSI and also in the stabilization of LHCII trimers (Kalisch et al. 2016). Therefore, changes in the MGDG/DGDG ratio affect the membrane organization and the protein folding and insertion, which exert an impact on the photosynthetic performance. Variations in the MGDG/DGDG ratios influence also the structural flexibility of the thylakoid membranes, as demonstrated by the significant alterations in the organization of the thylakoid membranes and their thermal stability (Krumova et al. 2010).

1.2.1. The structure of thylakoid membrane

Differentiation of the thylakoid membrane into stacked and unstacked regions (forming grana and stromal lamellae, respectively) is known for decades from transmission electron microscopy studies. In recent years, structural complexity of thylakoids become clear using more advanced microscopic methods. The grana exist as cylindrical stacks of flattened membrane discs closely appressed at their stromal faces and interconnected by the fret-like stromal lamellae (Austin and Staehelin 2011). The stromal lamellae thus provide contact multiple grana layers in the same stack. In addition to the stromal lamellae non-appressed membranes form two other regions, the non-appressed grana end membranes at the top and bottom of each stack and the junctional slits which connect the grana and stromal lamellae (Ruban and Johnson 2015).

In plants, the distribution of the different protein complexes is not homogenous. PSII is mainly found in the granum while PSI and the ATP synthase only in the stroma thylakoids and the end membranes of grana, grana margins. The cytochrome b6/f complex and the trimeric major LHCII, which serves both PSI and PSII, are found in both, grana and stroma thylakoids (Dekker and Boekema 2005). This lateral segregation of the protein complexes allows the formation of the different structure of the stroma and granum thylakoids. The trimeric LHCII actively participate in the close packing of granum thylakoids (Garab and Mustardy 1999).

The biological advantage of the structural and functional segregation of the two different thylakoid membranes, a unique feature for higher plants and green algae (Olive and Vallon 1991), is a widely investigated topic in photosynthesis. In the case of cyanobacterium, thylakoid membranes lacking lateral segregation of the protein complexes do not form grana structures. The evolutionary advantage of thylakoid membrane stacking is considered to be a higher efficiency of electron transport by preventing the fast energy trap PSI from outflowing excitation energy from the slower trap PSII, a phenomenon known as spillover (Johnson 2016). Another possible advantage of membrane stacking in thylakoids may be the segregation of the linear and cyclic electron transfer pathways, which might otherwise compete to reduce plastoquinone (Johnson 2016). Moreover, this lateral heterogeneity enables the flexibility in dynamic redistribution of the protein components, such that the plant can perform vital self-protective and repair processes that enable rapid responses to its environment (Ruban and Johnson 2015).

1.3. Photosynthetic light-harvesting

Photosynthesis begins with the absorption of light by pigment molecules located in the thylakoid membrane. In plants and green algae most of the light is absorbed by the photosynthetic pigments chlorophyll (Chl) *a* and *b* owning remarkable physicochemical properties allowing efficient light harvesting and ultrafast excitation energy transfer among antenna Chls. Thus energy from sunlight is captured by pigment-protein complexes (PPCs) that subsequently deliver it to reaction centres during 10–100 ps with the highest known quantum and thermodynamic efficiencies (Scholes et al. 2011). In other words, light harvesting count on the process of electronic energy transfer moving electronic excitation energy stored for a very short time (nanoseconds) by the excited states of molecules within highly organized networks of light absorbing chromophores to a target chromophore or trap (Olaya-Castro and Scholes 2011). Timescale of this process limits the size of the chromophore arrays connected to the reactive centre on so-called exciton diffusion length, i.e. how far excitation energy can migrate. The excitation energy flow to the reaction centres thus can be regulated by very fine structural changes in antennas. On this basis, photoprotective mechanisms switch from an arrangement of chromophores that optimizes trapping via energy transfer through the antenna to arrangement that works inefficiently due to excitation traps quenching the excited-states of Chls.

1.3.1. Photosynthetic pigments

The first step of the photosynthetic processes is the absorption of a photon by a photosynthetic pigment. As a result of evolution nature has selected a relatively small group of pigments to serve in the photosynthetic antenna complexes: Chls, carotenoids (Cars) and phycobilins. From them only Chl in plants and algae and bacteriochlorophyll in photosynthetic bacteria serve in photochemically active reaction centre. The antenna pigments are more versatile. The photosynthetic antenna pigments of plants include Chl *a* and *b* and several types of Cars including oxygenated Cars, called xanthophylls.

The majority of photosynthesizing organisms contain Chl *a,* which plays a central role in the photochemical energy conversion. Chl *a* is a magnesium containing chlorin ring, to which a phytol chain is esterified at pyrrole ring IV. Chl *b* is the main accessory Chl in higher plants and green algae. Chl *b* differs only in one functional group from Chl *a*, which confers a slightly lower lipophylic character and shifts of the major absorption bands in the red and blue towards the green.

Higher plant antenna xanthophylls, lutein, neoxanthin, violaxanthin and zeaxanthin are the most common xanthophylls on our planet. Xanthophylls absorb light in spectral region in which the sun irradiates maximally and transfer excitation energy to Chls. Xanthophylls also contribute to regulation of energy flow within the photosynthetic apparatus and to protection of photosynthetic apparatus against photoinduced damage caused by excess light absorption.

1.3.2. The structure of the individual light-harvesting complexes

Most of photosynthetic organisms possess an antenna system that increases optical cross-section of the photosystems. During the evolution of photosynthesis in eukaryotes, the membrane-associated phycobilisomes of the cyanobacteria have been substituted by membrane-integral pigment binding complexes, Light-harvesting complexes (Lhc) (Ballottari et al. 2012). All Lhc proteins are encoded by nuclear genes, are homologous to each other and share a similar structure. Although all Lhc antennas have three helix membrane-spanning regions and coordinate Chl *a*, Chl *b* and Car molecules, each Lhc has a specific pigment content which confers them distinct spectroscopic properties (Caffarri et al. 2014). Accordingly to the nomenclature for core subunits, PPCs of PSII and PSI are named Lhcb and Lhca, respectively.

The antenna complexes of PSII from higher plants are composed of 6 different Lhcb proteins Lhcb1-6. Subunits Lhcb1, Lhcb2 and Lhcb3 form heterotrimer of the major antenna complex of PSII, LHCII. Subunits Lhcb4, Lhcb5 and Lhcb6 occur only as monomers and are also commonly named as

CP29, CP26 and CP24, respectively (based on the apparent molecular weight on a SDS-PAGE obtained at the time of the first characterization). The structure of a monomeric subunit of trimeric LHCII was shown (Liu et al. 2004). Each monomer coordinates 8 Chls *a*, 4 Chls *b* and four xanthophylls (one N, two L and one V). The two L are located at sites L1 and L2 in the center of the molecule while N and V are located at the periphery in sites N1 and V1, respectively (Croce et al. 1999; Caffarri et al. 2001; Ruban and Horton 1999). The average distance between the Chls is around 10 A°, which leads to excitonic interactions between the pigments, resulting in fast energy transfer within the complex.

Crystal structure of CP29 at 2.8 Å resolution indicates that this complex binds 3 Cars and 13 Chls with Chls *a*/*b* ratio about 1.9 (Pan et al. 2011). CP29 differs from LHCII subunits in absence of a peripheral V1 site and also in the position of some Chls binding sites. The structure of CP26 is not available, nevertheless, biochemical data and sequence homology suggest that this complex has a similar amount of Chls (13-14 Chls) as CP29 and a Chls *a*/*b* ratio approximately 2 (Dall'Osto et al. 2005). CP24 differs from all the other PSII monomeric antennas. Evolution of this subunit is considered as a more recent, because it is found only in the land plant lineage while CP26, CP29 and LHCII are present in green algae as well (Koziol et al. 2007). Moreover, it has unusual pigment binding properties due to the lowest Chl *a*/*b* ratio approximately 1, binding only 10-11 Chls and 2 Cars in site L1 and L2 (Passarini et al. 2009).

The structural and pigment-binding characteristics of the individual Lhca complexes were always less elucidated than for the Lhcb complexes, mainly due the difficulties of purifying intact monomeric complexes. In plants, the absorption cross section of the PSI core is increased by four LHCI subunits Lhca1-4, which form a belt on one side of the PSI core (Ben-Shem et al. 2003) and bind 57 Chls and 13 Cars as revealed 2.8 Å resolution of Lhca from pea (Qin et al. 2015). These high-resolution structures are necessary to understand the molecular basis of light harvesting in Lhca, especially due to the fact that the Lhca contain several Chls with redshifted spectra (called red forms) which extend the light-harvesting capacity of PSI to the far-red region (van Amerongen and Croce 2013).

1.3.3. The structure and function of the photosystem II

The basic role of the PSII is to oxidize water molecules on the lumenal side and to reduce quinones at the stromal side of the thylakoid membrane using the energy of absorbed photons. During the last two decades electron and X-ray crystallography studies have provided more and more detailed information about this multisubunit protein complex achieving already a resolution of 1.9 Å (Guskov et al. 2009; Loll et al. 2005; Umena et al. 2011). The structure of the PSII core from higher plants is not available at present but it is supposed to be very similar to that of cyanobacteria. The PSII core is composed of four large integral membrane proteins (the products of genes PsbA–PsbD) containing 22 membrane-spanning helices and 14 additional transmembrane helices are formed by a number of small subunits. The products of genes PsbA and PsbD (D1 and D2 proteins, respectively) form a heterodimer which coordinates 6 Chls, 2 pheophytins and 2 plastoquinones (Q_A and Q_B) that participate in the electron transport chain. These complexes together with the two $cytb_{559}$ proteins form complex of reaction center (RC). PsbB and PsbC encode for the two inner antenna complexes (core antenna proteins CP47 and CP43) located on the side of D2 and D1, respectively. Core antenna proteins coordinate 29 Chl *a* (CP47: 16; CP43: 13) and 11-12 β-carotene molecules (Umena et al. 2011).

During the last decade, development of single particle cryo-electron microscopy and cryo-electron tomography enabled improvement of knowledge on the structure of external antenna system of PSII and the architecture of thylakoid membranes (Croce and van Amerongen 2011; Kouřil et al. 2012; Mustardy et al. 2008; van Amerongen and Croce 2013). A variable number of LHCII proteins can be bound to dimeric PSII core PPCs forming different PSII–LHCII supercomplexes (Dekker and Boekema 2005). The largest supercomplex purified so far named C2S2M2 (Caffarri et al. 2009) consist of dimeric core (C2) associated with 2 copies of each of the monomeric complexes CP29

(lhcb4), CP26 (lhcb5) and CP24 (lhcb6) and 4 LHCII trimers (lhcb1-3) (Boekema et al. 1999). Two LHCII trimers firmly bound on the CP26 sides (S-trimers) are composed of the products of the Lhcb1 and Lhcb2 genes (Hankamer et al. 2001), while the next two ones, moderately bound on the side of CP29 and CP24 (M-trimers), contain also the product of the Lhcb3 gene (Boekema et al. 1999). Except LHCII trimers contained in the PSII-LHCII supercomplexes there are also extra LHCII trimers that are either functionally connected to PSII (van Amerongen and Croce 2013) or located in the LHCII-only domains (Boekema et al. 2000).

1.3.4. The structure and organization of the photosystem I

The organization of the Lhc protein around the photosystems is different between PSII and PSI. Crystallographic model and single particle analysis revealed a single layer of Lhca proteins bound on one side of the core complex of plant PSI in order of Lhca1, Lhca4, Lhca2, Lhca3. Subunit PsaG is considered important for the anchoring of the Lhca antenna proteins to the PSI core (Ben-Shem et al. 2003).

In all conditions in which PSII is preferentially excited, part of the LHCII population moves to PSI to increase its antenna size, forming the PSI-LHCI-LHCII supercomplex (Lemeille and Rochaix 2010). The LHCII trimer binds on the opposite side of the Lhca's interacting with the PsaH subunit (Croce and van Amerongen 2013; Kouřil et al. 2005). However, this complex is very sensitive to most non-ionic detergents, but it is stable in digitonin (Kouřil et al. 2005). Excitation energy transfer from LHCII to PSI core is extremely fast, making LHCII a perfect light harvester for the system (Wientjes et al. 2013a).

1.4. Photoprotection mechanisms of the photosynthetic apparatus against photo-oxidative damage

Light reactions of photosynthesis are inevitably associated with production of potentially harmful reactive oxygen species (ROS). The oxidative stress is increased by unfavourable conditions either directly by excess photosynthetically active radiation, UV radiation and high temperatures, or indirectly by temperatures below optimum, drought or salinity. In most cases particularly PSII is a target of photooxidative damage (Pospíšil 2012; Ruban et al. 2012; Vass 2012).

Plants have evolved a comprehensive set of protective mechanisms that determine the resulting resistance and/or acclimation strategy to changing environmental conditions. Plants are capable to respond at different levels of organization: for example at the tissue level via optical screening by epidermal phenolics (Agati et al. 2011; Merzlyak et al. 2008; Štroch et al. 2008b), at the cellular level by chloroplast movements (Banas et al. 2012; Nauš et al. 2008; Wada 2013) and regulation of chloroplast number (Oguchi et al. 2003), or at the molecular level by regulation of protein (Bailey et al. 2001; Garab 2014; Timperio et al. 2012) and lipid (Harwood 1998; Lepetit et al. 2012) composition of the thylakoid membranes. All these processes with very different dynamics on the timescale from seconds to weeks lead to lowering of ROS formation or the detoxification of already formed ROS (for example by accumulation of the direct antioxidants such as low-molecular compounds such as phenolics and Cars).

Among the prompt regulatory responses (on the timescale from seconds to minutes), which helps plants and algae to survive under rapidly changing light conditions, the so-called non-photochemical quenching of Chl *a* fluorescence (NPQ) (Demmig-Adams et al. 2014; Goss and Lepetit 2015; Niyogi and Truong 2013; Ruban 2016; Ruban et al. 2012) is a crucial one. Mechanisms of NPQ processes that turn on and off rapidly (often called qE) differs in green algae, mosses and plants (Goss and Lepetit 2015; Niyogi and Truong 2013). According to a current concept the PsbS protein belonging to the family of LHC is important for NPQ in higher plants (Croce 2015). In lower plants (e.g. green algae, mosses) the stress-related LHC proteins (Lhcsr) overtake the role of PsbS in NPQ activation (Goss and Lepetit 2015; Niyogi and Truong 2013). In higher plants, qE process is triggered by acidification of the thylakoid lumen, which causes protonation of PsbS (Croce 2015) and its

monomerization (Correa-Galvis et al. 2016). Moreover, low lumenal pH activates VDE converting violaxanthin into zeaxanthin via antheraxanthin (Jahns and Holzwarth 2012). Resulting structural rearrangement of PSII is responsible for functional disconnection of part of LHCII from PSII core and formation of quenching centres within detached major LHCII (quenching site Q1) or in the remaining PSII antenna (quenching site Q2) (Jahns and Holzwarth 2012; Johnson and Ruban 2011). Whether LHCII aggregates in the light adapted state contains M trimers only or also bind CP24 is still under debate.

Upon exposure to excess light, several other mechanisms are attributed to NPQ, except the most rapid component qE operating in the range of seconds to minutes. Slower component reflects the enhancement of energy dissipation due to the accumulation of zeaxanthin (qZ) through the xanthophyll cycle, which develops in the time range from 10 to 30 min at moderate light (ML)(similarly as qE). Under very high light (HL) at longer illumination time (>30 min) dominates photoinhibition quenching (qI) (Jahns and Holzwarth 2012). Also light-avoidance movements of the chloroplasts within the plant cell significantly contribute to slower component of NPQ (Dall'Osto et al. 2014). Under low light (LL), the state transition component of NPQ operates in the timeframe of a few minutes and reflects the dynamic allocation of part of LHCII either to PSII or to PSI (qT) (Goldschmidt-Clermont and Bassi 2015; Minagawa 2011; Tikkanen et al. 2011). State transitions operate particularly under LL and are replaced by other mechanisms such as qE under ML and HL. In higher plants, state transitions do not significantly contribute to NPQ, in contrast to the situation in green algae (Jahns and Holzwarth 2012).

1.4.1. Acclimation of photosynthetic apparatus to different light intensity

Regulatory responses of the photosynthetic apparatus on the timescale of days to weeks to natural light regimes, so-called long-term acclimation, rely mostly on two types of adjustment, i.e. modulation of the relative amount of LHCII and changes in the PSI/PSII ratio adjusting the balance of excitation of both photosystems. A number of acclimation responses have been described for various plant species grown under different light conditions.

At the turn of the millennium, particularly biochemical studies on amount of accumulated proteins and photosynthetic pigments were performed. Significant increase in the amount of cytochrome b_6f complex and the activity of ATP synthase has been reported for several species grown under HL (de la Torre and Burkey 1990). Considerably elevated levels of PSII reaction centres (RCs) in response to HL have been demonstrated for *Arabidopsis* (Bailey et al. 2001; Walters et al. 1999), pea (Evans 1987; Leong and Anderson 1984), and mustard (Wild et al. 1986). On the contrary, only slightly enhanced amounts of PSI RCs at HL were reported for *Arabidopsis* (Bailey et al. 2001) and pea (Leong and Anderson 1984), but a dramatic increase in PSI content was observed in thylakoid membranes of plants grown under very LL (Bailey et al. 2001). It has been known for decades that the ratio of LHCII to PSII is decreased under HL growth conditions (Anderson et al. 1995). More recently, changes in LHCII protein composition (Bailey et al. 2001; Kouřil et al. 2013) or even in their individual isoforms (Albanese et al. 2016; Timperio et al. 2012) were described for *Arabidopsis* acclimated to different light intensities. Reduction of LHCII size in HL plants has often been assessed indirectly by increased ratio of Chl *a*/*b*, for example in barley (de la Torre and Burkey 1990; Kurasová et al. 2002; Štroch et al. 2004), *Arabidopsis* (Bailey et al. 2001; Kouřil et al. 2013), spinach (Lindahl et al. 1995), and pea (Leong and Anderson 1984). Furthermore, diminution of functional antenna size of PSII in HL-grown barley as compared with LL plants has been roughly assessed from the reduced ratio of the main Chl *b* and Chl *a* excitation bands in the Soret region of the 77 K fluorescence excitation spectra measured on leaf segments (Čajánek et al. 2002; Štroch et al. 2004) and by advanced methods based on Chl *a* fluorescence (Bielczynski et al. 2016; Wientjes et al. 2013b). Regarding changes in the composition of photosynthetic pigments, the Cars/Chls ratio increased in plants grown at HL conditions as well that was particularly due to relative increase VAZ pool (Bielczynski et al. 2016; Kurasová et al. 2002; Štroch et al. 2004). In consequence, the acclimation to HL results in enhanced capacity of NPQ, and enhanced convertibility of violaxanthin to

zeaxanthin (Bugos et al. 1999; Demmig-Adams 1998; Kurasová et al. 2002; Štroch et al. 2004). Part of VAZ pool pigments (bigger part may be expected for HL plants in comparison with LL ones) is formed by non-protein bound xanthophylls in the lipid phase of the thylakoid membrane. Z in the lipid phase of the thylakoid membrane is linked to an important photoprotective function of Z independent from its role in qE (Havaux and Niyogi 1999) and serves as antioxidant, additive to the photoprotective function of tocopherol (Havaux et al. 2007).

In the last decade, the structural response of PSII-LHCII supercomplexes in the thylakoid membranes after acclimation to different light intensity has been characterized (Albanese et al. 2016; Bielczynski et al. 2016; Kouřil et al. 2013). Reduction of LHCII size under HL conditions was related to the decreased amount of large C2S2M2 PSII-LHCII supercomplexes, while acclimation to very LL had no influence on large supercomplexes in comparison with ML (Albanese et al. 2016; Kouřil et al. 2013). The structural modification of PSII supercomplexes at HL is accompanied by a specific reduction of antenna protein subunits Lhcb3, Lhcb6 and M-LHCII trimers bound to the PSII cores (Albanese et al. 2016; Kouřil et al. 2013), while the Lhcb4.3 isoform increased in PSII–LHCII supercomplex response to HL intensities. These results suggest that the Lhcb3, Lhcb4.3 and Lhcb6 antenna subunits are major players in modulation of the PSII antenna size upon long-term acclimation to HL. On the other hand, the amount of the "extra" LHCII was increased in LL membranes, whereas in HL membranes their amount remained at the same level as in ML plants. Furthermore, occurrence of semi-crystalline PSII arrays was strongly reduced in HL plants as compared to LL and ML plants, probably due to the increased structural heterogeneity of PSII supercomplexes. Kouřil et al. (2013) found that the C2S2M2 supercomplexes in semi-crystalline arrays in LL plants were more densely packed than in HL or ML plants and suggested that the spacing between supercomplexes is important for efficient energy transfer between PSII under light-limiting conditions.

1.4.2. Thermal stability of photosystem II

As mentioned above, temperatures out of the range of optimum increase oxidative stress either directly such as in the case of high temperature stresses, or indirectly by cold stresses. Moreover, an elevated temperature can cause direct negative effects on photosynthetic assimilation of carbon dioxide. PSII is considered to be the most heat sensitive component of photosynthetic apparatus (Allakhverdiev et al. 2008; Zhang and Sharkey 2009). At the temperature from 42 °C to 48 °C the PSII donor side undergoes a disruption due to loss of oxygen evolution complex (Cramer et al. 1981; DelasRivas and Barber 1997). PSII acceptor side becomes gradually inactivated at temperatures above 40 °C by changed midpoint potential of the primary quinone acceptor Q_A (Pospíšil and Tyystjarvi 1999). The increasing permeability to protons can lead to dissipation of ΔpH and finally to loss of the thylakoid membranes integrity resulting in inability to maintain transmembrane electrochemical potential (Zhang et al. 2009). The disassembly of the chiral macrodomains occurs in the temperature range of 45 - 55 °C (Krumova et al. 2010; Varkonyi et al. 2009). At a temperature around 60 °C the PSII core denatures (Shi et al. 1998) and trimeric LHCII dissociate to its monomeric form (Dobrikova et al. 2003). Heat denaturation of LHCII monomers occurs at temperature between 70–80 °C (Lípová et al. 2010; Yang et al. 2006). The more stable PSI undergoes the major conformation transition at 60 °C to 70 °C, which is accompanied by the energetic disconnection of LHCI from PSI core, that denatures in a wide temperature interval 70–90 °C (Hu et al. 2004; Lípová et al. 2010). It should be noted that the mentioned denaturation temperatures of individual PPCs can be influenced by the type of temperature treatment or heating rate during linear heating (Krumova et al. 2005).

The analysis of temperature dependence of Chl *a* fluorescence parameters *in vivo* documented considerably different thermal stability of PSII function among plants species (Knight and Ackerly 2002), genotypes (Brestič et al. 2012) and its seasonal variations (Brestič et al. 2012; Froux et al. 2004). It has been proved that increased temperatures lead, in addition to adjustment of numerous photosynthetic processes and structures, to a relatively fast increase of PSII thermal

stability (Brestič et al. 2012; Ghouil et al. 2003). An improved thermal stability of PSII was also observed as a result of acclimation to other stress factors, e.g. drought (Epron 1997; Lu and Zhang 1999) and salinity (Chen et al. 2004; Wen et al. 2005). However, knowledge on the mechanisms that are responsible for the mentioned variability of PSII sensitivity to heat stress is still not complete and controversies remain.

The thermal stability of PSII can be increased by stable forms of PSII proteins as observed in the case of double mutation in PSII reaction centre protein D1 of mesophilic cyanobacterium (Dinamarca et al. 2011). More often the different thermal stability of PSII is attributed to lipid composition and/or the fatty acid composition of thylakoid membrane. Under conditions of heat stress changes in the ratio between the two major lipids, monogalactosyldiacylglycerol (MGDG) and digalactosyldiacylglycerol (DGDG) occur (Kalisch et al. 2016; Williams 1994), the chain length and the number of double bonds in FAs is affected (Harwood 1998). It is generally accepted that the thylakoid membrane lipids in higher plants respond to prolonged high temperature exposure with increased degree of fatty acid saturation (Gombos et al. 1994; Makarenko et al. 2014). On the contrary, studies on cyanobacterium Synechocystis suggest that thermal stability of PPCs does not depend on the lipid composition of the membranes (Laczko-Dobos and Szalontai 2009) or that lipid saturation *per se* is not a regulator of thermal stability (Nanjo et al. 2010). DGDG-deficient *Arabidopsis* mutant revealed lowered thermal stability of macrodomain organization of PPC in thylakoid membranes compared to wild type, and thus proved direct role of DGDG in the stabilization of thylakoid membranes at elevated temperatures (Krumova et al. 2010). Similarly, importance of DGDG in the enhanced thermal stability of LHCII trimers incorporated into liposomes was confirmed (Zhang et al. 2008). Heat shock proteins produced as a result of stress are important for protecting cells against high temperature and other stresses, as well as conferred heat tolerance to the photosynthetic electron transport chain in isolated chloroplasts (Allakhverdiev et al. 2008; Mathur et al. 2014).

1.5. Spectroscopy techniques for macro-organization of pigment-protein complexes in the thylakoid membrane

Low temperature steady-state Chl *a* fluorescence is one of the non-invasive tools to study the structural organization of thylakoids. This simple spectroscopic method is highly sensitive to the energy transfer between PPCs and to the aggregation of LHCII as well (Horton et al. 1996). The 77 K steady-state emission spectrum of higher plant thylakoid membranes is characterized by three clearly recognizable bands, two of which, at wavelengths of 685 and 695 nm, are attributed to PSII, and third band at 735 nm to PSI (Van Grondelle et al. 1994). More detailed fluorescence studies have shown that the fluorescence bands at 685 nm (F685) and 695 nm (F695) correspond to two different PPCs of PSII, the core antenna complexes CP43 and CP47, respectively (Dekker et al. 1995). The shoulder at 680 nm (F680) was ascribed to the LHCII and presence of LHCII aggregates leads to the appearance of the major emission band at 700 nm (F700) (Ruban et al. 1997). Fluorescence emission of PSI consists of at least two bands, emitting mainly at 720 nm (F720) and at 735 nm (F735) attributed to PS I core and LHCI, respectively (Van Grondelle et al. 1994).

The presence of the strong pigment–pigment interactions in photosynthetic membranes and isolated PPCs enables use of non-invasive techniques of polarization spectroscopy, such as linear dichroism and circular dichroism (CD). CD spectroscopy is a non-invasive method suitable for investigation of pigment-pigment interaction even in as complex systems as intact cells *in vivo*. CD is the absorption difference of the left and right circularly polarized light at a given wavelength. CD signals originate from the chirality of the molecules or from asymmetric interactions of the molecules. In photosynthetic apparatus containing highly organized system of Chls, CD signals originate from molecular systems of different complexity (Garab and van Amerongen 2009).

Chiral molecules exhibit optical activity, called intrinsic CD. Chls as a planar ring-structured molecules have electric and magnetic dipole moments nearly perpendicular to each other, which

results in weak CD signals. The band shapes of the intrinsic CD are identical with those of the absorption bands, their sign can be either positive or negative determining the handedness of the molecule. On grounds of symmetry of the pigment molecules the intrinsic CD signals in photosynthetic systems are weak, i.e. some 10^{-5} intensities per absorbance unit.

In the case of excitonic interaction of two or more pigment molecules a conservative band structure can be observed. That means that positive and negative CD bands can be observed, the areas of which gives zero in the energy spectrum (Devoe 1965). This is called exciton-coupled CD signal or excitonic CD. In photosynthetic systems the excitonic CD signal is typically by an order of magnitude higher than the intrinsic CD signal of the same pigment molecules. Excitonic CD is observed in PPCs or small Chl aggregates containing pigments localized close to each other, which allows participating in short-range dipole-dipole interactions. Excitonic CD is often used for fingerprinting of isolated PPCs, because it provides information on pigment-pigment interactions in these complexes (Garab and van Amerongen 2009).

In aggregates with sizes comparable with the wavelength of the visible light (hundreds of nanometres) and with high chromophore density, new anomalous CD bands with non-conservative band structure may be observed. That means that the intensity of the negative or positive component of a band-pair can vary independently from each other in the case of this type of CD. These signals are called Ψ (psi - polymer or salt-induced) type bands. Ψ-type CD can also be observed in non-absorbing regions, which originate from circular differential scattering and thus can provide useful information about the size of the aggregate (Garab et al. 1988). Measured CD signal is then composed of differential absorption (A_L-A_R) and differential light scattering (S_L-S_R) of the sample [CD = (A_L - A_R) + (S_L - S_R)]. The intensity of the Ψ-type bands depends on the extent of the long-range chiral order, the domain size and the direction of the chiral order (handedness) (Keller and Bustamante 1986). Photosynthetic pigments are able to form large chiral aggregates, so called chiral macrodomains, exhibiting intense Ψ-type CD signals due to long-range chiral organization or macroorganization of pigments bound within PPCs, possibly extending the pigment interactions in the thylakoid membrane system (Garab 2014; Garab 2016; Garab and van Amerongen 2009).

The CD signals of thylakoid membranes of green plants are dominated by intense bands with anomalous shape at around (−)674 nm, and (+)690 and (+)506 nm and are accompanied by long tails outside the main absorbance bands. Detailed analyses on detached leaves and isolated thylakoid membranes of wild-type and mutant plants provide more specific information on the origin of the major Ψ-type CD bands, which are summarized in the following findings (Garab 2014; Garab 2016; Garab and van Amerongen 2009; Toth et al. 2016):

- The chiral macrodomains disassemble upon mild detergent treatments and chaotropic effects. Nevertheless, detergent and chaotropic effects on the CD signal can be prevented by pre-treatment of the thylakoid membrane with glutaraldehyde that cross-links the proteins. These confirm that long-range ordered protein domains organized using weak protein–protein interactions result in the intense Ψ-type CD bands of thylakoid membranes.
- It is evident that multilamellar organization of grana is conducive to the generation of Ψ-type CD. However, the well-developed grana do not automatically generate Ψ-type CD bands. The various *Arabidopsis* mutants with altered antenna composition exhibit drastically different CD spectra while they retain the same wild type like granum structure. Thus role of the granum ultrastructure in generating Ψ-type CD signals could be in the induction or stabilization of the macro-domain organization of PPCs in the thylakoid membrane and the fast unstacking of the grana triggers a gradual disassembly of protein macro-domains. However, the occurrence of the positive Ψ-type CD bands requires only a few stacked layers.
- The impact of the PPCs composition on their long-range order in the membrane plane has been demonstrated using various *Arabidopsis* mutants with altered antenna composition. Examined mutants containing distinct PSII supercomplex structures, which have been

described earlier, reveal characteristic CD fingerprints. This suggests that the main positive Ψ-type bands (+)690 depend on LHCII contents of the thylakoid membranes. Further, the (+)506 nm band appears only in the presence of PSII–LHCII supercomplexes and does not depend on the xanthophyll composition of the membranes.

- The CD signatures of different wild-type leaves of dicotyledonous and monocotyledonous angiosperms are quite robust, characterized by very similar excitonic and Ψ-type CD bands. This suggests similar protein composition and macro-organization of PSII-LHCII supercomplexes in the granal thylakoid membranes.
- The chiral macrodomains of the photosynthetic membranes undergo gross (up to 80-90%) light induced reversible structural changes, which can be detected in the major Ψ-type CD bands. These light-induced changes are largely independent on the photochemical activity of the thylakoid membranes, although they are sensitive to the inhibitors of qE component of NPQ. In addition, the amplitude of light-induced CD changes exhibit linear correlation with the light intensity, even above the intensities that saturate the linear electron transport.
- Chiral macrodomains in isolated thylakoid membranes are also susceptible to elevated temperatures. This can be concluded from the decrease of the Ψ-type CD signals between 40 and 50 °C, while the excitonic CD signals persist even at 65-70 °C. These data reveal that the thermal stability of the chiral macrodomains is considerably lower than that of the PPCs. Thylakoid membranes preilluminated with strong actinic light exhibit even higher sensitivity to increased temperatures. In contrast, the excitonic interactions are essentially not affected by preillumination, suggesting that the majority of PPCs undergo no detectable light induced changes.

2. AIMS

During my PhD work, the following aims and goals were addressed:

I. To introduce CD spectroscopy at the Laboratory of spectral-optical methods at University of Ostrava in order to obtain technique that can provide information on the organization of PPCs in the thylakoid membranes, complementary to that obtained by low temperature Chl *a* fluorescence spectroscopy.

II. To demonstrate using spectroscopic techniques that isolation procedures of thylakoid membranes applied to *Arabidopsis*, barley leaves and especially spruce reflect the state of PPCs in intact leaves/needles.

III. To examine structural and functional stability of the PPCs in spruce thylakoid membranes by measuring their thermal stabilities and compare to model plants such as *Arabidopsis* or barley.

IV. To examine acclimation responses of pigment composition and PPCs organization in of thylakoid membranes to LL and HL, particularly in comparison with acclimation responses of model plants such as *Arabidopsis* and barley.

3. MATERIALS AND METHODS

In this section only the methods, results of which are directly shown in section 4 “Results and discussion”, are described. Details on other methods can be found in attached manuscripts.

3.1. Sample preparation

Arabidopsis (*Arabidopsis thaliana* L. cv. Columbia), spring barley (*Hordeum vulgare* L. cv. Bonus) and Norway spruce (*Picea abies* [L.] Karst.) were grown from seeds under controlled environmental conditions inside a HB 1014 growth chamber (Vötsch Industrietechnik, Balingen-Frommern, Germany) at photosynthetic photon flux density of 50 μmol photons m^{-2} s^{-1}, 20 °C, 65 % relative humidity and light/dark regime of 8/16 for *Arabidopsis* and 16/8 for barley and spruce. The

middle segments of dark adapted primary leaves/needles of 11–13 week-old *Arabidopsis*, 1-week-old barley or 3–4 week-old spruce seedlings were used for measurements on the intact leaves/ needles and isolation of thylakoid membranes. For purposes of the study of acclimation response in barley photosynthesis apparatus to different light intensities, barley seedlings were from seeds in growth chamber at 50, 300 and 1000 μmol photons m^{-2} s^{-1}, respectively termed LL, ML, and HL. Other growing conditions were the same as in the previous experiment with barley. For purposes of the study of acclimation response in spruce photosynthesis apparatus to different light intensities, spruce seedlings were grown from seeds in growth chamber at 100 mmol photons m^{-2} s^{-1} for 17 days. Other growing conditions were the same as in the previous experiment with spruce. Afterwards parts of seedlings were acclimated to low (LL, 20 mmol photons m^{-2} s^{-1}) and high (HL, 800 mmol photons m^{-2} s^{-1}) lights for 10 days, whereas control plants continued to grow under original (normal, control, moderate) light ML. Other growing conditions were the same as in the previous experiment with spruce.

For the purposes of experiments concerning photosynthetic pigment composition changes and functional state of the thylakoid membranes from barley during the individual steps of preparation and acclimation response in barley photosynthesis apparatus to different light intensities the modified method described by Ilík et al. (2002) was used (Karlický et al. 2010). For the purposes of experiments concerning the comparison of plant species studied, their thermal stability and acclimation response in spruce photosynthesis apparatus to different light intensities method for thylakoid membrane preparation according to Nosek (2012) was used (Karlický et al. 2016).

Separation of PPCs by clear native-polyacrylamide gel electrophoresis (CN-PAGE) was carried out using 4 % (w/v) focusing and 4.5–11.5 % (w/v) linear gradient polyacrylamide gel (acrylamide:bis acrylamide; 30% T and 2.67% C) enabling well distinguished separation of large PPCs such as PSI and PSII-LHCII supercomplexes (Järvi et al. 2011). BisTris system of cathode and anode buffers (pH = 7.0) were used with addition of β-DM (0.02 % w/v) and anionic detergent sodium deoxycholate (0.05 % w/v) to cathode buffer. Electrophoresis was performed at 4 °C in dark at gradual increase of voltage from 75 to 200 V (Järvi et al. 2011) with total running time about 3.5 h. Images of gels containing separated PPCs were captured by ChemiDoc MP gel imager (Bio-Rad Laboratories, Hercules, CA, USA) in transmitting white light or Chl *a* fluorescence excited by blue light with CCD detection. Relative amounts of individual PPCs in heat-treated membranes in comparison with membranes at 20 °C were evaluated from one-dimensional densitograms calculated from the green gel images using the Matlab software procedure according to Ilík et al. (2002).

3.2. Measurements

Chl *a* fluorescence spectra at 77 K were measured using an LS50B luminescence spectrofluorometer (Perkin-Elmer, Beaconsfield, United Kingdom) equipped with a custom-made Dewar-type optical cryostat. The Chl content was set to 5 μg/ml to avoid reabsorption (OD_{680} < 0.05 with optical pathlength of 0.1 cm). In experiment concerning the thylakoid membranes from barley during the individual steps of its preparation thylakoid membranes with 1,000 μg/ml Chl content diluted in membrane filter with defined pore size were used for measurement. Parameters for measurement of emission spectra and excitation spectra are described in Karlický et al (2016).

CD spectra were recorded in the range of 400–750 nm with a J-815 spectropolarimeter (Jasco, Tokyo, Japan). The spectra were recorded in steps of 0.5 nm with an integration time of 1 s, a band-pass of 2 nm and scanning speed of 100 nm min^{-1}. For measuring of spectra on intact leaf samples detached leaves were placed in between the two detachable glass windows of an optical cell of 0.2 mm path length, and were measured at the distance of the sample from the photomultiplier of 5 cm. Stacked thylakoid membranes were prepared by resuspension of isolated membranes at a Chl content of 20 μg ml^{-1} in medium containing 50 mM Tricine (pH = 7.5), 0.4 M sorbitol, 5 mM KCl and 5 mM $MgCl_2$. In order to obtain unstacked thylakoids displaying no Ψ-type CD bands, the thylakoid membranes at the same Chl concentration were washed in 50 mM Tricine buffer supplemented with

5 mM MEDTA (pH 7.5) and were sonicated (GM 3100; Bandelin Electronic, Berlin, Germany) on ice for 300 s using 0.5 s duty cycle and output value of 25%. CD spectra of thylakoid membranes were recorded in the cell with optical pathlength of 1 cm. The measurements of temperature-dependent changes of CD signal are described in Karlický et al. (2016).

PSII function in heat-treated leaf/needles was monitored using potential yield of PSII photochemistry (F_V/F_M) measured by pulse amplitude-modulated fluorometer PAM 101–103 (Walz, Effeltrich, Germany)(Karlický et al. 2016).

The ratios of Chl *a* to Chl *b* (Chl *a*/*b*) and of total Cars to Chls (Cars/Chls) were estimated spectrophotometrically (UV/VIS 550, Unicam, Leeds, England) from the pigment extracts according to Lichtenthaler (1987). In the case of suspensions, the pigments were extracted in 80% acetone. Because the single extraction of pigments (mainly β-carotene) from leaves in aqueous acetone solvent is incomplete (Dunn et al. 2004; Thayer and Björkman 1992), we used triple acetone extraction (80:100:100%) of pigments from leaves.

The contents of the individual Cars (lutein, neoxanthin, β-carotene, and the pool of xanthophyll cycle pigments, *i.e.* violaxanthin + antheraxanthin + zeaxanthin) expressed on a Chls basis were estimated by the gradient reversed-phase high-performance liquid chromatography (*TSP Analytical*, USA) according to Färber and Jahns (1998) with a minor modification (Kurasová et al. 2003) that are described in details in previous study (Štroch et al. 2008a).

4. RESULTS AND DISCUSSION

4.1. Structure-functional state of thylakoid membranes

Isolation of chloroplasts, thylakoid membranes from plant tissues and following separation of individual PPCs by native gel electrophoresis or ultracentrifugation is necessary for most of biochemical and some spectroscopic studies of photosynthetic apparatus concerning adaptation or acclimation mechanisms to changing environmental conditions. The interpretation of findings obtained from native gel electrophoresis is based on the assumption that they reflect the state of PPCs in intact leaves. In this section, I summarize used isolation procedures of thylakoid membranes applied to *Arabidopsis*, barley and spruce leaves/needles by primarily spectroscopic monitoring of the structure-functional state of PPCs that indicate the above mentioned assumption.

4.1.1. Isolation of thylakoid membrane for native electrophoresis

In the first study, we examined changes in photosynthetic pigment composition and functional state of the thylakoid membranes from barley leaves grown under low irradiance during the individual steps of preparation of samples that are intended for a separation of PPCs by non-denaturing polyacrylamide gel electrophoresis. Functional state of the thylakoid membranes preparations was evaluated by a determination of F_V/F_M, by an analysis of excitation and emission spectra of Chl *a* fluorescence at 77 K and CD spectra. All measurements were done at three phases of preparation of the samples: (1) in the suspensions of osmotically-shocked broken chloroplasts (RES1), (2) thylakoid membranes in extraction buffer containing Tris, glycine and glycerol (RES2) and (3) thylakoid membranes solubilized with a detergent decyl-β-D-maltosid (Dm).

Pigment composition was not pronouncedly changed during all steps of preparation of the thylakoid membrane. In comparison with the intact leaves and thylakoid membranes resuspended in RES1 medium, F_V/F_M of the membranes resuspended in RES2 ones was reduced to 0.723±0.018 (from 0.826±0.002 and 0.815±0.004, respectively) and to values close to zero in solubilized membranes. In 77-K Chl fluorescence emission spectra, thylakoid membranes solubilization resulted in a pronounced emission band with the maximum around 680 nm corresponding to emission of LHCII trimers detached from PSII core after Dm treatment (Fig. 1A). In comparison with intact leaves, the broad Chl *b* and Cars excitation band in the spectral region of 460-510 nm within PSII was slightly reduced in

RES1, RES2 and more pronouncedly in Dm samples, which are comparable to those LHCII trimers (Fig. 1B). In addition, disassembly of PSI and PSII supercomplexes after solubilization of the thylakoid membranes is accompanied by loss of chiral macrodomains in the thylakoid membrane as indicated disappearance of Ψ-type CD signal in CD spectra (Fig. 2). It is valuable to note that chiral macrodomains were not affected by the isolation of thylakoid membranes (Fig. 2). These results indicate that thylakoid membranes from barley leaves affected the pigment composition, macrodomain organization of PPCs in the thylakoid membranes and the functional state of the PSII complexes only slightly. Despite a functional disconnection of LHCII from PSII antenna core in Dm-solubilized thylakoid membranes, energy transfer from Chl *b* and Cars to emission forms of Chl *a* within LHCII trimers remained effective.

Similarly, isolation of photochemically active thylakoid membranes (or "broken chloroplasts") from one year old needles of Norway spruce was tested. Unfortunately, there were not conventional methods suitable for the isolation of highly active thylakoids for conifers, mainly for the following reasons. Firstly, highly fibrous character of needles complicates the isolation process due to difficulties of cells disruption without damaging the chloroplasts. And secondly, the high content of specific compounds (phenols, resin, tannin, etc.) that are released from the vacuole or other cell compartments of broken cells can cause either inhibition or degradation of some components of the photosynthetic electron-transport chain. Since previous isolation procedure used for barley (Attachment III; Karlický et al. 2010) did not provide highly active thylakoid membranes, we tested method specifically designed for conifers revealed moderately lower F_V/F_M than intact needles (about 0-12 %) and only slightly reduced Chl *b* and Cars bands in blue region of 77K Chl *a* fluorescence excitation spectra. Although the prepared thylakoid membranes seemed appropriate for the following experiments, this procedure reveals low yield of thylakoid suspension or poor solubilization under mild detergent condition, which complicates the separation of PPCs by native electrophoresis. For this reason we performed thylakoid membrane isolation from young spruce seedlings that proved to be convenient material for highly efficient preparation of photochemically active thylakoid membranes, sufficient yield of thylakoid suspension, and reasonable solubilization of PPCs under mild detergent condition. In addition, utilization of young spruce seedlings allows the use of conventional methods from herbaceous plants as described above (Attachment III; Karlický et al. 2010) or similar (Nosek 2012), which was used in the following experiments.

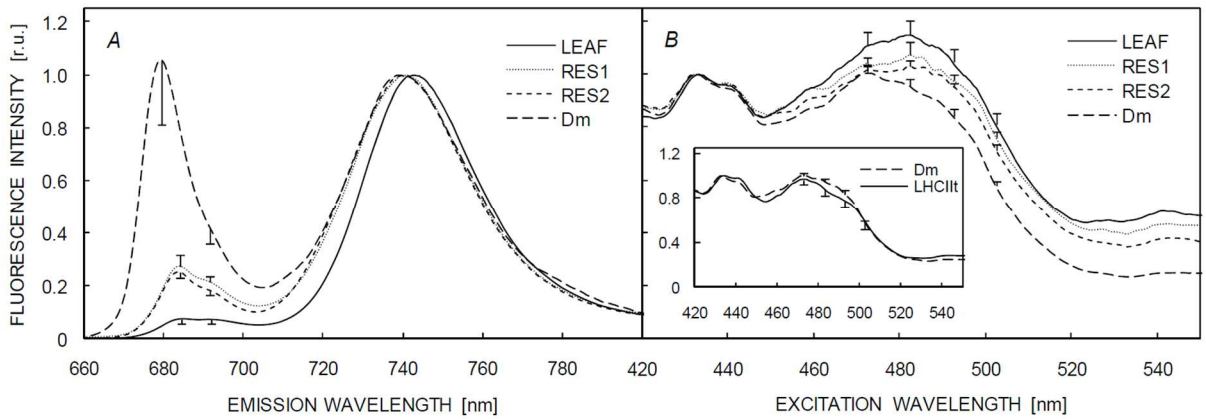

Fig. 1: *Chlorophyll a fluorescence emission (A) and excitation (B) spectra at 77 K of barley leaves and isolated thylakoid membranes suspended in RES1, RES2 and Dm media during the individual steps of the isolation procedure. The inset shows excitation spectra of Dm membranes and band containing LHCII trimers (LHCIIt) obtained by nondenaturing gel electrophoresis. The emission spectra were recorded at the excitation wavelength of 436 nm and normalized at the long wavelength maximum. The excitation spectra were measured at the emission wavelengths of 685 nm for leaves and the membranes and 681 nm for LHCIIt bands. The excitation spectra were normalized at the excitation maximum of chlorophyll a in the Soret region. The mean spectra from 6–12 samples are presented. Error bars indicate SD.*

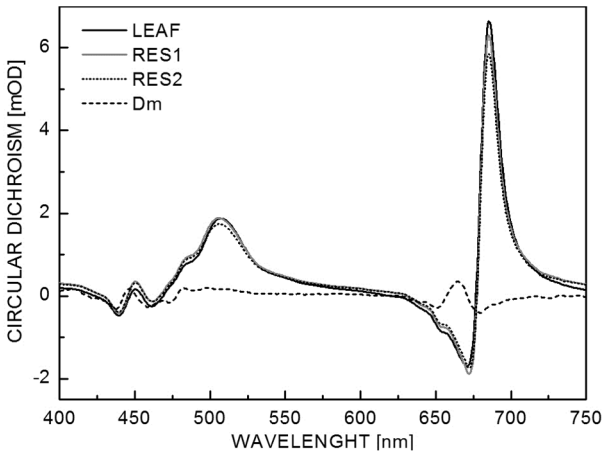

Fig. 2: *CD spectra of isolated thylakoid membranes of barley leaves and isolated thylakoid membranes suspended in RES1, RES2 and Dm media during the individual steps of the isolation procedure. The CD spectra were normalized to the absorbance at 678 nm. The spectra represent the means and SD of 3 samples.*

4.1.2. Spectral characteristics of pigment-protein complexes *in vivo* and *in vitro* – the similarities and particularities among plant species

Low temperature fluorescence emission spectra and CD spectra of intact leaves/needles, thylakoid membranes and isolated PPCs reveal spectral characteristics of PPCs both, *in vivo* and *in vitro*, which are specific for different plant species. Some of these spectral properties are summarized in this section.

Fluorescence emission spectrum of intact spruce needles at 77 K was reported long before (Špunda et al. 1994). In this spectrum, PSII emission from spruce dominates about 692 nm in contrast to *Arabidopsis* and barley having roughly the same intensity of both, emission at 685 nm and 692 nm (Fig. 3A). However, this was originally explained by strongly suppressed fluorescence band around 685 nm in the case of spruce needles due to the fluorescence reabsorption effect (Špunda et al. 1994), which was consistent with the general concept assuming the similar structure of PSII for higher plants.

Using highly efficient preparation of photochemically active thylakoid membranes and separation of PPCs by CN-PAGE we showed that main signatures of fluorescence emission spectra on intact leaves/needles remains at the level of isolated thylakoids (removal of reabsorption) and PSII-LHCII and PSI-LHCI supercomplexes (Fig. 3), despite that reabsorption has significant contribution to the shape of the emission spectrum *in vivo*. Indeed, 77K fluorescence emission spectra of isolated PSII-LHCII supercomplexes from spruce peaked at around 692 nm compared to those of *Arabidopsis* and barley, which revealed maximum at wavelength of 685 nm (Fig. 3D). Secondly, variability of position of LHCI emission maxima observed in intact leaves (Fig. 3A; *Arabidopsis*: 732 nm, barley: 743 nm, spruce: 738 nm) is also manifested on isolated PSI-LHCI supercomplexes (Fig. 3E). Other PPCs including parts of PSII supecomplexes like core complex of PSII or LHCII monomers and trimers showed almost the same spectra in all studied species (e.g. LHCII trimers, (Attachment I; Karlický et al. 2016)). The CD spectra of thylakoid membranes isolated from *Arabidopsis*, barley and spruce revealed similar character as described previously (Krumova et al. 2010; Varkonyi et al. 2009). Nevertheless, amplitude of the main Ψ-type CD band of *Arabidopsis* and barley membranes was much higher in comparison with spruce ones (Fig. 4A), which indicates much smaller size of the chiral macrodomains (Garab et al. 1991; Garab and Mustardy 1999) or a different organization of PSII superomplexes (Kovacs et al. 2006) in thylakoid membranes of spruce than in those of *Arabidopsis* and barley. In contrast to stacked thylakoid membranes spruce thylakoids did not exhibit significant changes compared to *Arabidopsis* and barley in the CD originating from short-range interactions in unstacked thylakoid membranes, which indicated similar composition of PPCs in the thylakoid membranes (Fig. 4B).

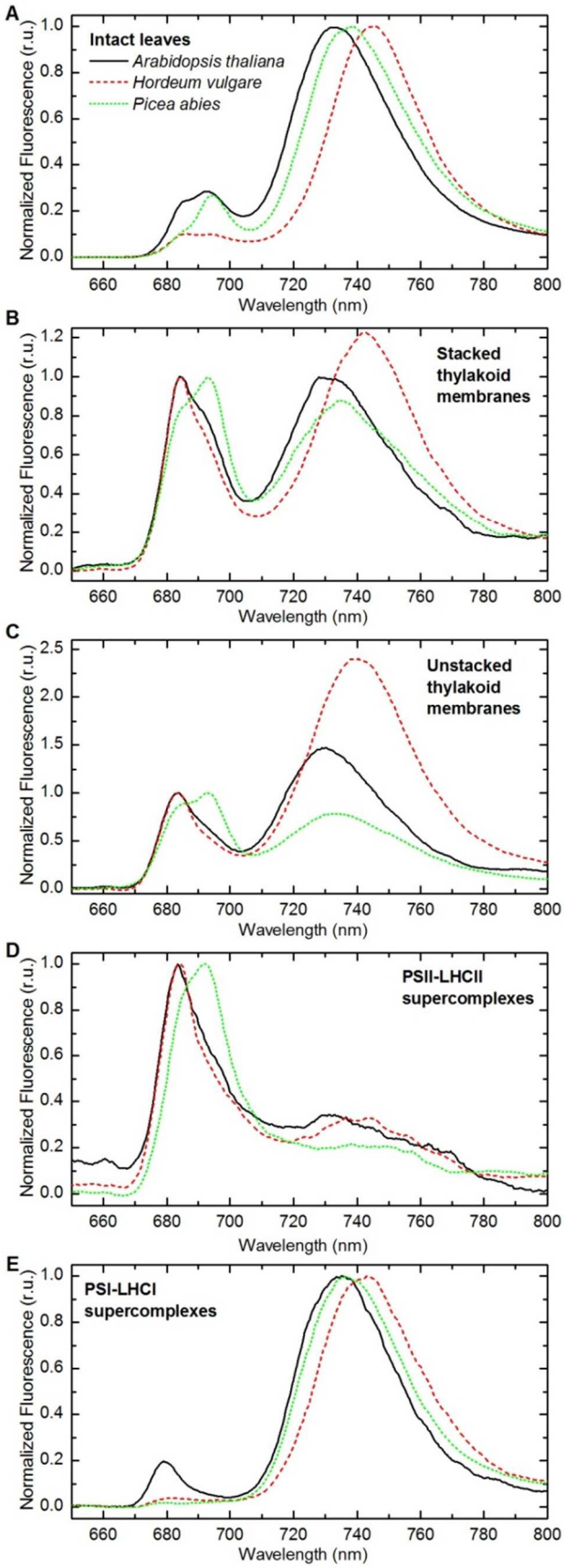

Red shift of 77K Chl *a* fluorescence emission maximum of PSII supercomplexes from spruce, smaller macrodomain organization in spruce membranes and absence of electrophoretic band containing LHCII-CP29-CP24 complexes in spruce thylakoid membranes (Fig. 8) strongly indicate different structural organization of LHCII in spruce PSII supecomplexes as compared to those from *Arabidopsis* and barley. Indeed, the loss of both Lhcb6 (CP24) and Lhcb3 proteins in some gymnosperm genera such as Picea was described very recently (Kouřil et al. 2016). Absence of these proteins in spruce led to modified structural organization of LHCII in PSII superomplexes similar to that observed in PSII supercomplexes of *Chlamydomonas reinhardtii* (Kouřil et al. 2016). It is useful to note that CD spectra of spruce thylakoid membrane revealed similarities with those of *C. reinhardtii* as regards the spectrum shape and magnitude of Ψ-type CD bands (Toth et al. 2016).

Fig. 3: *Normalized 77 K fluorescence emission spectra of intact barley leaves/needles (A), stacked (B) and unstacked (C) thylakoid membranes (total chlorophylls concentration of 4 μg ml^{-1} for), PSII supercomplexes (D), and PSI supercomplexes (E) isolated from Arabidopsis (black line), barley (red line) and spruce (green line) grown under low light conditions (50 μmol m^{-2} s^{-1}). Samples were excited at wavelength of 436 nm (preferential excitation of chlorophyll a). Typical spectra from the three independent experiments are displayed.*

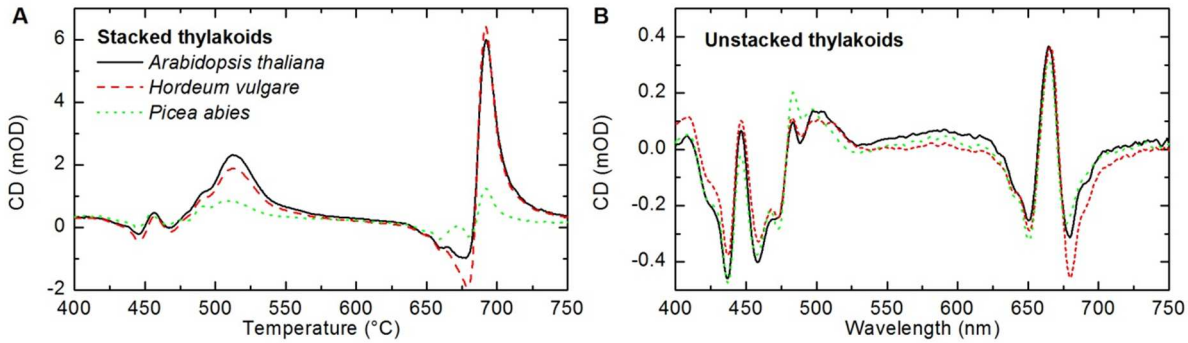

Fig. 4: *CD spectra of stacked (A) and unstacked (B) thylakoid membranes from Arabidopsis (solid black line), barley (dashed red line) and spruce (dotted green line). The CD spectra were normalized to the absorbance at 678 nm. The spectra represent the typical spectra from 4-5 independent experiments.*

4.2. Thermal stability of the thylakoid membranes from different species of higher plants

PPCs of photosynthetic apparatus in thylakoid membranes have dual requirement of structural stability: 1) to preserve the integrity of the membranes and the entire organelle, 2) to provide necessary flexibility to ensure the adaptability of the system that is evidently required in various steps of the multilevel regulatory system. The main objective of this work is to examine the structural and functional stability of the PPCs in spruce thylakoid membranes by measuring their thermal stabilities and compare to model plants such as *Arabidopsis* or barley. We have found that thermal stability of PSII photochemistry in spruce needles is higher than in other plants cultivated under the same temperatures. In addition, we studied whether higher thermal stability of PSII photochemistry found in spruce needles is accompanied with specific features of thylakoid membranes composition that can be related to the enhanced structural stability of PPCs in the thylakoid membranes.

4.2.1. Higher thermal stability of PSII photochemistry of spruce is accompanied by the maintenance of PSII macro-organization

Thermal stability of the PSII function was monitored via the measurement of the maximum quantum yield of PSII photochemistry (the parameter F_V/F_M) on intact leaves/needles exposed to linear heating. We found that F_V/F_M of *Arabidopsis* and barley leaves steeply decreased at 42 °C and almost complete PSII inactivation occurred at 46 °C. On the contrary, reduction of PSII photochemical activity was more gradual in needles of spruce seedlings at temperatures above 40 °C and still F_V/F_M values about 0.5 were observed at 46 °C (Fig. 5A).

Structural stability of PPCs in the thylakoid membranes was examined by measuring their thermal stabilities. On the plot of the temperature dependence of the main Ψ-type CD band pair differences in the thermal stability of the macrodomain organization of the PPCs between plant species studied can be seen (Fig. 5B). The T_ms of the main Ψ-type CD in spruce membranes is higher by about 6 °C in comparison with the *Arabidopsis* and barley membranes (Fig. 5B). Similarly as heat induced inactivation of PSII photochemistry, also decreases of Ψ-type CD bands with increasing temperature were less steep for spruce membranes compared to *Arabidopsis* and barley ones. T_ms of Ψ-type CD bands or band pair are summarised in Table 1. T_m values observed in spruce were significantly higher in comparison with those observed in *Arabidopsis* and barley by about 6 °C in the case of Ψ-type CD in red spectral region ($CD_{685-730}$, $CD_{685-673}$) and by about 4 °C for Ψ-type CD band in green spectral region ($CD_{505-550}$).

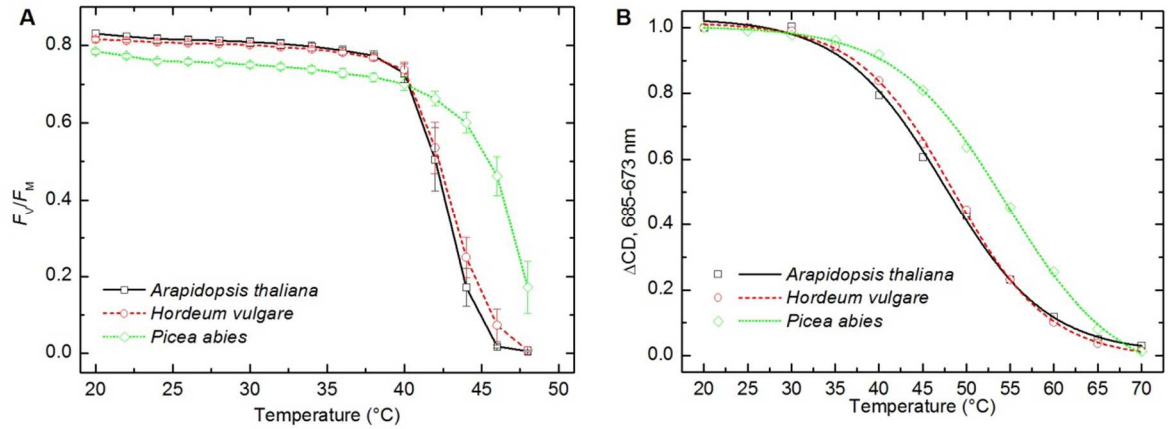

Fig. 5: *Temperature dependences of maximum efficiency of PSII photochemistry (F_V/F_M) measured on overnight dark-adapted Arabidopsis (black squares), barley leaves (red circles) and spruce needles (green diamonds)(A). Leaf or needle samples were exposed to linear heating of 1 °C min^{-1}. Mean values (points) and standard deviation (error bars) are presented (n = 5–6). Typical temperature dependences of the amplitude differences of the main Ψ-type bands at around (+)685 nm and (–)673 nm of the Arabidopsis, barley and the spruce thylakoid membranes exposed to gradual heating (B). Data points from one representative series fitted with a sigmoidal curve resulting transition temperatures (T_m) of 47.8 °C, 47.6 °C and 54.7 °C for Arabidopsis, barley and spruce, resp. Mean values and standard deviation of T_m from six independent experiments are presented in Table 1.*

Table 1 Transition temperatures (T_m) of selected CD bands or band pairs for Arabidopsis, barley and spruce stacked and unstacked thylakoid membranes

CD signal (nm)	*Assignment*	*T_m (Arabidopsis) (°C)*	*T_m (Barley) (°C)*	*T_m (Spruce) (°C)*
685–730	Ψ-type	47.9 ± 2.8^a	48.3 ± 2.2^a	54.1 ± 1.4^b
685–673	Ψ-type	47.5 ± 2.9^a	47.9 ± 1.9^a	54.3 ± 1.1^b
505–550	Ψ-type	47.8 ± 2.2^a	48.4 ± 1.2^a	52.4 ± 1.2^b
483–473	Excitonic (Chl *a*, LHCII trimers)	61.7 ± 0.4^a	61.1 ± 0.2^a	62.3 ± 0.7^a
665–650	Excitonic (Chl *b*, LHCII)	70.0 ± 0.3^a	67.4 ± 0.5^b	74.4 ± 0.5^c

The samples of thylakoid membranes were gradually heated in the range between 20 °C and 70 °C and between 20 °C and 80 °C for stacked and unstacked membranes, resp. The amplitudes for the individual bands were calculated from the difference in the intensity at specific wavelengths. T_m is defined as the temperature at which the intensity of the CD band is decreased to 50% of its value at 20 °C. T_m of Ψ-type CD bands or band pair were estimated from stacked thylakoid membranes and T_m of excitonic CD band pairs were calculated from unstacked ones. Mean values and standard deviations from five (n = 5) and four (n = 4) independent experiments are presented for stacked and unstacked membranes, resp. Data within a row followed by the same letter are not significantly different ($P > 0.05$).

In contrast to stacked thylakoid membranes, unstacked spruce membranes exhibited similar diminution of excitonic bands at elevated temperatures as *Arabidopsis* and barley ones. The excitonic CD band pair of (+)483 nm/(–)473 nm is specific for LHCII trimers and disappearance of this band pair indicates the monomerization of LHCII trimers, both in the thylakoid membranes and in the isolated LHCII (Garab et al. 2002; Yang et al. 2006). It can be clearly seen in Fig. 6A that the T_m of the LHCII trimers monomerization in the *Arabidopsis* and barley correspond well with that of spruce (Table 1). CD bands in red region at (–)650 nm, (+)665 nm and (–)680 nm are present in the CD spectra of both trimeric LHCII and monomeric LHCII (Yang et al. 2006). Therefore, temperature dependence of amplitude of (+)665 nm/(–)650 nm band pair indicates disintegration of LHCII monomers. It can be clearly seen in Fig. 6B that again the T_m of the LHCII monomers disintegration in the spruce membranes is higher by about 4 °C and 7 °C in comparison with *Arabidopsis* and barley ones, resp. (Table 1).

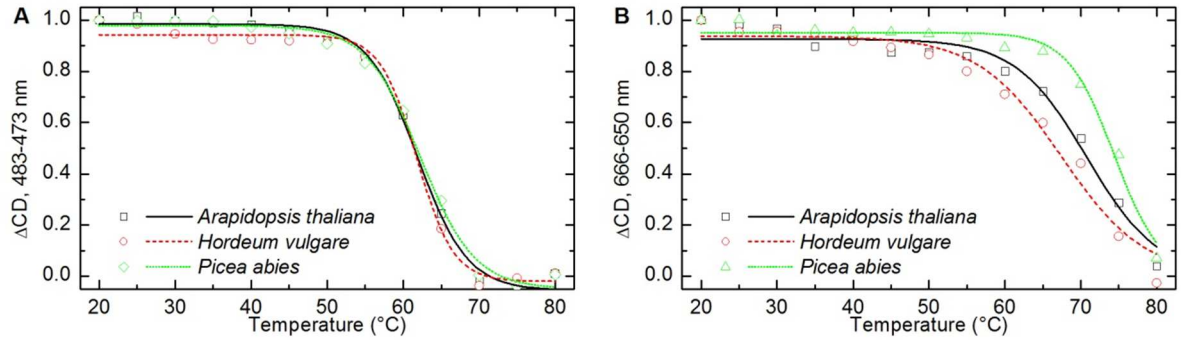

Fig. 6: *Typical temperature dependences of the amplitude differences of the excitonic bands at around (+)483 nm and (–)473 nm (D) and (+)666 nm and (–)650 nm (E) in the Arabidopsis (black), barley (red)and the spruce (green) membranes exposed to gradual heating. Data points from one representative series fitted with a sigmoidal curve resulting transition temperatures (T_m). Mean values and standard deviation of T_m from four independent experiments are presented in Table 1.*

In order to quantify the relation between thermal stability of PSII photochemistry and PPC macro-organization also Tm for F_V/F_M [$T_m(F_V/F_M)$] were expressed by fitting temperature-dependent data with sigmoidal Boltzmann function. Although T_m for the temperature dependence of Ψ-type CD signal [T_m(ΔCD685-673)] was always higher than T_m of F_V/F_M [$T_m(F_V/F_M)$], linear dependence of $T_m(F_V/F_M)$ on $T_m(T_m$(ΔCD685-673)) clearly demonstrated connection between thermal stability of the PSII photochemistry and ability to maintain PSII macro-organization in the thylakoids at elevated temperatures (Fig. 7). In addition to higher thermal stability of PSII structure and function for spruce in comparison with *Arabidopsis* and barley grown at same light and temperature these data revealed also higher thermal stability of PSII structure and function of both mature spruce needles and 3-4 weeks old seedlings in comparison with early developmental stage (2 weeks old seedlings).

It should be noted that despite of close correlation between the mentioned quantitative estimates of PSII thermal stability, T_m of Ψ-type CD was on average by 6 °C higher than T_m of F_V/F_M. Similarly, parameters derived from F_0 temperature curves occur at considerably higher temperatures than T_m of F_V/F_M and are usually tightly correlated together (Froux et al. 2004; Knight and Ackerly 2002). As a matter of fact, the decrease in F_V/F_M upon increasing temperatures is initiated due to a decrease in F_M with no increase of F_0, which indicate mainly a reversible increase of thermal dissipation in PS II (Berry and Bjorkman 1980; Epron 1997) and the increase of F_0 at higher temperatures reflects an irreversible inactivation of PSII photochemistry due to reaction centre disorganization (Berry and Bjorkman 1980). Hence, analyses of correlations between parameters derived from F_0 temperature curves and Ψ-type CD during heating could contribute to elucidation of suggested connection between thermal stability of PSII photochemistry and PPC macro-organization in thylakoid membranes.

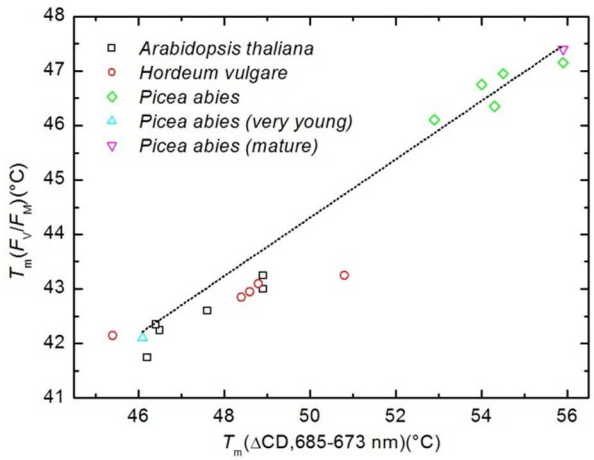

Fig. 7: *The dependence of transition temperature of PSII photochemistry (T_m (F_V/F_M)) on the transition temperature of amplitude differences of the main Ψ-type bands at around (+)685 nm and (–)673 nm (T_m (ΔCD, 685–673 nm)) estimated from sigmoidal fits of temperature dependence of F_V/F_M and ΔCD measured on samples exposed to gradual heating. Data points presenting independent cultivations of Arabidopsis (black) and barley plants (red), spruce seedlings (green), very young spruce seedlings (2-weeks old; light blue) and mature needles of 4-year spruce trees (magenta).*

4.2.2 Higher thermal stability of PSII macro-organization of spruce is associated with the maintenance of PSII supercomplexes in the thylakoid membrane

We have also attempted to explain whether the observed enhanced thermal stability of spruce membranes is connected with increased structural stability of individual PPCs at elevated temperatures. Therefore, CD spectra measurements of thylakoid membranes pre-heated 15 minutes at given temperature were performed together with directly observation of thermal stability of individual PPCs of thylakoid membranes using CN-PAGE separation (fog. 17). Among the separated PPCs, only PSII supecomplexes revealed considerably higher thermal stability in spruce thylakoids as compared to *Arabidopsis* and barley ones (Figs. 8,9A). The most heat sensitive PSII supercomplexes disappeared in the temperature range from 40 °C to 52 °C (Figs. 8,9A), thus roughly at the same temperatures as the Ψ-type CD signal (Fig. 9B). The most abundant LHCII trimers started to decrease at the temperature of 52 °C till 56 °C similarly as excitonic CD signal. Therefore, these results indicate that enhanced thermal stability of macrodomain organization of spruce is associated with the maintenance of PSII supercomplexes in the thylakoid membrane, rather than with more stable LHCII trimers.

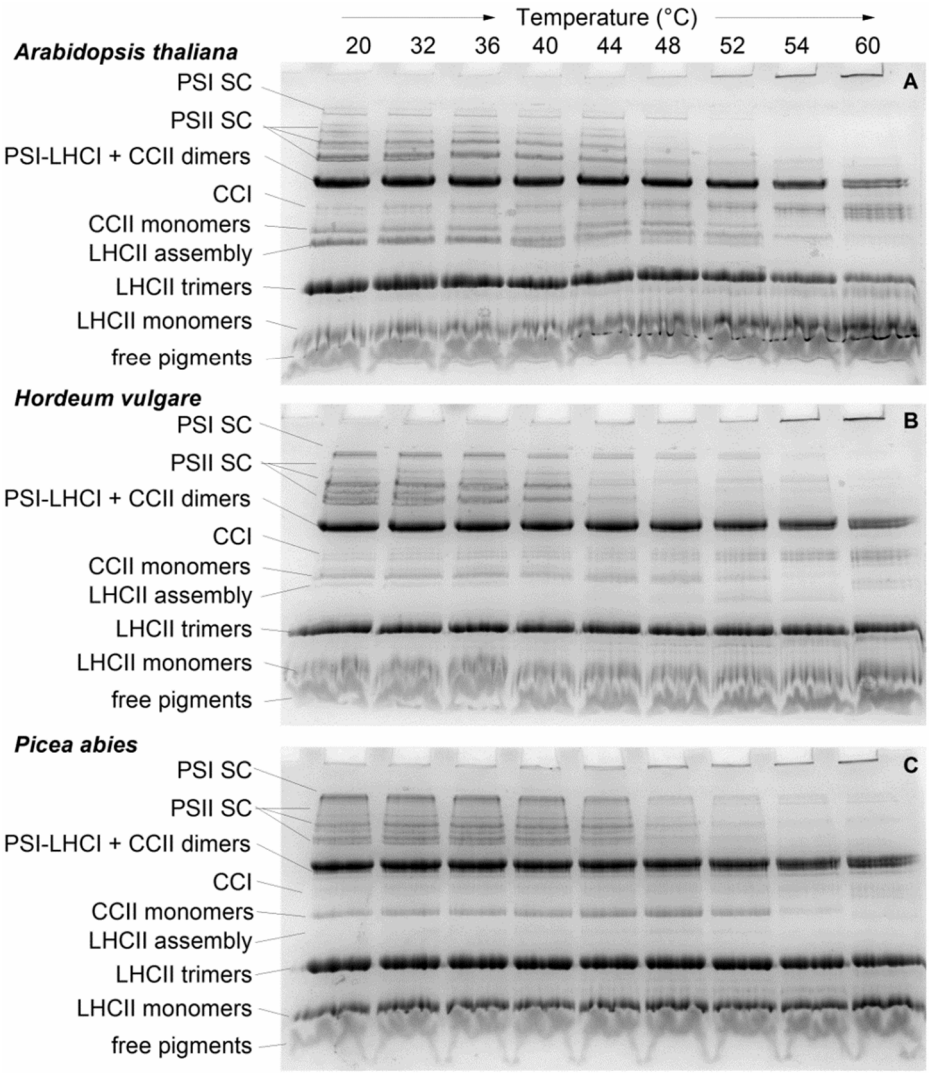

Fig. 8: *CN-PAGE separation of PPCs of thylakoid membranes from Arabidopsis (A), barley (B) and spruce (C) preheated to 20 - 60 °C for 15 minutes in the dark. Thylakoid membranes were solubilized using n-dodecyl-β-D-maltoside with detergent/chlorophyll ratio of 20:1 (Arabidopsis, barley) a 35:1 (spruce). Gel images were obtained as transmittance of white light using CCD camera ChemiDoc MP (BioRad). Typical electropherograms from the three independent experiments are displayed.*

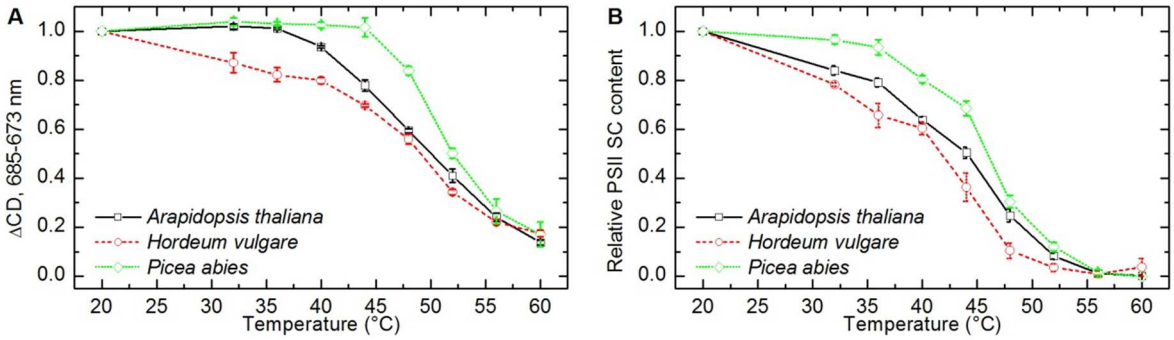

Fig. 9: *Temperature dependences of the amplitude differences of the main Ψ-type bands at around (+)685 nm and (–)673 nm of the Arabidopsis (black), barley (red) and the spruce (green) heat treated thylakoid membranes (A). Temperature dependences of the PSII supercomplexes stability determined from the green gel density profiles of same heat treated membranes (B). Temperatures experiments were carry out in the three independent experiments. Mean values (points) and standard deviations (error bars) from three independent experiments (n = 3) are displayed.*

Closer inspection of these analyses show the connection between the heat-induced decreases in the content PSII supercomplexes and macro-organization of PPCs in the thylakoid membranes that was assessed based on dependence of reduction of the amplitude differences of the main Ψ-type bands at around (+)685 nm and (–)673 nm on decrease in total content of PSII superomplexes in the heat treated thylakoid membranes (Fig. 10). This clearly non-linear dependence, with similarities for all plants species, revealed that 20% reduction of total content of PSII superomplexes in the heat treated thylakoid membranes did not cause significant change of Ψ-type CD signal. After disintegration of almost all PSII supercomplexes in thylakoid membranes by heat, Ψ-type CD signal was reduced to below 50% of the initial value. It is appropriate to note that LHCII-only domains also contribute to the Ψ-type CD signal (Garab et al. 1991; Garab and Mustardy 1999), which thermal stability cannot be determined by CN-PAGE, and could thus partially explain the observed residual Ψ-type CD signal after the disintegration of all PSII supercomplexes. Nevertheless, the fact that main part of PSII inactivation and reduction of PSII supercomplexes content occurs in a similar temperature range (40 – 46 °C) indicate that stability of PSII supercomplexes may be important for short-term resistance of photosynthetic apparatus against heat stress.

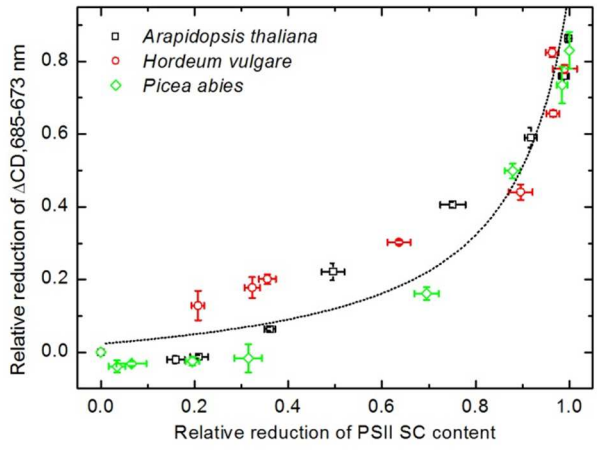

Fig. 10: *Dependence of heat induced reduction of the amplitude differences of the main Ψ-type bands at around (+)685 nm and (–)673 nm on the decrease in total content of PSII supercomplexes (SC) in the heat treated thylakoid membranes from Arabidopsis (black squares), barley (red circles) and spruce (green diamonds). Mean values (points) and standard deviations (error bars) from three independent experiments (n = 3) are displayed.*

Different composition of LHCII protein subunits and PSII-LHCII supercomplex structural organization (Kouřil et al. 2016) and thylakoid membrane lipids (Attachment I; Karlický et al. 2016) in spruce led us to propose factors that can affect the thermal stability of spruce thylakoid membranes.

- Different structure of the PSII supercomplexes from spruce resulting in smaller macrodomains, which may possess higher thermal stability itself.

- More free packing of PPCs that can be expected from higher fatty acids to Chl *a* ratio (Attachment I; Karlický et al. 2016) also could have the role in thermal stability of PSII. But as this ratio in spruce thylakoids was only by 10% higher than in *Arabidopsis* and barley we do not expect pronounced contribution of the higher lipid to protein ratio to the enhanced thermal stability of spruce PSII supercomplexes.
- Although, the relation of lipid desaturation and the thermal sensitivity of PSII is still unclear and data are contradictory (Allakhverdiev et al. 2008), increase in the degree of fatty acid saturation in lipids of spruce thylakoid membranes (Attachment I; Karlický et al. 2016) could be further factor responsible for the enhanced thermal stability of PSII.
- Moreover, considerably lower ratio of MGDG/DGDG in spruce thylakoid membranes can significantly affect membranes stability at higher temperatures (Krumova et al. 2010). Despite of lower MGDG/DGDG ratio in spruce thylakoids monomerization of LHCII trimers in *Arabidopsis*, barley and spruce occurred at the same temperature (T_m approximately 62 °C, Fig. 6A, Table 1) that is in agreement with Krumova et al. (2010). On the other hand, the thermal stability of LHCII monomers in spruce thylakoid membranes was significantly higher than in *Arabidopsis* and barley ones (Fig. 6B, Table 1).
- Possible role of interactions of LHCII and DGDG with FAs specific for gymnosperms (i.e. very long chain fatty acids, branched-17:0 fatty acid and Δ5-unsaturated fatty acids (Attachment I; Karlický et al. 2016; Moellering et al. 2009; Mongrand et al. 2001) on the thermal stability of LHCII proteins cannot be excluded.

Although we cannot distinguish between the contribution of these factors to resulting higher thermal stability of PSII function and structure in spruce thylakoid membranes, we suppose that different lipid-protein interaction together with different structure of PSII supercomplexes play a crucial role.

4.3. Long-term acclimation response of photosynthetic apparatus to different growth light intensity

Up to now it has been thought that protein composition of both photosystems is highly conserved among higher plants (Croce and van Amerongen 2011). Particularly the presence of Lhcb6 and Lhcb3 proteins has been determined as the characteristic evolutionary difference between the land plants and algae regarding the PSII protein composition, due to fact that *C. reinhardtii* is lacking both proteins (Ballottari et al. 2012). It has been proposed that absence of Lhcsr, involved in photoprotective ΔpH- and zeaxanthin-dependent energy dissipation in green algae such as *C. reinhardtii* (Koziol et al. 2007; Peers et al. 2009), and appearance of PsbS protein overtaking this function in higher plants is another evolutionary step from algae to land plants (Goss and Lepetit 2015; Niyogi and Truong 2013). Moreover, some evolutionary older land species, e.g. *Physcomitrella patens* retain both of these PSII regulatory proteins (Alboresi et al. 2010). Recently, the loss of both Lhcb6 (CP24) and Lhcb3 proteins was confirmed in some gymnosperm genera such as *Picea* (Kouřil et al. 2016), resulting in modified structural organization of LHCII trimers in PSII-LHCII supercomplexes of spruce in comparison to *Arabidopsis*, but similar to that observed in *C. reinhardtii* (Kouřil et al. 2016). Further, possible presence of the Lhcsr protein together with PsbS in some species of *Pinaceae* family was outlined (Dittami et al. 2010; Kouřil et al. 2016). In addition, in comparison with *Arabidopsis* different composition of lipids and fatty acids is known in spruce thylakoids (Attachment I; Karlický et al. 2016) or generally in gymnosperms (Mongrand et al. 2001), again more similar to that observed in evolutionarily older organisms such as mosses, ferns or algae as well (Karunen 1990; Mongrand et al. 2001). All these findings indicate that spruce could possess a different mechanism of NPQ and long-term acclimation response to different growth light intensity than other land plants. The aim of this work was to examine acclimation responses of pigment composition and PPCs organization in thylakoid membranes to LL and HL, particularly in comparison with acclimation responses of model plants such as *Arabidopsis* and barley.

Earlier, we studied acclimation responses of barley grown at 50, 300 and 1000 µmol photons m^{-2} s^{-1} using biochemical and spectroscopical analyses of leaves and individual PPCs in order to contribute to elucidation of processes associated with regulation of functional size of PSII antenna *in vivo* (details in attachment IV). Gradual reduction of PSII antenna size was revealed in barley leaves grown under LL, ML and HL light intensities by Chl *a*/*b* ratio and the 77K fluorescence excitation spectra of PSII. The excitation spectra of individual PSII-LHCII supercomplexes and LHCII trimers, separated from thylakoids isolated from LL, ML and HL plants, revealed no reduction of the Chl *b* and Car excitation bands with increasing growth light, suggesting that variations in the functional antenna size originate from changes in the macro-organization and/or composition of PPCs of thylakoid membranes. CD spectra of intact barley leaves revealed gradual decline in the long-range chiral order of PPCs with increasing growth light intensities. Analysis of the composition of LHCII proteins separated by CN-PAGE corresponded to the gradually reduced amounts of trimers forming major LHCII subunits, Lhcb1 and Lhcb2, and particularly the LHCII subunits related to PSII M-trimers, Lhcb3 and Lhcb6, with enhanced growth light intensity. Overall, the acclimation to different growth light intensity in barley were similar as described in *Arabidopsis* (Bielczynski et al. 2016; Kouřil et al. 2013), indicating the same main features of acclimation to different growth light intensity in dicotyledons (represented by *Arabidopsis*) and monocotyledons (barley), for the first time studied from this point of view. In order to identify possible peculiar HL responses in specific clades of monocotyledons or dicotyledons more detailed analysis would be needed.

In the following paragraphs I describe several interesting findings arising on the experiments with spruce seedlings. Norway spruce seedlings were grown from seeds in a growth chamber at 100 µmol photons m^{-2} s^{-1} (17 days). Afterwards parts of seedlings were acclimated to low (LL, 20 µmol photons m^{-2} s^{-1}) and high (HL, 800 µmol photons m^{-2} s^{-1}) lights for 10 days, whereas control plants continued to grow under original (normal) light (ML).

Firstly, modulability of the Chl *a*/*b* ratio and the amount of LHCII upon HL and LL acclimation is not a universal property of all land plants. This capability is lacking in bryophytes (Gerotto et al. 2011) and also in early diverging vascular plants, lycophytes (Ferroni et al. 2016). Previous study on mature spruce needles indicated that also photosynthetic apparatus of spruce could be unable to adjust light harvesting antennas during acclimation to different light intensity as determined by from Chl *a*/*b* ratios and fluorescence excitation spectra (Kurasová et al. 2003; Štroch et al. 2008a). Nevertheless, young spruce seedlings revealed increased Chl *a*/*b* ratio under HL (Table 2) indicating the ability to modulate the antenna size similarly as observed in different species of angiosperms (Bielczynski et al. 2016; Kouřil et al. 2013) (attachment IV). Likewise, decreases of Chl *b* and Cars excitation band (460-490 nm) in 77K fluorescence excitation spectra demonstrated reduced antenna size of both, PSII and PSI with increasing acclimation light intensity (Fig. 11A,B).

Secondly, the higher Cars/Chls ratio in HL spruce seedlings in comparison with LL and ML ones was particularly due to relative increase of lutein and VAZ pool (Table 2). Acclimation response of Car composition to HL in spruce differs from *Arabidopsis* (Bielczynski et al. 2016) or barley (attachment IV), which revealed more pronounced increase of VAZ pool size and only slight changes of lutein content. Again, such increased amount of lutein was observed in evolutionarily earlier plant species such as algal species *C. reinhardtii* acclimated to HL, in which concomitant accumulation of lutein and Lhcsr3 is likely responsible for enhanced capacity of excess energy dissipation in HL acclimated cells (Bonente et al. 2012). Very recently, it was demonstrated that pH-dependent and zeaxanthin-independent reductive quenching mechanism is active in Lhcsr1 from *Physcomitrella patens*, which result in formation of lutein radical cation and Chl *a* radical anion (Pinnola et al. 2016). Acclimation response of Car composition of spruce suggests possible presence of the Lhcsr protein in spruce.

Table 2 Pigment analysis of plants grown under different light conditions.

Light intensity	LL	NL	HL
Chl *a* /*b*	2,59 ± 0,04[a]	2,76 ± 0,05[b]	3,03 ± 0,10[c]
Car x + c/1000 Chl *a*	261,6 ± 4,7[a]	265,3 ± 3,2[a]	365,4 ± 15,4[b]
L/1000 Chl *a*	108,1 ± 1,1[a]	116,0 ± 7,5[a]	189,1 ± 9,0[b]
VAZ/1000 Chl *a*	25,7 ± 4,8[a]	26,2 ± 4,6[a]	44,0 ± 12,5[b]
N/1000 Chl *a*	33,2 ± 0,7[a]	35,8 ± 1,8[a]	35,9 ± 1,7[a]
α + β-Car/1000 Chl *a*	93,2 ± 1,6[a]	95,3 ± 2,9[a]	79,9 ± 5,1[b]
α Car/β-Car	1,52 ± 0,05[a]	1,31 ± 0,06[b]	0,37 ± 0,05[c]

Chlorophyll *a* /chlorophyll *b* (Chl *a* /*b*) and total carotenoids/Chl *a* (Car x + c/Chl *a*) ratios determined spectroscopically from 80% acetone needle extracts. The same extracts were used for the quantification by HPLC of the carotenoids per 1000 Chl *a*. The values represent the means SD of 6 determinations. Data within a row followed by the same letter are not significantly different (P > 0:05).L, lutein V, violaxanthin; A, antheraxanthin; Z, zeaxanthin; N, neoxanthin; α, β-Car, α, β - carotene.

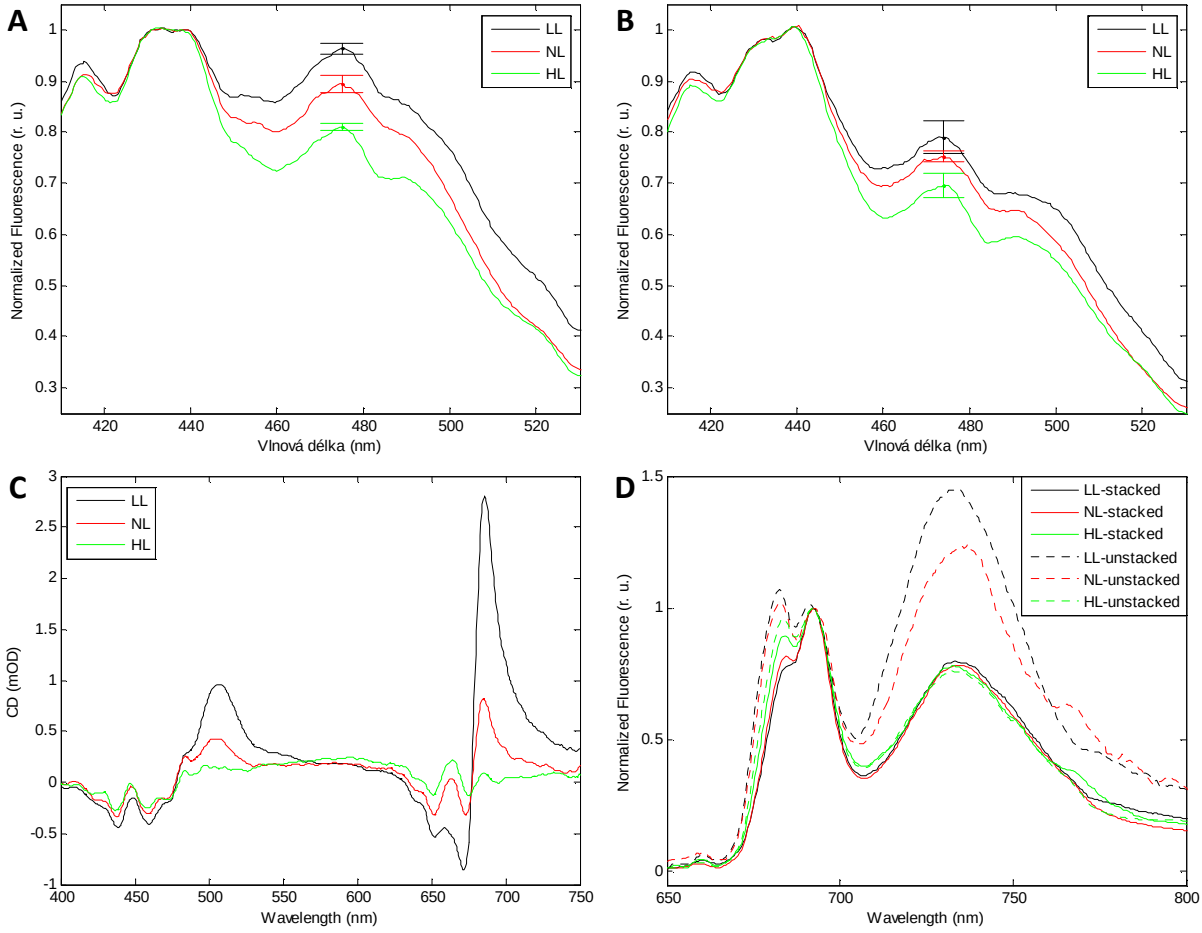

Fig. 11: *Normalized 77 K fluorescence excitation spectra of PSII (**A**) and PSI (**B**), room temperature circular dichroism spectra (**C**) and normalized 77 K fluorescence emission spectra (**D**) measured on stacked and unstacked (indicated in the legend) thylakoid membranes isolated from spruce seedlings acclimated to low (LL), normal (NL) and high (HL) intensity of light. Emission spectra were excited at wavelength of 476 nm and excitation spectra were collected at wavelength of 685 nm (PSII) and 735 nm (PSI). Average spectra and standard deviations from three independent experiments (n = 3) are presented.*

Thirdly, CD spectra of isolated thylakoid membranes demonstrated reduced macro-organisation of the PPCs in the thylakoid membranes under higher light intensities (Fig. 11C). HL spruce seedlings revealed almost none Ψ-type CD signal (Fig. 11C), that indicate disappearance of long-range ordered PSII-LHCII supercomplexes in the membrane plane in HL spruce. Similar response of reduced Ψ-type CD bands with increasing acclimation light intensities was observed in barley (attachment IV) although Ψ-type CD magnitudes were significantly greater than in spruce, under all light conditions (Fig. 12). Since Ψ-type CD signal originates from macrodomains consisting of the PSII-LHCII supercomplexes (the (+)685 and the (+)505 nm Ψ-type CD bands) and LHCII-only domain (the (+)685 and the (−)674 nm Ψ-type CD bands), main Ψ-type CD at (+)685 nm and (+)685/(+)505 Ψ-type CD ratio correlate with Chl *a*/*b* ratio, which roughly express LHCII/PSII core ratio (Toth et al. 2016) (Fig. 12). As seen in Fig. 12, this correlation is different for spruce and angiosperms species reflecting distinct structure of PSII-LHCII, building blocks of the long-range ordered domains.

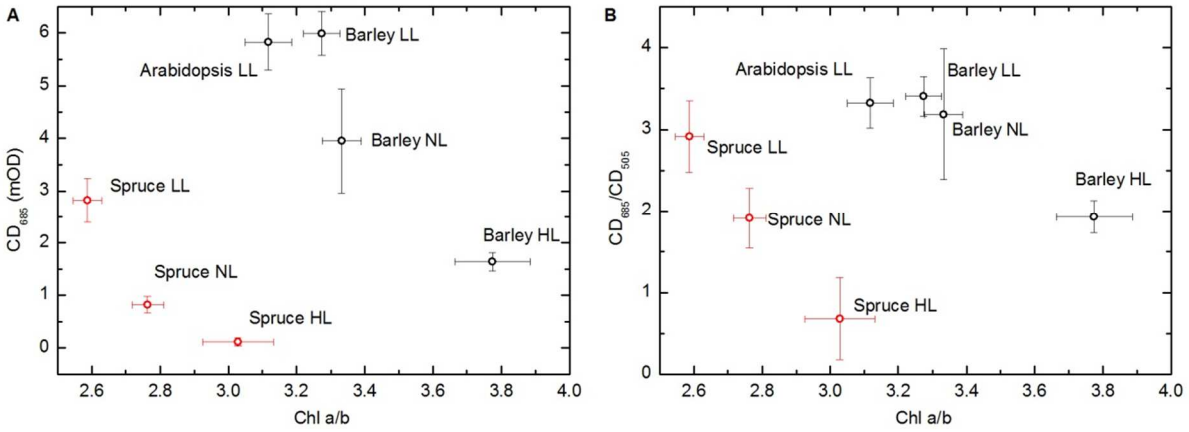

Fig. 12: *Correlation between the positive Ψ-type CD band and the Chl a/b ratios. Correlation of the amplitude of (+)685 with Chl a/b (A) and the correlation of the (+)685/(+)505 peak ratio with Chl a/b. The amplitudes of CD bands are normalized to the red maximum of the Chl a absorption band.*

Finally, in the presence of cations (NaCl and $MgCl_2$), LHCII is tightly connected with PSII in stacked grana regions (Kirchhoff et al. 2007), which resulted in high fluorescence emission from the PSII complexes (Fig. 11D). Depletion of cations in the buffer induced unstacking of the grana thylakoids accompanied by lateral disorganisation of PSII and LHCII (intermixing and randomization of the proteins, especially PSII, LHCII and PSI) and caused a spillover of excitation energy from LHCII to PSI (Kirchhoff et al. 2007) as indicated by increased fluorescence emission from the PSI complex (Fig. 11D). Almost identical 77K fluorescence emission spectra of HL spruce thylakoid membranes under stacked and unstacked conditions indicate very low segregation of PPCs in granal and lamellar thylakoids *in vivo*, under HL conditions.

5. CONCLUSIONS AND FUTURE PERSPECTIVES

I have investigated structure-functional characteristics of pigment-protein complexes, and their macro-organization and stability in thylakoid membranes in three different species of higher plants, Norway spruce belonging to the gymnosperms and model plants from angiosperms, *Arabidopsis* thaliana and spring barley. Information on the molecular organization and their structural stabilities were obtained mainly from spectroscopic techniques, including circular dichroism spectroscopy and low temperature fluorescence, as well as from biochemical analyses.

The results of my work can be summarized as follows:

I. We showed that main specific signatures of low temperature fluorescence emission spectra on intact leaves/needles remain at the level of isolated thylakoids after removal of reabsorption and PSII-LHCII and PSI-LHCI supercomplexes. Low temperature fluorescence

emission of PSII-LHCII supercomplexes from spruce peaked at around 692 nm compared to those of *Arabidopsis* and barley, which revealed maximum at wavelength of 685 nm.

II. Thylakoid membranes of spruce possess enhanced thermal stability of PSII photochemistry than in other plants (*Arabidopsis*, barley) cultivated under the same temperatures. Our data show that higher thermal stability of PSII photochemistry of spruce is accompanied by the maintenance of PSII macro-organization. In addition, clear-native polyacrylamide gel electrophoresis of preheated thylakoids demonstrated that higher thermal stability of PSII macro-organization of spruce is associated with the maintenance of PSII-LHCII supercomplexes in the membrane.

III. Photosynthetic apparatus of spruce revealed different long-term acclimation response to different growth light intensity than other higher plants such as barley (attachment 4) or *Arabidopsis*. In contrast to previous study on mature spruce needles (Kurasová et al. 2003; Štroch et al. 2008a), young spruce seedlings exhibit ability to adjust light harvesting antennas during acclimation to different light intensity, similarly as observed in other higher plants (Bielczynski et al. 2016; Kouřil et al. 2013) (attachment IV). The pronounced increase in lutein content in seedlings acclimated to HL differs from acclimation response of *Arabidopsis* (Bielczynski et al. 2016) or barley (attachment IV) characterized by only slight changes of lutein content.

In the following section I would like to address a few questions, work in progress and plans for the near future, which are not discussed or only marginally treated in the dissertation but nevertheless constitute important parts of work on this field:

I. During my research stay in Biological Research Centre in Szeged I have participated in experiments focused on signatures of oriented thylakoid membranes using anisotropic CD (attachment IV; Miloslavina et al. 2012). It was found that the anisotropic CD spectra of face- and edge-aligned stacked thylakoid membranes exhibit substantial differences in their Ψ-type CD bands. Also excitonic CD of unstacked thylakoid membranes revealed appreciable differences. Nevertheless, the theoretical approach has to be further developed in order to interconnect structural data with the spectral signatures. This might help to use the full potential of anisotropic CD to improve current understanding of Ψ-type CD in further studies.

II. Based on different structural organization of LHCII in spruce PSII-LHCII supercomplexes accompanied by red shift of 77K Chl *a* fluorescence emission maximum and smaller macrodomain organization in spruce membranes as compared to *Arabidopsis* and barley we started comparative spectroscopic experiments focusing on excitonic interactions and excitation energy transfer in PSII-LHCII supercomplexes of spruce and *Arabidopsis* (work is in progress).

III. Up till now long-term acclimation of spruce photosynthetic apparatus to different growth light intensity could not be studied biochemically on the level of PPCs using native electrophoresis due to difficulties with solubilization of thylakoid membranes from HL acclimated spruce seedlings. We found that this is caused by high contents of charged lipids, and that changes in the content of lipids and fatty acids play important role in long-term acclimation of spruce photosynthetic apparatus to different growth light intensity. Again the pronounced changes in lipid composition in spruce seedlings acclimated to HL correspond rather to the response of green algae thylakoids (*C. reinhardtii*) acclimated to HL than to that typically found in model higher plants

IV. As mentioned above, there are particular responses of spruce to HL including different acclimation strategy to HI, e.g. lutein accumulation indicating enhanced involvement of Lhcsr in photoprotective processes in spruce acclimated to HL and extremely altered macro-organization of PPCs suggesting loss of typical spatial segregation of PSI and PSII in granal and or stromal membranes. Thus altered lipid and protein composition is related to several structure-functional particularities. This opens an attractive field of future research aimed at elucidation of structural and functional flexibility of thylakoid membranes related to different

short- and long-term response of photosynthetic apparatus to changing environmental conditions. We plan an implementation of advanced biophysical methods such as small-angle neutron scattering, phosphorus 31 nuclear magnetic resonance spectroscopy, time-resolved fluorescence spectroscopy or anisotropic CD spectroscopy for further research in order to obtain additional information on the architecture of spruce thylakoid membranes and organization of PPCs, with focus on their flexibility.

6. REFERENCES

Agati G, Cerovic ZG, Pinelli P, Tattini M (2011) Environ Exp Bot 73: 3-9.
Albanese P et al. (2016) Biochim Biophys Acta 1857: 1651-1660.
Alboresi A, Gerotto C, Giacometti GM, Bassi R, Morosinotto T (2010) Proc Natl Acad Sci U S A 107: 11128-11133.
Allakhverdiev SI, Kreslavski VD, Klimov VV, Los DA, Carpentier R, Mohanty P (2008) Photosynth Res 98: 541-550.
Anderson JM, Chow WS, Park YI (1995) Photosynth Res 46: 129-139.
Austin JR, 2nd, Staehelin LA (2011) Plant Physiol 155: 1601-1611.
Bailey S, Walters RG, Jansson S, Horton P (2001) Planta 213: 794-801.
Ballottari M, Girardon J, Dall'Osto L, Bassi R (2012) Biochim Biophys Acta-Bioenerg 1817: 143-157.
Banas AK, Aggarwal C, Labuz J, Sztatelman O, Gabrys H (2012) J Exp Bot 63: 1559-1574.
Ben-Shem A, Frolow F, Nelson N (2003) Nature 426: 630-635.
Berry J, Bjorkman O (1980) Annu Rev Plant Phys 31: 491-543.
Bielczynski LW, Schansker G, Croce R (2016) Front Plant Sci 7: 105.
Boekema EJ, van Breemen JFL, van Roon H, Dekker JP (2000) J Mol Biol 301: 1123-1133.
Boekema EJ, van Roon H, van Breemen JFL, Dekker JP (1999) Eur J Biochem 266: 444-452.
Bonente G, Pippa S, Castellano S, Bassi R, Ballottari M (2012) J Biol Chem 287: 5833-5847.
Brestič M, Živčák M, Kalaji HM, Carpentier R, Allakhverdiev SI (2012) Plant Physiol Biochem 57: 93-105.
Bugos RC, Chang SH, Yamamoto HY (1999) Plant Physiol 121: 207-213.
Caffarri S, Kouřil R, Kereiche S, Boekema EJ, Croce R (2009) Embo J 28: 3052-3063.
Caffarri S, Tibiletti T, Jennings RC, Santabarbara S (2014) Curr Protein Pept Sc 15: 296-331.
Correa-Galvis V, Poschmann G, Melzer M, Stuhler K, Jahns P (2016) Nat Plants 2: 15225.
Cramer WA, Whitmarsh J, Low PS (1981) Biochemistry 20: 157-162.
Croce R (2015) Nat Struct Mol Biol 22: 650-652.
Croce R, van Amerongen H (2011) J Photochem Photobiol B-Biol 104: 142-153.
Croce R, van Amerongen H (2013) Photosynth Res 116: 153-166.
Čajánek M, Navrátil M, Kurasová I, Kalina J, Špunda V (2002) Photosynth Res 74: 121-133.
Dall'Osto L, Caffarri S, Bassi R (2005) Plant Cell 17: 1217-1232.
Dall'Osto L, Cazzaniga S, Wada M, Bassi R (2014) Philos Trans R Soc Lond B Biol Sci 369: 20130221.
de la Torre WR, Burkey KO (1990) Photosynth Res 24: 117-125.
Dekker JP, Boekema EJ (2005) Biochim Biophys Acta-Bioenerg 1706: 12-39.
Dekker JP, Hassoldt A, Pettersson A, vanRoon H, Groot ML, vanGrondelle R (1995) Photosynthesis: From Light to Biosphere, Vol I: 53-56.
DelasRivas J, Barber J (1997) Biochemistry 36: 8897-8903.
Demmig-Adams B (1998) Plant Cell Physiol 39: 474-482.
Demmig-Adams B, Garab G, Adams III W, Govindjee (eds) (2014) Non-Photochemical Quenching and Energy Dissipation in Plants, Algae and Cyanobacteria. Advances in Photosynthesis and Respiration, vol 40. Springer Netherlands, Berlin; Heidelberg.
Devoe H (1965) J Chem Phys 43: 3199-&.
Dinamarca J et al. (2011) PLoS One 6: e28389.
Dittami SM, Michel G, Collen J, Boyen C, Tonon T (2010) BMC Evol Biol 10.
Dobrikova AG et al. (2003) Biochemistry 42: 11272-11280.
Dunn JL, Turnbull JD, Robinson SA (2004) Funct Plant Biol 31: 195-202.
Epron D (1997) J Exp Bot 48: 1835-1841.
Evans JR (1987) Aust J Plant Physiol 14: 157-170.
Farber A, Jahns P (1998) Biochim Biophys Acta-Bioenerg 1363: 47-58.
Ferroni L, Suorsa M, Aro EM, Baldisserotto C, Pancaldi S (2016) New Phytol.
Froux F, Ducrey M, Epron D, Dreyer E (2004) Annals of Forest Science 61: 235-241.
Garab G (2014) Biochim Biophys Acta-Bioenerg 1837: 481-494.
Garab G (2016) Photosynth Res 127: 131-150.

Garab G et al. (2002) Biochemistry 41: 15121-15129.
Garab G, Kieleczawa J, Sutherland JC, Bustamante C, Hind G (1991) Photochem Photobiol 54: 273-281.
Garab G, Mustardy L (1999) Aust J Plant Physiol 26: 649-658.
Garab G, Ughy B, Goss R (2016) Subcell Biochem 86: 127-157.
Garab G, van Amerongen H (2009) Photosynth Res 101: 135-146.
Garab G, Wells S, Finzi L, Bustamante C (1988) Biochemistry 27: 5839-5843.
Gerotto C, Alboresi A, Giacometti GM, Bassi R, Morosinotto T (2011) Plant Cell Environ 34: 922-932.
Ghouil H, Montpied P, Epron D, Ksontini M, Hanchi B, Dreyer E (2003) Tree Physiol 23: 1031-1039.
Goldschmidt-Clermont M, Bassi R (2015) Curr Opin Plant Biol 25: 71-78.
Gombos Z, Wada H, Hideg E, Murata N (1994) Plant Physiol 104: 563-567.
Goss R, Lepetit B (2015) J Plant Physiol 172: 13-32.
Guskov A, Kern J, Gabdulkhakov A, Broser M, Zouni A, Saenger W (2009) Nat Struct Mol Biol 16: 334-342.
Hankamer B, Morris E, Nield J, Gerle C, Barber J (2001) J Struct Biol 135: 262-269.
Harwood JL (1998). In: Siegenthaler PA, Murata, N. (ed) Lipids in Photosynthesis: Structure, Function and Genetics. Kluwer Academic Publishers, Dordrecht, The Netherlands, pp 290–300
Havaux M, Dall'Osto L, Bassi R (2007) Plant Physiol 145: 1506-1520.
Havaux M, Niyogi KK (1999) Proc Natl Acad Sci U S A 96: 8762-8767.
Horton P, Ruban AV, Walters RG (1996) Annu Rev Plant Phys 47: 655-684.
Hu ZH, Xu YN, Jiang GZ, Kuang TY (2004) Plant Sci 166: 1177-1183.
Chen HX, Li WJ, An SZ, Gao HY (2004) J Plant Physiol 161: 257-264.
Ilík P, Krchňák P, Tomek P, Nauš J (2002) J Biochem Biophys Methods 51: 273-281.
Jahns P, Holzwarth AR (2012) Biochim Biophys Acta-Bioenerg 1817: 182-193.
Järvi S, Suorsa M, Paakkarinen V, Aro EM (2011) Biochem J 439: 207-214.
Johnson MP (2016) Essays Biochem 60: 255-273.
Johnson MP, Ruban AV (2011) J Biol Chem 286: 19973-19981.
Kalisch B, Dörmann P, Hölzl G (2016). In: Nakamura Y, Li-Beisson Y (eds) Lipids in Plant and Algae Development. Springer International Publishing,
Karlický V, Kurasová I, Ptáčková B, Večeřová K, Urban O, Špunda V (2016) Photosynth Res 130: 357-371.
Karlický V, Podolinská J, Nadkanská L, Štroch M, Čajánek M, Špunda V (2010) Photosynthetica 48: 475-480.
Karunen P (1990) Plant lipid biochemistry, structure and utilization: 30-32.
Keller D, Bustamante C (1986) J Chem Phys 84: 2972-2980.
Kirchhoff H, Haase W, Haferkamp S, Schott T, Borinski M, Kubitscheck U, Rogner M (2007) Biochim Biophys Acta-Bioenerg 1767: 1180-1188.
Knight CA, Ackerly DD (2002) Oecologia 130: 505-514.
Kouřil R, Dekker JP, Boekema EJ (2012) Biochim Biophys Acta-Bioenerg 1817: 2-12.
Kouřil R, Nosek L, Bartoš J, Boekema EJ, Ilík P (2016) New Phytol 210: 808-814.
Kouřil R, Wientjes E, Bultema JB, Croce R, Boekema EJ (2013) Biochim Biophys Acta-Bioenerg 1827: 411-419.
Kouřil R et al. (2005) Biochemistry 44: 10935-10940.
Kovacs L et al. (2006) Plant Cell 18: 3106-3120.
Koziol AG, Borza T, Ishida K, Keeling P, Lee RW, Durnford DG (2007) Plant Physiol 143: 1802-1816.
Krumova SB, Laptenok SP, Kovacs L, Toth T, van Hoek A, Garab G, van Amerongen H (2010) Photosynth Res 105: 229-242.
Krumova SB, Todinova SJ, Busheva MC, Taneva SG (2005) J Photochem Photobiol B-Biol 78: 165-170.
Kurasová I, Čajánek M, Kalina J, Urban O, Špunda V (2002) Photosynth Res 72: 71-83.
Kurasová I, Kalina J, Štroch M, Urban O, Špunda V (2003) Photosynthetica 41: 513-523.
Laczko-Dobos H, Szalontai B (2009) Biochemistry 48: 10120-10128.
Latowski D, Akerlund HE, Strzalka K (2004) Biochemistry 43: 4417-4420.
Lemeille S, Rochaix JD (2010) Photosynth Res 106: 33-46.
Leong TY, Anderson JM (1984) Photosynth Res 5: 117-128.
Lepetit B, Goss R, Jakob T, Wilhelm C (2012) Photosynth Res 111: 245-257.
Lichtenthaler HK (1987) Method Enzymol 148: 350-382.
Lindahl M, Yang DH, Andersson B (1995) Eur J Biochem 231: 503-509.
Lípová L, Krchňák P, Komenda J, Ilík P (2010) Biochim Biophys Acta-Bioenerg 1797: 63-70.
Liu ZF et al. (2004) Nature 428: 287-292.
Loll B, Kern J, Saenger W, Zouni A, Biesiadka J (2005) Nature 438: 1040-1044.
Lu CM, Zhang JH (1999) J Exp Bot 50: 1199-1206.
Makarenko SP, Konenkina TA, Suvorova GG, Oskorbina MV (2014) Russ J Plant Physiol 61: 119-123.
Mathur S, Agrawal D, Jajoo A (2014) J Photochem Photobiol B-Biol 137: 116-126.
Merzlyak MN, Melo TB, Naqvi KR (2008) J Exp Bot 59: 349-359.

Miloslavina Y et al. (2012) Photosynth Res 111: 29-39.
Minagawa J (2011) Biochim Biophys Acta-Bioenerg 1807: 897-905.
Moellering ER, Miller R, Benning C (2009). In: Wada H, Murata N (eds) Lipids in Photosynthesis: Essential and Regulatory Functions. Springer Netherlands, Dordrecht, The Netherlands, pp 139–155
Mongrand S, Badoc A, Patouille B, Lacomblez C, Chavent M, Cassagne C, Bessoule JJ (2001) Phytochemistry 58: 101-115.
Mustardy L, Buttle K, Steinbach G, Garab G (2008) Plant Cell 20: 2552-2557.
Nanjo Y, Mizusawa N, Wada H, Slabas AR, Hayashi H, Nishiyama Y (2010) Biochim Biophys Acta-Bioenerg 1797: 1483-1490.
Nauš J, Rolencová M, Hlaváčková V (2008) J Integr Plant Biol 50: 1292-1299.
Niyogi KK, Truong TB (2013) Curr Opin Plant Biol 16: 307-314.
Nosek L (2012) Usage of 2D-CN/SDS-PAGE for determination of changes in pigment-protein complexes from thylakoid membranes of stressed plants. Masters thesis, Palacký University Olomouc
Oguchi R, Hikosaka K, Hirose T (2003) Plant Cell Environ 26: 505-512.
Olaya-Castro A, Scholes GD (2011) Int Rev Phys Chem 30: 49-77.
Olive J, Vallon O (1991) J Electron Microsc Tech 18: 360-374.
Pali T, Garab G, Horvath LI, Kota Z (2003) Cell Mol Life Sci 60: 1591-1606.
Pan XW et al. (2011) Nat Struct Mol Biol 18: 309-U394.
Passarini F, Wientjes E, Hienerwadel R, Croce R (2009) J Biol Chem 284: 29536-29546.
Peers G et al. (2009) Nature 462: 518-U215.
Pinnola A, Staleva-Musto H, Capaldi S, Ballottari M, Bassi R, Polívka T (2016) Biochim Biophys Acta 1857: 1870-1878.
Pospíšil P (2012) Biochim Biophys Acta-Bioenerg 1817: 218-231.
Pospíšil P, Tyystjarvi E (1999) Photosynth Res 62: 55-66.
Qin XC, Suga M, Kuang TY, Shen JR (2015) Science 348: 989-995.
Ruban AV (2016) Plant Physiol 170: 1903-1916.
Ruban AV, Calkoen F, Kwa SLS, vanGrondelle R, Horton P, Dekker JP (1997) Biochim Biophys Acta-Bioenerg 1321: 61-70.
Ruban AV, Johnson MP (2015) Nat Plants 1: 15161.
Ruban AV, Johnson MP, Duffy CDP (2012) Biochim Biophys Acta-Bioenerg 1817: 167-181.
Shi H, Xiong L, Yang KY, Tang CQ, Kuang TY, Zhao NM (1998) J Mol Struct 446: 137-147.
Scholes GD, Fleming GR, Olaya-Castro A, van Grondelle R (2011) Nat Chem 3: 763-774.
Simidjiev I, Barzda V, Mustardy L, Garab G (1998) Biochemistry 37: 4169-4173.
Simidjiev I et al. (2000) Proc Natl Acad Sci U S A 97: 1473-1476.
Špunda V et al. (1994) Universitas Ostraviensis, Acta Facultatis Rerum Naturalium, Physica - Chemia 141: 37-52.
Štroch M, Čajánek M, Kalina J, Špunda V (2004) J Photochem Photobiol B-Biol 75: 41-50.
Štroch M, Kuldová K, Kalina J, Špunda V (2008a) J Plant Physiol 165: 612-622.
Štroch M, Lenk S, Navrátil M, Špunda V, Buschmann C (2008b) Environ Exp Bot 64: 271-278.
Thayer SS, Björkman O (1992) Photosynth Res 33: 213-225.
Tikkanen M, Grieco M, Aro EM (2011) Trends Plant Sci 16: 126-131.
Timperio AM, Gevi F, Ceci LR, Zolla L (2012) Plant Physiol Biochem 50: 8-14.
Toth TN et al. (2016) Biochim Biophys Acta 1857: 1479-1489.
Umena Y, Kawakami K, Shen JR, Kamiya N (2011) Nature 473: 55-60.
van Amerongen H, Croce R (2013) Photosynth Res 116: 251-263.
Van Grondelle R, Dekker JP, Gillbro T, Sundstrom V (1994) Biochim Biophys Acta-Bioenerg 1187: 1-65.
Varkonyi Z, Nagy G, Lambrev P, Kiss AZ, Szekely N, Rosta L, Garab G (2009) Photosynth Res 99: 161-171.
Vass I (2012) Biochim Biophys Acta-Bioenerg 1817: 209-217.
Wada M (2013) Plant Sci 210: 177-182.
Walters RG, Rogers JJM, Shephard F, Horton P (1999) Planta 209: 517-527.
Wen XG, Qiu NW, Lu QT, Lu CM (2005) Planta 220: 486-497.
Wientjes E, van Amerongen H, Croce R (2013a) Biochim Biophys Acta-Bioenerg 1827: 420-426.
Wientjes E, van Amerongen H, Croce R (2013b) J Phys Chem B 117: 11200-11208.
Wild A, Hopfner M, Ruhle W, Richter M (1986) Z Naturforsch (C) 41: 597-603.
Williams WP (1994) Prog Lipid Res 33: 119-127.
Williams WP (1998). In: Siegenthaler PA, Murata N (eds) Advances in photosynthesis. Lipids in photosynthesis. Kluwer Academic Publishers, Dordrecht, pp pp 103–118
Yamamoto HY, Higashi RM (1978) Arch Biochem Biophys 190: 514-522.
Yang CH, Boggasch S, Haase W, Paulsen H (2006) Biochim Biophys Acta-Bioenerg 1757: 1642-1648.

Zhang R, Cruz JA, Kramer DM, Magallanes-Lundback ME, Dellapenna D, Sharkey TD (2009) Plant Cell Environ 32: 1538-1547.
Zhang R, Sharkey TD (2009) Photosynth Res 100: 29-43.
Zhang YJ, Liu C, Liu SA, Shen Y, Kuang TY, Yang CH (2008) Biochim Biophys Acta-Bioenerg 1777: 479-487.

CURRICULUM VITAE

PERSONAL INFORMATIONS

Karlický Václav

Hlavní 1378, 739 11 Frýdlant nad Ostravicí

Vaclav.Karlicky@osu.cz

+420 597 092 156

Date of birth: 04/11/1982

Nationality: Czech

Education

- B.Sc.: University of Ostrava, Faculty of Science, Biophysics (2002-2005)
- M.Sc.: University of Ostrava, Faculty of Science, Biophysics (2005-2007)
- Ph.D.: Palacky University in Olomouc, Faculty of Science, Biophysics (2007- present)

Academic and professional appointments

2011-present: Department of Physics, Faculty of Science, University of Ostrava (Assistant professor)

2011-present: Global Change Research Centre ASCR (Junior Researcher)

Important research visits, fellowships

2011, 2013, 2016 - Laboratory of Photosynthetic Membranes, Institute of Plant Biology, Biological Research Centre, Hungarian Academy of Sciences, Szeged, Hungary, G. Garab and P.Lambrev, circular and linear dichroism of photosynthetic membranes

Fields of scientific interest

Study of response mechanisms of the assimilation apparatus of higher plants to short-term and long-term changes of light intensity and temperature, fluorescence and circular dichroism spectroscopy

Awards

1st place in young scientists competition, poster session, 8th International Conference "Ecophysiological aspects of plant responses to stress factors", September 16-19, 2009, Krakow, Poland

„Young Talents Award Certificate“ at international conference "Photosynthesis Research for Sustainability", July 24-30, 2011, Baku, Azerbaijan

„Best Poster Award Certificate“ at international conference "Photosynthesis Research for Sustainability", September 21-26, 2015, Colymbari, Crete, Greece

Short scientometry

Papers in the reviewed journal with impact factor 4

Papers in proceeding from conference – ISI Web of Science 2

Total number of citations: 12 (10 without self-citations)

H-index according ISI Web of Science: 2